



40th International Free-Electron Laser Conference

Trieste, Italy | August 22-26 2022
www.fel2022.org

Proceedings

Hosting Organization



Elettra Sincrotrone Trieste

ATTOSECONDS AT HARMONICS AT THE EUROPEAN XFEL: FIRST RESULTS AT SASE3

A. Trebushinin^{*}, G. Geloni[†], S. Serkez, G. Mercurio, N. Gerasimova
European XFEL, Schenefeld, Germany
M. Guetg, and E. Schneidmiller[‡], DESY, Hamburg, Germany

Abstract

We report on the observation of a substantial amount of single-spike spectra collected at the SASE3 beamline of European XFEL using a two-stage scheme (3 - 11 % with respect to all events). The undulators at the first stage were set to the resonance at the “fundamental”, and the undulators at the second stage operated at the “harmonic” of the fundamental, in this case, it was the 4th harmonic. In the experiments, we expected radiation generation in the second stage to start from the high level of bunching created in the first stage. Moreover, the nonlinear characteristic of harmonic bunching growth rate at the first stage leads to the most rapid growth of the most prominent spikes. After being amplified at the second stage this provides occasional single spike pulses in the time domain. With that, we expect these single spike events in the spectrum correspond to single spike events in the time domain. We estimated the *minimal possible* pulse duration for these pulses using Fourier transform of the experimental spectra amplitude where we assume a flat phase across a pulse spectrum. The typical duration was at the level of several hundreds of attoseconds (300-500 as). Considering the appearance frequency of single spike events, this method may be attractive for high repetition-rate free electron lasers for generating sub-femtosecond radiation pulses.

INTRODUCTION

High bunching at harmonics driven by the fundamental has drawn the attention of researchers in the past and described in numerous publications, e.g. [1–3]. Underlying effect consists in the fact that, the longitudinal phase space of the electron beam buckets “rotates” from nearly sin-like shape at the beginning of linear regime to a set of “strokes” in deep linear regime. This enhances the content of higher harmonics. The growth of bunching at harmonics is rapid and it reaches very shortly a sufficient level. This process is non-linear and is characterized by a power law dependence with respect to the fundamental ($b_n(t) \sim b_1^n(t)$), Fig. 1, where b_n denotes the bunching at the corresponding n -th harmonic.

Due to this power law dependence, spikes of bunching along the electron beam length are effectively being filtered: suppression of low value of bunching, increase of contrast, and reduction of the width of the spike follow, as depicted in Fig. 2.

^{*} andrei.trebushinin@xfel.eu

[†] gianluca.aldo.geloni@xfel.eu

[‡] evgeny.schneidmiller@desy.de

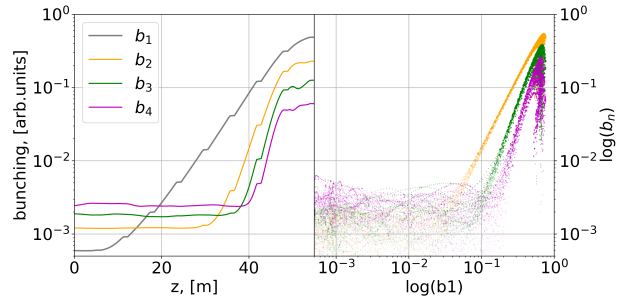


Figure 1: Simulation of the growth of the harmonics bunching with GENESIS 1.3 code, [4]. Left: evolution of the bunching factor for the fundamental (1st), 2nd, 3rd, and 4th harmonic. Right: dependence of the harmonics bunching factor on bunching factor at fundamental in log-log scale. The long plateau on the left corresponds to a negligible level of the higher harmonics content, followed by a linear dependence $b_n(t) \sim b_1^n(t)$, the slopes of the lines is 2, 3, 4 for the corresponding harmonics, which corresponds to linear regime, on the right a hook-like dependence represents saturation.

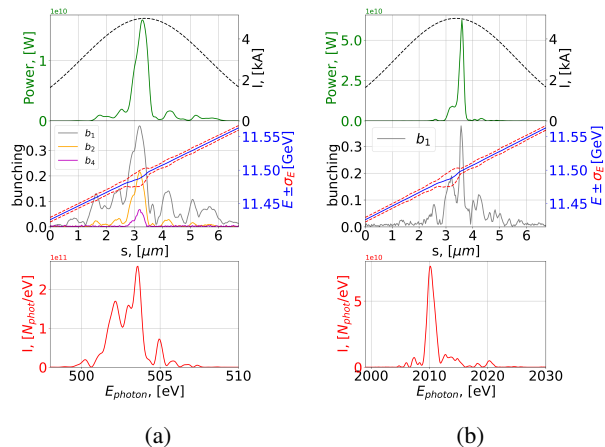


Figure 2: A first part of the FEL is tuned at the fundamental harmonic (a), while a second part lases at the fourth harmonic with respect to the first stage (b). The spikes of the harmonics were effectively filtered when compared to the bunching distribution of the fundamental harmonic. One may observe suppression of low values of bunching, increase in contrast, and reduction of the width of the spike.

The authors of [5] proposed to use this effect for generating sub-femtosecond pulses with two (or *multi*) stage

FIRST LASING OF THE THz SASE FEL AT PITZ*

M. Krasilnikov[†], Z. Aboulbanine, G. Adhikari, N. Aftab, P. Boonpornprasert, R. General, G. Georgiev, J. Good, M. Gross, L. Heuchling, A. Hoffmann, M. Homann, L. Jachmann, D. Kalantaryan, W. Köhler, G. Koss, X.-K. Li, A. Lueangaramwong, S. Maschmann, D. Melkumyan, F. Müller, R. Netzel, R. Niemczyk, A. Oppelt, B. Petrosyan, S. Philipp, M. Pohl, H. Qian, C. Richard, C. Rüger, A. Sandmann-Lemm, M. Schade, E. Schmal, J. Schultze, F. Stephan, G. Vashchenko, T. Weilbach, S. Weisse, DESY, Zeuthen, Germany
 B. Krause, E. Schneidmiller, M. Tischer, P. Vagin, M. Yurkov, DESY, Hamburg, Germany
 W. Hillert, Univ. Hamburg, Institut fuer Experimentalphysik, Hamburg, Germany
 A. Brachmann, N. Holtkamp, H.-D. Nuhn, SLAC, Menlo Park, CA, USA

Abstract

The Photo Injector Test Facility at DESY in Zeuthen (PITZ) develops a prototype of an accelerator-based high-power tunable THz source for pump-probe experiments at the European XFEL. The PITZ injector is also the site for the development and preparation of the high-brightness electron source for the main linac of the European XFEL and has the same pulse train structure as the X-ray photon source of the XFEL. For the proof-of-principle experiments on high-power THz generation an LCLS- I undulator (on loan from SLAC) is installed in the tunnel annex downstream of the existing accelerator. The extension of the beam line consists of a bunch compressor and a collimation system in the main PITZ tunnel, as well as a matching section, the undulator and the THz diagnostic setup in the tunnel annex. A Self-Amplified Spontaneous Emission (SASE) FEL is used to generate the THz pulses. High radiation power can be achieved by utilizing high charge (up to several nC) electron bunches from the PITZ photo injector. A beam energy of ~ 17 MeV is used to generate THz radiation with a centre wavelength of $100 \mu\text{m}$. The transport of this space charge dominated electron beam and its thorough matching into the planar LCLS-I undulator with a strong vertical focusing is one of the project challenges. The installation of the first THz beamline setup was finished in summer 2022 and commissioning with electron beam started. A specially developed procedure for a high charge beam matching into the undulator was successfully tested resulting in a first THz pulse generation. The start-up THz diagnostics is based on pyrodetectors. First measurements of the THz generation from 1 nC, 2 nC and 3 nC bunches have been taken, the statistics properties analysis corresponds to the expected SASE performance. The gain curve for the 3 nC case reflects the onset of saturation regime.

INTRODUCTION

The Photo Injector Test Facility at DESY in Zeuthen (PITZ) currently develops a prototype for a high-power tunable accelerator-based THz source for pump-probe experiments at the European XFEL [1]. A promising concept

to provide THz pulses with a pulse repetition rate identical to that of the X-ray pulses is to generate them using the PITZ photo injector. Because PITZ develops the high-brightness electron source for the European XFEL, properties of the photo injector are fully compatible with the XFEL one, especially both injectors maintain the same pulse train structure. To generate a high-power THz pulses a SASE FEL is considered as a main mechanism. One of the key parameters for the THz SASE FEL high performance is a high beam peak current of up to 200 A. The PITZ RF-gun with a Cs_2Te photocathodes is capable of generating electron bunches with charges of up to several nC (up to 5nC), making it suitable for the proof-of-principle experiments on the high-gain THz SASE FEL. The THz beamline has been designed and implemented as an extension of the existing PITZ linac in the tunnel annex [2]. A planar LCLS-I undulator (on-loan from SLAC) is used to generate the THz radiation. The undulator parameters (period of 3 cm and undulator parameter of ~ 3.5) demand an electron beam energy of ~ 17 MeV for the centre radiation wavelength of $\sim 100 \mu\text{m}$. The strong magnetic field with a horizontal gradient requires a thorough beam matching. Another challenge is the narrow vacuum chamber (height 5 mm, width 11 mm, and length ~ 3.5 m), which makes matching and transport of the space charge dominated electron beams a complicated task.

The THz beamline was successfully commissioned [3] with 100 pC beams, then high-charge transport and matching started. A special procedure was developed and experimentally tested before at the existing part of the PITZ linac [4] and then successfully applied at the newly installed THz beamline. The first THz SASE FEL lasing was first detected with 1 nC bunch charge, then the bunch charge was stepwise increased to 3 nC. The gain curves were measured for 1 nC, 2 nC, and 3 nC.

THz BEAMLIN

The previously existing PITZ beamline was extended by a bunch compressor and a collimator system in the first tunnel and a matching system, the LCLS-I undulator and THz diagnostics in the second tunnel annex (second PITZ tunnel) downstream of the existing accelerator [2]. The current THz beamline in the tunnel annex is shown in Fig. 1. The THz radiation is measured using pyrodetectors at two stations after the undulator [3]. To measure gain

*The project is supported by the R&D program of the European XFEL.

[†]mikhail.kraskilnikov@desy.de

MICROBUNCHING OF RELATIVISTIC ELECTRON BEAMS*

Alex H. Lumpkin[†], Argonne Associate, Argonne National Laboratory, Lemont, IL USA

Abstract

Microbunching in relativistic electron beams provides the opportunity for generation of coherent radiation at the wavelengths that characterize that periodic longitudinal modulation. Since microbunching is an inherent process in the free-electron laser (FEL) mechanism for both single-pass and oscillator configurations, studies of these properties can elucidate the fundamental interactions. Diagnostics of these microbunched electron beams can be performed using coherent optical transition radiation (COTR) imaging techniques. Four COTR-based experiments from SASE FELs to recent laser wakefield accelerated beams will be presented.

INTRODUCTION

Imagine that a relativistic charged-particle beam transiting the vacuum to a metal interface generates a burst of light in a few fs that is linear with the charge distribution. The unique angular distribution pattern with opening lobes of $1/\gamma$, where γ is the Lorentz factor, carries energy and divergence information, and the near-field image provides the beam transverse profiles. This works for a total charge of 100s of pC and sub-mm beam sizes. This is the description of optical transition radiation (OTR) [1,2]. Now imagine that the light is 5-6 orders of magnitude times brighter due to microbunching in the beam and the concomitant coherent enhancements at specific wavelengths. It's an experimentalist's dream realized.

One of the fundamental facets of microbunching in relativistic electron beams is the potential for generation of coherent radiation at the wavelengths that characterize that periodic longitudinal modulation. This microbunching is an inherent process in the free-electron laser (FEL) mechanism for both single-pass [3] and oscillator configurations. Besides the FEL output, diagnostics of these microbunched electron beams can be performed using coherent optical transition radiation (COTR) and imaging techniques in the former case. In these cases, the COTR from the microbunched portion of the beam in 6-D space generally dominates the images. We note that other mechanisms include the longitudinal-space-charge-induced microbunching in ultra-bright beams and laser-induced microbunching such as observed in laser wakefield accelerator (LWFA) beams. More recently, we consider the diagnostics of the TESSA FEL concepts where a seed laser copropagating with the electron beam through a short modulator and chicane may result in bunching fractions of $>10\%$ leading to COTR enhancements of >22 million. Examples of these past, present, and future investigations will be discussed.

* Work supported by the U.S. Department of Energy, Office of Science, Office of Basic Energy Sciences, under Contract No. DE-AC02-06CH11357.

[†] lumpkin@anl.gov

MICROBUNCHING MECHANISMS

Microbunching of an electron beam, or a z-dependent density modulation with a period λ , can be generated by several mechanisms:

In self-amplified spontaneous emission (SASE) induced microbunching (SIM) the electron beam is also bunched at the resonant wavelength and harmonics. This is narrow band.

The longitudinal space-charge-induced microbunching (LSCIM) starts from noise fluctuations in the charge distribution which causes an energy modulation that converts to density modulation following a dispersive section. This is a broadband case: e.g., LCLS-1 and APS linacs.

The laser-induced microbunching (LIM) occurs at the laser resonant wavelength (and harmonics) as the e-beam co-propagates through the wiggler with the 1-GW laser beam followed by a dispersive section. This is narrow-band. (TESSA prebuncher)

With very high-power lasers in the >100 -TW regime, the laser wakefield accelerator (LWFA) beams have been shown to be microbunched at 1-10 % at visible wavelengths [4,5].

To help the reader visualize the phenomenon, we consider one of the first time-domain observations reported by Ricci and Smith (2000) using off-phase rf acceleration at the end of their infrared FELO beamline [6]. Basically, at the phase of 90 degrees off crest for the accelerating structure, the electrons acquired different energies for their different arrival times. The downstream electron spectrometer then displayed the effective temporal information of the pulse with about 100-fs resolution in the focal plane. This was sufficient to display the longitudinal modulation at the FEL resonant wavelengths of 60 and 51 μm . Other FELOs of that generation did not have this configuration to display the longitudinal modulation. The indirect result was of course the FEL's optical power increased with the number of passes up to saturation of the process. However, for single-pass SASE or seeded FELs one can get access to the laser power and the electron microbunching after each undulator, in principle. In practice, this was done at ANL in 2000-2004, initially at visible wavelengths.

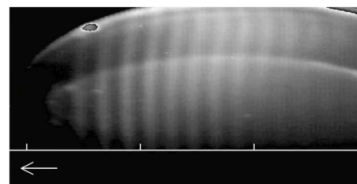


Figure 1: Early time-domain grey-scale image of electron beam microbunching at 60 μm from an FELO process and using an off-phase acceleration technique and

PROPOSAL FOR A QUANTUM FREE ELECTRON LASER DRIVEN BY ULTRACOLD ELECTRONS

B. H. Schaap*, S. Schouwenaars, O.J. Luiten
Eindhoven University of Technology, Eindhoven, Netherlands

Abstract

Operation of a Quantum Free-Electron Laser (QFEL) could provide fully coherent X- and gamma-rays in a compact setup. Imperative to experimental realization is allowing for decoherence of either spontaneous emission or space-charge to take place, having opposing constraints. Here, we discuss a comprehensive QFEL model that takes into account both decoherence effects. Then, we use this model to investigate the ultracold electron source (UCES) as a potential QFEL electron injector. The UCES, based on near-threshold photoionization of laser-cooled and trapped atomic gas, has the unique property of allowing highly charged electron bunches to be extracted while maintaining ultralow transverse emittance. We find that the ultracold electron bunches meet the stringent requirement for potential QFEL operation with commercially available laser systems

INTRODUCTION

Free-electron lasers (FELs) offer tunable and coherent X-ray pulses required for spatiotemporal imaging on the atomic and molecular scale. However, these machines are only available at specialized, costly, large-scale facilities and produce pulses with poor longitudinal coherence and pulse-to-pulse stability. One can scale down a FEL by the use of a laser undulator, which has significantly smaller wavelength than its magnetostatic counterpart, therefore requiring much lower electron beam energy. The resonant wavelength in a laser undulator of wavelength λ_0 is given by

$$\lambda_r = \frac{\lambda_0}{4\gamma_r^2} (1 + a_0^2 + X) \quad (1)$$

where γ_r is the resonant Lorentz factor of the electron beam, $a_0 = eE_0\lambda_0/(2\pi m_e c^2)$ is the laser strength parameter and $X = 4\gamma_r \lambda_c/\lambda_0$ is the recoil parameter with e the elementary charge, m_e the mass of an electron, c the speed of light, E_0 the laser electric field amplitude and $\lambda_c \approx 2.42$ pm the Compton wavelength. Besides red-shifting of the resonant wavelength, recoil parameter X is a measure for the relative momentum loss of an electron due to the emission of a X-ray photon. For the low electron beam energy required to reach the X-ray regime with a laser undulator, the recoil momentum $X\gamma_r mc$ can be larger than the FEL-induced momentum modulation $\rho\gamma_r mc$, where $\rho = (a_0\lambda_0\omega_p/(8\pi c)^{2/3}/\gamma_r)$ the Pierce parameter and $\omega_p = (e^2 n_e/(m_e \epsilon_0))^{1/2}$ the plasma frequency with n_e the electron density. If this is the case $\bar{\rho} = \rho/X < 1$, the quantum mechanical momentum transitions play a dominant role in operation of the FEL. The

dynamics of such a quantum free-electron laser (QFEL) can result in longitudinal spectral coherence similar to solid-state lasers even from self amplified spontaneous emission. [1].

However, detrimental effects of spontaneous emission [2] and space-charge [3] limit the quantum dynamics. Moreover, these effects have opposite constraints [4], making it impossible to operate in a regime where both effects are negligible. The opposite constraints become clear by rewriting the Pierce parameter to

$$\rho = \frac{\frac{1}{4}\sigma\beta}{\beta + \frac{\alpha_f}{6\pi X}} \quad (2)$$

with $\sigma = 4(\lambda_0\omega_p/(8\pi a_0 c)^{2/3}(1 + a_0^2)/\gamma_r)$ is the universally scaled space charge parameter and $\beta = \alpha_f a_0^2/(6\pi X)$ the scaled spontaneous emission rate and α_f the fine structure constant. In this work, we investigate the interplay between spontaneous emission and space charge in steady state QFEL dynamics using a comprehensive discrete Wigner model. Then, based on the results, we propose the ultracold electron source as potential QFEL driver.

THEORETICAL MODEL

Here, we combine the QFEL models that include microscopic space charge [3] and spontaneous emission [2]. These models describe the evolution of the periodic quasi-phase space distribution (discrete Wigner function) W_m of the electron beam during steady state FEL operation. The discrete Wigner function for a pure quantum state is given by [5]

$$\begin{aligned} W_m &= \frac{1}{\pi} \int_{-\pi/2}^{+\pi/2} d\vartheta' e^{-2im\vartheta'} \Psi^*(\vartheta - \vartheta') \Psi(\vartheta + \vartheta') \\ &= \frac{1}{2\pi} \sum_{n=-\infty}^{+\infty} \left[w_m^n + \sum_{m'=-\infty}^{+\infty} \frac{(-1)^{m-m'-1}}{(m-m'-\frac{1}{2})\pi} w_{m'+\frac{1}{2}}^n \right] e^{in\vartheta} \end{aligned} \quad (3)$$

where a periodic wave function $\Psi(\vartheta) = \sum_m c_m e^{im\vartheta}/\sqrt{2\pi}$ was assumed with ϑ the ponderomotive phase. The Fourier components of the wave function c_m are related to the Fourier components of the Wigner function w_m^n in the following way: $w_m^{2n} = c_{m+n}^* c_{m-n}$ and $w_{m+1/2}^{2n+1} = c_{m+n+1}^* c_{m-n}$. In particular, $w_m^0 = |c_m|^2$ is the occupation probability of the m -th momentum state ($p = m\hbar k$) *i.e.* the projection of the Wigner function, Eq. (3) on the momentum axis $\int_{-\pi}^{+\pi} d\vartheta W_m = |c_m|^2$. The projection on the position axis gives the probability density distribution $\sum_m W_m = |\Psi(\vartheta)|^2$.

* b.h.schaap@tue.nl

QUANTUM DIFFUSION DUE TO COHERENT RADIATION *

Gennady Stupakov

SLAC National Accelerator Laboratory, Menlo Park, CA, USA

Abstract

Quantum diffusion caused by synchrotron radiation plays an important role in circular electron and positron accelerators. It is, however, cannot be applied to FELs, because the original derivation of the quantum diffusion [1] assumes incoherent radiation. In this paper, we overcome this limitation and develop the theory of quantum diffusion for coherent radiation. We also give a new interpretation of the quantum diffusion as due to quantum fluctuations of the vacuum electromagnetic field.

INTRODUCTION

Quantum diffusion due synchrotron radiation in circular accelerators defines such important characteristics of the beam as its energy spread, the bunch length and the beam horizontal emittance [2]. The mechanism of the diffusion is usually interpreted in the following way: an emission of a photon of frequency ω causes a discontinuous jump $\hbar\omega$ in the energy of the particle; the stochastic component of these jumps leads to the particle's energy diffusion and the averaged smooth part of the accumulated jumps acts as a radiation reaction force. Based on this interpretation, the quantum diffusion coefficient can be expressed through the spectrum of the synchrotron radiation of a single particle [1–3]; in particular, the energy variance of an electron in the beam due to this diffusion is given by the following formula,

$$(\Delta W)^2 = \int \hbar\omega \frac{d^2 W_{\text{rad}}}{d\omega d\Omega} d\omega d\Omega, \quad (1)$$

where $d^2 W_{\text{rad}}/d\omega d\Omega$ is the energy radiated by an electron into a unit frequency interval $d\omega$ and a unit solid angle $d\Omega$. The energy variance Eq. (1) is not correlated between different electrons in the beam.

Fundamental in the existing derivation of quantum diffusion is an assumption of incoherent radiation. This means that it cannot be applied to FELs. On the other hand, the number of photons that a beam radiates during the passage of an undulator in an FEL can be many orders of magnitude larger than in a ring synchrotron. A natural question arises: how large is the quantum diffusion caused by the coherent radiation in an FEL? In this paper, we will give an answer to this question.

An attempt to generalize the original derivation of the quantum excitation [2] for the case of coherent radiation encounters the following problem: how the recoil momentum of a single photon is distributed between the group of electrons that are involved in coherent radiation of this photon (these are electrons located within the coherence volume for

a given type of radiation)? To overcome this problem, we have to return to quantum description of the electromagnetic field in terms of the creation and annihilation operators. At the same time we treat the beam as a classical current because the quantum effects in relativistic electron beams are negligible [4]. Such a combined treatment is well known in the literature [5, 6] and is relatively easy to apply to the problem at hand.

QUANTUM RADIATION OF A CLASSICAL CURRENT

The electromagnetic field of radiation is represented by the operator $\hat{E}(\mathbf{r}, t)$ that is expressed through the Heisenberg photon annihilation and creation operators, $\hat{a}_{k\nu}(t)$ and $\hat{a}_{k\nu}^\dagger(t)$,

$$\hat{E}(\mathbf{r}, t) = i \sum_{k\nu} c_k \left[\hat{a}_{k\nu}(t) e^{i\mathbf{k}\cdot\mathbf{r}} - \hat{a}_{k\nu}^\dagger(t) e^{-i\mathbf{k}\cdot\mathbf{r}} \right]. \quad (2)$$

Here \mathbf{k} is the wavenumber of the mode, $\nu = 1, 2$ denotes its polarization with the unit polarization vectors $\mathbf{e}_{k\nu}$ that are perpendicular to \mathbf{k} , $\mathbf{e}_{k\nu} \cdot \mathbf{k} = 0$, and $c_k = (2\pi\hbar\omega_k/V)^{1/2}$ with $\omega_k = ck$ and V the quantization volume. If radiation is emitted by a classical current $\mathbf{j}(\mathbf{r}, t)$, the time dependence of the Heisenberg operator $\hat{a}_{k\nu}(t)$ is given by the following equation [6]:

$$\hat{a}_{k\nu}(t) = \hat{a}_{k\nu}(0) e^{-i\omega_k t} + \alpha_{k\nu}(t), \quad (3)$$

where the amplitude $\alpha_{k\nu}(t)$ is

$$\alpha_{k\nu}(t) = \frac{2\pi i}{c_k} \int_{-\infty}^t dt' e^{-i\omega_k(t-t')} j_{\perp k\nu}(t'), \quad (4)$$

and $j_{\perp k\nu}(t)$ is the transverse component of the current projected onto the polarization vector $\mathbf{e}_{k\nu}$,

$$j_{\perp k\nu}(t) = \int \frac{d^3 r}{V} \mathbf{e}_{k\nu} \cdot \mathbf{j}(\mathbf{r}, t) e^{-i\mathbf{k}\cdot\mathbf{r}}.$$

In Eq. (3) we assumed that at $t = 0$ the field is in vacuum state (zero photons) and in Eq. (4) we integrate over time from $-\infty$ instead of 0 assuming that the current is zero for $t < 0$.

Let us now consider a bunch with the charge distribution $\rho(\mathbf{r})$ moving as a rigid body along the orbit given by the vector function $\mathbf{r}_0(t)$,

$$\mathbf{j}(\mathbf{r}, t) = \mathbf{v}(t)\rho(\mathbf{r} - \mathbf{r}_0(t)), \quad (5)$$

with $\mathbf{v}(t) = d\mathbf{r}_0(t)/dt$. Consider an electron located at coordinate \mathbf{a} relative to the center of the bunch which we associate with coordinate $\mathbf{r} = \mathbf{r}_0(t)$ and let us define its

* Work supported by the Department of Energy, contract DE-AC03-76SF00515.

EVOLUTION OF MICROBUNCHING IN DRIFT SECTIONS

S. Khan^{*†}, Center for Synchrotron Radiation, TU Dortmund University, Dortmund, Germany
 G. Perosa¹, F. Sottocorona¹, E. Allaria, A. Brynes, G. Penco, P. R. Ribič, S. Spampinati, C. Spezzani,
 M. Trovò, L. Giannessi², G. De Ninno³, Elettra-Sincrotrone Trieste SCpA, Basovizza, Italia
 E. Ferrari, E. Schneidmiller, DESY, Hamburg, Germany
¹ also at Università degli Studi di Trieste, Trieste, Italy
² also at Laboratori Nazionali di Frascati, INFN, Frascati, Italy
³ also at University of Nova Gorica, Nova Gorica, Slovenia

Abstract

The typical layout adopted in a seeded harmonic generation free-electron laser (FEL) is based on radiator undulators immediately following the dispersive section, in which the microbunching is created. With the advent of new and more complex seeding schemes, this solution cannot always be implemented and cases, where the bunched beam needs to be propagated in free space before entering the radiator, should be investigated. The evolution of the density modulation in a drift space may also play a role in long intra-undulator sections of short-wavelength FELs. The paper reports on recent studies aimed at investigating the impact of the bunching evolution in a drift space on coherent harmonic emission. Experimental results collected at the FERMI free-electron laser are compared with numerical predictions.

INTRODUCTION

The FERMI user facility [1] at the Elettra laboratory located near Trieste, Italy, provides powerful radiation in the spectral range from 100 to 4 nm with two free-electron laser (FEL) lines, FEL-1 and FEL-2. Both rely on the use of an external seed laser to initiate the process of FEL amplification and coherent emission in order to provide a high degree of longitudinal and transverse coherence enabling experiments not possible with other radiation sources. Until recently, FEL-1 [2] was based on high-gain harmonic generation (HGFG) [3, 4] with a single undulator (modulator) for seeding, a dispersive section to convert the laser-induced energy modulation into microbunching, and six undulators (radiators) for the FEL process. In order to extend its spectral range, FEL-1 is presently being upgraded to implement the echo-enabled harmonic generation (EEHG) [5–7] scheme employing two modulators and two dispersive sections to generate microbunching with higher harmonic content [8]. FEL-2 [9], on the other hand, is based on two successive modulator-radiator stages employing a fresh-bunch scheme (HGFG-FB) [10], and studies for a future upgrade have started [11].

In an externally seeded FEL, a dispersive section transforms a laser-induced energy modulation of the electrons into microbunches with a strongly increased charge density giving rise to longitudinal space charge (LSC) effects. In a single-stage HGFG scheme, the radiator is usually placed

* shaukat.khan@tu-dortmund.de

† Work supported by Heinrich-Hertz-Stiftung, MKW NRW, Düsseldorf.

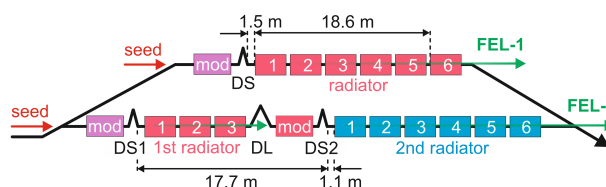


Figure 1: Schematic view of the seeded FEL lines of FERMI with modulators (mod), radiators, dispersive sections (DS), and a delay line (DL) for two-staged HGFG. Also indicated is the shortest drift from the respective DS to the radiator and the range of drift lengths used in the present study (not to scale, see also Table 1).

immediately after the dispersive section and the FEL process starts before LSC effects become significant. With the recent advent of more complex seeding schemes, such as HGFG-FB and EEHG mentioned above, the need may arise to transport the microbunched electrons through drift sections before entering the radiator. Here, LSC increases the energy spread within the microbunches causing a longitudinal elongation (debunching). On the other hand, the correlated energy spread between the microbunches can be reduced which was proposed as a way to improve the output of HGFG FELs at high harmonics [12].

In order to investigate these effects, measurements were performed at both FEL lines of FERMI, and experimental results are presented below together with preliminary numerical predictions.

EXPERIMENTAL SETUP

In contrast to other experimental studies (e.g. [13]), the layout of FERMI shown in Fig. 1 allows to study the evolution of microbunching under variation of the drift length before entering the radiator.

Experiments were performed in three different configurations: (i) a single undulator as radiator at FEL-1 preceded by zero to five undulators with open magnetic gap acting as a variable drift space, (ii) a four-undulator FEL at FEL-1 preceded by zero to two undulators with open gap, and (iii) the full six-undulator FEL of the second HGFG stage of FEL-2 with microbunching in the dispersive section of the first or the second stage. The experimental parameters are summarized in Table 1.

The FEL pulse intensity generated by different harmonics of the laser wavelength was recorded using an intensity mon-

GAUSSIAN RANDOM FIELD GENERATOR SERVAL: A NOVEL ALGORITHM TO SIMULATE PARTIALLY COHERENT UNDULATOR RADIATION

A. Trebushinin*, G. Geloni, and S. Serkez†
European XFEL, Schenefeld, Germany

Abstract

Wavefront propagation codes play pivotal roles in the design of optics at synchrotron radiation sources. However, they usually do not account for the stochastic behavior of the radiation field originating from shot noise in the electron beam. We propose a computationally efficient algorithm to calculate a single statistical realization of partially coherent undulator radiation fields at a given frequency under the approximation of quasi-homogeneity of the source. The proposed algorithm relies on a method for simulating Gaussian random fields. This algorithm is consistent with other well-established approaches, and, in addition, it possesses an advantage in terms of computational efficiency. It can be extended to other types of sources that follow Gaussian statistics. Finally, the demonstration of the algorithm is well suited for educational purposes.

INTRODUCTION

The wave optics approach allows to straightforwardly account for the effects related to fully coherent radiation. Nevertheless, the case of partially coherent radiation remains a sophisticated problem. The characteristics of synchrotron radiation heavily depend on the presence of the shot noise in an electron beam. Because of it, amplitudes and phases of the radiation exhibit stochastic fluctuations. In other words, radiation fields distributions change from realization to realization, and in order to obtain statistically meaningful intensities and correlation functions one needs to average over a statistical ensemble, so that the framework of statistical optics becomes quite natural.

Approaches for simulating partially coherent undulator radiation are proposed in several codes and in plenty of publications. Based on the framework of statistical optics, one can consider propagating the cross-spectral density function of the electric field by exploiting coherent mode decomposition methods, e.g. [1]. An alternative type of methods is based on Monte-Carlo-like simulations. One of the most well-known wave-optics simulation toolkits, Synchrotron Radiation Workshop (SRW) [2, 3] where the intensities are being summed up to form an intensity of the synchrotron radiation.

The algorithm we propose here relies on the generation of instances of the stochastic process, instead of dealing with ensemble-averaged quantities like correlation functions or averaged intensities. The method we propose is based on

Gaussian random field generator. In practice, we restrict complex Gaussian noise by the effective size and divergence of the radiation field. Introducing Gaussian noise, we effectively emulate the contribution of the shot noise accounting for all electrons at once. As a result the algorithm provides complex amplitude of a multimode field of the undulator radiation, suitable for propagation through a beamline. We call this method SERVAL (Synchrotron Emission Rapid eVALuator)¹. The results reported in this contribution were published in [4].

THEORETICAL BACKGROUND ON UNDULATOR RADIATION STATISTICAL PROPERTIES

Undulator radiation has an intrinsic stochastic structure caused by random distribution of electrons in a volume of $6D$ phase space. This distribution follows the shot noise statistics as the number of electrons located in the finite volume of the electron beam phase space is *discrete* and *random*. This shot noise is imprinted in the radiation structure. It manifests itself as longitudinal and transverse spikes in the radiation pulse as illustrated in Fig. 1. By its nature, those fields follow the same statistics as *thermal light*: both are described in terms of Gaussian random processes [5].

However in contrast with thermal sources, which are fully incoherent and whose coherent spot-size at the source is about the radiation wavelength, undulator sources are partially coherent, and they exhibit a coherent spot size equal to the single-electron diffraction size.

For the case of the thermal light, the relation of the spiky structure in the far zone with the source size is described by Van Cittert-Zernike theorem [6, 7]. This theorem relates the cross-spectral density in the far zone with the intensity distribution at the source via Fourier transform. For undulator radiation this theorem is only applied to the special case of quasi-homogeneous sources. Applicability of Van Cittert-Zernike theorem to undulator radiation was thoroughly reviewed in [8]. To assess the coherence properties of the source one should compare the natural size and divergence of the radiation from a single electron with the size and divergence of the electron beam.

Field Correlation

The electron beam length $c\sigma_T$ (c is the speed of light and σ_T is the electron beam duration) is almost always much

¹ This is a backronym. From the beginning we came up with this name SERVAL and only then decided that it stands for Synchrotron Emission Rapid eVALuator.

* andrei.trebushinin@xfel.eu

† svitozar.serkez@xfel.eu

BRINGING GENESIS TO THE CLOUD WITH SIREPO

C. C. Hall, P. Moeller, J. P. Edelen, E. Carlin, M. Keilman,
G. Khalsa, R. Naglar, R. O'Rourke, RadiaSoft LLC, CO, USA

Abstract

Genesis is widely used in the free electron laser community as a simulation tool for studying both simple and complex FEL systems. Until now, this has necessitated learning the command line interface, which can be challenging for new users. Sirepo Genesis provides an intuitive graphic interface for building Genesis simulations in the browser that can then be run using our cloud computing services. Our interface also provides the ability to export simulations for command line use, simulation post-processing with publication quality graphics and the power to share their results with the click of a button to anyone, anywhere, in the world. This poster describes our new GUI and highlights the notable features that have been developed.

INTRODUCTION

RadiaSoft has built a computer aided engineering (CAE) gateway called Sirepo [1], using our open source cloud computing framework of the same name [2–4]. Sirepo supports over 1,500 (and growing) free users, of whom approximately 200 are active in a given month. Sirepo is also available through a series of subscription programs. Sirepo Premium provides users enhanced support, greater access to compute cores, and scientific consulting from RadiaSoft scientists and engineers. The US Particle Accelerator School¹ is our first Sirepo Education customer and the NSLS-II is our first Sirepo Private customer. RadiaSoft supports a few university programs and workshops each year as a service to the community. Recent beneficiaries include Stanford University and the SAGE-S 2021 Summer Camp²

Sirepo is designed to bring scientific, engineering and educational softwares to the cloud, with a rich browser-based interface that works in any modern browser on any computing device. The number of supported codes is continuing to grow, with more features for code coupling and benchmarking. For particle accelerator modeling, we support: MAD-X, elegant, OPAL, Synergia, Zgoubi, Warp PBA (plasma-based accelerators with a cylindrical mesh and azimuthal modes), and JSPEC (electron cooling and intra-beam scattering in rings). For X-ray beamlines, synchrotron radiation and X-ray optics, we support: Shadow for ray tracing and the Synchrotron Radiation Workshop (SRW) for full physical optics. Other interesting apps include: Warp VND (using the Warp code as a 2D and 3D electrostatic PIC engine) to simulate thermionic converters and other vacuum nanoelectronic devices, and the Radia code for magnet design.

More recently, Sirepo is supporting our own app, called Activait, for the use of machine learning techniques to

analyze data. The newest app, called Controls, enables users to explore control system algorithms, using MAD-X as a virtual particle accelerator.

Some codes Sirepo supports are proprietary, e.g. FLASH for hydrodynamic and MHD plasma simulations. Proprietary codes are enabled through Sirepo's role-based authorization system. Authentication of users is secured through password-less logins via email using short-lived one-time tokens. For some codes, Sirepo also gives users the option to launch simulations on the Cori supercomputer at NERSC, if they have access to a NERSC repository. Sirepo supports the two-factor authentication mandated by NERSC.

Sirepo provides single sign-on access to an integrated Jupyter³ server, enabling interactive cloud computing with Python and other languages. All of the Sirepo-supported codes and associated dependencies are pre-installed, together with standard machine learning tools and libraries. Our Jupyter configuration supports a variety of graphics and numeric libraries including Matplotlib, Pandas, Plotly, Seaborn, and yt.

GENESIS IN SIREPO

We have recently added Genesis to the family of codes supported in Sirepo. Due to the uniqueness of Genesis the code the interface does not follow the same convention as many of our other particle accelerator design tools. When users enter the Sirepo Genesis app they have access to a sandbox with an array of examples from notable free electron lasers. Figure 1 shows a screenshot of the examples folder in the Genesis application. Note that users can start a simulation from scratch, import an existing simulation, or build off of one of the provided examples.

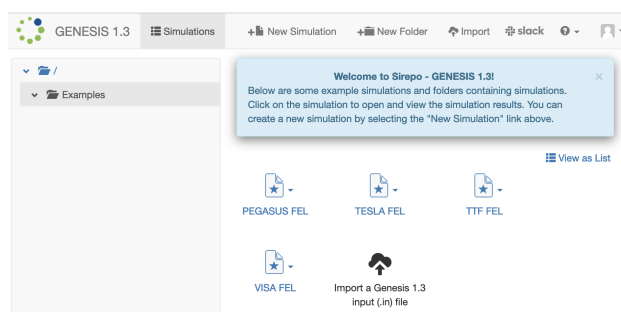


Figure 1: Screenshot of the examples folder for Sirepo Genesis.

The app allows users to configure and execute time-independent simulations. Users can adjust all parameters specified in the Genesis input file related to time-independent simulations. The full set of Genesis inputs are

³ <https://jupyter.org>

¹ <https://uspas.fnal.gov/>

² <https://conf.slac.stanford.edu/sage/>

SPECTROMETER-BASED X-RAY FREE-ELECTRON LASER PULSE DURATION MEASUREMENTS OF CHIRPED BEAMS

R. Robles^{1*}, A. Halavanau, A. Lutman, D. Cesar, G. Stupakov,
SLAC National Accelerator Laboratory, Menlo Park, USA
¹also at Stanford University, Stanford, USA

Abstract

Accurate measurements of the X-ray pulse duration produced by X-ray free-electron lasers (XFELs) typically rely on longitudinal electron beam phase space diagnostics, e.g. in a transverse deflecting cavity or TCAV, or from measurements of spectral correlations. All of the known spectral methods share the weakness that they will underestimate the pulse length in the case that the FEL spectrum is broadened due to the electron beam having an energy chirp. We present a statistical analysis of FEL radiation in the presence of a linear electron beam energy chirp which extends previous results by including an accurate description of the FEL gain process. In doing so, we show that with measurements of the spectral intensity correlations and the average spectrum, one can reconstruct the X-ray pulse length, e-beam chirp, and spectrometer resolution. Our approach is validated by comparison with 1D FEL simulations.

INTRODUCTION

Several methods exist to measure the pulse duration produced by XFELs. One can directly infer something about the XFEL pulse shape and duration if a longitudinal phase space diagnostic is available for the electron beam, such as a transverse deflecting cavity (TCAV) [1]. In practice, however, TCAVs can be difficult to operate and have a limited temporal resolution, about 2-4 fs, particularly at higher beam energies, and thus other methods which do not rely on knowledge of the e-beam phase space pose interest. It has been known for decades that the fluctuations of spectral intensity of the radiation emitted by electron beams stores information about the bunch length [2–5]. A technique applied to the XFEL by Lutman *et al* in [6, 7], showed that by evaluating the spectral intensity correlations, one can reconstruct not only the pulse duration but also the resolution of the spectrometer used to measure the XFEL spectra. A similar approach was recently taken in [8] to unveil slightly more information about the time-frequency correlations of the XFEL pulses. Both of these approaches, as well as other approaches based on studying intensity correlations, are inaccurate if the electron beam has a time-energy correlation or chirp. The presence of the e-beam chirp broadens the FEL spectrum and results in these measurements underestimating the pulse duration [9]. This inability stems from the assumption, in those models, that each electron emits

radiation centered around the same central frequency ω_0 defined by the FEL resonance condition.

The behavior of the FEL gain process in the presence of a linear e-beam energy chirp is well-understood, however, and an appropriate Green's function was derived by Krinsky and Huang in [9]. These spectral correlation-based measurements should be extendable to include the chirp. We present a revised analysis of FEL intensity fluctuations in the presence of a linear energy chirp and non-zero spectrometer resolution. By fitting to both the spectral intensity correlation function and the average spectrum, we are able to extract all three parameters - the X-ray pulse length, the electron beam chirp, and the spectrometer resolution. There is inherent uncertainty in this method which stems from ambiguity in the value of the SASE bandwidth, however, we demonstrate that the impact of that uncertainty is negligible on practical measurements. We validate our approach by using it to reconstruct the beam parameters of 1D FEL simulations.

CALCULATION OF SPECTRAL INTENSITY CORRELATION

In an experiment, one typically has access to spectral intensity measurements of the FEL field via spectrometer. The measurement is a convolution of the true intensity spectrum with a spectrometer resolution function:

$$\tilde{S}(\omega) \equiv \int \frac{d\omega'}{2\pi} e^{-\frac{(\omega-\omega')^2}{2\sigma_m^2}} |\tilde{E}(\omega')|^2 \quad (1)$$

where σ_m is the spectrometer resolution. The measured spectral intensity correlation is then defined as

$$G_2(\delta\omega) \equiv \frac{\langle \tilde{S}(\omega - \frac{\delta\omega}{2}) \tilde{S}(\omega + \frac{\delta\omega}{2}) \rangle}{\langle \tilde{S}(\omega - \frac{\delta\omega}{2}) \rangle \langle \tilde{S}(\omega + \frac{\delta\omega}{2}) \rangle} - 1 \quad (2)$$

We utilize an integral form of this equation given by Eq. (A5), in [6], omitted here for brevity. We now compute two quantities: the spectral field correlation $\langle \tilde{E}(\omega - \frac{\delta\omega}{2}) E^*(\omega + \frac{\delta\omega}{2}) \rangle$ and the spectral intensity correlation $\langle |\tilde{E}(\omega - \frac{\delta\omega}{2})|^2 |E^*(\omega + \frac{\delta\omega}{2})|^2 \rangle$. We will do this within the framework of [9], which treated a 1D FEL in the high-gain regime including the effects of a linear energy chirp. In this model, the SASE electric field takes the form

$$E(t) = \sum_j e^{i\omega_j(\frac{z}{c} - (t-t_j))} g(t-t_j) h_{1d}(t_j) \quad (3)$$

where $\omega_j = \omega_0 + ut_j$ is the frequency of light emitted by the j -th electron which is the central frequency ω_0 offset by a

* This work was supported by the Department of Energy, Laboratory Directed Research and Development program at SLAC National Accelerator Laboratory, under contract DE-AC02-76SF00515.

ORIGIN OF ECHO-ENABLED HARMONIC GENERATION*

Vladimir N Litvinenko, Stony Brook, NY, USA

Abstract

In this paper I present an overview of two preprints that were published at Budker Institute of Nuclear Physics in 1980. These original publications describing harmonic generation technique which has the same foundation as Echo-Enabled Harmonic Generation (EEHG). They recently become available online, but they are still unknown to FEL community. This paper is an attempt to current this omission.

INTRODUCTION

When I first read about EEHG [1], it vaguely reminded me of a theory developed at Novosibirsk Institute of Nuclear Physics (BINP) in late 1970s. But I was not 100% sure that my memory of decades-old events was correct.

Recently, the BINP made their preprint available on the web [2] and I was able to confirm that technique proposed by I.G. Idrisov and V.N. Pakin [3, 4] based on the similar principles to those described in [1]. In this presentation I would like to briefly review these original papers and give credit to early inventors of this innovative high-harmonic generation technique.

These papers, see Fig. 1, were written in Russian in form of preprints and were not available outside the Iron Curtain – a typical totalitarian method of preventing the exchange of information. Hence, in general, only people from BINP had direct exposure to these findings. The goal of this short

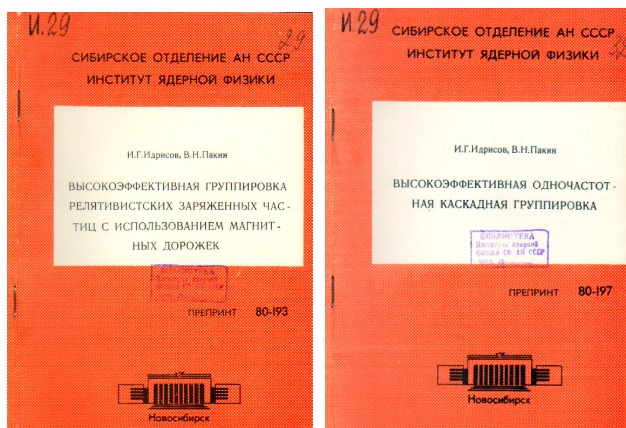


Figure 1: Cover pages of the two preprints.

paper is to give historic perspective on EEHG and to provide FEL community with references to these original papers. I attempted to translate snippets of the original texts and use as many as possible of original illustrations. Unfortunately, quality of some illustrations is poor.

* Work supported by DE-SC0020375 grant from the Office of High Energy Physics, US Department of Energy.

CONTENT OF TWO PREPRINTS

It is impossible to include all text, formulae, figures, and tables from two preprints in this 4-page paper. When it is necessary, I will put in brackets references to these preprints. For example, Fig. 3 or Eq. [4](5) will mean Fig. 3 in Ref. [3] and Eq. (5) in Ref. [4], correspondingly. Similarly, Section [3](2.3) means section 2.3 in Ref. [3].

Abstract [3](1) We demonstrate possibility of high efficiency bunching of relativistic beams using magnetic compressors. We show that amplitude of the current in first harmonic is possible to increase to $1.9 \cdot I_0$ and the current in 10th harmonic to $1.8 \cdot I_0$ (where I_0 is the current in un-bunched beam), or even higher.... High efficiency in amplitudes of high harmonics is achieved using strong compression (to be exact – over-compression using large $R56 - VL$) at initial stages and very strong (increasing) energy modulation in the later stages of the bunching.

Abstract [4](1) We show in this paper that using strong compression (e.g. over-compression) in first compressors, followed by increasing amplitude of energy modulation in the following steps of cascade bunching system allows to increase efficiency of the modulation to $1.76 \cdot I_0$, $1.94 \cdot I_0$ and $1.98 \cdot I_0$ (where I_0 is the current in un-bunched beam) using two, three and four cascades, correspondingly.

[4](2) KINEMATIC APPROACH

[4](2.1) Cascade Bunching

Figure 2 [4](1) shows a typical schematic of cascade bunching.

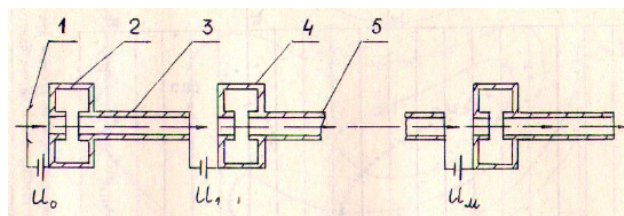


Figure 2: [4](1) Schematic of multi-stage bunching.

A continuous beam with current I_0 from the cathode (1) is accelerated to energy eU_0 and passes through first RF cavity (2), where its energy (velocity) modulated by RF voltage U_{m1} . The drift (3) turns energy modulation into density (current) modulation.... This process is repeated with U_1, U_2, \dots representing modulation at each stage.

[4](2.2) Idealized Equations for Phase Motion – Efficiency of Harmonic Generation

For simplification, let's consider a reference particle which does passing all cavities at zero-crossings:

$$U_1 = U_2 = \dots = 0$$

FIRST COMMISSIONING OF THE PROOF-OF-PRINCIPLE EXPERIMENT ON A THz SASE FEL AT THE PITZ FACILITY

P. Boonpornprasert*, Z. Aboulbanine, G. Adhikari, N. Aftab, R. General, G. Georgiev, J. Good, M. Gross, L. Heuchling, A. Hoffmann, M. Homann, L. Jachmann, D. Kalantaryan, W. Köhler, G. Koss, M. Krasilnikov, X.-K. Li, A. Lueangaramwong, S. Maschmann, D. Melkumyan, F. Müller, R. Netzel, R. Niemczyk, A. Oppelt, B. Petrosyan, S. Philipp, M. Pohl, H. Qian, A. Sandmann-Lemm, C. Richard, C. Rüger, M. Schade, E. Schmal, J. Schultze, F. Stephan, G. Vashchenko, T. Weilbach
 Deutsches Elektronen-Synchrotron DESY, Zeuthen, Germany
 B. Krause, E. Schneidmiller, M. Tischer, P. Vagin, M. Yurkov
 Deutsches Elektronen-Synchrotron DESY, Hamburg, Germany
 A. Brachmann, N. Holtkamp, H.-D. Nuhn
 SLAC, Menlo Park, CA 94025, United States

Abstract

Research and development of an accelerator-based THz source prototype for pump-probe experiments at the European XFEL are ongoing at the Photo Injector Test Facility at DESY in Zeuthen (PITZ). A proof-of-principle experiment to generate THz SASE FEL radiation using an LCLS-I undulator driven by an electron bunch from the PITZ accelerator has been prepared. After four years of designs and construction, the first commissioning with an electron beam was started in July 2022. This paper presents and discusses the experience and results of the first commissioning.

INTRODUCTION

The European XFEL has planned to perform THz pump-X-ray probe experiments at the full bunch repetition rate for users. A promising concept to provide the THz pulses with a pulse repetition rate identical to that of the X-ray pulses is to generate them using an accelerator-based THz source [1, 2]. The Photo Injector Test Facility at DESY in Zeuthen (PITZ) is an ideal machine as a prototype for developments of the THz source [3]. Proof-of-principle experiments to generate the THz SASE FEL by using an LCLS-I undulator driven by a high-charge (2-4 nC) electron bunch from the PITZ accelerator has been planned and studied. Start-to-End simulations for this setup, i.e. beam momentum of about 17 MeV/c, a photocathode laser pulse duration of 10 ps FWHM and a peak current of 200 A, yielded a THz pulse energy of about 0.5 mJ at a central wavelength of 100 μm [4-6].

The PITZ beamline has been extended and improved for the proof-of-principle experiments. A schematic overview of the PITZ beamline and the extension into a tunnel annex currently under installation is shown in Fig. 1. The beamline extension consists of a bunch compressor, an LCLS-I undulator, two beam dumps, magnets, screen stations, and other diagnostic devices. More information on the progress of the beamline extension is reported in [7].

* prach.boonpornprasert@desy.de

In July 2022, screen stations and magnets in the straight section of the extended beamline were installed and operable. We performed the first commissioning of the extended beamline by transport and matching a beam with a bunch charge of 100 pC through the undulator. Then, the transport and matching were repeated with higher bunch charges, 500 pC and 1 nC, respectively. We also measured the output radiation from the undulator using a THz pyroelectric detector.

CORRECTION AND STOP COILS

Beam transport and matching through the undulator are crucial for the first commissioning. For beam momentum of about 17 MeV/c, the transverse gradient of the undulator will lead to a significant off-axis trajectory in the horizontal plane [8]. To compensate the effect of the horizontal gradient on the beam path, a pair of correction coils was designed and installed at the undulator as shown in Fig. 2.

Five identical pairs of short coils are installed uniformly along the longitudinal axis of the undulator. Each pair of short coils is designed to stop a 20 MeV/c beam inside the undulator by horizontally bending the beam up to 10 mrad (applied a current of 3.3 A) to the vacuum pipe for measuring energy gain curve of the SASE FEL. Figure 3 shows the design of the stop coils and the first pair of stop coils installed at the undulator.

BEAM COMMISSIONING

For the first beam commissioning in the undulator, an electron beam with a 100 pC bunch charge was considered, which is much lower than our nominal charge of 4 nC. With a lower bunch charge, the hardware, e.g., screen stations and magnets, could be tested while being protected from high radiation exposure. A smaller beam size is achievable at lower charges, which is beneficial to transport the beam in the narrow vacuum chamber and to test the matching procedure in the undulator. The machine and beam parameters are summarized in Table 1, where the gun and booster phases are the relative phases with respect to the maximum mean momentum gain (MMMGM).

OPTICAL-CAVITY BASED SEEDED FEL SCHEMES TOWARD HIGHER REPETITION RATE AND SHORTER WAVELENGTHS

G. Paraskaki*, S. Ackermann, DESY, Hamburg, Germany
G. Geloni, European XFEL, Hamburg, Germany
B. Faatz, C. Feng, B. Liu, H. Sun, SARI, Shanghai, China

Abstract

More and more high-gain SASE FELs operate at high repetition rates, either in burst or in continuous wave mode of operation, offering an unprecedented number of electron bunches per second. External seeding techniques provide high quality FEL pulses of full coherence and shot-to-shot stability but cannot keep up with MHz repetition rates of such FELs due to their dependence on the seed laser repetition rate. One attractive solution to overcome this limitation is to employ an optical cavity to store radiation that acts as a seed for the electron bunches arriving at high repetition rates. Such a scheme not only allows seeded operation at multi-MHz repetition rates but also introduces the possibility to achieve seeded radiation at shorter wavelengths, overcoming the hurdle of insufficient power availability of seed laser systems in the vacuum ultraviolet (VUV) wavelength range. Here, we present different optical-cavity-based schemes and we give an overview of their unique capabilities together with simulation results.

INTRODUCTION

Most high-gain Free-Electron Laser (FEL) facilities have so far delivered radiation which is transversely coherent, but longitudinally contains spikes that are not correlated in time. The main reason for this is that the radiation is built up from noise in a single pass and the statistics of the initial noise cause a noisy output [1]. Several schemes have been proposed to increase the longitudinal coherence of FEL radiation without the decrease in the pulse energy implied by monochromatization. However, this has turned out to be a challenge, especially at high repetition rates and some wavelength ranges.

One promising direction to improve the longitudinal coherence is a scheme called self-seeding [2, 3], where the amplification process of the radiation starts from noise. The amplified FEL radiation is then monochromatized and serves as a seed for further amplification in a second stage where a clean spectrum can be achieved. This scheme works well for hard x-rays and high repetition rate when heat loading of crystals is not critical [4]. The disadvantage is that it has relatively large intensity fluctuations.

Another interesting direction is to use external seeding techniques [5, 6] to achieve fully coherent FEL pulses. In this paper, we focus on the limits of external seeding and present a scheme that overcomes them. The limitations are

twofold, namely the limit of available energy of the seed laser at short wavelength and at high repetition rates. Typically, at wavelengths below 200 nm the intensity of seed lasers reduces significantly. And with the required seed energy, there is no laser available that exceeds approximately a few tens of kHz repetition rate. For these reasons, in this paper we study an alternative solution aiming at external seeding without the need of a high repetition rate and powerful seed laser system.

The simulations shown in this paper make use of the high gain harmonic generation (HG) external seeding scheme [5, 7]. We increase the repetition rate of the scheme by using an optical cavity that recirculates a seed at high repetition rates. The FEL process is simulated with Genesis 1.3 [8] while the treatment of the radiation field in the optical cavity is done in ocelot [9]. As examples, we show simulations performed using parameters of FLASH [10] and of the Shenzhen FEL.

SIMULATIONS PERFORMED

For this study, parameters for FLASH and for the Shenzhen FEL have been taken as example, as shown in Table 1. Because the main interest is in the shortest achievable wavelength, which should be 4 nm at FLASH and 2.5 nm at the Shenzhen FEL, only the shortest seed wavelength, which is assumed to be 50 nm is studied in this paper.

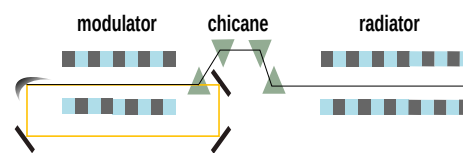


Figure 1: Geometry simulated for FLASH for a cavity-based HG setup. Important simulation parameters are given in Table 1.

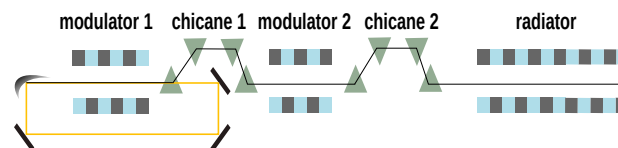


Figure 2: Geometry simulated for the Shenzhen FEL for a cavity-based harmonic optical klystron. Important simulation parameters are given in Table 1.

In both schemes, the process can be initiated by an external seed laser, which seeds the first bunch in a train. After

* georgia.paraskaki@desy.de

GENERATION OF X-RAY VORTEX BEAMS IN A FREE-ELECTRON LASER OSCILLATOR

N.S. Huang, Shanghai Synchrotron Radiation Facility, Shanghai, China

H.X. Deng*, Shanghai Advanced Research Institute, Chinese Academy of Sciences, Shanghai, China

J.W. Yan, European XFEL, Schenefeld, Germany

Abstract

Light with orbital angular momentum (OAM) provides new insights into a wide range of physical phenomena and has engendered advanced applications in various fields. Currently, research interest in X-ray OAM is rapidly expanding. Here, we report a straightforward method capable of generating intense OAM beams from an X-ray free-electron laser oscillator (XFEL). This method leverages Bragg mirrors and longitudinal-transverse mode coupling to enable mode selection in a conventional XFEL configuration, thereby natively producing fully coherent hard X-ray beams carrying OAM. Simulation results indicate that fully coherent hard X-ray OAM beams can be generated without the need for optical mode converters. This simple approach can significantly advance the creation of X-ray OAM while stimulating the development of novel experimental methods.

INTRODUCTION

Optical vortices are spirally phased beams, which have a phase dependence of $\exp(il\phi)$, where l denotes the topological charge and ϕ denotes the azimuthal coordinate in the plane perpendicular to the beam propagation. As demonstrated, the orbital angular momentum (OAM) of optical vortices is l [1]. The past few decades have seen a succession of breakthroughs in vortex and OAM applications, including ultra-high resolution imaging, microparticle manipulation using optical tweezers, high-capacity communications, quantum optics, and laser thermal noise reduction in gravitational wave detection. Although X-ray OAM is much less common, the interaction of matter and X-ray optical vortices is expected to give rise to new phenomena. This capability allows X-ray OAM to open up new opportunities for characterizing different material properties. In particular, XFEL is able to provide unprecedentedly bright X-ray vortices, which will significantly stimulate the development of experiments and methods.

Recent advances have led to the generation of OAM beams in single-pass seeded XFEL with fundamental Gaussian mode lasers and helical undulators [2]. Generally, two schemes have been developed to generate FEL OAM pulses. The first scheme uses spirally microbunched electron beams to produce OAM light, which can be generated by the high harmonic interaction of the lasers and electron beams in a helical undulator. The second one is based on the harmonic emission of the helical undulator, which carries OAM natively. In this scheme, the electron beam is microbunched

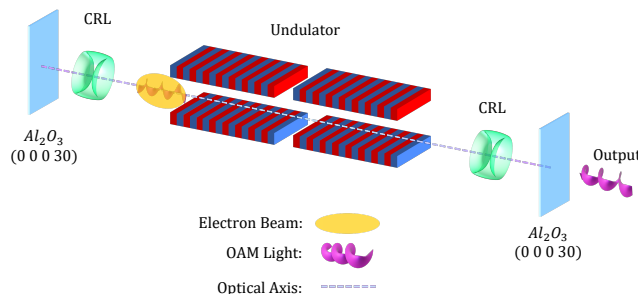


Figure 1: Scheme to generate X-ray OAM beams by using a typical configuration of the XFEL. Compound refractive lenses (CRLs) are used for X-ray focusing.

at harmonic wavelength of a helical undulator via a fundamental Gaussian mode lasers, and then sent to pass through the helical undulator to generate OAM light. This scheme is also compatible with after burner mode.

Unlike single-pass FELs to produce OAM beams, XFEL is well suited to produce coherent radiation with high power and high repetition rates in the hard X-ray regime. XFEL to generate OAM beams (see Fig. 1) can use a newly proposed method [3], which essentially facilitates the preservation of OAM beam amplification at the fundamental wavelength and avoids the need for external optical elements. The method is very simple, as it requires only the adjustment of the resonant condition of XFEL operation. The method is based on the important fact that the resonant condition for each transverse mode is slightly different. As a result, the gain profile of each transverse mode is shifted over the spectrum. The combined effect is that XFEL can operate in a specific spectral regime in which radiation in a high-order transverse mode can be obtained at maximum gain. Because the laser saturation state is only governed by the gain and cavity loss, this effect enables XFELs to select transverse modes that carry OAM.

OAM MODES IN XFEL

We start with the Laguerre–Gaussian (LG_p^l) modes that can possess arbitrary OAM [1], where l denotes any real integer for the azimuthal mode and p is zero or any positive integer for the radial mode. With the LG_p^l basis modes, the transversely dominated FEL radiation fields can be described

* denghx@sari.ac.cn

SIMULATION STUDIES FOR THE ASPECT PROJECT AT EUROPEAN XFEL

J. W. Yan*, G. Geloni, C. Lechner, S. Serkez, European XFEL, Schenefeld, Germany
Y. Chen, M. Guetg, C. Heyl, E. Schneidmiller
Deutsches Elektronen-Synchrotron DESY, Hamburg, Germany

Abstract

Intense attosecond pulses generated by x-ray free-electron lasers (XFEL) are promising for attosecond science, for example, to study the quantum mechanical motion of electrons in molecules. This paper presents numerical simulations of the generation of attosecond soft and hard x-ray FEL pulses with the chirp-taper and the enhanced self-amplified spontaneous emission methods, based on the parameters of the European XFEL. To overcome the coherence time barrier, a modification of the chirp-taper scheme is used in the case of soft x-rays. The results show that several hundred attosecond pulses can be obtained at both 700 eV and 6 keV photon energies.

INTRODUCTION

As a new generation of light sources, x-ray free-electron lasers (XFELs) are indispensable tools for a wide range of research fields. The demand for attosecond XFEL pulses is increasing rapidly in recent years. Several methods have been proposed to shorten the FEL pulse duration [1]. Many of these schemes employ an external laser to modulate an electron beam and let only a short part of the electron beam lase effectively, such as the chirp-taper [2, 3] and the enhanced self-amplified spontaneous emission (ESASE) schemes [4].

In the chirp-taper scheme, an electron beam is modulated through the interaction with a few-cycle intense laser in a few-period wiggler, and a strong energy chirp is introduced, which inhibits lasing. Reverse taper is used to compensate this effect in a short part of the electron beam, the one with the strongest energy chirp. In addition to the energy modulation, the ESASE scheme relies on the creation of high-current spikes in short parts of the electron beam, with the help of a dispersive section (a chicane) following the energy modulator. Due to the high current levels, in the ESASE scheme, space-charge interactions play a particularly important role. We are currently setting up a project dedicated to the generation AttoSecond Pulses with eSASE and Chirp-Taper schemes (ASPECT) at the European XFEL [5]. ASPECT will initially serve two of the three SASE line at the European XFEL, SASE1 and SASE3, which are respectively specialized in the production of hard and soft x-rays.

The schematic layout of the ASPECT project is shown in Fig. 1. The energy modulation section is placed before SASE1, where external laser and electron beam interact in a two-period wiggler. The energy-modulated beam can be transported to both SASE1 and SASE3. The ESASE scheme

is enabled by the two chicanes located, respectively, before SASE1 and SASE3.

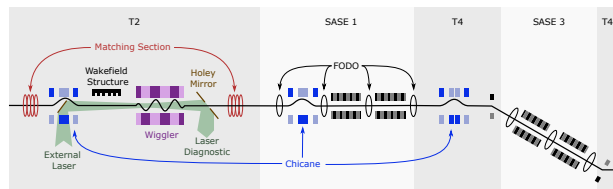


Figure 1: Schematic layout of the ASPECT project.

CHIRP-TAPER SCHEME

We analyze the performance of the chirp-taper scheme for two case studies covering the generation of hard (6 keV) and soft (700 eV) x-ray radiation. A 14 GeV electron beam with a flat-top current of 2500 A is used in both simulations. The electron beam is modulated by a laser with a wavelength of 1030 nm, a pulse energy of several mJ (see below) and an FWHM pulse duration of 4 fs in the two-periods wiggler with a period of 0.7 m. The simulations for the hard and soft x-ray cases are respectively based on the parameters of SASE1 and SASE3 [5], made up of 5 m-long segments, respectively with 40 mm and 68 mm period, followed by 1.1 m-long intersections.

Hard X-Ray Case

In the hard x-ray case, the pulse energy of the laser is selected as 4 mJ. The energy modulation induced by the laser is calculated by theoretical analysis [6] and three-dimensional numerical analysis [7, 8]. As shown in Fig. 2, the two methods yield very similar results. An energy modulation amplitude of around 30 MeV can be obtained.

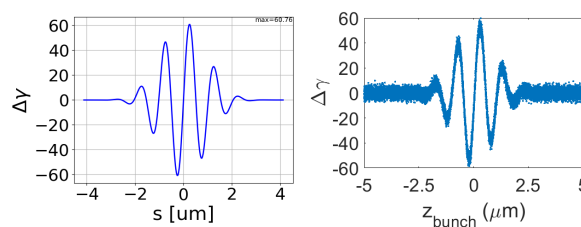


Figure 2: Energy modulation induced by the laser, obtained by theoretical analysis (left) and three-dimensional simulation (right). The bunch head is to the right.

A reverse step-taper is applied in SASE1, and the dimensionless undulator parameter K increases by 0.0013 in each undulator segment. Figure 3 shows the evolution of the

* jiawei.yan@xfel.eu

UNAVERAGED SIMULATION OF SUPERRADIANCE IN FEL OSCILLATORS

R. Hajima[†], National Institutes for Quantum Science and Technology, Kizugawa, Japan

Abstract

Generation of few-cycle FEL pulses with a high extraction efficiency was achieved at infrared FEL oscillators. The observed lasing can be understood as superradiance, radiation from bunched electrons in the slippage region. In the superradiant FEL oscillators, the high-extraction efficiency is accompanied by significant energy variation of the electrons during the undulator. Therefore, numerical studies of such FELs should be conducted by unaveraged simulation codes, in which macroparticles are not bound to specific bunch slices. In this paper, evolution of optical pulses in superradiant FEL oscillators is studied by using one-dimensional and three-dimensional unaveraged codes.

INTRODUCTION

Few-cycle optical pulses are generated with a high-extraction efficiency at a free-electron laser oscillator operated with specific parameters: slippage length, bunch length, gain parameter, cavity length detuning, and round-trip loss [1,2]. In this lasing, the peak intensity (I_p) and the pulse duration (τ) show the scaling law with respect to the number of electrons contributing to the lasing, $I_p \propto N^2$, $\tau \propto 1/N$. Since this scaling law is identical to that of superradiance in a two-level system [3], the lasing is also called superradiance in an FEL oscillator.

Thanks to the few-cycle pulse generation with high-extraction efficiency, a superradiant FEL oscillator operated in infrared wavelengths can provide high-intensity laser pulses exceeding the threshold of tunneling ionization of atoms and molecules, $\sim 10^{13}$ W/cm², and could potentially be used for intense light field science including high-harmonic generation for attosecond X-ray pulses [4].

The study of superradiant FELs also leads to a deeper understanding of the resonant light-matter and light-electron interactions through analogies with superradiance in two-level systems.

Numerical simulations are essential for experimental planning and data analysis of superradiant FEL oscillators, as well as for a deeper understanding of the physics of the high-efficiency few-cycle pulse generation. However, it has been found that so-called average codes widely used in FEL simulations do not give correct results in simulations of superradiance FEL oscillators and that unaveraged codes are necessary. In this paper, we report on superradiance FELO simulations using one-dimensional and three-dimensional unaveraged codes.

SUPERRADIANCE IN TWO-LEVEL SYSTEMS

In order to compare the role of quantum fluctuations in superradiance in two-level systems with the role of shot noise in superradiant FEL oscillators, here we review the Bloch sphere representation of superradiance in two-level systems and calculate pulse waveforms of the superradiance.

The Bloch sphere is a geometrical representation to describe a pair of mutually orthogonal states and their superposition. Here we define the north and south poles of the Bloch sphere as the upper and lower levels in a two-level system and assume all the atoms are initially in the upper level. If there were no quantum fluctuations, all atoms would continue to exist in the upper level, like an inverted pendulum maintaining its posture, and no radiation would occur from the system. In a realistic system, due to quantum fluctuations originating from spontaneous radiation and background thermal radiation, the atoms in the upper level decay to the lower level to emit cooperative radiation, i.e., superradiance [5,6,7].

The radiation waveform from the two-level system was calculated according to the paper [4] and plotted in Fig. 1, in which the initial tipping angle to simulate the quantum fluctuation was assumed to be $\theta_i = 10^{-3}, 10^{-4}, 10^{-5}$. It is shown that the evolution of the pulses depends on the initial tipping angle and the faster the pulses rise with the larger θ_i .

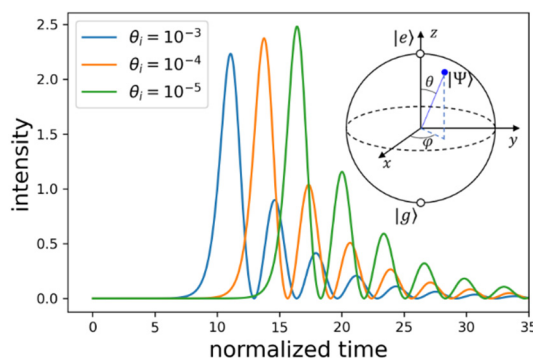


Figure 1: Superradiance of a two-level system calculated by the Burhan-Chiao model with different initial tipping angles, $\theta_i = 10^{-3}, 10^{-4}, 10^{-5}$. The Bloch vector representation of the two-level system is also depicted.

[†] hajima.ryoichi@qst.go.jp

LASER-INDUCED GAS BREAKDOWN AT KU-FEL

R. Hajima[†], National Institutes for Quantum Science and Technology, Kizugawa, Japan
H. Zen, H. Ohgaki, Kyoto University, Uji, Japan

Abstract

We have observed laser-induced breakdown of gases at KU-FEL, the FEL oscillator at Kyoto University, in which few-cycle FEL pulses are generated due to superradiance. In the thermionic cathode mode with a repetition rate of 2856 MHz and a wavelength of 10 μm , the breakdown was observed in air, nitrogen, and argon, while weak luminescence from nitrogen was observed in the photocathode mode operation (29.75 MHz, 8.7 μm). We discuss the mechanism of each phenomenon. The difference in the two operation modes can be explained by the diffusion of electrons between the micropulses.

INTRODUCTION

Free-electron laser oscillators operated in the superradiant regime provide ultrashort infrared pulses with durations of only a few optical cycles. In such lasing, the peak intensity of FEL pulses increases in proportion to the square of the number of electrons. The intensity of the FEL pulses after appropriate focusing, thus, can exceed the threshold of tunnel ionization in atoms and molecules ($> 10^{13} \text{W/cm}^2$), making it possible to develop intense light field science in the long-wavelength infrared region (8-15 μm), where solid-state lasers are difficult to be applied [1].

In this paper, we report recent results from gas-induced breakdown experiments at KU-FEL, the FEL oscillator at Kyoto University, which can be operated in the superradiant regime to produce few-cycle FEL pulses with a high extraction efficiency [2,3].

LASER-INDUCED GAS BREAKDOWN

Laser-induced gas breakdown occurs by the multiphoton ionization process at low pressures and in the case of short pulses (sub-nanosecond). For high-pressure cases, collision cascade ionization dominates [4,5]. Since our experiment is in the high-pressure case, the collision cascade ionization is reviewed here.

The breakdown is initiated by a few free electrons, seed electrons, in the illuminated region. Seed electrons are produced by multiphoton ionization of gas molecules or airborne particles. Cosmic radiation is also a source of seed electrons. Once seed electrons are produced, the electrons gain energy from the laser field by inverse bremsstrahlung, the three-body collision of a photon, an electron, and a heavy particle, and after a number of collisions, the electron energy becomes high enough to induce another ionization. This cascade ionization continues until a sufficient number of free electrons are produced to induce

breakdown in the focal spot. The number of free electrons at the breakdown is about 10^{13} [5].

The number of electrons, n , in the cascade process varies according to [4,5]

$$\frac{dn}{dt} = (v_i - v_a)n - \nabla^2(Dn) - \beta n^2,$$

where v_i is the ionization frequency, v_a is the attachment frequency, D is the diffusion, and β is the recombination coefficient. The electron energy (ε) gained by the inverse bremsstrahlung is given by

$$\frac{d\varepsilon}{dt} = \frac{e^2 E_{rms}^2 v_{eff}}{m(\omega^2 + v_{eff}^2)},$$

where E_{rms} is the rms electric field of the laser, e and m is the electron charge and mass, ω is the laser frequency and v_{eff} is the effective electron heavy particle collision frequency. The effective collision frequency for air is $v_{eff} = 5.3 \times 10^9 p$, with p in torr [6].

Assuming the number of initial and final free electrons in the cascade process, $n_i = 1$ and $n_f = 10^{13}$, we can evaluate the number of cascade generation $k = \ln(n_f/n_i)/\ln 2 \approx 43$. The laser energy deposition for achieving the breakdown, then, must be larger than kE_I , where E_I is the ionization energy. This requirement of the energy deposition leads to the threshold of the laser energy fluence, F_{th} , for the breakdown, neglecting the particle and energy loss:

$$F_{th} = \frac{kE_I(v_{eff}^2 + \omega^2)}{4\pi r_c c v_{eff}},$$

where r_c is the classical electron radius. For a laser wavelength of 10 μm , and nitrogen gas of $1.0 \times 10^5 \text{ Pa}$, we obtain $F_{th} = 8 \text{ J/cm}^2$. Once the laser wavelength and the pulse length are given, the intensity threshold for the gas

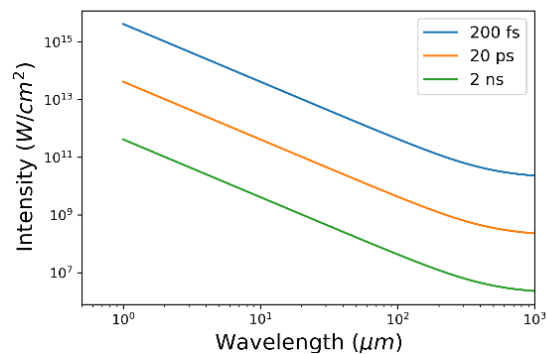


Figure 1: Laser-induced breakdown threshold calculated for nitrogen of $1.0 \times 10^5 \text{ Pa}$ and laser pulses with different durations, 200 fs, 20 ps, and 2 ns.

[†] hajima.ryoichi@qst.go.jp

ANALYSES SUPPORTING THE 2-COLOR UPGRADE TO THE IR FEL AT FHI, BERLIN*

A. M. M. Todd[†], AMMTodd Consulting, Princeton Junction, USA

W. B. Colson, WBC Physics, Carmel, USA

D. H. Dowell, SLAC, Menlo Park, USA

S. C. Gottschalk, STIMagnetics, Woodinville, WA, USA

J. W. Rathke, JW Rathke Engineering Services, Centerport, USA

T. J. Schultheiss, TJS Technologies, Commack, USA

L. M. Young, LMY Technology, Lincolnton, GA, USA

W. Schöllkopf, M. De Pas, S. Gewinner, H. Junkes, G. Meijer, G. Helden, FHI, Berlin, Germany

Abstract

This paper provides a summary of the analyses that led to the definition of the 2-color upgrade of the IR FEL at the Fritz-Haber-Institut (FHI), Berlin. We briefly cover several different aspects of the design, beginning with the beam dynamics of the second far-IR (FIR) beamline, engineering considerations of that physics design, and the FEL physics that defined the short-Rayleigh-range undulator, as well as aspects of the undulator design itself. Additionally, we touch on the approach to 2-color operation and considerations for the FIR optical transport to users. The status of commissioning is described in a parallel paper [1].

INTRODUCTION

The FHI mid-IR (MIR) FEL first lased on February 14, 2012 [2]. Since November 2013, it has provided continuous 3 to 60 μm radiation service to users, resulting in more than 80 peer-reviewed publications [3].

In 2018, FHI embarked upon an ambitious upgrade project to add a FIR FEL beamline that could deliver radiation from 5 to 166 μm . By adding a 2-degree deflecting cavity right after the second linac, alternately, 2-color, 500 MHz pump-probe radiation can be delivered to experiments on the MIR and FIR beamlines, which are separated by 4 degrees, when the new FEL is commissioned.

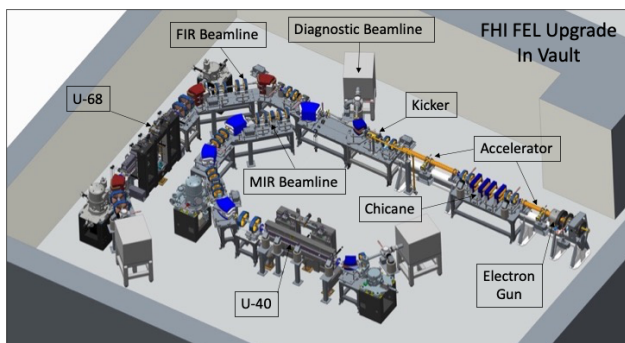


Figure 1: Engineering schematic showing the FHI FEL MIR and FIR electron beamlines in the vault.

This paper describes the analysis that underpinned the FIR FEL physics and engineering design illustrated in Fig. 1. It touches on the beam dynamics and engineering analyses of the electron beamline, the undulator FEL physics and engineering, the FIR optical transport and scanner magnet calibration measurements used in the beam dynamics calculations.

BEAM DYNAMICS

We concentrate on the most difficult 18 MeV energy operation at the longest wavelengths (166 μm with the minimum 32 mm undulator gap). Figure 2 shows a TRACE3D [4] plot for the FIR electron beamline beginning after the accelerator at the left edge to the beam dump at the right edge. Note that the dispersion trace (gold) goes to zero at the center of the U-68 undulator indicating that the 94-degree pre-undulator FIR bend is achromatic. The horizontal U-68 match has a waist in mid-undulator, while the near constant vertical trace illustrates the proper match in the vertically focusing undulator.

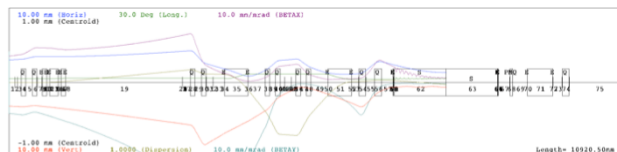


Figure 2: TRACE3D 5e beam envelope simulation of the FIR electron beamline with achromaticity in the centre of the undulator (gold trace) and an excellent match (horizontal/blue - vertical/red) to the U-68 undulator (62 and 63).

Using identical post-linac parameters, the corresponding Fig. 3 TSTEP [5] simulation for this case shows the revised FIR achromat delivers a 2.5 ps, 100 keV FWHM beam to the FIR undulator for FEL physics analysis.

The most difficult operating scenario will occur for 2-color FEL operation where, for any given beam energy, we are short of beam matching variables on the U-68 beamline. Our plan is to utilize quadrupoles QB05 and QB06 after linac 2, and QC04 and QC05 ahead of U-68, to produce waists in the middle and the near constant matched vertical beam size through U-68, at the longest wavelength. For the MIR beamline, we use the matched FIR values for the two magnets after linac 2, adjusting QC01 and QC02,

* Work supported by the Max-Planck-Gesellschaft, Munich, Germany.

[†] ammtodd@fhi-berlin.mpg.de

MODELLING OF SUB-WAVELENGTH EFFECTS IN A FEL OSCILLATOR

P. Pongchalee^{1,2,3}, B.W.J. McNeil^{1,2}

¹SUPA, Department of Physics, University of Strathclyde, Glasgow, UK

²Cockcroft Institute, Warrington, WA4 4AD, UK

³ASTeC, STFC Daresbury Laboratory, Warrington, WA4 4AD, UK

Abstract

Previous studies of FEL oscillators typically use averaged simulation codes which cannot model sub-wavelength effects, such as Coherent Spontaneous Emission from the electron pulse. In this paper, the unaveraged FEL simulation code Puffin is used with the optics code Optical Propagation Code (OPC) to model a FEL oscillator in three dimensions, enabling sub-wavelength effects to be modelled at the FEL interaction and cavity length scales. Results show that coherence spontaneous emission (CSE) can drive the FEL interaction during the start-up phase in the cavity. Further, cavity detuning effects at the sub-wavelength scale can have an effect upon the FEL output from start-up through to the steady state output. While the effects are demonstrated here at a fundamental level, it can be expected that they may be reduced due to limitations such as electron beam and/or cavity length jitter at the radiation wavelength scale. Such effects will need to be further investigated.

INTRODUCTION

When modelling the short pulse effects here, both the coherent and shot-noise spontaneous emission from the electron beam are taken into consideration. CSE has the potential to dominate the overall amplification of the FEL start-up process in an undulator when it is operating, particularly in the low-gain regime of FEL operation. CSE is primarily caused by a short electron beam that has a fine structure at the wavelength scale, such as a sharp-edge rectangular beam. For a short-pulse FEL oscillator, a better understanding of such sub-wavelength effects is needed and a preliminary study is presented here.

Previously, Puffin [1] and OPC [2] were operated together to simulate a RAFEL oscillator model operating in the steady-state [3], but without considering any detailed effects of coherence spontaneous emission (CSE). The effect of CSE occurs with relatively short electron bunch lengths e.g. when they are shorter or comparable to the slippage length. The use of an unaveraged FEL code, Puffin enables the modelling of CSE effects and, together with OPC, can simulate the optical components for an optical cavity at the sub-wavelength scale. A full 3D unaveraged model of a short pulse FEL oscillator can be achieved.

In this paper an FEL oscillator design operating with the near-concentric resonator in the mid-infrared regime is then described. We first demonstrate the simulation of the FEL oscillator when the optical cavity length is detuned from resonance by integer factors of 0.05 of a radiation wavelength.

THE SIMULATION MODEL

FEL and Optics Codes

The conversion of the radiation field between Puffin and OPC has been described in [3]. The two codes are run sequentially starting from, the Puffin simulation of electron/light interaction inside the undulator. The output field at the undulator exit from Puffin is then translated into OPC format to propagate further in the optical oscillator including mirrors and optical path length adjusting due to cavity non-resonance. OPC propagates the radiation field to the undulator entrance, where it is translated back into Puffin field format and is used as a seed for the Puffin input file for the subsequent pass.

Simulation Parameters

In the example presented here, we use parameters as given in Table 1. The parameters used are very similar to those of the IR-FEL of [4]. A curved pole undulator is used to keep the beam size constant throughout the undulator length [5]. The undulator module of length 1.8m consists of the 40 periods of $\lambda_u = 4.5$ cm. The symmetric transverse size of the beam is matched into the curved undulator lattice with $\sigma_{x,y} = 311.8\mu\text{m}$. The temporal shape of the beam current is rectangular of duration 400 fs. The electron beam energy and undulator parameters give a radiation wavelength in the mid-infrared wavelength regime of $6\mu\text{m}$. The electron beam length is then equal to 20λ .

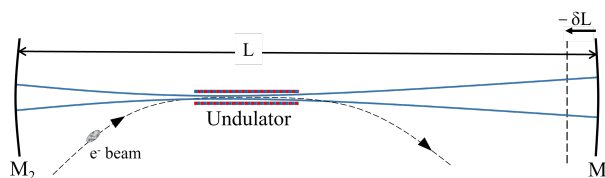


Figure 1: a diagram of the FEL oscillator used in the simulation

The optical cavity is designed as a near-concentric resonator with a Rayleigh length of 52 cm. Two mirrors make up the optical cavity (see Fig. 1). The first mirror is placed after the undulator exit with an output coupling that can be partially transmissive or use a hole out-coupling. The second mirror that forms the simple cavity is then placed before the undulator entrance. When the distance between the two mirrors gives a round-trip propagation time equal to the electron beam repetition rate, the cavity has zero length detuning. The optical beam waist position will be in the cen-

REPORT ON THE FELIX WAVELENGTH RANGE EXTENSION

Victor Claessen[†], Marije Barel, René van Buuren, Alexander van der Meer, Paul Pijpers, Britta Redlich, Michel Riet, Wouter Stumpel, Guus Tielemans, Arjan van Vliet, Bryan Willemsen, FELIX Laboratory, Radboud University and NWO, Nijmegen, The Netherlands
Stephen Gottschalk, STI Magnetics, Woodinville, WA, United States

Abstract

The FELIX Laboratory, located at Radboud University in Nijmegen, The Netherlands, is operating a suite of FELs serving an international user community with infrared and THz radiation from 5 to 1500 micron operating three FELs in parallel and providing beam to 16 dedicated user end stations. Recently, FELIX has upgraded its most frequently used FEL-2 beamline. The 38 period, 65 mm Halbach-type SmCo undulator, originally built for the UK-FEL project in the mid 80's, which had been successfully used for the short-wavelength FEL for almost 30 years, was replaced by a new undulator. This 50 period, 40 mm NdFeB hybrid undulator was built in close collaboration with STI magnetics and the FEL group of FHI/MPG in Berlin. Together with a new resonator cavity it allows an extension of the fundamental range from 5 μm to sub-3 μm , while keeping the desirable good spectral overlap with the longer wavelength FEL-1 branch. The upgraded FEL-2 beam line produced first light at the end of April 2022 and commenced serving regular user experiments in early May.

DESIGN

Undulator

Driven by user request for more power in the 2000 – 3000 wavenumber range (i.e. 3 – 5 μm), we decided to upgrade the FEL2 undulator. With the estimated parameters (Table 1) for our accelerator, we did calculations with software constructed on Benson's version [1] of FEL CAD [2] to determine appropriate undulator parameters.

Table 1: FELIX FEL-2 accelerator parameters

Parameter	Value
Beam energy	25 – 50 MeV
Pulse length	0.7 ps
Energy spread	0.3%
Emittance	50 mm mrad
Bunch charge	200 pC

Table 2: U40 undulator parameters

Parameter	Value
Type	Planar hybrid, NdFeB
Period	40 mm
# of periods	50
Length	2 m
K_{RMS}	0.5 – 1.6

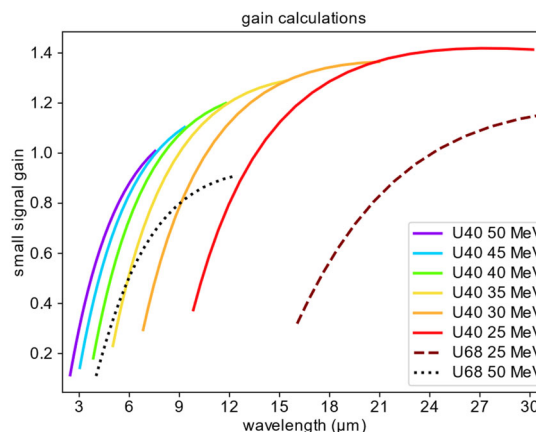


Figure 1: gain calculations for the proposed 40 mm undulator for FEL-2 showing that the 3 – 30 μm region is well covered (solid lines), offer more gain in the 3 – 5 μm region than the 68 mm undulator (dotted line), and maintain good overlap with the highest energy of FEL-1 (dashed line).

As it turns out, the best results (Table 2) were obtained using a 40 mm undulator (Fig. 1) similar to that of the FHI FEL [3], and this design was therefore accepted with slight modifications.

Resonator

A new resonator (Table 3) was built around the new undulator. Since optical cavity stability is more critical at lower wavelengths, particular care was taken to isolate the cavity mirrors from vibrations in the laboratory by mounting them on heavy blocks of granite (Fig. 2).

Table 3: Resonator parameters

Parameter	Value
Type	near-concentric
Frequency	25 MHz
Length	5.9993 m
Rayleigh range	0.85 m
Outcoupling hole	0.9, 1.2, 1.6, 2.1, 2.8, 3.7 mm

[†] victor.claessen@ru.nl

LASING PERFORMANCE OF THE EUROPEAN XFEL*

W. Decking[†], M. Scholz, Deutsches Elektronen-Synchrotron, Hamburg, Germany

Abstract

The European XFEL operates with 3 different SASE FELs served by variable gap undulators. In addition, the electron energy of the superconducting linear accelerator is varied between 8.0 and 17.5 GeV to cover a photon energy range from 250 eV to 30 keV. We will present SASE performance data collected over the past 5 years of operation and compare them with theoretical predictions.

INTRODUCTION

The European XFEL is in operation since 2017 [1]. With its powerful superconducting accelerator, a flexible beam distribution system and three long, moveable gap, undulators it can provide a wide range of X-ray radiation spanning two orders of magnitude from 250 eV to 30 keV. In this paper we will focus on the peak and average performance of the FELs operated in standard self-amplified spontaneous emission (SASE) mode. Other operation modes like Hard X-ray Self-Seeding are implemented but will not be considered here.

The superconducting accelerator can accelerate up to 27000 bunches/second to an energy of 17.5 GeV. It is operated in burst mode, i.e. with a 10 Hz repetition of a 600 μ s long RF pulse that accommodates electron bunches with a repetition rate of up to 4.5 MHz. bunches are produced in a radio-frequency photo-injector at charges between 20 pC to 1 nC. Operating ranges of the accelerator and undulator parameters are summarized in Table 1.

Table 1: Accelerator and undulator parameters

	Range	Typical
Energy - GeV	8 – 17.5	14
# of bunches/s	10 – 27000	13500
Bunch charge pC	20 – 1000	250
	SASE1/2	SASE3
K Parameter	3.9 – 1.65	9.0 – 4.08
Number of 5 m cells	35	21

Bunches are distributed with a fast kicker system into two electron beamlines, where one is presently hosting the hard X-ray undulator SASE2, while the other passes the beam through the hard X-ray undulator SASE1 first, before entering the soft X-ray undulator SASE3. The fast kicker system can also discriminate between SASE1/SASE3 bunches by applying a bunch specific betatron oscillation, thus suppressing lasing in either of the two undulators. The kicker system also allows to send individual bunches into a beam dump before the undulators, this gives the opportunity to vary the average X-ray power by up to 3 orders of magnitude (i.e. 1 to 1000 pulses per RF burst) on user demand.

* Work supported by European XFEL GmbH

[†] wimfried.decking@desy.de

MOP: Monday posters, Coffee & Exhibition

LASING PERFORMANCE DATA

In the following we will present an analysis of all FEL intensity data that has been collected over the last 5 years. Electron energies between 8.0 and 17.5 GeV are covered, with pre-dominant operation at 14 GeV (75 % of the time). Only data points at 250 pC bunch charge have been considered. The FEL intensity is measured with an X-ray gas monitor (XGM) [2] providing a data-point every 0.1 s. One should note that the XGM signal observed is an averaged signal with a sliding average of 30 s. The data is processed by binning the respective intensity values into 1 keV (Hard X-ray undulators), resp. 0.1 keV intervals, where the average is calculated after removing the lower 10% of the measurements (attributed to tuning or early operation), and the upper 1% (attributed to gain switching in the XGM, leading temporarily to too high values). In addition, the data is compared to the calculated maximum intensity at saturation for optimized electron energies [3].

A gain curve is measured by successively moving the 5 m long undulator segments (cells) out of resonance and monitoring the XGM signal. In addition, a fast and more sensitive, but uncalibrated, signal (“HAMP”) is used to obtain reliable data at low intensities. The calibration is obtained in intensity regimes where the XGM continues to measure reliably.

SASE1

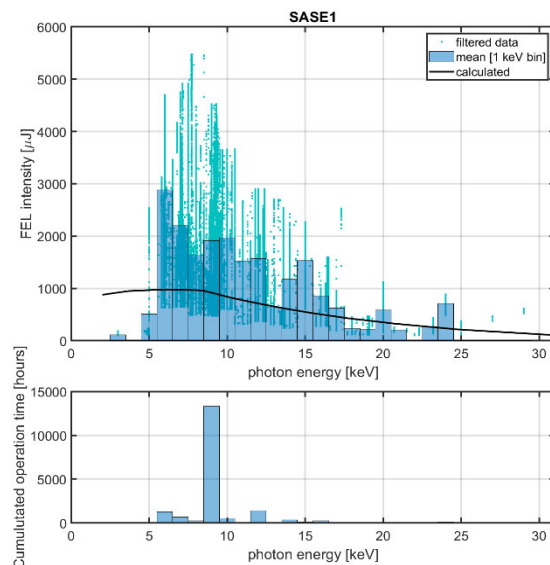


Figure 1: Upper plot: 5-year SASE intensities at SASE1 (cyan dots), and the average value in selected photon ranges (blue bars), compared to calculated intensities for optimized electron energies (black line). Lower plot: Cumulated operation hours within the respective photon energy range.

FLEXIBLE OPERATION MODES FOR EUXFEL

M. W. Guetg*, B. Beutner, J. Branlard, F. Brinker, W. Decking, I. Hartl, R. Kammering, D. Lipka, N. Lockmann, N. Mirian, E. Schneidmiller, H. Tünnemann, T. Wamsat, DESY, Hamburg, Germany
G. Geloni, N. Gerasimova, N. Kujala, S. Serkez, XFEL GmbH, Schenefeld, Germany

Abstract

A major challenge in single-linac-multiple undulator setups like EuXFEL is generating individually shaped photon pulses for each of the undulator lines, especially when working in an operation mode where a single pulse train, or cw stream, feeds all undulator lines. This work presents the experimental verification of a flexible delivery scheme feeding all three undulator lines of EuXFEL with electron bunches individually shaped in charge, compression and optics from a single RF pulse burst.

SETUP

European XFEL (EuXFEL) consists of a single linac which feeds three undulator lines. All undulator lines are fed in parallel, receiving electron pulses that originate from RF pulse trains with a repetition rate of 10 Hz. Each pulse train consists of up to 2700 pulses with a maximal repetition rate of 4.5 MHz. A beam distribution system with a fast and a slow kicker system distributes the pulses between the three undulator lines. The fast kicker system works on a bunch-to-bunch rate and is used to dump superfluous pulses as well as to create soft-kicked pulses for lasing suppression in the fresh-bunch [1, 2] setup. The slow kicker system is used to distribute the beam into one of the two undulator branches.

In most operation modes, the first part of each RF pulse train is used to stabilize the beam through transverse and longitudinal intra-train feedbacks and then dumped after the linac without passing any undulator lines and subsequently not producing any X-rays. The next part of the train is sent in bulk towards the first undulator line (Fig. 1, colored in purple). The following part is dumped again in order to provide a transition time (about 30 μ s) which is required to relax the slow kicker of the beam distribution system. The last part of the pulse train is used to deliver pulses to two undulator lines that follow one another (Fig. 1, colored in blue and green). Each of the three lines is operated exclusively by allowing the lasing only in one line while suppressing it in the other two. To maximize the available RF time for each experiment, the two serial undulators receive bunches in an interleaved mode. In summary, there are two undulator lines which receive beam in an interleaved mode with a maximum repetition rate of 4.5 MHz and one undulator line which is separated by about 30 μ s from the other lines. The repetition rate and number of pulses at each undulator line can be lowered by dumping individual pulses in the linac dump.

* marc.guetg@desy.de

METHODS

We investigated two options to shape the duration of pulses within a single pulse train, which is necessary to provide pulses of different durations for each of the undulator lines. The first option is to exploit the gun laser system, which consists of an acoustic-optical modulator (AOM) in front of the amplifier [3, 4]. This system is designed to keep the charge constant along the entire pulse train, however, this system is also able to create pulses of varying charge along the pulse train. The achievable charge profiles along the pulse train underlie only two limitations. First, the charge cannot be larger than what the laser pulse allows for an unattenuated pulse. Second, there have to be high charge pulses in regular intervals to prevent building up an inversion state in the laser gain medium. Since the AOM is able to react at a 4.5 MHz scale, this system is able to customize the bunch length for all three undulator lines even if the two serial undulator lines are operated in an interleaved mode.

The second option for longitudinal shaping along the pulse train is to use the RF system, which allows to modulate both amplitude and phase of wave in the cavity along the pulse train [5, 6], thereby effectively changing the energy chirp and thus compression of the beam. The maximal frequency of transitions between different states depends on the characteristics of the klystron as well as the quality factor of the super-conducting RF cavity and allows for different compression states for different sections of the pulse train, but not for the individual pulses of the train. Therefore, this option is only suitable when the undulator lines are operated in a non-interleaved mode.

These two options are not exclusive. Combining the two techniques allows to operate with lower charge while still correcting the compression setting individually for optimal performance of all undulator lines. Furthermore, there is the possibility to use multiple RF flat-tops in phase and amplitude in the gun to correct for the different space charge in the low energy regime and thus improve the optical mismatch by exposing the electron to a different electric field.

RESULTS

Reducing the charge is the most flexible way to reduce the pulse duration. It allows for nearly full flexibility of the pulse patterns within a pulse train. Unfortunately, changing the charge leads to different effective compression given similar RF settings, which in turn leads to a miscompressed beam as shown in Fig. 2. It is important to note that the increase in electron pulse duration does not necessarily transfer to the photon pulse, which could still be significantly shorter due

STATUS OF THE FREE-ELECTRON LASER USER FACILITY FLASH

K. Honkavaara*, C. Gerth, M. Kuhlmann, J. Roensch-Schulenburg,
L. Schaper, S. Schreiber, R. Treusch, M. Vogt, J. Zemella
Deutsches Elektronen-Synchrotron DESY, Hamburg, Germany †

Abstract

FLASH, the free-electron laser user facility at DESY, delivers XUV and soft X-ray radiation for photon experiments since 2005. It is driven by a superconducting linear accelerator, and has two undulator lines (FLASH1 and FLASH2). A third electron beam line hosts the plasma-wakefield experiment FLASHForward. Presently, the FLASH facility is undergoing an extensive refurbishment and a substantial upgrade (FLASH2020+). In this paper we summarize the FLASH operation in 2019-2021, and report on the main upgrades realized in a shutdown from November 2021 to August 2022.

INTRODUCTION

FLASH [1–5] at DESY (Hamburg, Germany) is a XUV and soft x-ray FEL user facility. It originates from the TESLA Test Facility (TTF) Linac [6], which was constructed at DESY in mid 1990's to test the feasibility of high gradient superconducting accelerator technology. The present FLASH facility (originally called “VUV-FEL at TTF2”) was constructed in 2003-2004. User operation started in summer 2005, and since summer 2014 two undulator lines (FLASH1 and FLASH2) are operated in parallel. FLASH2 user operation started in April 2016.

In order to keep FLASH a state-of-the-art FEL user facility, refurbishments and upgrades are on-going within the framework of the FLASH2020+ project [7–9]. The main goals are to establish a high repetition rate seeding (up to 1 MHz) at FLASH1, and to extend the wavelength range at FLASH2 down to the oxygen K-edge (2.3 nm). Installation of an APPLE III undulator as a third-harmonic afterburner at FLASH2 will enable FEL radiation with variable, in particular circular polarisation, well suited for magnetic studies, e.g. at the L-edges of Fe, Co and Ni.

The first upgrade shutdown started in November 2021 with the goal to increase the electron beam energy to 1.35 GeV. High repetition rate seeding is planned to be installed in 2024/25.

This paper reports on the status of the FLASH facility and its operation in 2019-2021, and summarizes the main installations during the 2021/22 shutdown. Part of this material has been presented in previous conferences, most recently in [10, 11].

FLASH FACILITY

FLASH consists of a photoinjector, a superconducting linac, two undulator lines (FLASH1 and FLASH2), and two

experimental halls. A schematic layout of the facility as it was operated until November 2021 is shown in Fig. 1. In addition, FLASH hosts a seeding experiment Xseed [12], and a plasma-wakefield experiment FLASHForward [13].

The photoinjector, consisting of a normal conducting RF-gun with an exchangeable Cs₂Te photocathode, and three injector lasers, generates a high quality, bunched electron beam. The superconducting linac has seven TESLA type 1.3 GHz accelerator modules with eight 9-cell Niobium cavities each. The maximum electron beam energy, before the energy upgrade in 2022, was 1.25 GeV. A third harmonic (3.9 GHz) module, to linearize the longitudinal phase space, is installed downstream of the first accelerator module. Two magnetic chicane bunch compressors (C-shape and S-shape) are used to compress the electron bunches to the peak currents required for the lasing process. FLASH2 has an additional bunch compressor downstream of the extraction beamline.

Superconducting RF cavities allow operation with long RF-pulses (up to 800 μ s), and thus with long electron bunch trains. The number of electron bunches (1 to 500 in user operation), and their spacing within the bunch train, is variable, e.g. 500 bunches with 1 μ s (1 MHz) spacing, or 50 bunches with 10 μ s (100 kHz) spacing. The bunch train is shared between FLASH1 and FLASH2, which are operated simultaneously [14], both with the full 10 Hz bunch train repetition rate. The switching between FLASH1 and FLASH2 within the bunch train is realized by a kicker-septum system downstream of the last accelerator module. FLASH2 and FLASHForward electron beam lines are separated from each other in the end of the extraction line by a DC-dipole, and thus only one of them can be operated at a given time.

FEL radiation is produced using the SASE (Self Amplified Spontaneous Emission) process. FLASH1 has six 4.5 m long fixed gap (12 mm) undulator modules, FLASH2 twelve 2.5 m long variable gap (minimum 9 mm) undulators. FLASH1 photon wavelength range in the fundamental is from 4.2 nm to slightly above 50 nm. In addition, FLASH1 has a planar electromagnetic undulator downstream of the SASE undulators, and can deliver, on request, also tunable THz radiation (1-300 THz) [15]. FLASH2 provides FEL radiation at wavelengths between 4 nm and 90 nm (fundamental). Thanks to variable gap undulators, fast automated wavelength scans are possible at FLASH2.

Both FLASH1 and FLASH2 have an own transverse deflecting RF structure (TDS) for longitudinal electron bunch diagnostics. FLASH1 has an S-band TDS (“LOLA”) [16] located upstream of the SASE undulators, and FLASH2 has, downstream of its undulators, two variable polarization X-band structures (“PolariX”) [17].

* katja.honkavaara@desy.de

† for the FLASH team

CORRUGATED STRUCTURE SYSTEM FOR FRESH-SLICE APPLICATIONS AT THE EUROPEAN XFEL

W. Qin*, M. Guetg, W. Decking, N. Golubeva, J. Guo†, S. Liu, T. Wohlenberg, I. Zagorodnov
Deutsches Elektronen-Synchrotron, Hamburg, Germany
E. Gjonaj, Technische Universität Darmstadt, Darmstadt, Germany

Abstract

Fresh-slice lasing using wakefield induced time-dependent orbit oscillation is capable of producing high intensity two-color XFEL pulses and high power short pulses at femtosecond level. At the European XFEL, a corrugated structure system for fresh-slice applications for both the hard x-ray beamline SASE1 and the soft x-ray SASE3 beamline is being developed and implemented. In this contribution, we present the novel design of the corrugated structure system.

INTRODUCTION

X-ray free-electron lasers (XFELs) [1–5] have been significant over the past decade in a broad range of scientific experiments by providing the brightest x-ray pulses. Utilizing various methods, from injector laser shaping to special accelerator and undulator configuration, the XFEL pulses are highly customizable in time and frequency domain. Fresh-slice techniques, which selectively suppress or enable the FEL lasing in localized slices of the electron bunch in different undulator sections, have been very successful in providing tailored x-ray pulses with high efficiency. Many fresh-slice schemes [6–9] employ a parallel-plate corrugated structure [10, 11] to produce transverse to longitudinal correlation from the dipole wakefield of the structure. Meanwhile, non-zero quadrupole wakefield of such structures can cause slice-dependent mismatch [12, 13] and sometimes hinder the advanced applications. The quadrupole effect is usually compensated by orthogonally placed modules or minimized by using small incoming electron bunch sizes.

As the first high-repetition-rate XFEL facility, the European XFEL [4] has seen significant progress in advanced lasing scheme development since operational in 2017. The European XFEL consists of three undulator lines: the hard x-ray lines SASE1 and SASE2 and the soft x-ray line SASE3. The electron bunches are distributed via long pulse KL kicker [14] to the south branch (SASE2) or the north branch (SASE1/3). The SASE3 undulator line is located after the SASE1 undulators, and hence shares the same electron beam path with SASE1. Parallel operation of SASE1 and SASE3 [15–17] is enabled by using bunch-by-bunch KS fast kickers [18] to steer the SASE3 bunches such that they present large orbit oscillation in SASE1 undulators and remain fresh for lasing in SASE3 undulators.

The common beam path shared by SASE1 and SASE3 makes it possible to setup wakefield-based fresh-slice appli-

cations for two beamlines with only one corrugated structure. Meanwhile, it also places challenges to the design of the corrugated structure system since it is preferable to operate SASE1 and SASE3 in parallel, i.e., having only one of the two beamlines operate in fresh-slice mode while the other beamline operate in standard mode. Besides, the system has to accommodate the megahertz repetition rate of electron bunches with a distance much below 1 mm between the electron bunches and the corrugated structure.

In this paper, we present the design of the corrugated structure system for fresh-slice applications at the European XFEL. The corrugated structure is located after the SASE2 bunch extraction area and before the SASE1 undulator. Special optics has been designed to allow small distance between the electron bunches and the corrugated structure. Long pulse kickers combined with correctors are designed to separate the SASE1 and SASE3 bunches in the corrugated structure area. Furthermore, a novel L-shape configuration of the corrugated structure has been designed to compensate the quadrupole component of the wakefield. This paper is arranged as the following. We first introduce the special optics and bump orbit design. Then we show the wakefield of the L-shaped corrugated structure. In the last section we present our discussions and conclusion.

OPTICS AND ORBITS

The existing optics before the SASE1 undulator line is a FODO transport line followed by a matching section. The average beta function is about 30 m with peak up to about 50 m. The existing optics is challenging for the corrugated structure operation in two aspects. First, the large beta function makes the time-dependent focusing effect caused by the quadrupole wakefield component significant. Second, a large beta function corresponds to large beam halo extension and can cause significant particle loss in the corrugated structure and further deposit large amount of radiation dose in the undulators, especially when it is operated at a megahertz repetition rate [19].

A special optics with low beta function in both x and y directions around the corrugated structure area has been designed. Two new quadrupoles are inserted in the beamline to help create the low beta region as well as match back to the designed undulator optics. The special optics maintains the possibility to switch back to nominal optics. The created low beta region, as shown in Fig. 1(a), has a beta function of about 9 m to 12 m in both x and y planes over 6-meter-long corrugated structure area (indicated as red rectangle in Fig. 1(b)). The low beta optics reduces the electron beam

* weilun.qin@desy.de

† Currently at Zhangjiang Laboratory, Shanghai, China

AN ATTOSECOND SCHEME OVERCOMING COHERENCE TIME BARRIER IN SASE FELs

E.A. Schneidmiller*, Deutsches Elektronen-Synchrotron DESY, Hamburg, Germany

Abstract

In Self-Amplified Spontaneous Emission Free Electron Laser (SASE FEL) based short-pulse schemes, pulse duration is limited by FEL coherence time. For hard X-ray FELs, coherence time is in a few hundred attosecond range while for XUV and soft X-ray FELs it is in the femtosecond regime. In this paper the modification of so-called chirp-taper scheme is developed that allows to overcome the coherence time barrier. Numerical simulations for XUV and soft X-ray FEL user facility FLASH demonstrate that one can generate a few hundred attosecond long pulses in the wavelength range 2 - 10 nm with peak power reaching hundreds of megawatts.

INTRODUCTION

Attosecond science [1] is rapidly developing nowadays thanks to the laser-based techniques such as chirped-pulse amplification and high-harmonic generation. There are also different schemes proposed for generation of attosecond X-ray pulses in free electron lasers [2–9]. Many of these schemes make use of a few-cycle intense laser pulse to modulate electron energy in a short undulator, and then to make only a short slice (a fraction of wavelength) efficiently lase in a SASE undulator. In particular, in the chirp-taper scheme [7], a slice with the strongest energy chirp is selected for lasing by application of a strong reverse undulator taper that compensates FEL gain degradation within that slice. The lasing in the rest of the bunch is strongly suppressed due to uncompensated reverse taper.

Creation of a short lasing slice can also be done without using a laser. In particular, nonlinear compression of multi-GeV electron beams [10] and self-modulation in a wiggler of a bunch with the special temporal shape [11] allowed to generate a few hundred attosecond long pulses at the Linac Coherent Light Source (LCLS). However, creation of sub-femtosecond features in the electron bunch at lower electron energies (≈ 1 GeV) is problematic.

Typically, pulse duration in SASE-based short-pulse schemes is limited by FEL coherence time [12]. For hard X-ray FELs, coherence time is usually in a few hundred attosecond range. For such a case an adequate choice of a laser could be a Ti:Sapphire system providing a few mJ within 5 fs (FWHM) with the central wavelength at 800 nm. However, for XUV and soft X-ray regimes the coherence time is in femtosecond range, and a longer wavelength laser is needed [13] to match a lasing slice duration and coherence time. In this contribution a simple method, proposed in [14], is described.

* evgeny.schneidmiller@desy.de

PRINCIPLES OF OPERATION

Conceptual representation of the attosecond scheme is shown in Fig. 1. Few-cycle laser pulse is used to modulate a central part of an electron bunch in energy in a short (typically, two-period) modulator undulator. The wavelength λ_L is chosen such that the lasing slice is much shorter than FEL coherence length. In particular, for generation of attosecond pulses in XUV and soft X-ray regime one can consider Ti:sapphire laser. A typical shape of energy modulation after the modulator undulator is shown in Fig. 2.

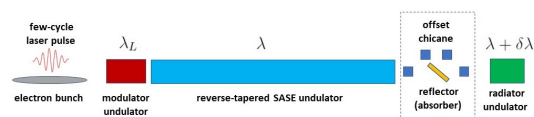


Figure 1: Conceptual scheme for generation of attosecond pulses. Dashed rectangle illustrates a particular realization of suppression (separation) of a radiation background from the SASE undulator.

Then the bunch enters a long SASE undulator tuned to a wavelength λ . The undulator is operated in the same way as in the classical chirp-taper scheme [7]: it is reverse-tapered to compensate for the energy chirp within the central slice (positioned at $t = 0$ in Fig. 2). In this way the FEL gain degradation within this slice is avoided, and the amplification proceeds up to the onset of saturation. The rest of the bunch suffers from the uncompensated reverse taper, and the lasing is strongly suppressed (except maybe for two satellites positioned around $t = \pm 2.7$ fs on Fig. 2 with the negative time derivative). The difference with the standard scheme is that now the central lasing slice is much shorter than FEL coherence time. The distribution of bunching (density modulation amplitude) is rather narrow and is localized at the end of that slice but the radiation slips forward, and a relatively long pulse (on the order of coherence time) is produced. The next task is to get rid of this relatively long radiation pulse (as well as of the background radiation from the rest of the bunch) while preserving the bunching. This can be done in different ways. In Fig. 1 a possible realization is illustrated: an offset chicane with a reflector or absorber inside. Alternative options are discussed below in this Section: excessive reverse taper, an achromatic bend, a kick with a quadrupole, a dogleg, and a harmonic afterburner.

Finally, the microbunched beam radiates in a short radiator undulator. The bunching is strong in the central slice, it is weaker in the two satellites around $t = \pm 2.7$ fs, and much weaker in the rest of the bunch. Note that reverse tapering is

SASE OPTIMIZATION APPROACHES AT FLASH

J. Roensch-Schulenburg*, M. Czwalinna, K. Honkavaara, A. Eislage, V. Kocharyan,
M. Kuhlmann, S. Schreiber, R. Treusch, M. Vogt, J. Zemella
Deutsches Elektronen-Synchrotron DESY, Hamburg, Germany

Abstract

The free-electron laser FLASH at DESY can produce SASE-FEL pulses from the extreme ultraviolet to the soft X-ray regime. A superconducting linear accelerator drives two undulator lines (FLASH1 and FLASH2). The FLASH1 undulator beam line contains six fixed gap undulator which implies that the SASE wavelength can only be changed via the electron beam energy, while FLASH2 contains twelve variable gap undulators. Preparing different charges and compression schemes in the two parts of the bunch trains for the two undulator beamlines allows to adjust the phase space in wide range and meet the various requirements of photon pulse trains properties. In order to improve the SASE performance, reference files for standard energies and standard charges are regularly prepared. In the FLASH2 undulator beamline beam-based alignment and phase shifter scans have been applied to improve SASE operations and FEL beam quality. Improving set-up and tuning procedures allow to decrease setup times and optimize performance and stability. Procedures and optimization of FEL parameters towards a reliable SASE-FEL operation as well as the achieved results are discussed.

INTRODUCTION

FLASH [1–5] at DESY (Hamburg, Germany) is a free-electron laser (FEL), operated as a user facility since summer 2005. FLASH contains a normal conducting RF photo-injector with Cs₂Te-cathode and a superconducting linac which allows the acceleration of long bunch trains with several thousand electron bunches per second in 10 Hz bursts of up to 800 μs length. Downstream of the first accelerator module a third harmonic module is installed, to linearize the longitudinal phase space distribution of the bunch, followed by bunch compressor at a beam energy of 150 MeV. Another bunch compressor is installed after the third accelerator module, where the beam has reached an energy of 450 MeV.

The bunch trains are divided into two parts generated by two independent photo-injector lasers with selectable charge. A kicker-septum combination after the seventh accelerator module allows to split the bunch trains and serve two beamlines in parallel. The RF properties of the two beamlines can be chosen independently within a certain range allowing to adjust the phase space properties of the bunches. In standard operation the two beamlines are the undulator beamlines FLASH1 and FLASH2. FLASH2 beam can be diverted towards the plasma wakefield acceleration

experiment FLASHForward in the FLASH3 beamline [6] by means of a DC dipole.

The FLASH1 beamline contains a seeding experiment Xseed [7], followed by a transverse deflecting structure (LOLA) [8] for longitudinal diagnostics. The SASE (Self Amplified Spontaneous Emission) undulator consists of six 4.5 m long fixed gap undulators. The fundamental wavelength of the FEL radiation based on the SASE ranges from 4.2 nm to about 50 nm.

The upgrade project "FLASH2020+" [9, 10] includes an energy upgrade from 1250 MeV to 1350 MeV which extends the wavelength range deeper into the water window and a seeding concept at FLASH1 using variable gap undulators.

The FLASH2 beamline contains an additional bunch compressor to further increase the flexibility of the compression. The undulator beamline in FLASH2 contains twelve 2.5 m long variable gap undulator segments. The tunable gap allows to control the undulator parameter K and thus the lasing wavelength in a certain range, depending on the electron beam energy. Behind these undulators a novel Apple-III type undulator will be installed next year as an afterburner which will cover the L-edge of the magnetic 3d metals (at about 1.8 to 1.4 nm) with variable polarization in the third harmonic of the FEL radiation. FLASH2 was equipped recently with a transverse deflecting structure (PolariX) [11, 12].

REFERENCE FILES

Since the FLASH1 undulators are fixed gap undulators employing each wavelength change in FLASH1 goes along with an energy change and thus a new setup of the linac and a new setup in beamline FLASH2. Smaller energy changes can be reached by scaling the magnet currents with the beam energy, but larger changes require a change in the optics. In order to improve the SASE performance and reduce the setup times, reference files for the standard energies 450 MeV, 750 MeV, and 1100 MeV are regularly prepared. The setup is done close to the theoretical energy profile. The goal is to prepare three reproducible, well-documented starting points (reference files) from which a non-expert can reach all standard machine states with a decent SASE pulse energy and long bunch trains with at most moderate beam losses, essentially by scaling the magnet currents. For the 450 MeV-reference file all accelerating modules after the second bunch compressor (ACC4,5,6 and 7) are set to zero voltage. For the 750 MeV-reference file only the last two accelerating modules (ACC6 and 7) are set to zero. In the 1100 MeV-reference file all accelerating modules are used at a high gradient, but not the maximum gradient.

Table 1 indicates the energy/wavelength ranges in which the reference files are applied. Beam energies smaller than

* juliane.roensch@desy.de

A COMBINATION OF HARMONIC LASING SELF-SEEDED FEL WITH TWO-COLOR LASING

J. Rönsch-Schulenburg*, M. Kuhlmann, E. Schneidmiller, S. Schreiber, M. Vogt
Deutsches Elektronen-Synchrotron DESY, Hamburg, Germany

Abstract

The free-electron laser FLASH at DESY can produce SASE-FEL pulses in the extreme ultraviolet to the soft X-ray region. The flexibility of the variable gap undulators in the FLASH2 beamline opens a wide range of scientific opportunities. Different advanced lasing schemes have been tested in the past years, like the "frequency doubler" scheme, "two-color lasing", and "harmonic lasing self-seeded FEL" (HLSS). A recent user experiment required parameters not yet provided: a similar power in the fundamental and the third harmonic. To fulfill these requirements, a new way of lasing had to be developed ad hoc. A combination of HLSS and two-color lasing has been identified as the appropriated scheme to deliver a tailored two-color beam to the user experiment. In this article we describe difficulties of the setup and discuss the results achieved.

INTRODUCTION

FLASH [1–5] at DESY (Hamburg, Germany) is a free-electron laser (FEL) user facility. FLASH has been operated as an FEL user facility since summer 2005. FLASH's superconducting linac allows the acceleration of long bunch trains with several thousand electron bunches per second in 10 Hz bursts of up to 800 μ s length. The bunch trains are divided into two parts with, in a certain range, independent RF-properties. A kicker-septum-based beam-switchyard allows to serve two beamlines in parallel. FLASH consists of two undulator beamlines (FLASH1 and FLASH2) and a plasma wakefield acceleration experiment FLASHForward (FLASH3) [6]. In FLASH1 the generation of FEL radiation based on the SASE (Self Amplified Spontaneous Emission) process is defined by the electron beam energy, due to fixed gap undulators. The fundamental FLASH1 wavelength provided for user experiments ranges from 4.2 nm to about 50 nm. In addition, FLASH1 hosts a seeding experiment Xseed [7]. In order to continue the operation of FLASH as a state-of-the-art FEL user facility, a substantial upgrade and refurbishment project, "FLASH2020+" was initiated. It includes seeding at FLASH1 using variable gap undulators [8]. The undulator beamline in FLASH2 contains twelve variable gap undulator segments. The tunable gap allows to control the undulator parameter K and thus the lasing wavelength in a certain range, depending on the electron beam energy. These variable gap undulators allow to implement novel techniques for radiation generation in addition to the standard SASE FEL operation at varying wavelength, ranging from 4 nm to about 90 nm.

60% of the available operation time is dedicated to user experiments. Every experiment has its own requirements of photon pulse properties and demands on quality and stability. We optimize each individual setup in order to fulfill all the requested parameters of the experiments.

TWO COLOR LASING AT FLASH

Employing novel lasing schemes potentially allows to significantly optimize the radiation properties, like increasing of the FEL pulse energy, improvement of the longitudinal coherence, control of polarization, extension of the wavelength range and multi-color mode of operation. Different innovative FEL developments have been realized at FLASH2. Using "Post-saturation undulator tapering" an increase of the radiation pulse energies above 1 mJ has been established [9, 10] and also high contrast of the afterburner radiation with reverse undulator tapering scheme has been demonstrated [11, 12].

The frequency doubler scheme [13] allows the operation in a two-color mode (with double frequency) and operation at shorter wavelengths with respect to the standard SASE scheme. At FLASH2 operating in the water window has been demonstrated with a wavelength of 3.1 nm.

Applying Harmonic Lasing Self Seeded FEL (HLSS) [14, 15] a significant increase in spectral brightness has been achieved and the coherence time has been increased noticeable. The HLSS scheme starts with harmonic lasing in the linear regime in the first part of the undulator. In the second part of undulator the K is reduced such that the harmonic becomes the fundamental and the harmonic output serves as "seed" which reduces the gain length and increases the FEL pulse energy. The graph in the middle of Fig.1 describes schematically the undulator setting for the HLSS.

Two-color lasing [16] can be set up in different configurations, but at FLASH2 a scheme based on alternating undulator tunes was found to be beneficial. The graph on top in Fig.1 shows a schematic of the setup for two-colors lasing based on alternating tunes. All odd undulator segments are tuned to the wavelength λ_1 and all even segments to λ_2 . The amplification in the FEL process of the electromagnetic wave with the wavelength λ_1 is disrupted as soon as the electron bunch leaves a segment tuned to the wavelength λ_1 and enters a segment tuned to λ_2 . However, energy modulations in the electron bunch, continue to get transformed into density modulations. Due to its longitudinal dispersion, the additional bunching in the λ_2 undulator segment quickly radiates a stronger field than the one coming from the previous λ_1 segment, which is diffracted in addition, and the FEL process continues with higher amplitudes. Thus, in

* juliane.roensch@desy.de

SASE-FEL STOCHASTIC SPECTROSCOPY INVESTIGATION ON XUV ABSORPTION AND EMISSION DYNAMICS IN SILICON

D. De Angelis[†], E. Principi, D. Fausti¹, L. Foglia, R. Mincigrucci, E. Pedersoli, J. S. Pelli Cresi, K. J. Prince, F. Capotondi, Elettra-Sincrotrone Trieste, Trieste, Italy
 E. Razzoli, C. Svetina, Paul Scherrer Institut, Villigen, Switzerland
 Y. Klein, S. Schwartz, Physics Department and Institute of Nanotechnology and advanced Materials, Bar Ilan University, Ramat Gan, Israel
 I. A. Vartaniants, Deutsches Elektronen-Synchrotron DESY, Hamburg, Germany
¹also at Department of Physics, Università degli Studi di Trieste, Trieste, Italy

Abstract

Time-resolved high-resolution emission/absorption spectroscopy appears to be strategic in fundamental matter physics investigation as well as in functional materials characterization. For example, chemical activity can be investigated on the basis of absorption edge spectroscopy, magnetic spin status can be probed via resonant dichroic effects by means of Faraday (in transmission) or Kerr (in reflection) effects, molecular chirality can be resolved with high accuracy using combining photons with variable energy and polarizations. Typically, all such applications of high-resolution time resolved absorption spectroscopy require a pulsed radiation source and narrow bandwidth emission line, along with a large data statistic to resolve level the characteristic signal from the sample above the instrumental noise. In this work we will demonstrate a novel experimental approach, originally demonstrated in hard X-ray regime, aimed to retrieve high resolution absorption and emission spectra with sub-picosecond time resolution, by exploiting the stochastic nature of the wide-band self-amplified spontaneous emission (SASE) FEL radiation provided tuning FERMI in optical klystron mode. We got advantage of the two spectrometers available at the TIMEX beamline to reconstruct a 2D emission/absorption spectrum map of a Si crystalline thin film sample. To do so, we applied the singular value decomposition approach on a large ensemble of incoming and outgoing single-pulse spectra; by applying Tikhonov regularization, we were able to obtain absorption spectra with an energy resolution of few tens of meV (comparable to the maxima resolution of the used spectrometer). Moreover, emission lines due to spontaneous emission of the electron de-excitation are clearly resolved after the inversion of the ensemble of spectra fluctuation before and after the sample. Finally, by using this stochastic approach correlating the spectral fluctuation of the source to sample response, we performed a time resolved characterization of the Si L_{23} -edge and Si emission line at 99.3 eV, by pumping the Si sample with the visible laser (390 nm) below damage threshold (i.e. deposit on the sample surface about 20 mJ/cm²). Using this approach, we were able to combine time resolved XAS and XES spectra, and we ascribed the observed dynamics to a

consequence of the bond softening phenomenon occurring in our sample after the visible light excitation.

INTRODUCTION

In the last decades, the introduction of soft X-ray radiation from synchrotron sources gave an impressive boost to the study of the electronic and structural properties of condensed matter. Their high brilliance, together with their high energy resolution, allow nowadays to spectroscopically characterize samples with high chemical and structural sensitivity. For this reason, synchrotron spectroscopy is extensively used in an increasingly large ensemble of scientific field. Soft X-ray emission/absorption spectroscopy with high-resolution (tens of meV) and picosecond time resolution appears to be strategic in fundamental matter physics investigation as well as in functional materials characterization. FELs have been considered as extremely powerful tools for their capability of delivering high brilliance and high coherent radiation. Such characteristics boosted the research on nonlinear photonics, condensed matter physics in extreme pressure and temperature condition, diffraction and projection imaging. Free-electron laser appeared as a steppingstone to the investigation of the femto- and picosecond timescale dynamics in condensed matter systems. Indeed, nowadays a pump probe scheme is typically implemented in the experimental scheme in order to bring the sample in the excited state to measure its dynamics with the short FEL pulses. Such a measurement approach appears to be of large interest in the context of chemical reaction, structural, electronic and magnetic dynamics and it is widely employed also at FERMI, using the FEL radiation as probe or pump, together with a UV-Vis-IR laser. Recently, also the possibility to have a FEL-FEL pump-probe scheme at FERMI has been introduced with the commissioning of the AC-DC delay line [1]. It is clearly of great interest to introduce spectroscopic techniques in the FEL framework, taking advantage from its peak high brilliance and, in case of seeded FEL, its high energy resolution. Nevertheless, there were some issues, up to now, preventing the efficient implementation of high-performance spectroscopic techniques in combination with FEL strong points.

* Work supported by Elettra-Sincrotrone Trieste

[†] dario.deangelis@elettra.eu

FEL PERFORMANCE OF THE EuPRAXIA@SPARC_LAB AQUA BEAMLINE

F. Nguyen*, A. Petralia, A. Selce, ENEA–Frascati, Frascati, Italy
C. Boffo, Fermilab, Batavia IL, USA

M. Castellano, M. Del Franco, Z. Ebrahimpour, M. Ferrario, A. Ghigo, L. Giannessi,
A. Giribono, A. Marcelli, C. Vaccarezza, F. Villa, INFN–LNF, Frascati, Italy
A. Cianchi, F. Stellato, University of Tor Vergata and INFN–Roma Tor Vergata, Rome, Italy
M. Coreno¹, CNR–ISM and Elettra, Trieste, Italy
P. Iovine, University La Sapienza, Rome and INFN–Napoli, Naples, Italy
N. Mirian, DESY, Hamburg, Germany
M. Opromolla, V. Pettrillo, University of Milan and INFN–Milano, Milan, Italy
¹ also at INFN–LNF, Frascati, Italy

Abstract

The AQUA beamline of the EuPRAXIA@SPARC_LAB infrastructure consists of a Free-Electron Laser facility driven by an electron beam with 1 GeV energy, produced by an X-band normal conducting LINAC followed by a plasma wakefield acceleration stage, with the goal to deliver variable polarization photons in the 3-4 nm wavelength range. Two undulator options are considered for the AQUA FEL amplifier, a 16 mm period length superconducting undulator and an APPLE-X variable polarization permanent magnet undulator with 18 mm period length. The amplifier is composed by an array of ten undulator sections 2m each. Performance associated to the electron beam parameters and to the undulator technology is investigated and discussed.

INTRODUCTION

The EuPRAXIA project is expected to realize and demonstrate use of plasma accelerators delivering high brightness beams up to 1-5 GeV for users [1]. During the first phase, the Free-Electron Laser (FEL) facility EuPRAXIA@SPARC_LAB will be constructed at the INFN-LNF laboratory [2]. This will be driven by the beam accelerated to 1 GeV energy within the plasma wakefield accelerator (PWFA) scheme, where a properly tailored electron bunch is injected into the plasma wave [3].

The AQUA¹ FEL beamline of the project will be operated in Self-Amplified Stimulated Emission (SASE) mode with 3-4 nm target wavelength, *i.e.* 310-410 eV photon energy, where water is almost transparent to radiation, while nitrogen and carbon are absorbing and scattering. This range belongs to the so called *water window*, where for instance 3D images of biological samples can be obtained processing several X-ray patterns by means of coherent diffraction imaging experiments: an ideal technique that could allow to reconstruct images of viruses or cells in their native environment [4].

CHOICE OF THE UNDULATORS

Table 1 shows the electron beam values expected and assumed for the undulators assessment and for evaluating the AQUA FEL performance. The Linac driving the AQUA

Table 1: Electron Beam Parameters

Quantity	Value
Charge Q	30 pC
Energy E_{beam}	1 GeV
Peak current I_{peak}	1.8 kA
RMS bunch length σ_z	2 μm
Proj. normalized x, y emittance ε_n	1.7 mm mrad
Slice normalized x, y emittance ε_n	0.8 mm mrad
Proj. fractional energy spread $\sigma_{\delta,p}$	0.95 %
Slice fractional energy spread $\sigma_{\delta,s}$	0.05 %

FEL includes two pairs of eight X-band accelerating cavities, separated by a magnetic bunch compressor and followed by the PWFA module. The final design of the layout is still in progress, with the following main features:

- peak current from the S-band photoinjector;
- slice energy spread goal of 0.05 % or lower;
- energy spread and transverse quantities under control operating at 0.85 GeV/m accelerating gradient.

In addition to the coherent imaging opportunities mentioned before, the chance to have variable and selectable X-rays allows to study [5] chemical properties of materials by means of switchable FEL polarization. Thus, the main requests to the undulator configuration are the following:

- deflection strength $K \approx 1$ at resonant $\lambda \approx 3\text{-}4\text{ nm}$;
- selectable linear and circular polarization;
- some contingency in the total active length;
- some flexibility in the wavelength tuning range.

Figure 1 shows the FEL saturation length as a function of undulator period and resonant wavelength, evaluated with

* federico.nguyen@enea.it

¹ Water in Latin.

SIMULATION STUDIES OF SUPERCONDUCTING AFTERBURNER OPERATION AT SASE2 BEAMLINE OF EUROPEAN XFEL

C. Lechner*, S. Casalbuoni, G. Geloni, B. Marchetti,
S. Serkez, H. Sinn, European XFEL, Schenefeld, Germany
E. Schneidmiller, DESY, Hamburg, Germany

Abstract

European XFEL is a multi-beamline x-ray free-electron laser (FEL) user facility driven by a superconducting accelerator with a nominal photon energy range from 250 eV to 25 keV. An afterburner undulator based on superconducting undulator technology is currently being planned to enable extension of the photon energy range towards harder x-rays. This afterburner undulator would be installed downstream of the already operating SASE2 FEL beamline, emitting at the fundamental or at a harmonic of the upstream SASE2 undulator. In this contribution we present a first simulation study of the impact of undulator mechanical tolerances for operation of the afterburner undulator at the fundamental of SASE2.

INTRODUCTION

European XFEL plans to develop superconducting undulator (SCU) technology as part of its facility development program. Combining the high electron beam energies available at European XFEL [1] with short-period SCUs allows for the generation of harder x-rays. At the exit of the already existing SASE2 hard X-ray permanent magnet undulator (PMU) beamline, the installation of six SCU modules, each housing two 2-meter-long superconducting undulator coils in a cryostat, is planned resulting in a total magnetic length of 24 m. In between the two 2-meter-long SCU coils there are two sets of superconducting Helmholtz coils to correct for the field integrals and a superconducting phase shifter. Between each module there is a room temperature intersection with a permanent magnet phase shifter, quadrupole and diagnostics, as in the PMU line. A detailed description of the European XFEL SCU afterburner project is given in Ref. [2].

In the SASE2 PMU beamline the high-brightness electron bunches arriving from the superconducting linear accelerator of European XFEL drive the self-amplified spontaneous emission (SASE) FEL process [3–6]. During this exponential amplification process, longitudinal density and energy modulations at a period given by the fundamental light wavelength $\lambda_1 = \frac{\lambda_u}{2\gamma_0^2} (1 + K^2/2)$ are generated. Close to saturation, these microbunches can carry rich harmonic content (at even and odd harmonics), which is the result of non-linear harmonic generation (NHG) [3–5, 7, 8].

After undergoing pre-conditioning by the FEL process in the SASE2 PMU, the bunched electrons enter the SCU beamline. If the SCU is tuned to the same wavelength as

the PMU ($\lambda_{1,SCU} = \lambda_{1,PMU}$), the power growth continues in the SCU. The SCU can also be tuned to harmonic h of the PMU ($\lambda_{1,SCU} = \lambda_{1,PMU}/h$). In the case $h = 2$ that was studied in Ref. [9], the $h = 2$ bunching generated in the PMU drives coherent emission at the fundamental of the SCU. In Ref. [9], simulations of the photon performance of the SCU at photon energies between 30 keV and 60 keV (for operation of the SCU at $h = 1$ or $h = 2$) are described. The estimated number of photons per pulse is larger than $3 \cdot 10^9$ in 30 fs (at 60 keV) and exceeds the number of photons per pulse calculated in Ref. [2] for a $1 \times 1\text{-mm}^2$ pinhole at 30 m from typical short-period undulators at high energy diffraction limited storage rings by more than two orders of magnitude in pulses more than 5000 times shorter [2].

In this contribution, the impact of undulator tolerances on the photon output (at $h = 1$) is studied.

SIMULATIONS

The numerical simulations are based on the FEL simulation code “GENESIS 1.3”, version 2 [10] and on software built around functionality provided by the OCELOT software package [11, 12] to set up, control, and post-process the simulation runs. As the two undulator beamlines in the system under study have different undulator periods (SASE2: 40 mm, SCU: 18 mm), each undulator beamline requires a dedicated run of “GENESIS 1.3”. At the beginning of the first run, an ideal flat-top electron bunch distribution is generated with the initial slice parameters as compiled in Table 1. After tracking the electron bunch and light field along the SASE2 PMU, they are stored in files. For operation of the SCU at the identical wavelength as the SASE2 PMU ($h = 1$),

Table 1: Simulation parameters ($h = \lambda_{1,PMU}/\lambda_{1,SCU}$).

Parameter	Value
electron beam energy	16.5 GeV
initial energy spread	3 MeV
bunch peak current	5 kA
bunch length	1 μm
normalized emittance	0.4 mm mrad
$\langle\beta\rangle$	30 m
SCU operation at harmonic h	$h = 1$ or $h = 2$
undulator period of SCU	18 mm
maximum K parameter of SCU	3.06
total magnetic length of SCU system	24 m

* christoph.lechner@xfel.eu

PROPOSED FEL SCHEMES AND THEIR PERFORMANCE FOR THE SOFT X-RAY FREE ELECTRON LASER (SXL) AT THE MAX IV LABORATORY

F. Curbis*, W. Qin[†], M. Pop, S. Pirani

S. Werin Physics Department, Lund University, Lund, Sweden

J. Andersson, L. Isaksson, B. Kyle[‡], F. Lindau, E. Mansten, H. Tarawneh,
P. Fernandes Tavares, S. Thorin, A. Vorozhtsov, MAX IV laboratory, Lund, Sweden

P. Eng-Johnsson, Atomic Physics, Lund University, Lund, Sweden

V. Goryashko, P. Salen, FREIA Laboratory, Uppsala University, Uppsala, Sweden

A. Nilsson, M. Larsson, S. Bonetti, Stockholm University, Stockholm, Sweden

Jonas A. Sellberg, KTH Royal Institute of Technology, Stockholm, Sweden

Abstract

The existing MAX IV 3 GeV linac could drive, with minor improvements, a soft X-ray Free Electron Laser and the aim of the SXL project has been so far to deliver a conceptual design of such a facility in the 1–5 nm wavelength range. The project was initiated by a group of Swedish users of FEL radiation and the design work was supported by the Knut and Alice Wallenberg foundation and by several Swedish universities and organizations (Stockholm, Uppsala, KTH Royal Institute of Technology, Stockholm-Uppsala FEL center, MAX IV laboratory and Lund University). In this paper we will focus on the baseline FEL performance based on two different accelerator operation modes (medium and short pulses) and give some hints of future developments after the first phase of the project, such as two-pulses/two-colours and HB-SASE.

INTRODUCTION

The Science case for a Swedish Soft X-ray FEL was initially defined during an international workshop held in Stockholm in March 2016 with more than 100 participants [1]. The original idea was to take advantage of the existing 3 GeV linac at the MAX IV laboratory, which was from the conceptual phase thought to be a driver for a Free-electron laser, and "quickly" build a beamline in the Short Pulse Facility (SPF) [2] area. With the support of the Wallenberg foundation, some major universities in Sweden contributed, together with the MAX IV laboratory, to a conceptual design report (CDR) that was ready in March 2021 [3]. The CDR focuses on different aspects of the SXL as a FEL user facility (science, experimental stations, beamline, undulators, linac driver, electron gun source, timing and synchronization). These matters were investigated from a conceptual point of view in order to satisfy the needs of the user case and design a competitive and up-to-date machine. While initially limiting the scope we kept in mind possible future upgrades and different modes of operations.

A new workshop has been held in Stockholm in June 2022 to renew the Science Case.

* francesca.curbis@maxiv.lu.se

[†] now at Deutsches Elektronen-Synchrotron DESY, Hamburg, Germany

[‡] now at ISIS Neutron and Muon Source, STFC/RAL, Didcot, UK

OVERVIEW OF THE SXL FEL

SXL (Soft X-ray laser) will cover a wavelength range from 1 to 5 nm with rather short pulse duration (from tens of femtoseconds down to a few femtoseconds, in the first phase) [4]. This source can accommodate the user requirements for a large variety of experiments in four main areas: AMO physics, condensed matter, Chemistry and Life Science [5]. The underlying idea in the conceptual design phase has been to keep the machine flexible for future expansions and enhancing some typical features like the embedded broad spectrum of pump sources. Table 1 summarizes the main parameters of the SXL photon beam.

Table 1: Main SXL Parameters

Wavelength range	1 – 5nm
Photon energy	≈ 0.25 – 1 keV
Pulse duration	1 – 30 fs
Repetition rate	100 Hz
Energy per pulse	0.015 – 1.5 mJ
Peak brightness	10^{-33} Ph./s/mm ² /mrad ² /0.1%BW

The Existing Linac

The SXL will be driven by the 3 GeV S-band linac currently injecting into the MAX IV 1.5 and 3 GeV storage rings and the Short Pulse Facility (SPF). As of today, a photo cathode gun and two bunch compressors can provide 100 fs long pulses for the SPF with a normalised emittance below 1 μm. In the MAX IV linac the bunches are compressed using two double-achromat structures (BC1 and BC2), which provide also passive magnetic linearization. A detailed description of the MAX IV linac and its performance can be found elsewhere [6, 7]. The baseline FEL performance is based on two different accelerator operation modes: a high charge-medium pulse (1A) and a low charge-short pulse (1B). Both pulses display a residual energy chirp which is not typical in other FELs, but at the same time a very high peak current can be achieved, which help the FEL process. More details about beam dynamics, collective effects and technical solutions that will be adopted can be found in the SXL CDR [3]. The layout of the MAX IV linac with the upgrades envisaged for SXL is shown in Fig. 1.

SHORT FEL PULSES WITH TUNABLE DURATION FROM TRANSVERSELY TILTED BEAMS AT SwissFEL

P. Dijkstal¹, E. Prat*, S. Reiche, Paul Scherrer Institut, Villigen, Switzerland
¹also at Department of Physics, ETH Zurich, Switzerland

Abstract

FEL pulses with an easily tunable duration are of great benefit to user experiments with high requirements on the temporal resolution. A transverse beam tilt is well suited to shorten the pulse duration in a controlled manner. We consider three methods of tilt generation: rf deflecting structures, lattice dispersion in combination with an energy chirp, and transverse wakefields from C-band accelerating cavities. We use monochromator scans in combination with an energy-chirped beam to diagnose the reduction in pulse duration.

INTRODUCTION

Exploration of matter and its dynamics on the sub-nanometer space and sub-femtosecond time scales are allowed by the recent progress in X-ray free-electron lasers (XFELs). Some experiments require photon pulses that are shorter than those emitted in the standard operation mode of SASE hard X-ray FEL facilities. For reference, the Aramis undulator beamline at SwissFEL [1] usually delivers pulse durations in the range of 40–60 fs (all pulse durations refer to FWHM: full width at half maximum values). For example, an experiment at LCLS [2] performed double-core-hole spectroscopy on CO molecules, and requested X-ray pulses with durations of about 10 fs [3]. Also at SwissFEL, several times over the past two years users requested pulses with durations between 5 and 20 fs.

Most methods of short pulse generation are based on suppressing the SASE process for selected longitudinal parts (slices) of the bunch. Different slice properties of the electron beam can be spoiled or interrupted: the energy spread [4, 5]; the transverse optics matching [6]; the emittance [7–9]; and the trajectory (beam tilt, this contribution).

A beam tilt is a correlation between the transverse (x, x' or y, y') and temporal (t) coordinates of particles in a bunch. For an efficient FEL process, the electron beam needs to be aligned to the path of the emitted photon beam. Parts of the beam that travel off-axis receive a collective steering effect (i.e., dipole kicks) from the quadrupoles, such that their trajectory oscillates. Therefore, all parts of a linearly tilted beam except one region, usually the core, travel off-axis in an undulator section and do not have a constant transverse overlap with the FEL pulse. The threshold of orbit misplacement, above which the FEL process is suppressed, depends on the photon energy and on electron beam parameters such as the transverse beam size [10–12]. This method of selective FEL pulse suppression is routinely used at LCLS [13–

15] and at SwissFEL [16, 17]. In this contribution we perform a systematic comparison of three methods of beam tilt generation.

SwissFEL

We report on measurements at the SwissFEL facility [1], schematically shown in Fig. 1. Electron bunches with a nominal charge of 200 pC originate from an rf photocathode with a repetition rate of up to 100 Hz and are accelerated to an energy of up to 6 GeV in several accelerating sections. Two bunch compressors (BC1 and BC2), acting in the horizontal plane, shorten the bunch length. An isochronous energy collimator is located after the last accelerating section (Linac 3). Two rf transverse deflecting structures (TDS) [19], streaking in the vertical plane, can be used in combination with a profile monitor [20] to measure longitudinal electron properties such as bunch length and current profile, as well as horizontal slice properties such as slice emittance, beam tilt and optics mismatch [21]. The Aramis undulator beamline contains 13 planar variable-gap undulator modules with a period of 15 mm, a maximum undulator parameter (K) of 1.8 and a total length of 4 m. The FEL radiation wavelength can be set between 1 and 7 Å. Photon pulse energies and spectra are measured by a gas detector [22] and a single-shot photon spectrometer (PSSS), respectively [23, 24]. In case the acceptance of the PSSS (approx. 0.76%) is insufficient, a monochromator followed by a photodiode is suitable for measuring the average spectral intensity over a larger photon energy range.

Furthermore, the recently developed passive streaker diagnostics allow for an indirect reconstruction of the FEL power profile through measurements of the electron beam longitudinal phase space after the undulator section [18]. At the time the measurements discussed later were performed, this type of diagnostics was not yet available.

BEAM TILT GENERATION

We consider three different ways to impose a mostly linear beam tilt (streaking the beam), as previously suggested [25]:

- A) A TDS after Linac 3 directly imposes a linear beam tilt through time-dependent electromagnetic fields.
- B) A beam can excite transverse electromagnetic fields (wakefields) that act back on itself. The head does not experience a deflecting force and remains unperturbed on its trajectory. Trailing slices experience progressively growing forces. The C-band accelerating rf cavities in Linac 3 with their periodic surface modulation (see Fig. 3) are suitable for this purpose.

* eduard.prat@psi.ch

TWO-COLOR FEL BY LASER EMITTANCE SPOILER

C. Vicario[†], C. Arrell, S. Bettoni, A. Dax, P. Dijkstal, M. Huppert, E. Prat, S. Reiche, A. Trisorio
Paul Scherrer Institut, Villigen, Switzerland
A. Lutman, SLAC National Accelerator Laboratory, Menlo Park, CA

Abstract

A novel and noninvasive method for two-color X-ray generation is demonstrated at SwissFEL. In the setup, a short laser pulse is overlapped with the primary photocathode laser to locally spoil the beam emittance and to inhibit the FEL emission. This, together with a chirped electron pulse, results in X-ray emission at two colors delayed in time. High-energy, high-stability, independent control of the duration and of the intensity of the two colors are demonstrated. The laser emittance spoiler enables shot-to-shot selection between one and two-color FEL emission and further, it is compatible with high repetition-rate FELs, as it does not contribute to beam losses.

INTRODUCTION

X-ray free electron lasers (FELs) are largely used for time-resolved studies of photoinduced processes at ultra-fast timescale with wide applications in biology, femtochemistry, physics and material science [1-5].

These experiments are usually carried out by combining a conventional laser pump pulse with an X-ray FEL probe. For such studies, the reduction of the temporal jitter between the pump and the probe pulses down to fs- level is a persistent challenge [6]. X-ray pump, X-ray probe experiments employing a two-color FEL are expected to drastically reduce the temporal jitter while the two-wavelengths can be tuned to selectively excite and to probe two different resonances [7, 8].

A two-color FEL output can be achieved by the uneven tuning of the undulator resonance or by the manipulation of the electron bunch properties, see references in [9]. Both approaches are implemented with a dedicated setting of the accelerator or the undulator which is often not optimized for FEL output and required a long preparation time.

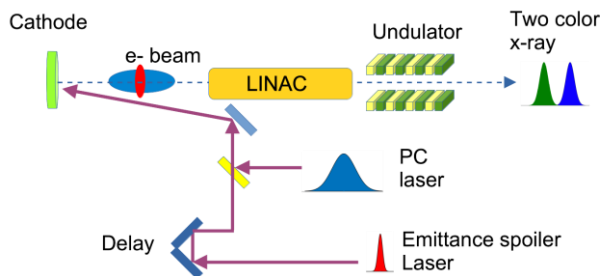


Figure 1: Layout of the two-color FEL scheme based on the laser emittance spoiler.

EXPERIMENTAL SETUP

This proceeding reports on a new method for the generation of a two-color FEL by electron beam emittance spoiling realized with a second photocathode laser [9]. Different from other techniques, the present method is able to produce two-color X-rays using the optimal FEL settings as it does not require a dedicated accelerator and undulator re-tuning. In this way it is possible to reduce the preparation time and save beam-time for the user experiment. The two-color by laser emittance spoiler enables shot-to-shot switching between two and single color. It is directly applicable to high-average power x-ray FELs because it is not introducing beam losses such as in the case of the two-color obtained with double-slot foil. The laser emittance spoiler concept is sketched in Fig. 1. A ps-laser pulse (emittance spoiler) is overlapped on the longer photocathode (PC) laser. The excess of charge spoils locally the slice emittance, preventing the FEL amplification. The part of the bunch not interacting with the laser spoiler still produces FEL emission at two wavelengths due to the linear energy chirp accumulated along the linear accelerator.

We experimentally demonstrated the two-color FEL by laser emittance spoiler at the hard X-ray branch of SwissFEL (Aramis) [1]. At the photoinjector, 300 MeV, 200 pC electron bunches at 100 Hz are generated from a Cs₂Te photocathode in a RF gun. The linear accelerator boosts the beam energy up to 3.15 GeV for the soft x-ray FEL (Athos) and to 5.8 GeV for the Aramis FEL. Two bunch compressors at 0.3 and 2.1 GeV reduce the bunch length to a few tens of fs. The Aramis undulator consists of 13 planar variable-gap modules of 4 m length each and magnetic period of 15 mm. This line produces radiation over the photon energy range 2-12 keV. The FEL pulse energies and spectra are measured by a gas detector and a single-shot spectrometer, respectively.

Table 1: Parameters of the PhotoCathode (PC) and the emittance spoiler laser.

Parameters	Nominal PC laser	Emittance-spoiler laser
Wavelength (nm)	260	260
Pulse duration (ps)	6.6	0.95
Diameter (mm)	1	2
Generated bunch charge (pC)	200	11-34

[†] email address carlo.vicario@psi.ch

SUPERRADIANT AMPLIFICATION TO PRODUCE ATTOSECOND PULSES IN SOFT X-RAY REGIME VIA LINEAR REVERSE TAPER WITHIN UNDULATOR SECTION

Longdi Zhu ¹, Sven Reiche, Paul Scherrer Institute, Villigen, Switzerland
Eugenio Ferrari, DESY, Hamburg, Germany

¹also at Swiss federal institute of technology Lausanne (EPFL), Lausanne, Switzerland

Abstract

Laser pulses of sub-femtosecond duration can be used to track the motion of electrons in the inner shell, which is needed in a variety of advanced experiments. Although this has been accomplished in XUV and hard X-rays in a free-electron-laser facility, it remains a challenge in the soft X-ray region due to the relatively high photon energies and large slippage in the undulator. In this contribution, we present a method to achieve a pulse sequence of ~ 120 attosecond each in average at 293.8 eV photon energy (4 nm wavelength), which covers the K-shell absorption of Carbon. The key is to create a linear undulator taper within each undulator module by rotating a transverse gradient undulator (TGU) at a small angle. The TGU technique is usually referred to minimise the energy spread effect in Laser-driven plasma accelerator, while in this paper we demonstrate that it can also be used to generate short pulses.

INTRODUCTION

Free-electron-laser (FEL) is an X-ray light source [1]. It has many advantages, such as gigawatt power, femtosecond pulse duration and tunable wavelength, opening up experimental opportunities for multiple scientific disciplines including biology, chemistry and physics [2–6]. In this proceeding, we present a method of generating attosecond pulse train (APT) at 4nm radiation wavelength, a scale at which the SASE coherence length is rather large. The consequence of the large coherence length is that the FEL spikes slip out of the electrons and increases the pulse duration, which is the main difficulty in soft x-ray regime.

The compensation of slippage by undulator taper has been discussed in [7, 8], we extend the range of radiation wavelength to 4 nm, where radiations slide significantly into fresh slices and bunch electrons, it is called superradiant regime [9–16]. The compensation of slippage effect is difficult as the process of superradiance is highly non-linear. In this contribution, we propose an original method, combining the energy modulation, phase shifter and taper inside an undulator module. The novelty of the method lies on the strong reverse [17, 18] taper within undulator section by rotated TGU [19] to reduce the effective period number in undulator. If the taper is reverse and its strength is extreme large, only the electrons on which FEL spike stands can effectively lase, while others are suppressed [18]. Based on the parameters in SwissFEL Athos undulator, the simulation result using GENESIS 1.3 code [20] shows that it is possible

to generate pulse trains averaging ~ 120 attosecond, which is much shorter than typical pulse duration in SASE, which is several femtosecond [21].

METHOD

Step 1: Energy Modulation by Seeding Laser

Assuming an electron beam, cold and long, beam current is homogeneous everywhere, travelling through a modulator and a main undulator. The energy modulation is induced by the interaction between electron beam and an external conventional laser, the laser Rayleigh length z_R matches the modulator length $L_m = N_m \cdot \lambda_m$, where N_m is the modulator period number [22]. For relativistic electrons with velocity $\beta_s \approx 1$, the modulated electron is supposed to have same periodicity as the laser beam [22]. The result of the seeding is a sinusoidal energy modulated beam with large amplitude. For the following discussion we choose a fixed value for the achieved energy modulation of 1% and a laser wavelength of 800 nm.

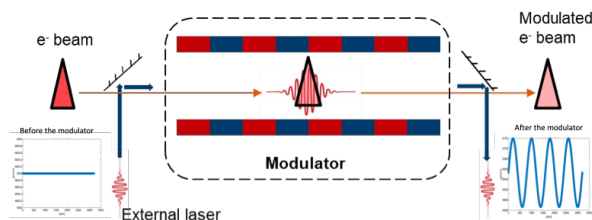


Figure 1: The external Ti-Sapphire 800 nm seeding laser induces a large energy modulation in modulator.

We are interested in the linewidth of resonance $\Delta\omega/\omega \approx \frac{1}{N_u}$, in the undulator. As we assume cold beam, the linewidth is not limited by energy spread, nor emittance. For high-gain case, if electrons do not lose significant energy compared to the total energy, the linewidth is of the order of ρ - FEL parameter [23, 24]. Since the amplitude of energy modulation is 1% and the FEL parameter $\rho \sim 10^{-3}$, for given undulator parameter K, only electrons within the linewidth satisfy the resonance condition and lase significantly photons. The gain in the rest of electron bunch (for both the unmodulated beam fraction and modulated beam with chirp of opposite direction) are strongly reduced or even suppressed, when electrons are out of resonance. Therefore, it is not the whole electron beam that is emitting light, but the resonant electron beam, which is very short.

LOW-EMITTANCE BEAM INJECTION FROM SACLA TO SPring-8

T. Hara[†], RIKEN SPring-8 Center, Sayo, Japan
On behalf of RIKEN-JASRI joint project team

Abstract

The SACLA linear accelerator has been successfully used as a full-energy injector of the SPring-8 storage ring since 2020. The beam injection from SACLA is a part of the SPring-8 upgrade project, called SPring-8-II, which requires low-emittance beams for injection due to its small beam aperture. In order to perform the beam injection in parallel with XFEL operation, three accelerators are virtually constructed in a control system of SACLA. Thus, the electron beam parameters, such as beam energies, are independently tuned for the beam injection and two XFEL beamlines. By shutting down a dedicated old injector, electricity consumption has been reduced by roughly 20-30 % and additional maintenance costs are no more necessary.

INTRODUCTION

The beam injection from SACLA has been started as a part of the SPring-8 upgrade project, called SPring-8-II [1, 2]. A small dynamic aperture is a common issue for all recent low-emittance storage rings with multi-bend optics [3]. In SPring-8-II, traditional off-axis beam injection will be employed using an in-vacuum septum magnet and low-emittance beams [4]. Thus, the low-emittance beam of SACLA is indispensable for beam injection.

Figure 1 is a schematic layout of the SACLA facility [5]. There are two XFEL beamlines (BL2, BL3) and a soft x-ray FEL beamline (BL1). BL1 operates independently from the SACLA main linear accelerator by using a dedicated 800 MeV linear accelerator, which was originally

constructed as SCSS, a proto-type accelerator of SACLA [6, 7]. BL2 and BL3 share the electron beam of the SACLA main linear accelerator. A switchyard is installed at the end of the linear accelerator and 60 Hz electron bunches are distributed pulse by pulse [8, 9]. For the beam injection, the electron bunches are deflected to a beam transport line named XSBT (XFEL to Storage ring Beam Transport).

The use of SACLA as an injector not only brings small emittance, but also it contributes to electricity saving and facility related cost reduction. In case of a dedicated injector, accelerators should be always maintained in operating condition just for sparsely occurred top-up injection. On the other hand, a linear accelerator of XFEL is already in operation to provide photon beams to its users, so no additional electricity or operation cost is required by just using a small number of electron bunches for top-up injection.

BEAM INJECTION

Figure 2 shows the stored current of SPring-8 during the beam injection from SACLA. It takes about 10 minutes to fill up the ring with 100 mA, which is a nominal stored current of SPring-8. During the 10 Hz injection, XFEL operation is suspended. Once the stored current reaches 100 mA, it is maintained by top-up injection, which is performed in parallel with XFEL operation. When the stored current decays below a certain threshold, SPring-8 sends a request of beam injection to SACLA. A typical frequency of top-up injection is 2-3 times every minute.

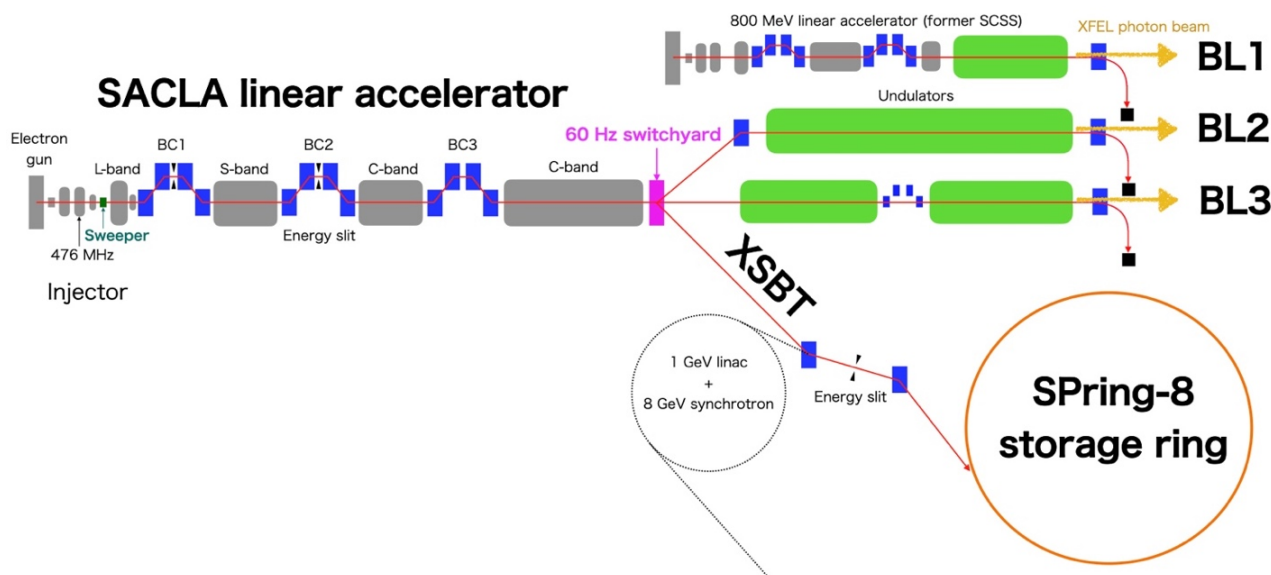


Figure 1: Schematic layout of the SACLA facility.

[†] toru@spring8.or.jp

DETAIL STUDY FOR THE LASER ACTIVATING REFLECTIVE SWITCH FOR THZ FREE ELECTRON LASER

K. Kawase[†], National Institutes for Quantum Science and Technology, Kizugawa, Japan

Abstract

THz free electron laser at SANKEN, Osaka university generates a train of THz pulses with the interval of 27 MHz in the repetition of 5 Hz. The number of pulses in a train is about 100. Single pulse energy exceeds 200 μ J at the carrier frequency of 4.5 THz. To extract a single pulse from the train, the reflective switch of the electron-hole plasma on the surface of Gallium Arsenide wafer driven by the Ti:sapphire laser pulse was constructed and the characteristics of the switch is studied. By evaluating also the characteristics of silicon and germanium wafers, the comparison experiments are performed. In addition, the study for carrier dynamics with the time scale of microseconds by measuring the variations of reflected and transmitted THz pulses with the interval of 27 MHz are being conducted. We report the recent results of the switching for the THz pulse and its time evolution in this conference.

INTRODUCTION

A free electron laser (FEL) oscillator is that the light is amplified and oscillated by going roundtrip inside a cavity similar to conventional lasers. A part of the light inside the cavity is extracted according to the coupling of the resonator mirror. In case of the radiofrequency linac, the electron beam consists of the bunch train with the duration of a few ten picoseconds for each bunch, thus, the FEL has also a form of the bunch train with the similar duration. On the other hand, an isolated pulse is more useful depending on the experimental demands. Therefore, the researches of the semiconductor reflective switching driven by visible or near infrared pulse lasers have been conducted at several FEL facilities [1 - 9].

The semiconductor reflective switching is that the intense laser pulse generates the high dense carrier plasma on the surface of the semiconductor sheet, which is undoped with high transparency on the wavelength range from mid to far infrared, and the plasma reflects the FEL pulses in a short time. When the plasma density on the surface of the semiconductor exceeds a critical density, the reflectivity is high, but the reflection, absorption and transmission of the FEL competes when the density is lower than that. Because the characteristics of the reflection, absorption and transmission of the radiation depends on the carrier density, the evolution of the carrier density is a fundamental property on the response of the semiconductor reflective switches. Thus, the detail studies for the evolution of the laser activating reflective switching for different semiconductors are useful and interesting. We performed the experimental studies of the evolution of reflective switching for gallium

arsenide (GaAs), germanium (Ge) and silicon (Si) using the FEL at the range of THz frequency.

EXPERIMENT

The experiments were conducted using THz FEL at the Institute of Scientific and Industrial Research, Osaka University (SANKEN THz-FEL, formerly named ISIR THz-FEL). This FEL covers the wavelength range from 50 to 100 μ m (3 to 6 THz) in practical. The pulse interval is 27 MHz and the duration of a pulse train is about 8 μ s. The repetition of operation is 5 Hz. The details of the accelerator and FEL apparatuses are shown in the previous reports [10].

The THz FEL beam is transported inside the vacuum duct and extracted to the experimental area through a diamond window. The beam is down-collimated with two off-axis parabola mirrors and injected to the semiconductor wafer as the switching material with Brewster's angle. Samples was undoped semiconductor wafers of GaAs, Ge and Si with the thickness of 0.5 mm. The pulse energy reflected from the switch and the energy of transmitted pulse train were measured by energy meter system (Coherent, Inc.). As the sensor heads, J10MB-LE with higher sensitivity for the reflected pulse and J50MB-LE with lower sensitivity for the transmitted train were used. For time resolved measurements, the pyroelectric detector (P5-00, Moletron, Inc.) was used.

As a driving laser for the semiconductor reflective switching, Ti:sapphire regenerative amplifier laser system with the nominal FWHM pulse duration of 100 fs (Spitfire, SpectraPhysics, Inc.) was used. The laser pulses are synchronized to the timing system of the linac. The irradiation timing on the wafer was tuned with the optical delay line consisting of two mirrors mounted on the motorized linear stage with the stroke of 100 mm and the cable delay line installed in the laser timing system. The irradiation fluence was tuned with the half waveplate before the polarizer. The photograph of the experimental setup is shown in Fig. 1.

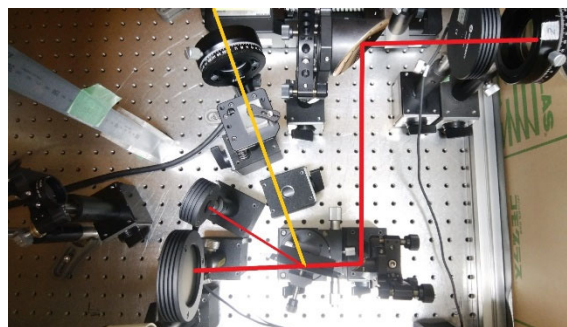


Figure 1: Experimental setup.

[†] kawase.keigo@qst.go.jp

CASCADED AMPLIFICATION OF ATTOSECOND X-RAY PULSES: TOWARDS TW-SCALE ULTRAFAST X-RAY FREE-ELECTRON LASERS*

P. L. Franz[†], Z. Guo, R. Robles, Stanford University, Stanford, CA, USA
D. K. Bohler, D. Cesar, X. Cheng, T. Driver, J. P. Duris, A. Kamalov, S. Li,
R. Obaid, N. S. Sudar, A. L. Wang, Z. Zhang, J. P. Cryan, A. Marinelli
SLAC National Accelerator Laboratory, Menlo Park, CA, USA

Abstract

The natural time scale of valence electronic motion in molecular systems is on the order of hundreds of attoseconds. Consequently, the time-resolved study of electronic dynamics requires a source of sub-femtosecond pulses. Pulses in the soft x-ray domain can access core-level electrons, enabling the study of site-specific electron dynamics through attosecond pump/probe experiments. As time-resolved pump/probe experiments are nonlinear processes, these experiments require high brightness attosecond x-ray pulses. The X-ray Laser-Enhanced Attosecond Pulses (XLEAP) collaboration is an ongoing project for the development of attosecond x-ray modes at the Linac Coherent Light Source (LCLS). Here we report development of a high power attosecond mode via cascaded amplification of the x-ray pulse. We experimentally demonstrate generation of sub-femtosecond duration soft x-ray free electron laser pulses with hundreds of microjoules of energy. In conjunction with the upcoming high repetition rate at LCLS-II, these tunable, high intensity attosecond capabilities enable new nonlinear spectroscopic techniques and advanced imaging methods.

INTRODUCTION

Valence electronic motion in molecular systems is on the order of hundreds of attoseconds. Consequently, the time-resolved study of electron dynamics requires a source of sub-femtosecond pulses.

The X-Ray Laser-Enhanced Attosecond Pulses (XLEAP) collaboration is an ongoing project for the development of attosecond capabilities at the Linac Coherent Light Source (LCLS). The XLEAP project has previously demonstrated the generation of isolated soft x-ray attosecond pulses with pulse energy millions of times larger than any other source of isolated attosecond soft x-ray pulses, with a median pulse energy of 10 μJ and median pulse duration of 280 as at 905 eV photon energy [1]. Here we report the recent development of a high power attosecond mode via cascaded amplification of the x-ray pulse. We experimentally demonstrate generation of soft x-ray free electron laser pulses with hundreds of microjoules of energy.

* This work was supported by US Department of Energy Contracts No. DE-AC02-76SF00515.

[†] FRANZPL@STANFORD.EDU

CASCADED AMPLIFICATION

A density perturbation is introduced in the electron beam by laser pulse stacking at the photocathode [2]. The perturbation is amplified to a high current spike by acceleration and then beam compression in downstream wigglers and a magnetic chicane.

In the first cascade stage, the undulator taper is matched to the energy chirp of the electron beam at the current spike to produce the initial enhanced self-amplified spontaneous emission (ESASE) [3] x-ray pulse. The bunch is then delayed relative to the pulse by a second magnetic chicane, allowing the radiation to slip onto a fresh slice of the bunch. This seeds the FEL process and amplifies the pulse in the second cascade stage (Fig. 1).

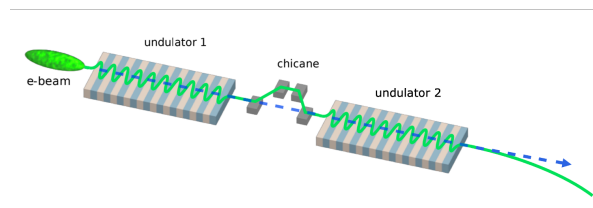


Figure 1: Schematic of the two-stage cascade. Cathode shaping has been used to create an ESASE current spike in the electron beam prior to the first undulator stage.

PRELIMINARY RESULTS

We have experimentally demonstrated the generation of soft x-ray pulses with hundreds of microjoules of energy using cascaded amplification in two FEL stages at LCLS. Figure 2 shows the pulse energy as a function of the number of undulator sections in the second stage. Using ten undulators the highest energy shots have over 300 μJ of pulse energy.

The highest energy pulses also have sufficient bandwidth to have sub-femtosecond duration near the fourier transform limit (Fig. 3). Previous XLEAP configurations have been within a factor of 2 of the fourier transform limit [1].

In the electron beam phase space, energy loss from reamplification in the second stage is seen as the lasing spike in the head of the beam (Fig. 4). The ESASE pulse initially lases at the current spike near the center of the beam, and is then slipped ahead to the fresh, non-chirped head of the beam. Energy loss from lasing in the head is visible when the second undulator stage is inserted, indicating that amplification of the ESASE pulse is taking place. Figure 5

COMPARISON OF TRANSVERSE COHERENCE PROPERTIES IN SEEDED AND UNSEEDED FEL

M. Pop*, F. Curbis, S. Werin, Physics department, Lund University, Lund, Sweden
 A. Simoncig, C. Spezzani, D. Garzella, E. Allaria, G. De Ninno, G. Perosa,
 G. Penco, L. Foglia, L. Giannessi, M. Zangrando, M. Trovo,
 M. Manfredda, N. Mahne, N. Mirian, P. R. Ribic,
 S. Di Mitri, S. Spampinati, Elettra-Sincrotrone, Trieste, Italy
 G. Geloni, European XFEL, Hamburg, Germany
 N. Mirian, Deutsches Elektronen-Synchrotron (DESY), Hamburg, Germany

Abstract

The transverse coherence of the source is an important property for FEL experiments. Theory and simulations indicated different features for seeded and unseeded FELs but so far no direct comparison has been pursued experimentally on the same facility. At FERMI FEL one has the unique possibility to test both SASE and seeded configurations under the same operating conditions. In this contribution we present the experimental results of the characterization of transverse coherence with special attention to the evolution of this fundamental property.

INTRODUCTION

Novel investigation techniques such as diffractive imaging [1] and X-ray holography [2] require high levels of transverse coherence from the free electron laser (FEL) source. An X-ray FEL is usually driven by a high current, low emittance and low energy spread electron beam. To achieve ultra relativistic velocities and high currents, the electron beam is accelerated by a linear accelerator and compressed by dispersive sections called bunch compressors. After acceleration the beam is then fed through an undulator line called radiator where the interaction between the electrons and the electromagnetic field, which they themselves produce, exponentially amplifies the latter. The resulting FEL radiation is highly brilliant and highly coherent.

Taking advantage of the capabilities of FERMI FEL-2, we were able to study two distinct modes of operating an FEL: self amplified spontaneous emission (SASE) and seeded. The first option is able to produce gigawatts of power by directly sending the electrons through the radiator, without any prior phase space shaping [3–6]. The longitudinal coherence of SASE radiation can be improved if the FEL is seeded [7–9]. The most common seeding scheme, in the XUV range, is the high gain harmonic generation or HGHG. First, an external laser co-propagating with the electron beam inside an undulator, called modulator, imprints an energy modulation onto the electron beam. Then the energy modulation is transformed into density modulation in a dispersive section. Such density modulation exhibits bunching not only at the fundamental harmonic but, with diminishing intensities, also at higher harmonics. By this mechanism

HGHG FELs can produce longitudinally coherent radiation at harmonics of the wavelength of an external, optical laser.

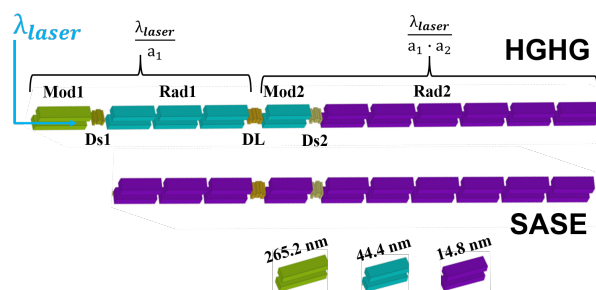


Figure 1: Schematic layout of FERMI FEL-2 operated in cascaded HGHG (top) and SASE (bottom) modes. The undulators are color-coded by the resonant wavelength they were set during the experiment.

Previous work showed that both SASE [10, 11] and seeded [12] FELs reach high degrees of transverse coherence. Furthermore, semi-analytical and simulation studies indicated that in a SASE FEL the transverse coherence is built up during the amplification process, reaching a maximum before intensity saturation. Aiming at qualitatively comparing the evolution of transverse coherence, this contribution presents the first experimental confirmation of the early saturation of this property in SASE FELs. A more in-depth description and analysis is presented in the original paper describing this experiment [13].

EXPERIMENTAL SETUP

The aim of our experiment was to estimate the transverse coherence properties of the FERMI FEL-2, operated in cascaded HGHG (seeded) and SASE modes. By progressively tuning out radiators, it is possible to obtain a transverse coherence gain curve which can be used to investigate how coherence is built up in the two types of FEL.

FERMI FEL-2 is usually run in fresh-bunch cascaded HGHG mode [14], which can produce longitudinally coherent pulses down to a few nanometers. However, for this

* corresponding author: mihai.pop@maxiv.lu.se

FEL RESONANCE OF CIRCULAR WAVEGUIDE MODES

A. Fisher*, P. Musumeci

Department of Physics and Astronomy, University of California Los Angeles, USA

Abstract

The THz gap is a region of the electromagnetic spectrum where high average and peak power radiation sources are scarce while scientific and industrial applications grow in demand. Free-electron laser coupling in a magnetic undulator can provide radiation generation in this frequency range, but slippage effects require the use of relatively long and low current electron bunches in the THz FEL, limiting the amplification gain and output peak power. The introduction of a waveguide can contain the radiation and match the radiation group velocity to the electron beam longitudinal velocity, allowing strong compression of the beam to provide seeding for a high efficiency THz FEL. We discuss the resonance and implementation of the waveguide modes in GPTFEL and consider simulations of the THz FEL, targeting resonance with the TE11 and TE12 modes.

INTRODUCTION

Recent experimental results have shown that large energy conversion efficiencies in a THz free electron laser can be achieved with strong undulator tapering and by introducing a waveguide to match the radiation group velocity to the electron beam longitudinal velocity [1]. The experiment relied on the coupling between the helical trajectory of the electrons and the fundamental lowest frequency TE11 mode of the waveguide. In this paper, we consider the resonance of higher order waveguide modes beyond the TE11 mode.

The paper is organized as follows. First we define the circular waveguide modes in general form. Next we describe the implementation in GPTFEL [2] and compare the simulated gain lengths in a untapered undulator amplifier to analytical expressions from the 1D theory. Finally, we compare single-mode and multi-mode simulations of a THz FEL at zero-slippage resonance for the TE11 mode and then the TE12 mode using planned experiment parameters.

CIRCULAR WAVEGUIDE MODES

TE and TM modes for a circular waveguide are written in terms of the the longitudinal fields H_z and E_z , respectively. For brevity, we present equations only for TE radiation modes as they couple more effectively to the electron beam in the undulator. A general description of circular waveguide modes can be found in most electrodynamics textbooks [3].

The discrete TE waveguide modes are solutions of a 2D Helmholtz equation

$$\left[\frac{\partial^2}{\partial \rho^2} + \frac{1}{\rho} \frac{\partial}{\partial \rho} + \frac{1}{\rho^2} \frac{\partial^2}{\partial \phi^2} + k_{\perp}^2 \right] H_z = 0, \quad \frac{\partial H_z}{\partial n} \Big|_{\rho=R} = 0$$

$$H_z^{mn} = H_0 J_m(k_{mn} \rho) e^{\pm im \phi} \quad (1)$$

* afisher000@g.ucla.edu

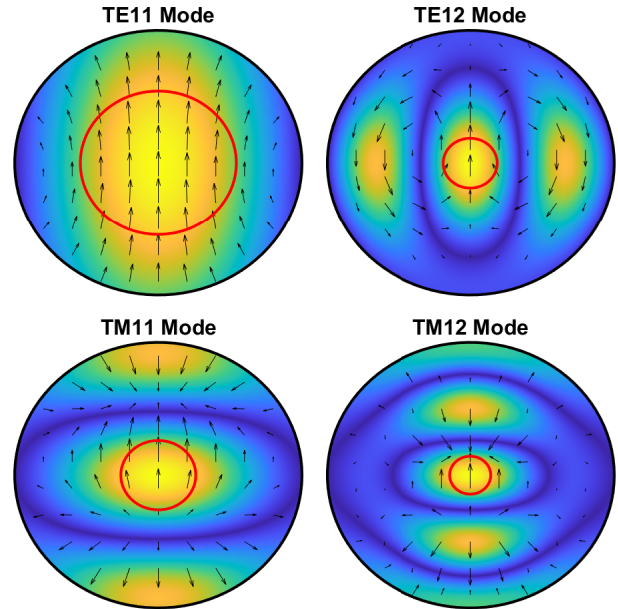


Figure 1: Waveguide Modes. Red circles show electron trajectory and amplitude of $\vec{v}_z \cdot \vec{E}_{\perp}^{mn}$ is shown by colormap.

for $m = 0, 1, \dots$ and $n = 1, 2, \dots$ where $k_{mn} = w_{mn}/R$, w_{mn} is the n^{th} zero of the derivative of the m^{th} Bessel function ($J'_m(w_{mn}) = 0$), R is the waveguide radius, and H_0 is a normalization constant. The transverse fields are given by

$$\vec{E}_{\perp}^{mn} = \frac{-i\omega\mu}{k_{mn}^2} [\hat{z} \times \nabla_{\perp} H_z^{mn}] \quad (2)$$

$$\vec{H}_{\perp}^{mn} = \frac{\omega\epsilon}{k_z} [\hat{z} \times \vec{E}_{\perp}^{mn}] \quad (3)$$

We choose $H_0 = \frac{\sqrt{2}k_{mn}}{\mu\omega}$ to normalize $|\vec{E}_{\perp}^{mn}|^2$ to 1.

Due to the symmetry of the spiraling electron trajectory, only TE and TM modes with $m = 1$ allow for net energy exchange with an electron over an undulator period. The first four of these modes are shown in Fig. 1. The red circles show the trajectory radius of the electron beam at the zero-slippage resonance and the colormap shows the amplitude of $\vec{v}_e \cdot \vec{E}_{\perp}^{mn}$.

The ratio of electron beam trajectory radius to waveguide radius is essentially independent of resonant frequency or beam energy and is given by $\frac{r_{\text{traj}}}{R} = \frac{K}{\sqrt{1+K^2}} \frac{\beta_z}{w_{mn}}$ where K is the undulator strength parameter, and β_z is the dimensionless relativistic longitudinal velocity. For TM modes, w_{mn} is the n^{th} zero of the m^{th} Bessel function ($J_m(w_{mn}) = 0$). While there are tight trajectory tolerances to ensure an effective energy exchange, the decreasing ratio suggests that higher modes could be used to target high frequencies in

SYNCHRONIZED TERAHERTZ RADIATION AND SOFT X-RAYS PRODUCED IN A FEL OSCILLATOR

M. Ruijter*, A. Bacci, I. Drebot, M. Rossetti Conti, A. R. Rossi, S. Samsam¹, L. Serafini
INFN-Section of Milan, Milan, Italy

¹also at Università La Sapienza, Rome, Italy

M. Opromolla², V. Petrillo², Università degli Studi di Milano, Milan, Italy

²also at INFN-Section of Milan, Milan, Italy

Abstract

We present a scheme to generate synchronized THz and Soft X-ray radiation pulses by using a Free-Electron Laser Oscillator driven by a high repetition rate (of order 10-100 MHz) energy recovery linac. The backward THz radiation in the oscillator cavity interacts with a successive electron bunch, thus producing few 10^5 Soft/Hard X-ray photons per shot (namely 10^{12} - 10^{13} photons/s) via Thomson back-scattering, synchronized with the mJ-class THz pulse within the temporal jitter of electron beams in the superconducting linac (< 100 fs). Detailed simulations have been performed in order to assess the capability of the scheme for wavelengths of interest, between 10 and 50 μm for the TeraHertz radiation and 0.5 – 3 nm for the X-rays.

INTRODUCTION

Researches at the science frontiers need tunable, brilliant and coherent radiation pulses. Two synchronized different wavelengths are required for testing phenomena on different time scales or for pump and probe experiments [1–3]. The combination of THz radiation sources with the most advanced X-ray facilities is so promising that the laboratories allocating the most brilliant X-ray sources, namely Synchrotrons and Free-Electron Lasers (FELs), are also endowed with THz sources to be coupled with the X-rays [4,5]. However, in this way, these experiments can be exclusively carried out in huge laboratories, limiting the diffusion of this research technique. Regarding the THz generation, much interest converges on FELs, widely tunable and delivering high quality pulses presenting energy stability, polarization, spectral and spatial optimal distribution. THz FELs operate mainly as oscillators, i.e. they are equipped with resonators confined by mirrors [6–10]. This operational mode guarantees compactness, relaxed requirements of the electron bunch quality and the fact that oscillators are suitable for Super Conducting (SC) Linacs, allowing the generation of powerful quasi-cw light. The dual source (THz plus X-rays) we expose here (see also [11]) exploits the fact that the THz radiation generated by the passage of successive electron bunches in the FEL undulator, driven by a SC ERL, propagates at each round trip inside the cavity, first forward towards the front mirror and then backward to the rear mirror. After the reflection, the radiation hits a successive electron bunch in a condition suitable for Thomson back-scattering. THz

FEL intracavity pulses with mJ-class energy at 15-50 μm of wavelength, driven by 20-100 MeV energy electron bunches, can deliver up to few 10^5 soft X-ray photons per shot by Thomson back-scattering at a rate of 10-100 MHz and synchronized with the THz radiation. The total of 10^{12} - 10^{13} X photons generated per second can be useful in many imaging fields (see Ref. [3]). This source is more compact and less expensive than Synchrotrons and Soft X-ray FELs, can be developed in small/medium size laboratories, hospitals or university campuses and represents an elementary upgrade of a basic THz FEL Oscillator. Section II describes the generalities of the double source constituted by a THz Free-Electron Laser Oscillator and by a X-ray Thomson source driven by the same electron beam. Section III presents the numerical results of the FEL and Thomson sources. We conclude by presenting considerations about the optimal layout and discussing the possibility of developing such a device.

DUAL SOURCE GENERALITIES

A SC Energy Recovery Linac (ERL) is required because the FEL Oscillator is based on the passage of successive electron beams at large repetition rate inside the undulator and the energy recovery option allows for sustainable radiation generation. The ERL is similar to those described in [9, 10]. Table 1 presents values of the electron beam parameters given by start to end simulations. The electron beam provides THz radiation with interesting properties and, at the same time, suitable for driving Thomson back-Scattering.

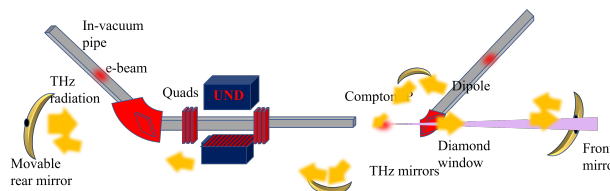


Figure 1: Dual source of THz and X-ray radiation. The cavity is constituted by four mirrors. The Thomson interaction point is on the right. E-beam and THz radiation interact at angle.

Figure 1 shows an option based on a four mirror cavity of the radiation source layout. After the first reflection off-axis, the radiation is obliquely sent to the Thomson interaction point (IP) by a second mirror, the scattering taking therefore place at a small angle. The THz radiation circumvents the

* Marcel.Ruijter@mi.infn.it

A PULSE SHAPER FOR DIRECT GENERATION OF 515 nm 3D ELLIPSOIDAL PULSES AT PITZ

A. Hoffmann†, J. Good, M. Gross, C. Koschitzki, M. Krasilnikov, H. Qian, F. Stephan
DESY, Zeuthen, Germany

Abstract

In this paper, a cathode laser pulse shaper at 515 nm is presented that will be used for emittance optimizations. In case alkali antimonide photocathodes are used, the shaped green pulses can be applied directly for photoemission while Cs₂Te photocathodes requires second harmonic generation to provide UV laser pulses. Recent tests of CsK₂Sb photocathodes in the high gradient RF gun at PITZ are first steps for the future usage of green laser pulses, which would simplify the requirements for the photocathode laser system, especially for CW operation cases envisioned in future. As long the alkali antimonide photocathodes are not in regular use yet, the laser pulses need to be converted into the UV. The green pulse shaper still simplifies the laser system since two conversion stages from IR to green to UV were needed in the past, which dilutes the quality of the shaped laser pulses. In this paper, a pulse shaper for 515 nm wavelength is presented that is expected to further improve the beam emittance generated by 3D ellipsoidal laser shaping.

INTRODUCTION

X-ray free electron lasers require short, high-brightness electron bunches with up to 1 nC charge. However, high charge and low emittance are conflicting goals due to space charge. To overcome this limitation an electron bunch with linear space charge force should be used which simplifies the electron transport [1]. The electron distribution with a linear space charge field is a uniform ellipsoidal electron bunch. To generate such electron distributions with high bunch charge in photoinjectors, the driving photocathode laser pulse should have a 3D ellipsoidal shape [2]. At the Photo Injector Test Facility at DESY in Zeuthen (PITZ), we investigate the generation of 3D ellipsoidal laser pulse shapes experimentally, among other techniques, mainly by spatial light modulator (SLM) pulse shapers [3-7].

For Cs₂Te photocathodes UV laser pulses have to be used and pulse shaping devices in that wavelength range have either low efficiency or are not suited for high average power. Pulse shaping schemes in the NIR are well established for 800 nm or 1030 nm, but frequency conversion of the shaped pulses to UV is limited by a compromise between conversion efficiency and pulse shape preservation.

In this paper, we present a pulse shaper that operates at 515 nm being a good compromise of having powerful lasers and the availability of efficient pulse shaping devices

for operation with 1 MHz repetition rate at several watts of average power. The wavelength of 515 nm has the advantage of direct pulse shaping for CsK₂Sb photocathodes without any frequency conversion step involved and for Cs₂Te only one conversion section for second harmonic generation (SHG) is required to achieve 257 nm wavelength.

The pulse shaper is based on a liquid crystal on silicon spatial light modulator (LCOS SLM) in a 4f zero dispersion stretcher geometry for applying amplitude shaping of chirped pulses. First experiments showing the preservation of a parabolic pulse shape in the UV are presented.

PULSE SHAPER AND DIAGNOSTICS

Green laser pulses (515 nm, 10 μJ, 265 fs, 1 MHz) are sent through a transmission grating stretcher to generate 10 ps chirped pulses, which afterwards enter the pulse shaper.

Amplitude Shaping

With the advance of LCOS SLMs shaping of femtosecond pulses became a standard technique for generation of user-specified waveforms [8]. Here, we use amplitude shaping of chirped picosecond pulses to mask the desired pulse shape from a Gaussian distribution that is coupled temporally and spectrally. A folded 4f zero dispersion stretcher of a cylindrical lens with the LCOS SLM in the image plane allows for shaping one spatial component and the spectrum. The amplitude shaping is realized by insertion of a quarter-wave plate in the beam path of the shaper. The second pass over the transmission grating at the exit of the shaper serves as a polarization filter. After image rotation by 90 degrees a second shaper is entered allowing to shape the other spatial component. With this, full 3D control over the pulse shape becomes possible. As feedback for the pulse shape optimization a high-resolution Czerny-Turner imaging spectrometer is used.

SHG FROG

Frequency-resolved optical gating (FROG) is a general method for measuring the spectral phase of ultrashort laser pulses and the standard technique for characterizing ultrashort laser pulses. In a FROG measurement a pulse gates itself in a nonlinear-optical medium and the resulting gated piece of the pulse is then spectrally resolved as a function of the delay between the two pulses. Retrieval of the pulse from its FROG trace is accomplished by using a two-dimensional phase-retrieval algorithm [9].

† andreas.hoffmann@desy.de

RF PERFORMANCE OF A NEXT-GENERATION L-BAND RF GUN AT PITZ

M. Krasilnikov*, Z. Aboulbanine, G. Adhikari, N. Aftab, P. Boonpornprasert, M.-E. Castro-Carballo, G. Georgiev, J. Good, M. Gross, A. Hoffmann, L. Jachmann, W. Koehler, C. Koschitzki, X.-K. Li, A. Lueangaramwong, D. Melkumyan, R. Niemczyk, A. Oppelt, S. Philipp, M. Pohl, B. Petrosyan, H. Qian, C. Richard, J. Schultze, G. Shu, F. Stephan, G. Vashchenko, T. Weilbach, DESY, Zeuthen, Germany

M. Bousonville, F. Brinker, L. Knebel, D. Kostin, S. Lederer, L. Lilje, S. Pfeiffer, M. Hoffmann, R. Ritter, H. Schlarb, S. Schreiber, H. Weise, M. Wenskat, J. Ziegler, DESY, Hamburg, Germany

Abstract

A new generation of high-gradient normal conducting 1.3 GHz RF gun with 1% duty factor was developed to provide a high-quality electron source for superconducting linac driven free-electron lasers like FLASH and European XFEL. Compared to the Gun4 series, Gun5 aims for a ~50% longer RF pulse length (RF pulse duration of up to 1 ms at 10 Hz repetition rate) combined with high gradients (up to ~60 MV/m at the cathode). In addition to the improved cell geometry and cooling concept, the new cavity is equipped with an RF probe to measure and control the amplitude and phase of the RF field inside the gun. The first characterization of Gun5.1 included measurements of RF amplitude and phase stability (pulse-to-pulse and along 1 ms RF pulse). The dark current was measured at various peak power levels. The results of this characterization will be reported.

INTRODUCTION

The Photo Injector Test Facility at DESY in Zeuthen (PITZ) develops, tests and characterizes high brightness electron sources for FLASH and European XFEL for more than 20 years. Since these user facilities operate superconducting accelerators in pulsed mode, the corresponding normal-conducting L-band RF gun also has to operate with long RF pulses at 10 Hz repetition rate. To obtain high electron beam quality from a photocathode RF gun, a high acceleration gradient at the cathode is required. The peak RF electric field of 60 MV/m at the cathode is considered as a goal parameter for a high brightness L-band photogun. Therefore, the RF gun has to provide stable and reliable operation at high average RF power. The previous gun cavity generation (Gun4) had a maximum RF pulse length of 650 μ s, which implies a maximum of 27000 electron bunches per second. Growing interest from the FEL user community for even longer pulse trains motivated developments of the next generation of normal conducting L-band gun cavity (Gun5), which aims for 1 ms RF pulses. Combined with 6.5 MW of peak RF power, this results in a very high average power of ~65 kW. In addition to the improved resonator shape and cooling, Gun5 has a built-in RF probe to directly control the phase and amplitude of the RF field in the cavity. RF conditioning faces issues of

stability and reliability. Aspects of pulsed heating and dark current should also be considered.

GUN5.1 SETUP AT PITZ

The RF gun cavity is a 1½-cell normal conducting copper cavity operating in a π -mode standing wave at 1.3 GHz. The Gun5 design includes several major improvements over the Gun4-generation, which are aimed at improving the performance of the gun. An elliptical shape of the internal geometry was applied in order to optimize the distribution of the peak electric field over the cavity surface [1]. Detailed studies to reduce the dark current resulted in an elliptical shape of the cathode hole at the back wall of the cavity [2]. In order to control the RF field in the cavity directly, an RF probe has been integrated in the front wall of the full cell. An optimized cavity cooling system and improved rigidity [1] should mitigate the challenges associated with the 1% duty cycle.

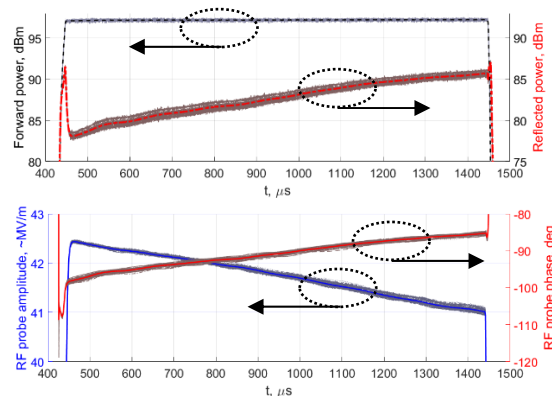


Figure 1: RF signals from 1 ms pulses. Top plot – directional coupler signals. Bottom plot: corresponding RF probe (pickup) signals.

The Gun5.1 RF feed setup was taken over from the waveguide distribution system of the previous generation of guns (Gun4.x) [3], including two waveguides (WG1,2) with two 5MW directional couplers (WG1,2 5 MW), followed by RF windows and a T-combiner in vacuum. The combined RF feed can be controlled by the 10 MW directional coupler (as was the case in recent Gun4.x generation setups) or by the newly installed RF pickup in the cavity. Typical RF signals for 1 ms RF pulses are shown in Fig. 1,

DEVELOPMENT AND TEST RESULTS OF MULTI-ALKALI ANTIMONIDE PHOTOCATHODES IN THE HIGH GRADIENT RF GUN AT PITZ

S.K. Mohanty¹, H. Qian, Z. Aboulbanine, G. Adhikari, N. Aftab, P. Boonpornprasert, J. Good, M. Gross, A. Hoffmann, M. Krasilnikov, A. Lueangaramwong, R. Niemczyk, A. Oppelt, F. Stephan, T. Weilbach, DESY, Zeuthen, Germany

D. Sertore, L. Monaco, Istituto Nazionale di Fisica Nucleare - LASA, Segrate, Italy
G. Guerini Rocco, C. Pagani, Università degli Studi di Milano & INFN, Segrate, Italy
W. Hillert, University of Hamburg, Germany

G. Loisch, DESY, Hamburg, Germany

¹also at INFN-LASA, Segrate, Italy

Abstract

Multi-alkali antimonide photocathodes can have high quantum efficiency, similar to UV sensitive (Cs₂Te) photocathodes, but with the advantages of photoemission sensitivity in the visible region of the light spectrum and a significant reduction in the mean transverse energy of photoelectrons. A batch of three KCsSb photocathodes was grown on molybdenum substrates via a sequential deposition method in a new preparation system at INFN LASA. Afterward, the cathodes were successfully tested in PITZ's high gradient RF gun. This contribution summarizes the experimental results obtained in both the preparation chamber and the RF gun. Based on those findings, we are now optimizing the recipe of KCsSb and NaKSb(Cs) photocathodes for lower field emission and longer lifetime, and the measurements for the latest photocathode with the improved recipe are also presented.

INTRODUCTION

High brilliance and high current electron beam with MHz repetition rate are the critical components for next-generation X-FEL [1,2]. To obtain these features, it requires an electron source of high quantum efficiency ($\geq 1\%$), low thermal emittance (< 1 mm. mrad/mm), and long lifetime (> 1 week) [3]. In recent years, different studies show that owing to its high QE (quantum efficiency), low emittance, and fast response time in the visible range, KCsSb-based photocathode material has emerged as a prominent candidate for these applications. However, these cathodes have some limiting factors like their high sensitivity towards the vacuum condition, which reduces their lifetime inside the RF guns.

This kind of photocathode material has successfully been demonstrated in various DC and continuous wave (CW) guns at low gradients (< 20 MV/m) [4,5], and the parameters like QE and thermal emittance are found to be very promising. Recently, it has been demonstrated that these kinds of cathodes can sustain a month of long continuous operation inside a QWR SRF gun [6]. However, to improve the brightness of the electron beam in next-generation CW guns, it requires even higher cathode gradients (30-40 MV/m) for various applications.

So, our current research domain is mainly focused on developing these materials and exploring their feasibility for high gradient operation at the PITZ RF gun for a future upgrade of the European XFEL facility. For the development part of the KCsSb-based photocathodes, DESY collaborated with INFN LASA, which has long-standing experience in studying and growing of semiconductor-based photocathode material. The first batch of three KCsSb cathodes with different thicknesses has been prepared and successfully tested at the PITZ RF gun. In this paper, the preparation and test results of these photocathodes are presented.

PHOTOCATHODE PREPARATION

As it is reported in previous papers [7-10], a reproducible recipe has been established for KCsSb photocathode in our R&D development system at INFN LASA. As it is described, the molybdenum substrates used in the R&D setup were not suitable to be loaded into an RF gun. So, another UHV preparation chamber has been prepared similar to Cs₂Te photocathode preparation system, which is suitable for producing the cathode film on the standard INFN Mo plugs. The new UHV preparation system has been equipped with the standard UHV devices (pressure gauges, a residual gas analyzer, and manipulators), two vacuum pumps (a combination of sputter-ion pump and NexTorr from SAES Getters), and a newly designed Mo plug heater. A custom-made source for Sb and commercially available Cs, Na, and K dispensers are used for the deposition. Each source is carefully pre-heated before starting of the deposition and calibrated to have the proper evaporation rate during the cathode growth. The usual deposition rate of 1 nm/min is used for the deposition in this case. A total number of four Mo plugs were polished to a mirror-like finishing (reflectivity $> 54\%$ at 543 nm w.r.t. 57% theoretical [11]) to allow reflectivity measurements during and after the photocathode growth. All samples are ultrasonically cleaned before loading them into the UHV system. Before the deposition, each cathode plug was heated up to 450 °C for at least one hour to remove the eventual residuals on the surface. By following the R&D experiences, three KCsSb cathodes have been prepared through a sequential deposition method. Out of which, two are thin (Sb=5 nm) and one thick (Sb=10 nm) cathodes. The detailed recipe parameters of produced photo cathodes are discussed in the

† sandeep.mohanty@desy.de

RADIO-FREQUENCY-DETUNING BASED MODELING AND SIMULATION OF ELECTRON BUNCH TRAIN QUALITY

Y. Chen*

Deutsches Elektronen-Synchrotron DESY, Hamburg, Germany

Abstract

A numerical study is carried out on the quality of the electron bunch train produced from a photoinjector based on a frequency-detuning dependent gun coupler kick. The impact of the kick on the emittance of the bunch train is modelled via three-dimensional electromagnetic field maps calculated at detuned frequencies of the gun cavity within long radio-frequency pulses. Beam dynamics simulations are performed in the so-called frequency-detuning regime. Preliminary results are presented and discussed.

INTRODUCTION

Radio-Frequency (RF) photoinjectors provide high brightness electron bunches for modern linear accelerator based free-electron lasers (FEL) [1–7]. At the European XFEL [2] (EuXFEL), the photoinjector [8] consists of an L-Band RF gun, a TESLA type 1.3 GHz module (A1), a 3rd harmonic RF section (AH1), a laser heater and beam diagnostics, as shown in Fig. 1. The 1.6-cell 1.3 GHz RF gun [9] can be operated with an electric field gradient of 60 MV/m on the cathode surface with long RF pulses of up to 650 μ s at 10 Hz, allowing the production of 27000 bunches per second at the EuXFEL. The RF power is provided by a 10 MW multi-beam klystron and fed to the gun from the input waveguide via a door-knob transition into the rotationally symmetric coaxial coupler and the gun cavity. A frequency-detuning dependent transient coaxial RF coupler kick is observed and characterized within the RF pulse in [10]. The impacts of the effect on the electron bunch quality along the train are more pronounced towards longer RF pulse operation of the FEL.

Since the first lasing of the EuXFEL in May 2017 [11], a growing trend in the RF pulse length of the gun has been shown for routine user experiments, i.e. from averagely 100 μ s in 2017 to first-time operating with 600 μ s by the end of 2019, subsequently, stably running with 500 μ s and above until the present. With more pronounced frequency-detuning over longer RF macropulses, potential impacts of the above-mentioned RF coupler kick on the bunch quality along the train should be further studied.

METHODOLOGY

Experiments have shown the existence of frequency detuning of the gun cavity within the RF macropulse due to pulse heating [10]. Within the RF pulse, individual electron bunches along the train see the transverse coaxial coupler kick of the gun. The kick is varied as a function of the

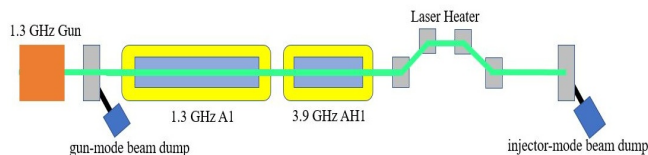


Figure 1: Schematic view of the European XFEL photoinjector (not to scale).

frequency detuning of the gun cavity. Thus, the variable kick added to different bunches along the train and the resulting impact onto the bunch quality can be modelled as these bunches passing through the gun while experiencing disturbed and detuned RF field distributions of the gun cavity. This method requires RF field calculations at detuned frequencies as well as corresponding beam dynamics simulations using these field maps, as presented in the following two sections.

ELECTROMAGNETIC FIELDS

The three-dimensional calculation of the disturbed RF cavity field due to the gun coupler kick is based on the frequency domain solver of Computer Simulation Technology [12]. A computational model with its coordinate system is described in [10]. The frequency detuning (Δf) is defined as the difference between the RF drive frequency (f) and the cavity resonance frequency (f_0), i.e. $\Delta f = f - f_0$. In the following example, the S11 parameter, defined as the ratio of the reflected power over the forward power for a resonant cavity, is tuned to about -25 dB at the resonance. Figure 2 shows the disturbed transverse electric (E_y) and magnetic (H_x) field profiles at different detuned frequencies of the gun cavity, covering a detuning range up to +15 kHz towards a deeper over-heating state of the gun.

SIMULATIONS

Beam dynamics simulations are performed using ASTRA [13]. A simulation setup is sketched in Fig. 1. Electron bunches are tracked with on-crest RF phasing until the exit of the A1 module. The final beam energy is 150 MeV. Note, in addition, that a three-dimensional TESLA cavity field map of the A1 module is also applied [14, 15].

Figure 3 shows a comparison of the projected transverse emittance evolution along the beamline between two simulation cases. One of the cases (blue curve) serves as a reference, in which, under ideal conditions, no coupler kick effects are considered. In the other case (orange curve), a specific situation is emulated: a bunch travels through the gun and the A1 module both of which are described by the

* ye.lining.chen@desy.de

PHOTOCATHODES FOR THE ELECTRON SOURCES AT FLASH AND EUROPEAN XFEL

D. P. Juarez-Lopez*, F. Brinker, S. Lederer, S. Schreiber
Deutsches Elektronen-Synchrotron DESY, Hamburg, Germany
L. Monaco, D. Sertore, INFN Milano - LASA, Segrate, Italy

Abstract

The photoinjectors of FLASH at DESY (Hamburg, Germany) and the European XFEL are operated by laser driven RF-guns. In both facilities cesium telluride (Cs_2Te) photocathodes are successfully used since several years. We present recent data on the lifetime and quantum efficiency (QE) of the photocathodes currently in operation. In addition we present the latest data of the cathode #680.1 which holds the operation record time of 1452 days with a total charge extracted of 32.2 C.

INTRODUCTION

The FLASH accelerator is a free-electron laser (FEL) user facility since 2005 [1–4], located in DESY (Hamburg, Germany) and provides ultra-short femtosecond laser pulses in the extreme ultra-violet and soft X-ray wavelengths range with unprecedented brilliance to two photon experimental halls. The macro-pulse repetition rate is 10 Hz with a usable length of the RF pulses of 800 μs . With a micro-bunch frequency of 1 MHz up to 8000 bunches per second are accelerated at FLASH. The bunch charge depends on the requirements on the FEL-light and is usually within a span of 20 pC to 1 nC. After the electron beam is accelerated to 1.25 GeV, the electron bunches are distributed into two different undulator beamlines.

The European XFEL [5] is the longest superconducting linear accelerator in the world driving a hard X-ray free-electron laser. The accelerator is operated by DESY. After a successful commissioning in 2016 [6] and first lasing in May 2017 [7], first user periods have been successfully accomplished [8]. The European XFEL runs now in full swing delivering high brilliance femtosecond short X-ray pulses in the energy range of 0.25 to 25 keV. The European XFEL uses upgraded TESLA type superconducting linac technology similar to FLASH with 10 Hz macro-pulse repetition rate. With a micro-bunch frequency of up to 4.5 MHz and an RF-pulse length of 600 μs , the European XFEL can deliver 27000 bunches per second.

ELECTRON SOURCES

The electron sources of FLASH and the European XFEL are very similar. Both photoinjectors are driven by a normal conducting 1.3 GHz L-band RF-gun, based on the design by [9]. Cs_2Te cathodes have been chosen to generate the photoelectrons bunches in both facilities. The electron bunches

at FLASH are generated by three drive laser systems operating at a wavelength of 262 nm and 257 nm [10], while both laser at the European XFEL operates at 257 nm. All Cs_2Te photocathodes have a high quantum efficiency (QE) that keeps the required average laser power for multi-bunch operation in a reasonable regime. The vacuum pressure in the RF-guns during operation is in the low 10^{-9} mbar range. These excellent vacuum conditions are crucial for the lifetime of Cs_2Te cathodes.

Currently the accelerating field at the photocathode during standard operation at FLASH is 50 MV/m and 54 MV/m for the European XFEL. In both facilities the whole gun setups are interchangeable between each other. Gun 3.1 was in operation at FLASH since 2013 [11] and has been exchanged in December 2019 for Gun 4.4 due to a leak in the cooling water circuit. Installed in 2013, Gun 4.3 was the first RF-gun operated at the European XFEL, during commissioning phase and first user runs. In December 2017 it was exchanged for Gun 4.6 and serves now as hot spare.

The photocathodes are either prepared at INFN-LASA in Milano, Italy, [12] or at DESY Hamburg. The transfer to the accelerators is done with ultra-high-vacuum (UHV) transport boxes, maintaining a pressure in the low 10^{-10} mbar range. The transport boxes can be equipped with up to four cathodes, one place is void. In both facilities a very similar load-lock transfer system is used to insert the Cs_2Te photocathodes under the required UHV conditions into the RF guns [12].

QUANTUM EFFICIENCY AND LIFETIME

QE Measurement Procedure

The QE is monitored after cathode production in the lab where the spectral response is measured with a Hg-lamp for 6 different wavelengths. A QE map is generated after production to understand its uniformity and to be able to compare the map afterwards with in situ measurements.

In situ, the cathode performance is monitored on regular bases. The QE measurements in the gun are always taken under comparable conditions, such as:

- The on-crest accelerating field during the measurements is in the order of 52 MV/m.
- The charge is measured with a toroid right after the RF-gun (uncertainty 1%).
- The launch phase is set to 38° w.r.t. zero crossing. This phase was chosen years ago and kept as reference for all QE measurements.

Regarding the phase, the measurement is neither at the on-crest phase nor at the launch phase during standard operation

* pavel.juarez@desy.de

GENERATION OF A SUB-PICOSECOND SHEET ELECTRON BEAM USING A 100 fs LASER

M. Asakawa[†], S. Yamaguchi, Y. Karaki, H. Matsubara, Y. Miyajima, R. Michishita, T. Shirai, R. Horii and S. Yoshimatsu, Kansai University, Suita, Japan
M. Nakajima, Institute of Laser Engineering Osaka University, Suita, Japan

Abstract

In this paper, we present the experimental results of a pulsed sheet-like photoelectron bunch generated by irradiating an elliptically focused 100 fs laser. The sheet-like bunch has the same space-charge limitation as the circular bunch. In the contrast, the anisotropic diverging property of the sheet-like bunch was observed: the diverging angle along the minor axis of the photoemission area was greater than that along the major axis. In addition, the net diverging angle of the sheet bunch seemed to be smaller. Based on our results, we propose a new kind of Peirce gun to compensate for the diverging angle along the minor axis.

INTRODUCTION

One of the most promising electron sources is the sub-picosecond laser driven DC photoelectron gun, capable of producing an ultrashort electron bunch with a duration of less than 1 ps and a charge of 10 pC and has been developed specifically for use as an ultrafast electron microscope instrument [1-3]. However, for the radiation source application, which requires a charge of 100 pC, electrons suffer from a strong self-field at the emission surface due to the ultrashort pulse duration, which causes them to increase their phase space volume, as previously reported [4].

In contrast, the sheet electron beam formation is being investigated for high-power microwave sources because the sheet electron beam interacts efficiently with the planar radiative structures [5-8]. Several methods have been studied to form the sheet electron beam: a round beam produced by the thermionic cathode Pierce gun was transformed into a sheet beam using a quadrupole magnet or an asymmetric solenoid lens, a specially designed sheet beam Pierce gun, and direct emission from a blade-like metallic cathode. Those studies aimed to produce a DC or long pulse current.

In this paper, we will present a preliminary attempt to generate a sheet-like electron bunch via photoemission using an elliptically focused 100 fs laser. The focal spot was an ellipse with an ellipticity of 43. With this ellipticity, the circumference of the sheet-like bunch is 4.2 times longer than that of a round beam with the same cross-section. Thus, the sheet-like bunch has a larger surface area. According to Gauss's law, the electric field on the surface of the sheet-like bunch should be significantly reduced. Based on this idea, we investigated the diverging angle of the sheet-like bunch.

[†] asakawa@kansai-u.ac.jp

EXPERIMENT

Figure 1 shows the experimental apparatus. The driving laser was a Ti:sapphire laser operated at a repetition rate of 1 kHz. At the fundamental wavelength of 800 nm, the average power was 2.5 W and the pulse-duration was 92 fs. At a third harmonic generator, the laser pulse was converted to the ultraviolet pulse with a wavelength of 266 nm (4.65 eV) and an average power of 200 mW. Then, the UV pulse passed through a pair of beam-splitters, changing the injection angle of the laser to the splitters by rotating them, with the transmitted power regulated from 0 to 150 mW. The UV pulse was focused by a convex lens or a cylindrical lens to generate a round electron bunch or a sheet-like bunch, respectively. Finally, the UV pulse was irradiated in a tungsten cathode ($\phi = 4.52$ eV), which was held at the negative voltage, by passing through a single crystalline quartz window placed in the vacuum vessel. With the convex lens, the spot area on the cathode formed an ellipse of $\pi \times 1.5$ (horizontal direction) $\times 0.75$ (vertical direction) mm^2 due to the injection angle of 60° . The injection angle also resulted in an optical path difference of $2 \times 1.5 \text{ mm} \times \sin 60^\circ$ in the incident plane, resulting in a time lag of 8.7 ps at most. The cylindrical lens was placed so that the laser spot had the same area: the expected size was $\pi \times 0.185 \times 6 \text{ mm}^2$ and the ellipticity was 32. The electron bunch in the region of the emission area should form a line-like shape rather than a sheet because of the short duration of the drive laser. In this case, the time lag was reduced to $2 \times 0.185 \text{ mm} \times \sin 60^\circ / 3 \times 10^{11} \text{ mm/s} = 1.1 \text{ ps}$.

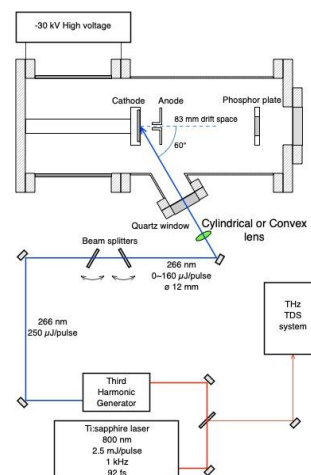


Figure 1: Experimental apparatus.

EXPERIMENTAL DEMONSTRATION OF TEMPORALLY SHAPED PICOSECOND OPTICAL PULSES FOR DRIVING ELECTRON PHOTOINJECTORS

R. Lemons^{*}, N. Neveu, J. Duris, A. Marinelli, C. Durfee, S. Carbajo

SLAC National Accelerator Laboratory, 2575 Sand Hill Rd, Menlo Park CA, 94061, USA

Colorado School of Mines, 1500 Illinois St, Golden CO, 80401, USA

University of California, Los Angeles, 420 Westwood Plaza, Los Angeles, CA 90095

Abstract

Next-generation electron photoinjector accelerators, such as the LCLS-II photoinjector, have increasingly tight requirements on the excitation lasers, often calling for tens of picosecond, temporally flat-top, ultraviolet (UV) pulse trains to be delivered at up to 1 MHz. We present an experimental demonstration of temporal pulse shaping for the LCLS-II photoinjector laser resulting in temporally flat-top pulses with 24 ps durations. Our technique is a non-collinear sum frequency generation scheme wherein two identical infrared optical pulses are imparted with equal and opposite amounts of spectral dispersion. The mixing of these dispersed pulses within a thick nonlinear crystal generates a second harmonic optical pulse that is spectrally narrowband with a designed temporal profile [1]. In the experiment, we achieve upwards of 40% conversion efficiency with this process allowing this to be used for high average and peak power applications. These narrowband pulses can then be directly upconverted to the UV for use in driving free electron laser photocathodes. Additionally, we present a theoretical framework for adapting this method to shape optical pulses driving other photoinjector-based applications.

INTRODUCTION

In photoinjectors, electrons are generated via the photoelectric effect with laser pulses comprised of light above the work function of the material. During emission, the temporal intensity profile of the laser pulse can significantly affect electron bunch quality. A key measure of quality is the transverse emittance, ϵ_x , defined as [2]

$$\epsilon_x = \sqrt{\langle x_i^2 \rangle \langle x_i'^2 \rangle - \langle x_i x_i' \rangle^2} \quad (1)$$

where x is the transverse position and x' is the corresponding angle with respect to the ideal trajectory. For generation of x-rays from x-ray free electron lasers (XFELs), it is critical to have electron bunches that are generated with low emittance ($< 1.5 \mu\text{m}$), narrow energy spread ($\Delta E/E < 10^{-3}$), and good spatial uniformity [3]. The latter two quantities can be improved to some extent after generation through the use of spatio-temporally shaped IR lasers in laser heaters [4–6], however initial transverse emittance is dominantly controlled through the temporal intensity profile of the excitation laser

pulse. Conventionally implemented photoexcitation laser profiles are Gaussian in time though other commonly sought-after laser distributions are shown to reduce transverse emittance such as flat-top spatiotemporal profiles resembling cylinders [7] or 3D ellipsoids such that the beam size and intensity vary as a function of time [8].

Producing excitation laser pulses with non-Gaussian temporal intensity profiles and duration on the order of 10s of picoseconds is non-trivial. Pulses of the temporal duration lack the spectral content for shaping methods such as spatial-light modulators [9] or acousto-optic modulators [10] to be effective and are shorter than the response time for direct temporal electro-optic modulators [11]. Additionally, the high-repetition rate and pulse energy requirements of next-generation XFELs such as LCLS-II [12] approaches or exceeds the material damage threshold for these devices [13] further complicating their use for shaping the excitation laser pulses. One method that has seen promise for pulse shaping for XFEL facilities is pulse stacking [14] where multiple copies of a short pulse are coherently added in time to generate the desired composite intensity profile. However, pulses generated with the method have been shown to induce unwanted microbunching [15, 16] on the electron bunch resulting in increased emittance relative to Gaussian distributions. Furthermore, the series of nonlinear conversion stages to upconvert infrared (IR) light to UV light below 270 nm [17, 18] present in all XFEL photo-excitation laser systems is detrimentally affected by non-zero phase structure on the pulses, distorting temporal profiles, complicating shaping efforts, and limiting the applicability to high average power, 24/7 facilities.

We present a non-collinear sum frequency generation (NC-SFG) technique that inherently incorporates temporal intensity shaping [1]. Our method is characterized by the mixing of two highly dispersed pulses (Fig. 1) which combine during sum-frequency generation to generate a pulse with a tailored temporal intensity profile. We expand on Raoult et al [19] of efficient narrowband second harmonic generation in thick crystals by adding third-order dispersion to simultaneously shape the output pulse. This method, which we call dispersion controlled nonlinear shaping (DCNS), can be broadly used to tailor pulses for the reduction of transverse emittance in photoinjector-based instrumentation.

^{*} rlemons@slac.stanford.edu

REAL-TIME PROGRAMMABLE SHAPING FOR ELECTRON AND X-RAY SOURCES

Jack Hirschman^{*1,2}, Randy Lemons^{2,3}, Ravi Saripalli², Federico Belli⁴, and Sergio Carbajo^{2,5,6}

¹Department of Applied Physics, Stanford University, 348 Via Pueblo, Stanford, CA 94305, USA

²SLAC National Accelerator Laboratory, 2575 Sand Hill Rd, Menlo Park, CA 94025, USA

³Colorado School of Mines, 1500 Illinois St, Golden, CO 80401, USA

⁴School of Engineering and Physical Sciences, Heriot-Watt University, Edinburgh, EH14 4AS, UK

⁵Electrical and Computer Engineering Department, UCLA, 420 Westwood Plaza, Los Angeles, CA 90095, USA

⁶Physics and Astronomy Department, UCLA, 475 Portola Plaza, Los Angeles, CA 90095, USA

Abstract

The next generation of augmented brightness X-ray free electron lasers (XFELs), such as the Linac Coherent Light Source-II (LCLS-II), promises to address current challenges associated with systems with low X-ray cross-sections. Typical photoinjector lasers produce coherent ultraviolet (UV) pulses via nonlinear conversion of an infrared (IR) laser. Fast and active beam manipulation is required to capitalize on this new generation of XFELs, and controlling the phase space of the electron beam is achieved by shaping the UV source and/or via IR shapers [1, 2]. However current techniques for such shaping in the UV rely on stacking pulses in time, which leads to unavoidable intensity modulations and hence space-charge driven microbunching instabilities [3]. Traditional methods for upconversion do not preserve phase shape and thus require more complicated means of arriving at the desired pulse shapes after nonlinear upconversion [4]. Upconversion through four-waving mixing (FWM) allows direct phase transfer, convenient wavelength tunability by easily changeable phase matching parameters, and also has the added advantage of greater average power handling than traditional $\chi(2)$ nonlinear processes [5, 6]. Therefore, we examine a possible solution for e-beam shaping using a machine learning (ML) implementation of real-time photoinjector laser manipulation which shapes the IR laser source and then uses FWM for the nonlinear upconversion and shaping simultaneously. Our presentation will focus on the software model of the photoinjector laser, the associated ML models, and the optical setup. We anticipate this approach to not only enable active experimental control of X-ray pulse characteristics but could also increase the operational capacity of future e-beam sources, accelerator facilities, and XFELs [7].

*jhirschm@stanford.edu

INTRODUCTION AND MOTIVATION

Ground-up design of high power chirped pulse amplification (CPA) systems is not trivial. Choosing the correct hardware and determining limitations for a particular laser system—such as damage thresholds for optics [8] and amplifiers as well as bandwidth limitations for shaping—can be a challenging task, especially for systems involving custom design amplifiers, pre-CPA programmable pulse shapers, or a series of up-/down-conversion stages. Start-to-end (S2E) software models can greatly inform laser system design decisions and aid in understanding limitations or trade-offs in performance parameters. To an even greater extent, as we enter new stages of ML-driven photonics and optical system design [9], the need for S2E-based data generation to inform these ML models and reduce parameter searches in the lab will become increasingly desired. Furthermore, the potential symbiosis between experiment and software model means experiment can improve the S2E models, which in turn can drive improvements in the system design. This relationship with experiment-corrected software model design could even open the possibility for using these models for material design via inverse engineering.

At LCLS-II, we are developing real-time adaptable photoinjector shaping techniques to increase the electron beam brightness and enhance future modes of X-ray lasing operation, some of which may require advanced models, such as machine learning, to determine optimal spatio-temporal distribution of the photoinjector laser pulses. Thus, we have developed and used this S2E model to both determine the limitations of our pulse shaping techniques and to generate data for training the ML models.

MODEL AND RESULTS

The LCLS-II photoinjector laser system starts with an IR mode-locked oscillator shaped in spectral phase and amplitude by an acousto-optic programmable dispersive filter,

UNIVERSAL TOOL FOR THz RADIATION ANALYSIS

M. Gerasimov, E. Dyunin, J. Gerasimov, A. Friedman

Department of Electrical and Electronic Engineering, Ariel University, Ariel, Israel

Abstract

We present here a tool for the 3D THz Radiation Analysis. The tool is a homemade simulation built from scratch in a Python code. A final goal of the simulation is a design of a Transmission Line (TL) for a wide tunable broad-spectrum THz radiation source. The TL is designed to be a component of the construction of an innovative accelerator at the Schlesinger Family Center for Compact Accelerators, Radiation Sources & Applications (FEL). A 3D space-frequency tool for a diagnostic of radiation pulse perform by the Wigner Distribution Function (WDF). This EM field is converted to geometric-optical ray representation at any desired resolution. WDF's representation allows to describe the dynamics of field evolution in future propagation, which allows us to determine an initial design of the TL. The EM field representation in terms of rays gives access to the Ray Tracing method and future processing, operating in the linear and non-linear regimes. A parallel processing, with graphics cards can be used which provides great flexibility and as a future preparation that able to apply advanced libraries such as machine learning. The tool can be used to study the phase-amplitude and spectral characteristics of multimode radiation generation in a free-electron laser (FEL), operating in various operational parameters.

INTRODUCTION

Terahertz (THz) radiation refers to electromagnetic waves which lengths are 80 – 1000 μm (corresponding to the 3.75 – 0.3 THz). A main THz radiation feature is transmission through various types of media as plastics, ceramics, paper, textiles wood, etc. They enable to perform non-destructive analysis, also, can detection hidden internal substances. Thus, THz research and applications have become widely popular and accessible [1,2]. In other side, the THz propagation is not straightforward. It has light waves properties on one hand and an electromagnetic on the one other. Hence, the THz propagation calculation is not trivial task. A goal of this work is a characterization of ultra-short of THz source. The source is a FEL under construction at the Schlesinger Family Center for Compact Accelerators, Radiation Sources & Applications, Ariel University Ariel University [3]. This result will impact to planning of an early design of Transmission line (TL) under development. Figure 1 is showing THz FEL Setup (with the TL). A heart is a 6 MeV hybrid photo-injector has been designed and constructed, based on a smaller-scale prototype previously built in UCLA's Particle Beam Physics Laboratory.

Using classical calculation methods as well as commercial software like CST, FDTD, HFSS not achieved a desired result. These contents supposed to supply a limited solution to general problems, because that's how they are

designed. It is mostly an environment with a well-defined geometry and likewise the function of the signal itself must have a defined function. Otherwise no calculation will be performed. It is true that the numerical calculation of the problem can also be used. In these cases, reference files built in programs such as MATLAB, PYTHON, etc. are often used. In this case even definition of the initial signal is a problem. The FEL supposed to produce a defined pulse as in a single shot regime. But in reality, it is completely different. As it is already known in advance, each pulse will be different from the previous one due to many influencing parameters, such as: exact laser frequency, exact optical path, laser impact at exactly the same point on the cathode, if all this is met then in addition, the electron beam must pass evenly and radiate in exactly the same direction. Besides, the electron beam must enter the wiggler in exactly the same place. And finally, there are also mechanical vibrations of each component, temperature dependence and many other parameters. Apart from everything that has been detailed so far, the FEL is in the construction stages therefore at this stage an approximate model of the EM field obtained in the previous studies is used [4]. The model represents a total electromagnetic (EM) field on the edge of the source in the frequency domain in terms of cavity eigenmodes, realized in WB3D numerical code.

As mentioned above, the classical methods and the use of commercial software are not suitable in our case, due to excessive demand of memory and calculation resources an extended explanation is shown in the work [5]. This work approach is based on a transform to a light field [6]. In other words, the EM field is represented in terms of optical geometric rays. This representation allows the use of simple geometrical optics techniques, the characterization of the field beam on the aperture. The rays' directions of the allow diagnose the propagation of the EM field in a free space.

In most cases, the WDF [7] is calculated analytically, or calculated in more complicated cases. In this work we calculate the WDF for the general case. The simulation is built in such a way that it will allow future integration of artificial intelligence (AI) techniques. AI will be integrated in the future and should design the smart mirrors for transferring radiation in the most efficient way.

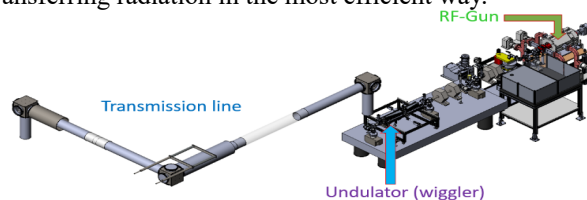


Figure 1: THz FEL Setup at the Schlesinger Center.

BRILLIANT X-RAY FREE ELECTRON LASER DRIVEN BY RESONANT MULTI-PULSE IONIZATION INJECTION ACCELERATOR

P. Tomassini^{1*}, ELI-NP, Magurele, Romania

¹also at CNR-INO, Pisa, Italy

L. Giannessi², A. Giribono, INFN-LNF, Frascati, Italy

²also at ELETTRA, Trieste, Italy

F. Nguyen, ENEA, Frascati, Italy

L. A. Gizzi³, CNR-INO, Pisa, Italy

³also at INFN, Pisa, Italy

Abstract

Laser Wakefield Accelerators are now sufficiently mature to provide GeV scale/high-brightness electron beams capable of driving Free Electron Laser (FEL) sources. Here, we show start-to-end simulations carried out in the framework of the EuPRAXIA project of a Free Electron Laser driven by an LWFA accelerator with the Resonant Multi-Pulse Ionisation Injection (ReMPI) setup. Simulations with this model using a 1 PW Ti:Sa laser system and a 20 cm long capillary, show the injection and acceleration of an electron beam up to 4.5 GeV, with a slice energy spread and a normalized emittance below 4×10^{-4} and 80 nm, respectively. The transport of the beams from the capillary exit to the undulator is provided by a matched beam focusing with a marginal beam-quality degradation. Finally, 3D simulations of the FEL radiation generated inside an undulator show that $\approx 10^{10}$ photons with central wavelength of 0.15 nm and peak power of ≈ 0.3 GW can be produced for each bunch. Our start-to-end simulations indicate that a single-stage ReMPI accelerator can drive a high-brightness electron beam having quality large enough to be efficiently transported to a FEL undulator, thus generating X-ray photons of brilliance exceeding 10^{31} ph/s/mm²/mrad²/0.1% bw.

INTRODUCTION

The use of Laser Wake Field Accelerators (LWFA) to produce beams capable of driving an FEL had been envisaged decades ago [1] due to their potentialities in terms of flexibility and compactness of the source. As the beam-quality required to drive an FEL is extremely demanding, high-quality both particle injection and acceleration schemes are required. In the last decade, therefore, a focus on high-quality injection and acceleration schemes has been provided. Remarkably, this long-term activity led to the first demonstration of FEL lasing in the X-ray range by beams produced a LWF accelerator with a density downramp injector, leading to a ≈ 500 MeV high-brightness beam with an estimated normalised emittance of about 200 nm [2]. Recently, an all-optical, high-quality injector using a Two-Color scheme [3] in a resonant wakefield excitation framework, has been proposed and numerically tested in different scenarios [4]. In the Resonant Multi-Pulse Ionisation injection (ReMPI), a tightly

* paolo.tomassini@eli-np.ro

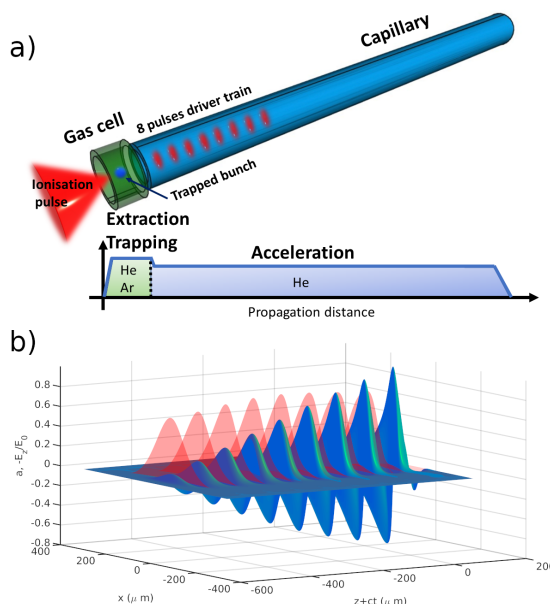


Figure 1: a) The LWFA layout with the ReMPI framework. The target consists of a 2mm long gas-cell filled with a mixture of He and Ar (50% + 50%). A 20 cm long He-filled capillary is placed just after the gas-cell. The large amplitude plasma wave excited by the train is able to catch and accelerate newborn electrons extracted by the fourth-harmonic ionizing pulse. The energy boosting up to 4.5 GeV is obtained by matching the transverse capillary size so as to guide a pulse with waist $w_{\text{matched}} = 65 \mu\text{m}$. Inside the capillary, the sub-pulses in the train remain well focused for the whole section, thus providing an efficient driver for the about 4.3 GeV of energy boost. b) Wakefield longitudinal electric field map (blue color) resonantly excited by the train of pulses (red color). Snapshot after 3cm of propagation.

focused, short-wavelength pulse acts as an *ionization* pulse as in the Two-Color scheme. Such a pulse extracts electrons from a dopant (e.g. Nitrogen, Argon or Krypton) and can be obtained by frequency doubling (or more) a portion of the Ti:Sa pulse. The remaining largest portion of the Ti:Sa pulse is time shaped as a sequence of (sub) pulses and focused on the target with a long parabola. Such a train of pulses is devoted to the resonant excitation of a large-amplitude

STABLE MULTI-DAY PERFORMANCE OF A LASER WAKEFIELD ACCELERATOR FOR FEL APPLICATIONS

J. P. Couperus Cabadağ*, S. Bock, Y.-Y. Chang, A. Debus, R. Gebhardt, A. Ghaith, U. Helbig, A. Irman, A. Koehler, M. LaBerge, R. Pausch, T. Püschel, U. Schramm, S. Schöbel, K. Steiniger, P. Ufer, O. Zarini, Helmholtz-Zentrum Dresden - Rossendorf, Dresden, Germany
E. Roussel, Univ. Lille, PhLAM, Lille, France
M.E. Couprie, M. Labat, Synchrotron SOLEIL, Saint-Aubin, France
M. C. Downer, University of Texas at Austin, Austin, Texas

Abstract

We report on the operation of the DRACO Laser Driven electron source for stable multi-day operation for Free Electron Laser (FEL) applications. The nC-class accelerator can deliver charge densities around 10 pC/MeV, <1 mrad rms divergence at energies up to 0.5 GeV and peak currents of over 10 kA [1]. Precise characterisation is paramount for controlled operation, including: spectrally resolved charge diagnostic, coherent optical transition radiation (TR) to resolve microbunch beam structures [2] and TR-based multioctave high-dynamic range spectrometry for sub-fs resolved characterisation of the 10 fs rms electron bunches [3]. Achieved stability allows for systematic exploration of demanding applications, resulting in the recent demonstration of the first LWFA based Beam-driven Plasma Wakefield Accelerator (LPWFA) [4]. Fulfilling the high demands required for FEL operation, the COXINEL manipulation line [5,6] developed at Synchrotron SOLEIL has recently been installed at our facility. Based on successful beam transport of over 13000 shots within 9 experimental days during commissioning, we were able to demonstrate the very first operation of a seeded FEL driven by a laser plasma accelerator [7].

INTRODUCTION

Plasma based wakefield acceleration is an acceleration technique able to achieve extremely high accelerating gradients, not limited by the vacuum breakdown limit, which has the potential to complement conventional accelerators where downsizing is desired. In Laser-plasma Wakefield Acceleration (LWFA), an ultrashort intense laser-pulse propagates through an optically transparent plasma and excites a plasma wake by displacing plasma electrons from its path by ponderomotive force [8]. Alternatively, in beam driven plasma wakefield acceleration (PWFA), a charged particle beam's space charge field similarly excites a plasma wake [9, 10]. For sufficiently high laser driver intensity or peak-current driver beam, all plasma electrons are completely expelled from the driver vicinity, thereby creating a co-propagating near-spherical shaped ion cavity [11, 12], which is able to sustain accelerating gradients above 100 GV/m [13]. Nowadays, compact LWFAs are hosted in many high-power laser facilities worldwide, and are able to provide electrons beams up to several GeVs [14], sub-percent energy spread [15], emit-

tances down to 0.1 mm mrad [16], nanocoulomb charges [1, 17] and inherently short bunch durations in the few femtoseconds range [2, 18] leading to peak currents exceeding 10 kA [1, 2, 19]. LWFA research is currently in a transition phase where a significant ongoing effort to understand and control the underlying physical phenomena takes place aiming at further quality improvement continues [20], while simultaneously a strong effort is being made to improve LWFAs' stability, aiming at applications [21]. Here we present the current status of the DRACO Laser Plasma Accelerator (LPA), and the ongoing effort to achieve stable performance for secondary applications, such as FEL or LPWFA operation.

DRACO LASER PLASMA ACCELERATOR

The DRACO LPA, located at the Helmholtz-Zentrum Dresden-Rossendorf, is driven by the 100 TW line of the 30 fs dual-arm 100 TW & 1 PW DRACO laser system [22]. The DRACO laser is located in a separate room and after compression is transported in-vacuum to a radiation shielded accelerator hutch, which is schematically depicted in Fig. 1. Before experiment and while operating at full laser amplification mode, a wavefront sensor (Phasics SID4) located at the accelerator (see Fig. 1) in closed loop with a deformable mirror at the laser compressor chamber provides focal spot optimization. The spectral phase is measured with spectral-phase interferometry for a direct electric field reconstruction (SPIDER-A.P.E.) in parallel with self-referenced spectral interferometry (WIZZLER-fastlite) in closed loop with an acousto-optic programmable dispersive filter (DAZZLER-fastlite) for correction of dispersion mismatch along the laser amplifier and laser beam transport chain. The LPA performance is further optimized by phase correction on the second order (group velocity) dispersion at the DAZZLER. Active beam stabilization within the amplification system in conjunction with online diagnostics for laser near field and far field monitored at the accelerator hutch (see Fig. 1) ensure shot-to-shot pointing stability. A few-cycle probe beam [23], derived from the main laser pulse, allows to monitor driver laser self-focussing and formation of the wakefield accelerating structure. A sample wakefield is shown in Fig. 2.

Accelerated electron beams can be diagnosed for charge, energy-distribution, (single plane) divergence & pointing using a 0.4 m long 0.9 T permanent magnet dipole. Phosphor-

* j.couperus@hzdr.de

A NOVEL METHOD FOR GENERATING HIGH-REPETITION-RATE AND FULLY COHERENT EUV FREE-ELECTRON LASER

H. X. Yang^{1,2}, J. W. Yan³, H. X. Deng^{4,*}

¹Shanghai Institute of Applied Physics, Chinese Academy of Sciences, Shanghai, China

²University of Chinese Academy of Sciences, Beijing, China

³European XFEL GmbH, Schenefeld, Germany

⁴Shanghai Advanced Research Institute, Chinese Academy of Sciences, Shanghai, China

Abstract

High-brightness extreme ultraviolet (EUV) light source is strongly required for high-resolution photoelectron spectroscopy, imaging experiments, and EUV lithography. In this work, the self-modulation technique is introduced into seeded FELs, such as high-gain harmonic generation (HG), to significantly reduce the requirement of the seed laser power by enhancing coherent energy modulation. Numerical simulations demonstrated that the modified HG configuration with the self-modulation technique could generate high-repetition-rate, fully coherent, stable, and kilowatt-scale EUV pulses at a more compact linac-based light source.

INTRODUCTION

High-brightness extreme ultraviolet (EUV) light source is a prerequisite for fundamental science. In terms of EUV high-resolution photoelectron spectroscopy and imaging experiments, high brightness and full coherence characteristics are essential. In terms of EUV lithography (EUVL), high average power (higher than 1 kW) and high stability characteristics are more critical. A high-power, fully coherent, and stable EUV light source is urgently required. Over the past decades, synchrotron radiation (SR) has been supplied as a standard tool for advanced research [1]. The SR light source's limitations are the longitudinally incoherent and the order of tens of picoseconds of pulse duration. With accelerator and undulator technology advancements, free-electron lasers (FELs) with high-intense and ultra-fast characteristics have made enormous progress in cutting-edge applications [2], which is the most promising high-power EUV light source.

Generation of high-brightness EUV radiation pulses requires the combination of a high-repetition-rate electron beam and various operating mechanisms. The steady-state microbunching mechanism-based photon source and storage-ring-based FEL are promising EUV light sources because the electron beam repetition rate in the storage ring can easily reach 100 MHz [3, 4]. However, the drawbacks of the electron beam in the storage ring are the low peak current, the induced energy spread that can limit the FEL extracted power, and the multiple turns stability remains experimentally demonstrated. Besides, the energy recovery linac (ERL) based light source with the self-amplified spontaneous emis-

sion (SASE) scheme [5, 6] is another method to produce kW-scale EUV pulses [7]. However, generating high-quality electron beams with high beam energy and high peak current is challenging. The total length of the ERL-FEL typically reaches over 100 m to improve the efficiency of extracted radiation power. Moreover, SASE FEL suffers from longitudinally incoherent and significant shot-to-shot jitter due to the initial shot noise of the electron beam.

Currently, most FEL facilities are based on linac that can produce electron beams with small energy spread, high peak current, and low emittance, thus achieving high single-pass FEL gain. The challenge of producing high average power kW scale EUV from single-pass FEL sources is the demand for high-repetition-rate electron beam or high beam energy. With the advanced superconducting radiofrequency technology, continuous-wave electron beam generation and FEL light source becomes feasible. Seeded FELs inherit the characteristics of the external seed laser, which can generate fully coherent and stable FEL pulses [8–10]. To generate high-repetition-rate EUV pulses in seeded FELs, such as high-gain harmonic generation (HG) [8], a UV seed laser of several MHz is required, challenging for state-of-the-art laser technology. Recently, the self-modulation technique has been demonstrated theoretically and experimentally in seeded FELs to reduce the power requirement of the seed laser at least two orders of magnitude by amplifying coherent energy modulation [11]. Thus, externally seeded FELs introducing the self-modulation technique have excellent potential to produce high-repetition-rate, fully coherent, and stable EUV pulses.

In this work, we demonstrate the feasibility of the single-pass FEL facilities to produce high-repetition-rate, fully coherent, and stable kW-scale EUV generation, with its potential application to EUVL. After upgrading the linac and laser systems, this modified HG configuration with the self-modulation technique is compatible with existing seeding beamlines.

PHYSICAL DESIGN

In a standard HG, an external seed laser interacts with the electron beam in a modulator undulator and imprints a sinusoidal energy modulation. After a dispersion section, the energy modulation is transferred into a density modulation and radiators resonate at the target harmonic of the seed laser. Typically, the energy modulation amplitude is proportional to the harmonic number n . For amplifying the FEL

* denghx@sari.ac.cn

HIGH HARMONIC LASING USING ATTOSECOND ELECTRON PULSE COMBS IN PHOTON-INDUCED NEAR-FIELD ELECTRON MICROSCOPY

Y. Pan[†], M. Krueger, Physics Department and Solid State Institute, Technion, Haifa, Israel
I. Kaminer, Department of Electrical and Computer Engineering, Technion, Haifa, Israel

Abstract

We propose a new high harmonic lasing mechanism using attosecond electron pulses, which can serve as promising ultra-bright extreme ultraviolet/soft X-ray attosecond laser sources.

INTRODUCTION

Attosecond laser pulses in the extreme ultraviolet/soft X-ray (XUV/SXR) spectral regions are presently available for attosecond pump-probe spectroscopy and extreme ultraviolet lithography for chip manufacturing, ultrafast atomic-scale microscopy, and nonlinear X-ray optics. There are two main approaches to produce attosecond light pulses: high-harmonic generation (HHG) in gas-phase or solid-state matter based on the three-step model [1-3], and X-ray free-electron lasers (XFELs) based on self-amplified spontaneous emission (SASE) and laser seeding processes of relativistic free electrons traveling through an undulator [4, 5].

Here, we propose a novel route of producing attosecond laser pulses, based on the generation of attosecond electron pulse trains in photon-induced near-field electron microscopy (PINEM) [6-8], combined with the SASE principle for light amplification. Our scheme relies on high-density nanotip arrays emitting dense electron bunches [9] that are subsequently modulated with a PINEM-type interaction, enabling high-gain for amplification of XUV/SXR high harmonic radiation.

SETUP

In analogy with the three-step model of HHG (ionization, acceleration, and recombination of an initially bound electron), we call our PINEM-HHG laser scheme the “three-tip” model (see Fig. 1a)), which can create both attosecond electron pulses and attosecond light pulses in a phase-coherent manner: the first tip emits electron pulses triggered by femtosecond laser pulses, with up to 102 electrons per laser pulse per tip [10]; the second tip modulates the electrons through a PINEM interaction with IR light (~ 800 nm) [7] and creates periodically bunched attosecond electron pulses [11]; the last tip serves as a radiation antenna for generating attosecond XUV/SXR pulses when interacting with the electron pulse train. Our scheme thus combines a tip emitter, a tip modulator, and a tip radiator.

In order to enhance the attosecond radiation power further, we replace the three tips with high-density nanotip arrays. The first tip is replaced by a 2D array (pitch of 100 nm) for generating a high electron charge density, thereby increasing it from 102 to 107 per laser pulse [9]. We also increase the PINEM interaction time (increasing the interaction length to 100 nm, with acceleration gradient field 1

GV/m) by introducing an array modulator with ten nanotips (pitch of 100 nm). As a result, we can achieve the widely spread PINEM spectrum of the order of a few hundred electronvolts, which as a crucial parameter limits the cut-off frequency of the radiation. Indeed, we find a linear scaling law of the cut-off frequency because it linearly depends on the laser-induced energy spread. At last, we realize SASE of XUV/SXR lasing radiation with an array radiator with 100 nanotips with a pitch of 800 nm (to match the period of electron pulse trains), respectively.

RESULTS

In order to assess the efficiency of PINEM-HHG, we devise a fully quantum theory approach based on quantum electrodynamics in the strong-field regime. Typical features of PINEM-HHG are shown in Fig. 1b)-1d). Fig. 1b) shows the HHG spectrum from an attosecond bunched free electron with PINEM spectrum with a spread of 160 eV. The HHG spectrum has a plateau shape and a cut-off at harmonic order $n_{\text{cut-off}}=150$, corresponding to the PINEM spread. Fig. 1c) shows the linear dependence of the cut-off frequency on the laser coupling strength $2|g|$ and hence on the laser field strength, which is similar to the linear power law in intra-band solid-state HHG [3]. A Fourier transform to the time domain reveals a radiative attosecond pulse train (see Fig. 1d)). We find that the pulse duration in the trains is 20 as, which is on the order of the atomic unit of time (inset of Fig. 1d)) and can hardly be achieved from FEL of relativistic beams [12]. In total, the best-case theoretical estimation of the superradiant XUV/SXR photon emission is $N_{\text{ph}}=(N_e N_{(\text{tip}3)})^2 \Delta v_{\text{sp}} \sim 10^{11}$ photon/pulse, with $N_e=10^7$, $N_{(\text{tip}3)}=100$ [9] and the emitted photon number per single electron $\Delta v_{(q, \text{sp})} \sim 10^{-7}$. The N_e^2 -dependence stems from the superradiance where many electrons emit coherently, and the $N_{(\text{tip}3)^2}$ -dependence from the SASE process when the photons are emitted spontaneously from the attosecond electron pulses and radiation emission builds up exponentially, until saturation. It is worthy to compare with the practical assessment of the first lasing in LCLS ($\sim 10^{13}$ photon/pulse), in which the beam has bunched electrons of the order of 10^9 [5]. However, we stress that practical challenges, such as the large source size of the emitter array and the Coulomb repulsion inside the high-charge electron bunches, will likely render our approach less efficient due to the increase of both the transverse and longitudinal beam emittance. The Coulomb repulsion effect may be mitigated by working at higher electron energies or at longer light pulses and accordingly longer wavelengths (mid/far IR).

From the perspective of free electrons, our PINEM-HHG scheme has many differences compared to atomic HHG and high-harmonic FEL [19]. First, the spectral spread of the electron beam in PINEM is about 1eV, less

FREE ELECTRON LASER SEEDED BY BETATRON RADIATION

A. Ghigo, M. Galletti, V. Shpakov, INFN-LNF, Frascati, Italy
 A. Curcio, CLPU, Villamayor, Salamanca, Spain
 V. Petrillo¹, Milan University, Milano, Italy
¹also at INFN-Mi, Milano, Italy

Abstract

In this paper the use of betatron radiation as a seed for the Free Electron Laser (FEL) is presented. The scheme shown can be adopted from all FEL driven by plasma accelerated electron beams via Particle or Laser Wake Field Acceleration. Intense radiation in the region of X ray characterized by a broad spectrum, the betatron radiation, is indeed produced in the plasma acceleration process from the electron passing through the ionized gas. It is proposed to use this radiation, suitably selected in wavelength and properly synchronized, to stimulate the emission of the Free Electron Laser.

INTRODUCTION

The possibility of using a plasma accelerated electron beam to generate Free Electron Laser (FEL) radiation has recently been proven [1]. The European EuPRAXIA project aims to develop FEL facilities using laser wake field acceleration and particle wake field acceleration (PWFA) techniques. In particular, in the INFN Frascati Laboratories, the headquarters of the EuPRAXIA project, an infrastructure will be built that will use the PWFA to generate FEL radiation in X-rays region [2]. The electron beam produced by a low emittance injector is accelerated by an X-band linac and a plasma acceleration section. Due to the intense transverse forces generated in the plasma wave, the electrons of the bunch oscillate emitting the so called betatron radiation. The radiation is emitted in a wide bandwidth in the X ray region and the basic idea is to select a narrow portion of the betatron radiation spectrum with a monochromator and to send this radiation superimposed on the same electrons beam that generated it, towards the magnetic undulator, as shown in Fig.1 [3]. The betatron radiation acts as seed of the Free Electron Laser emission: in EuPRAXIA, if the selected photon energy is matched with undulator fundamental wavelength (4nm), the seeding scheme enhances the number of photons per pulse and improves the pulse-to-pulse temporal stability as happens in the self-seeding scheme [4]. To extend the FEL emission spectrum towards high frequencies, the gap of the undulator can be opened. However, in these conditions, the SASE gain is no longer sufficient to saturate with the parameters of the beam expected at the accelerator output and with the nominal undulator length. It can be shown that by injecting the selected betatron radiation at the highest frequency that the most open undulator would have, it is possible to considerably extend the range of frequencies in which the FEL can saturate.

EXPERIMENTAL SET-UP

In the particle wake field plasma acceleration, a high charge electron bunch, the *driver* bunch, generates the plasma shape, losing energy, while a following low charge bunch, the *witness* bunch, is accelerated. Before entering in the FEL undulator, at the plasma chamber exit, the *driver* and *witness* bunches are dispersed, due to the different energy, in a dispersive section composed by four dipole magnets in a chicane configuration. The deviation angle in the first chicane dipole is large enough to separate the witness from the driver bunch. A collimator, or beam scraper, can be placed to stop the driver bunch. The betatron radiation propagates straight into the vacuum chamber and, as soon as the electron beam is deflected from the straight path, the first optical element of the monochromator is installed. The betatron radiation is selected in bandwidth and reflected back in the direction of the undulator overlapping the electrons that are leaving the chicane, in the first part of the undulator. Because of the very short electron bunch a perfect synchronization at the entrance of the undulator, at level of tens of femtosecond, is needed. The electron and photon beams started automatically synchronized because generated from the same electron beam. The trajectory length of the photons in the monochromator must compensate the path of the electrons that pass through the magnetic chicane and the delay of the electron, that travel with relativistic factor $\gamma=2000$, respect to the photon arrival time.

BETATRON RADIATION

Betatron radiation is the radiation emitted by electrons accelerated in plasma channels. Betatron radiation is emitted forward, and it is due to the betatron oscillations driven by the focusing fields inside the plasma bucket. Due to the very short scale of the betatron oscillations period (typically from mm down to microns, depending on the background electron plasma density), the typical energy of the photons emitted via betatron radiation falls in the X-rays.

Theoretical Introduction

If the scale of the electron energy gain is much longer than the betatron period, it can be assumed that the acceleration occurs adiabatically compared to the betatron dynamics. This allows using the following formula for the energy irradiated I by a single electron per unit photon energy E and

SPECTRAL CONTROL OF THz SUPER-RADIANT SPONTANEOUS UNDULATOR RADIATION DRIVEN BY ULTRASHORT ELECTRON BEAM WITH ENERGY SPREAD

S.Y. Teng, S.H. Chen, Department of Physics, NCU, Taoyuan, Taiwan
 W.Y. Chiang, M.C. Chou, H.P. Hsueh, W.K. Lau, A.P. Lee, NSRRC, Hsinchu, Taiwan
 P.T. Lin, Department of Engineering and System Science, NTHU, Hsinchu, Taiwan

Abstract

Intense coherent THz radiation has been generated from an 18-period, hybrid-type U100 planar undulator as it is driven by short relativistic electron pulses produced from the NSRRC photoinjector. However, it is observed that the number of output optical pulse cycles is much less than the number of undulator periods and therefore the radiation spectral bandwidth has been broadened. It is found that the dispersion of undulator with excessive energy spread is responsible for this undesired broadening of THz radiation spectrum. In this study, instead of using rectilinear rf bunch compression (i.e. velocity bunching) in photoinjector linac, we investigate the feasibility of using nonlinear magnetic bunch compression for spectral bandwidth control of coherent THz undulator radiation.

INTRODUCTION

THz radiation is a promising tool for scientific research in a variety fields such as semiconductor, quantum material and biology imaging etc. A linac-based tunable narrow-band THz radiation source has been constructed for novel light source development as well as user applications in NSRRC. It is a superradiant THz FEL facility with a photoinjector linac system providing sub-picosecond few tens MeV electron beam using the so-called velocity bunching technique. Superradiant THz spontaneous undulator radiation (THz SSUR) is then generated from a gap tunable planar undulator as the sub-picosecond beam passing through the device. Velocity bunching is a convenient way and cost effective way to produce ultrashort bunches from photoinjector. However, beam energy spread and the orientation of electron distribution in longitudinal phase space cannot be controlled easily especially when beam energy is not a free parameter and is determined by the resonant condition of undulator radiation. As a result, bunch lengthening of electron beam with excessive energy spread due to undulator dispersion leads to a decrease of output radiation amplitude with time. In this study, we investigate the possibility of using nonlinear dog-leg compressor for manipulation of electron distribution in longitudinal phase space in order to control emission spectrum of the superradiant undulator radiation.

The experimental setup and results of NSRRC THz SSUR source are described and summarized in the next section. Simulation results of photoinjector using ASTRA [1] and the electron beam manipulation through the dog-leg bunch compressor via ELEGANT [2] under different

compression ratios are discussed in the third section. In section 4, we describe the results of a self-developed algorithm in which particle motions in the undulator are tracked and the emission profile and spectra are calculated. Conclusions and the direction for future study are discussed in the last section.

EXISTING NSRRC THz FEL

Schematic layout of the NSRRC THz FEL facility is shown in Fig.1. Currently, an electron beam of maximum kinetic energy up to 62 MeV and a bunch charge of 460 pC are available from the photoinjector system. The electron bunches can be tightly compressed via velocity bunching during rf acceleration when the linac is operated near zero crossing phase. A wrap-around solenoid magnet is installed at the first 2 meters of the 5.2-m booster rf linac to assist beam focusing. In previous experimental study [1], an ultrashort beam of 490 fs bunch duration has been obtained and $\sim 20 \mu\text{J}$ super-radiant THz undulator radiation at 0.6 THz is produced from an 18-periods, U100 planar undulator.

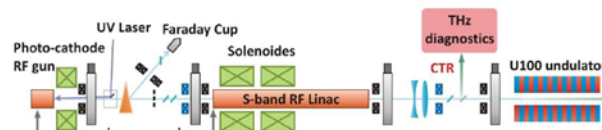


Figure 1: Schematics of the NSRRC THz FEL.

Interferogram of the THz output signal as detected by the Golay cell in auto-correlation measurement shows that the undulator radiation power reduce dramatically with time (Fig. 2). The main reason of this time-dependent power reduction is due to a significant reduction of beam bunching factor when the ultrashort beam with much energy spread traveling along an undulator which has inherent dispersion. In other words, while we are expecting a radiation bandwidth of $1/N_u$ in ideal situation, the coherent radiation power is broadened significantly to $\sim 15\%$.

FACILITY CONCEPT OUTLINES FOR A UK XFEL

D. J. Dunning[†], J. A. Clarke, L. S. Cowie, N. R. Thompson, P. H. Williams, ASTeC, STFC Daresbury Laboratory and the Cockcroft Institute, Warrington, UK,
J. L. Collier, J. S. Green, Central Laser Facility, STFC Rutherford Appleton Laboratory, Didcot, UK
J. P. Marangos, Department of Physics, Imperial College London, Blackett Lab, London, UK

Abstract

In early 2019, the UK initiated a project to develop the science case for a UK XFEL, featuring a diverse team of UK scientists and international advisors. Accelerator scientists were engaged to highlight potential future accelerator developments and to develop concept outlines for a facility design meeting the requirements for world-leading capabilities. The UK XFEL Science Case, featuring the concept outlines, was published in late 2020. Subsequent exercises further demonstrated the support of the UK community and the project is soon to enter a more detailed design phase. The concept outlines are reviewed and next steps outlined.

INTRODUCTION

This paper describes the development of facility concept outlines as part of the Science Case for a UK XFEL, which was published in 2020 [1]. The first section outlines the requirements from each of the different science areas, while the second collates them and describes how they impact key technology choices. The third section sets out concept outlines to meet the requirements. The final section outlines next steps for the project, which is funded for a 3-year conceptual design and options analysis phase starting soon.

REQUIREMENTS BY SCIENCE AREA

Each of the Science Case areas set out visions for world leading science, with requirements summarised below, including for photon energy and repetition rate in Fig. 1.

Physics and X-ray Photonics

The key requirements are attosecond pulses (~100 as) across a broad range of photon energies, from 200 eV to hard X-ray, with sub-femtosecond synchronisation to optical lasers. Combination with electrons and other FEL pulses is also of interest. Control of pulse properties, such as polarisation, and through seeding are also highlighted. High repetition rates (> 10 kHz) are strongly preferred as in many examples the anticipated signals are weak and much data must be taken for high fidelity measurements.

Matter in Extreme Conditions

The main requirements are X-ray pulses with high pulse energy (mJ to orders of magnitude higher) and high photon energy (up to 30 – 50 keV), in combination with very high-energy optical lasers. Rep. rate is generally less demanding, due to being relatively low in the high energy lasers that compress the material. However higher rates could be beneficial where the X-ray beam is used to isochroically

heat samples. Narrow bandwidth (~10 meV), two-colour capability and sub- μm spot sizes are also called for.

Quantum and Nanomaterials

The key requirements of this science area are soft to very hard X-rays (up to ~50 keV would open up new opportunities), in combination with pump sources across a broad range of wavelengths (THz to visible), as well as two-colour FEL capability. Sub-femtosecond synchronisation is important in all cases. Repetition rate can be as low as 10 Hz in some experiments, due to sample recovery times, but high average flux is needed in others.

Chemical Sciences and Energy

An important requirement is to combine XFEL pulses with a multitude of different sources: accelerator-based THz, electron pump sources, along with numerous synchronized laser-based sources. The X-rays should be soft to very hard (> 25 keV for some experiments) and high repetition rate (1 kHz to 1 MHz). For some experiments, a relative bandwidth below 1×10^{-4} is needed. Two-colour FEL operation is also important, with the possibility of delivering various combinations of soft and hard X-rays.

Life Sciences

This area calls for hard X-rays (5 – 25 keV) at rep. rates from 1 kHz to potentially 1 MHz, depending on detector capabilities. Some applications require precise control of the X-ray pulse properties: stability of pulse energy, carrier frequency, instantaneous bandwidth and spectrum. Hard X-ray pulses with up to 4% bandwidth, demonstrated at SwissFEL [2], are of interest. Two-colour FEL operation with large variation in temporal (fs – μs) and energy separation is important, as well as combination with electrons.

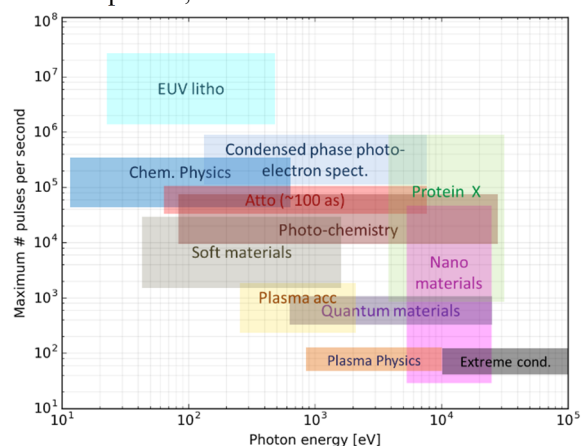


Figure 1: Requirements of different areas of the science case in terms of photon energy and repetition rate.

[†] david.dunning@stfc.ac.uk

FAST-GREENS: A HIGH EFFICIENCY FREE ELECTRON LASER DRIVEN BY SUPERCONDUCTING RF ACCELERATOR

P. Musumeci, A. Fisher, P. Denham, J. Jin, Y. Park

Department of Physics and Astronomy, University of California Los Angeles, Los Angeles, CA, USA

R. Agustsson, L. Amoudry, T. Hodgetts, M. Ruelas, A. Murokh

RadiaBeam Technologies, Santa Monica, CA, USA

A. Lumpkin, A. Zholents Argonne National Laboratory, Lemont, IL, USA

D. Broemmelsiek, S. Nagaitsev, J. Ruhan, J. Santucci, G. Stancari, A. Valishev

Fermilab National Laboratory, Batavia, IL, USA

J. Edelen, C. Hall and D. Bruhwiler

RadiaSoft, Boulder, CO, USA

Abstract

In this paper we'll describe the status of the FAST-GREENS experimental program aiming at the demonstration of the high gain TESSA regime using a strongly tapered helical undulator at the FAST facility in Fermilab. The first phase of the experiment is based on the use of the compressed 220 MeV electron beam from the FAST linac and two strongly tapered helical undulators aiming at the generation of high power radiation at 515 nm. We present time-dependent simulation results based on GENESIS and GPTFEL showing that up to 5% conversion efficiency can be achieved in less than 2 m active interaction length.

INTRODUCTION

Improving the conversion efficiency of relativistic electron beam power into coherent short wavelength radiation is at the center of both scientific and industrial interests as it would enable light sources to reap the benefits of 100 years development in the wall-plug efficiency of charged particle accelerator technology. In the X-ray, it would facilitate ultrahigh intensity X-ray laser pulses for single shot coherent imaging and Schwinger-field physics exploration, in the EUV it would meet the demands of fast throughput material processing (EUV-lithography) and at visible wavelengths it would enable high efficiency, high average and peak power lasers. It is helpful to note that state-of-the-art X-ray sources based on the Free Electron Laser principle take advantage of only a minimal fraction ($< 0.1\%$) of the available power stored in the beam with most of it simply wasted on the beam dump.

The TESSA program aims at fundamentally addressing this limitation in electron-based coherent radiation generation by exploiting a deeper understanding of the interaction of relativistic electrons with the electromagnetic field in tapered undulator systems, and leveraging the progress in high brightness beam generation and control [1, 2].

The physical concept behind our approach is the so-called Tapering-Enhanced-Superradiant-Stimulated-Amplification regime of FELs where high intensity seed and pre-bunched electron beams are used in combination with strongly tapered undulators to sustain high gradient deceleration over

extended distances and convert a large fraction of the beam energy into coherent radiation [3]. The main advantages of this coupling scheme are the absence of nearby boundary or media (i.e. this is a vacuum plane-wave interaction), so that there are basically no mechanisms for the energy to flow out of the particle-field system [4]. In TESSA, the initial conditions for the system allow for particle deceleration at a very high average energy exchange rates (typically in excess of 10 MV/m) larger than in any known FEL, in order to beat the onset of sideband instabilities which have been known for decades to set the limit on tapered FEL energy exchange [5]. Previous experiments based on the TESSA concept [6] demonstrated efficiencies as high as 30% in the far-infrared. Nevertheless, they were carried out in a very low gain amplification regime resulting in a strong background signal from the seed laser which precluded obtaining direct measurements of the transverse and spectral profiles of the amplified radiation. A recent application of the TESSA concept in the THz regime demonstrated 10% conversion efficiency in 1 m long tapered helical undulator at 160 GHz [7].

The TESSA initiative at FAST is aimed at demonstrating record high extraction efficiency lasing in a strongly tapered undulator [8]. We seek to obtain the first experimental measurements of spectral and spatial properties of the 515 nm radiation amplified in the high gain TESSA regime (Fig.1). The experiment will start in single-pass mode, but eventually we plan to take advantage of the unique high repetition rate of the FAST linac to demonstrate a very high average power source based on this principle. This source would be intrinsically synchronized with the electron beam and could be used for high flux gamma ray and polarized positron production [9, 10].

Nominal parameters for the FAST beam are reported in Table 1. The experiment is designed assuming an electron beam with 1000 pC charge, compressed to 600 Amp by the magnetic chicane compressor with a normalized emittance of < 3 mm-mrad and a relative energy spread of 0.1%. The intense green seed pulse of nominal peak power 1 GW (2 mJ in 2 ps in order to homogeneously seed the entire bunch temporal current profile) is obtained from an Yb-based laser

SIMULATIONS OF ULTRAHIGH BRIGHTNESS BEAMS FROM A PLASMA PHOTOCATHODE INJECTOR

L. H. A. Berman*, A. F. Habib, T. Heinemann, G. G. Manahan, A. Sutherland,
D. Campbell, A. Hewitt, A. Dickson and B. Hidding,
Scottish Universities Physics Alliance, Department of Physics,
University of Strathclyde, Glasgow G4 0NG, UK
The Cockcroft Institute, Warrington, UK

Abstract

Plasma photocathode injectors may enable electron beams with normalised emittance at the nm-rad level from a Plasma Wakefield Acceleration (PWFA) stage [1]. At these emittance levels, and currents at the kA-level, they are ultrahigh 5D brightness beams with the potential to drive advanced light sources. The feasibility of plasma photocathodes was demonstrated at the first Facility for Advanced Accelerator Experimental Tests (FACET-I) at the Stanford Linear Accelerator (SLAC) [2]. Further experiments will aim at realisation of the full 5D and 6D brightness potential at FACET-II [3]. However, a series of milestones must be reached before these beams can be utilised for FELs. For example, electron beams accelerated in plasma-based accelerators inherently have a significant energy chirp due to the multi-GV/m accelerating gradients involved. Since energy chirp and energy spread can be detrimental to the high-gain FEL interaction, an approach has been developed for energy spread minimisation of ultrahigh 5D brightness beams towards ultrahigh 6D brightness via the escort beam approach [4]. Here we discuss ongoing efforts within the framework of the PWFA-FEL project [5], aiming at direct single-bunch production of ultrabright beams with reduced energy spread using beamloading. We present considerations and results aiming at a balanced optimisation of energy spread, peak current, and emittance from direct plasma photocathode production, and their application to FELs.

INTRODUCTION

Plasma-based particle acceleration uses a plasma as the accelerating medium instead of conventional RF cavities [6]. Either an electron bunch or an intense laser pulse acts as a ‘driver’ that is sent through the plasma, transversely expelling the plasma electrons but having negligible impact on the heavier ions. This creates a cavity (or ‘blowout’) devoid of electrons that trails the driver, resulting in an internal longitudinal E-field of gradient on the order of tens of GV/m. This ‘wakefield’ can trap and accelerate an electron ‘witness’ bunch. Both the laser and beam-driven varieties, respectively known as laser and plasma wakefield acceleration (LWFA and PWFA), have already been used to demonstrate multi-GeV energy gain [7, 8], with a current record of energy doubling of electrons to 84 GeV [9]. This took less than a metre compared to the km-scale linac that would be needed

to achieve a comparable energy gain. If a plasma-based accelerator could be used to drive an FEL this would open up huge additional capacities, and potentially capabilities.

This prospect has gained a lot of interest, and FEL gain has recently been demonstrated for the first time using beams from plasma-based accelerators in the EUV at 27 nm [10] and the IR at 820 nm [11]. However, FEL gain in the x-ray region has not yet been achieved due to the increasingly stringent requirements on the electron witness beam. A key parameter is the normalised transverse beam emittance ε_n since this determines the minimum FEL wavelength that can be accessed via the Pellegrini criterion, $\varepsilon_n \leq \gamma \lambda_r / 4\pi$, where λ_r is the resonant FEL wavelength and γ is the beam Lorentz factor. The other key parameter is the slice energy spread σ_γ / γ of the electron beam, which should be smaller than ρ according to $\sigma_\gamma / \gamma \leq \rho$. Both thresholds are difficult to reach for beams from plasma accelerators today, and increasingly so for lower electron energies and harder resonant wavelengths. Because the electron beam quality obtainable from plasma accelerators is both determined and limited by currently used electron beam generation methods, the x-ray range may remain out of reach. Electron beams of higher quality are necessary for overcoming these limitations in future plasma-based accelerators.

Beam brightness is an important figure of merit for determining suitability for FEL operation [12]. Here we define 5D brightness as $B_{5D} = 2I_{\text{peak}} / \varepsilon_n^2$, where I_{peak} is peak current, and 6D brightness as $B_{6D} = B_{5D} / \sigma_E 0.1\% \text{BW}$ which also takes into account the correlated (projected) energy spread σ_E . Indeed, the obtainable witness beam quality depends heavily on the injection method. Self-injection methods tend to produce lower quality beams due to their dependence on highly nonlinear processes, whereas controlled injection methods may achieve higher beam quality due to the increased stability [13–15].

A novel electron injection method that goes one step further and promises decoupled control over witness properties, and electron beam quality orders of magnitude beyond state-of-the-art is the plasma photocathode injection, also known as ‘Trojan Horse’ (TH) [1]. In this method the plasma wave blowout is set up in a mixture of two gases, one with a low ionisation threshold (LIT) and one with a high threshold (HIT). Initially only the LIT gas is preionised into a plasma with the HIT gas remaining in a neutral state. An electron bunch driver sets up a wake in the LIT plasma. A low-intensity laser pulse incident in arbitrary orientation then

* lily.berman@strath.ac.uk

IMPROVING THE REALISTIC MODELING OF THE EEHG SEED SECTION IN START TO END SIMULATIONS

P. Niknejadi*, S. Ackermann, P. Amstutz, M. Dohlus, E. Ferrari, T. Lang, G. Paraskaki, L. Schaper, E. Schneidmiller, S. Schreiber, M. Vogt, M. Yurkov, DESY 22607 Hamburg, Germany
 W. Hillert, F. Pannek, D. Samoilenko, Institute for Experimental Physics
 University of Hamburg 20148 Hamburg, Germany
 S. Reiche, Paul Scherrer Institut 5232 Villigen PSI, Switzerland
 F. Curbis, M. Pop, Lund University and MAX IV Laboratory 22484 Lund, Sweden

Abstract

A tunable and multicolor light source with near Fourier-limited pulses, controlled delay, and fully coherent beam with precisely adjustable phase profiles enables state-of-the-art measurements and studies of femtosecond dynamic processes with high elemental sensitivity and contrast. The start-to-end (S2E) simulations efforts aim to take advantage of the available global pool of software and past and present extensive efforts to provide realistic simulations, particularly for cases where precise manipulation of the beam phase space is concerned. Since tracking of beams with billions of particles through magnetic structures and handover between multiple codes are required, extensive realistic studies for such cases are limited. Here we will describe a workflow that reduces the needed computational resources for the echo-enabled harmonic generation (EEHG) seed section of the FLASH2020+ project.

INTRODUCTION

The rapid progress in the field of x-ray free-electron lasers (XFELs) has opened a new era for photon science [1–4]. The progressively improved properties of x-rays have led to sources with higher brightness by ten orders of magnitude over previously available sources. Consequently, modeling and diagnostics of current and future XFELs have become more and more challenging. For instance, modeling externally seeded free-electron laser (FEL) requires noise suppression and smooth handshaking between multiple codes [5–13]. At FLASH, the first high-gain FEL, an upgrade with a strong emphasis on the research and development towards a fully coherent light source is ongoing. This upgrade program, FLASH2020+ [14, 15], peruses high-harmonic generation at high repetition rates in a superconducting seeded FEL. One of this program's goals is to study advanced concepts in beam dynamics, accelerator, and FEL physics through realistic and reliable S2E simulations.

A BRIEF OVERVIEW OF METHODS

In the past year, our focus has been mainly on improving EEHG [16] modeling, which needs multiple handovers between particle tracking and FEL codes. Due to the fine structure of the electron beam in the EEHG scheme, the task

involves simulating a large number of particles, which requires a large amount of memory and limits the possible studies to be conducted on electron beam properties, FEL performance, and properties of the output radiation. The relevant parameters are listed and discussed in reference [14]. In Fig. 1, the adopted workflow for the FLASH2020+ upgrade [15] simulation is shown above the dashed line. In addition, a few of the simulation codes [17–19] reviewed for short segments of the beamline are also listed below the line.

Electron Beam

Seeded FEL output's sensitivity to electron parameter deviations or jitters plays an essential role in the machine's stability. In ideal simulations, we often ignore or isolate the effects of chirp [20], inter-beam scattering, and coherent or incoherent synchrotron radiation [21]. Realistic modeling of the electron beam in the seed section would require (1) starting the simulations in the seed section with a high number of particles and (2) altering simulation codes for chicanes and modulators. To achieve the former, earlier steps of simulations, i.e., gun, and acceleration, need to be modeled with a high number of particles. Therefore, for the full S2E, the electron beam is simulated in sub-bunches using ASTRA [5]. The realistic acceleration and compression are modeled in Impact-Z [6]. However, since these two steps are computationally expensive and time-consuming, elegant and SelaV were benchmarked against Impact-Z for "quiet start" simulations to speed up the scans needed for determining the optimal working points [7, 8, 11]. While Impact-Z simulations are still in progress, the preliminary optimized beam in elegant is matched and transported to the start of the seed section and then upsampled to be a suitable input for the FEL codes. A detailed analysis is performed to understand contributing factors to microbunching and complement the S2E simulations [22, 23]. More importantly, these studies help identify the simulation artifacts, mainly in the noise distribution, in simulations and improve the model.

For the latter, the challenge is up and downsampling the beam for transition between elegant and FEL codes in the seed section. For instance, the genesis output at each modulator's end needs to be downsampled to be a suitable input file for elegant simulations in each chicane. While large particle files are often downsampled for plotting and output of PIC simulations for plasma-accelerators are upsampled

* pardis.niknejadi@desy.de

SIMULATIONS OF SEEDING OPTIONS FOR THz FEL AT PITZ

G. Georgiev*, P. Boonpornprasert, M. Krasilnikov, X.-K. Li
Deutsches Elektronen-Synchrotron DESY, Zeuthen, Germany
W. Hillert, University of Hamburg, Hamburg, Germany

Abstract

A THz FEL is under commissioning at PITZ as a proof-of-principle experiment for a high power and high repetition rate THz source and as an option for THz-driven experiments at the European XFEL. Some of these experiments require excellent coherence and CEP stable THz pulses. In SASE regime, the coherent properties of the FEL radiation are limited. A seeding scheme can be used instead of SASE to improve the coherent properties and shot-to-shot stability. Several options for seeding are considered in simulation for the THz FEL at PITZ: external laser pulse, pre-bunched electron beam, energy modulated electron beam and additional short spike on top of a smooth beam profile. The improvements over SASE in energy, spectral and temporal stability of the THz pulse are presented.

INTRODUCTION

The scientific opportunities of using terahertz (THz) radiation in modern x-ray free electron lasers (FELs) are recognized by the user community of the European XFEL [1]. Intense THz pulses are required for research of non-linear physics in THz-driven pump-probe experiments. The desired THz source is high-power, tunable and operates at a high repetition rate. An accelerator-driven source is a promising option. One concept of accelerator-driven source that matches the requirements is a THz FEL. At present, a proof-of-principle experiment of THz FEL source has achieved first lasing at the Photo Injector Test Facility at DESY in Zeuthen (PITZ) [2]. For this experiment, a LCLS-I undulator was installed in a second tunnel as an extension to the already existing PITZ accelerator.

In addition to high intensity, the ideal THz source should deliver identical and carrier-envelope phase stable pulses with good synchronization (low arrival time jitter). Typically in SASE regime FELs demonstrate significant shot-to-shot fluctuation due to the stochastic nature of the SASE process. This fluctuation manifests itself as final intensity, arrival time and spectral profile differences between shots of the FEL. To achieve more stable shot-to-shot performance, a seeding method is applied to the FEL. Several seeding options are studied in simulation for the THz FEL at PITZ and a summary of the results is given in this text.

SEEDING OPTIONS

The simulations are performed for four seeding options:

- External laser pulse,
- Pre-bunched electron beam [3],
- Energy modulated electron beam, and

- Short electron beam spike on top of main beam current profile.

A common FEL seeding method is the inclusion of a laser pulse along the electron beam in the undulator. In this setup, the FEL acts as an amplifier and inherits the coherent properties of the initial seeding radiation. The main simulation parameter of this seeding option is the seeding pulse power - it has to dominate over the beam noise.

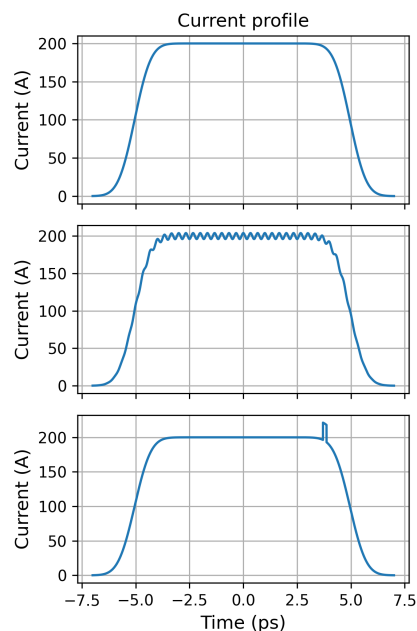


Figure 1: Electron beam current profile for SASE (top), pre-bunched beam with $b = 10^{-2}$ (center) and short 25 A spike (bottom).

Another technique is to deliver longitudinally density-modulated electron beam with the same periodicity as the FEL radiation, also called pre-bunched electron beam, to the undulator. An example is shown in the middle plot of Fig. 1, note the relatively small modulation amplitude. The main parameter of the simulation is the initial bunching factor b [4] given by:

$$b = \frac{1}{N_e} \left| \sum_{k=1}^{N_e} e^{-i\omega t_k} \right|, \quad (1)$$

where ω is the FEL resonant frequency, N_e is the number of electrons/macroparticles in the beam and t_k is the time coordinate of the k th particle. Sufficient pre-bunching will drive the FEL process and define the properties of the radiation pulse. The density-modulations generated in the simulation code Genesis 1.3 [5] for different bunching values are shown in Fig. 2.

* georgi.georgiev@desy.de

FIRST DEMONSTRATION OF PARALLEL OPERATION OF A SEEDED FEL AND A SASE FEL

S. Ackermann, Ph. Amstutz, F. Christie, E. Ferrari, S. Hartwell, M.M. Kazemi, P. Niknejadi, G. Paraskaki, J. Rönch-Schulenburg, S. Schreiber, M. Vogt, L. Schaper, J. Zemella, Deutsches Elektronen-Synchrotron DESY, Hamburg, Germany
E. Allaria, Elettra-Sincrotrone Trieste S.C.p.A., Trieste, Italy
W. Hillert, S. Mahmoodi, F. Pannek, D. Samoilenko, A. Thiel, Hamburg University, Hamburg, Germany

Abstract

The FLASH facility houses a superconducting linac powering two FEL beamlines with MHz repetition rate in 10 Hz bursts. Within the FLASH2020+ project, which is taking care of facility development, one major aspect is the transformation of one of the two FEL beam lines to deliver externally seeded fully coherent FEL pulses to photon user experiments. At the same time the second beam line will use the SASE principle to provide photon pulses of different properties to users. Since the electron beam phase space conducive for SASE or seeded operation is drastically different, here a proof-of-principle experiment using the existing experimental seeding hardware has been performed demonstrating the possibility of simultaneous operation. In this contribution we will describe the setup of the experiment and accelerator. Finally, we will discuss the results and their implications also for the FLASH2020+ project.

INTRODUCTION

FLASH, the Free-Electron Laser user facility in Hamburg, has been delivering high brilliance soft X-ray FEL pulses for user experiments since 2005 [1, 2]. Also, FLASH had been equipped with hardware to study seeded FELs [3]. To address the growing demand of beam time requests, the facility has been upgraded with a second FEL beam line in 2014 [4]. The next upgrade project, FLASH2020+ [5, 6], aims for several augmentations of the facility. Two key components are the higher electron beam energy of now 1.35 GeV and the implementation of external seeding, namely HGHG [7, 8] and EEHG [9] at the high repetition rates FLASH can offer.

Experimental Setup Within the User Facility

The FLASH FEL, as seen in Fig. 1, is driven by a superconducting linear accelerator and can provide up to 800 electron bunches, separated by 1 μ s per so-called macro pulse. The bunches can be divided between FLASH1 and FLASH2 during each macro pulse, expending about 50 μ s of the burst. This also allows for different RF-parameters for the two bunch trains. The macro pulses are generated at a repetition rate of 10 Hz. In the FLASH1 electron beam line, just upstream the SASE undulators, the experimental seeding hardware called Xseed is located. The setup consists of a seed laser injection where two seeds of a wavelength of 267 nm are coupled in the last dipole of the energy collimation area. For the laser-electron interaction, two planar

electromagnetic modulators of orthogonally oriented deflection planes are used, separated by a dispersive chicane of sufficient strength for EEHG seeding. A second, less strong dispersive section completes the modulation section. The electron beam then passes to 10 m of radiator undulators, before the generated radiation is reflected into a diagnostic section inside another chicane. The electron beam is transported through a transverse deflecting structure and dipole magnet before it hits a screen and finally a diagnostic beam dump. During user operation none of the aforementioned components are influencing the beam. Due to the limited repetition rate of the used laser system only one bunch per macro pulse can be used for experimental seeding, while the remaining burst can be used for FLASH2.

EXPERIMENTAL SETUP

The experimental program to achieve parallel operation as a side goal was conducted in June 2021. The parameters used for the demonstration of true parallel operation can be found in Table 1.

Table 1: Parameters Used During the Demonstration of Parallel Operation

Electron bunch		
Energy	E	685 MeV
Charge	C	400 pC
Duration	$\tau_{e,rms}$	391 fs
Peak current	A_{peak}	770 A
Norm. emittance	ϵ_x	0.68 mm mrad
	ϵ_y	0.48 mm mrad
Mismatch para.	μ_x	1.10
	μ_y	1.07
Mismatch ampl.	M_x	1.56
	M_y	1.44
Dispersion	D_x	≤ 5 mm
	D_y	≤ 10 mm
Seed laser		
Wavelength	λ_{seed}	267 nm
Duration	$\tau_{seed,fwhm}$	200 fs

Six-Dimensional Overlap

The six-dimensional overlap between electron bunch and seed laser pulses at each modulator is achieved by first using

STATUS OF THE SEEDING UPGRADE FOR FLASH2020+ PROJECT

E. Ferrari*, S. Ackermann, M. Beye, I. Hartl, S. Hartwell,
 T. Lang, S. Mahmoodi, M. Mohammad Kazemi, P. Niknejadi, G. Paraskaki,
 L. Schaper, S. Schreiber, M. Tischer, P. Vagin, J. Zemella, J. Zheng
 Deutsches Elektronen-Synchrotron (DESY), Hamburg, Germany
 Enrico Allaria Elettra-Sincrotrone Trieste S.C.p.A., Basovizza, Italy.
 Margarit Asatryan, Wolfgang Hillert, Fabian Pannek, Dmitrii Samoilenko, Andreas Thiel
 University of Hamburg, Hamburg, Germany.

Abstract

In the framework of the FLASH2020+ project, the FLASH1 beamline will be upgraded to deliver seeded FEL pulses for users. This upgrade will be achieved by combining high gain harmonic generation and echo-enabled harmonic generation with a wide-range wavelength-tunable seed laser, to efficiently cover the 60–4 nm wavelength range. The undulator chain will also be refurbished entirely using new radiators based on the APPLE- III design, allowing for polarization control of the generated light beams. With the superconducting linac of FLASH delivering electron beams at MHz repetition rate in burst mode, laser systems are being developed to seed at full repetition rates. In the contribution, we will report about the progress of the project.

To implement seeding in FLASH1, we anticipate to utilize two harmonic generation seeding approaches for efficiently cover the tuning range for users, namely HGHG [3] and EEHG [4]. For the longer wavelengths (>20 nm), we foresee to employ HGHG. In fact, by looking at the bunching curve as a function of the harmonic number as reported in Fig. 2, one can observe the higher efficiency in generating coherent bunching of HGHG than for EEHG in this wavelength range.. For harmonic numbers ≥ 15 , i.e., for shorter wavelengths, we plan to rely on EEHG.

Such an ambitious upgrade requires new dedicated state-of-the-art seed lasers and laser transport beamlines, new modulators and radiators undulators, magnetic chicanes, as well as numerical simulations to investigate and optimize the setup.

INTRODUCTION

In the context of the FLASH2020+ project, the whole FLASH machine is undergoing a notable series of upgrades and refurbishments that include the installation of a laser heater, exchange of bunch compressor chicanes as well as an electron beam energy upgrade. They will be realized during two long shutdown periods, the first ending in August 2022 and the next one scheduled for July 2025.

Full seeding capabilities will be implemented at the FLASH1 beamline to provide users with fully coherent and stable FEL radiation at the Fourier limit, with continuous wavelength tunability below 40 nm and full wavelength range spanning from 60 to 4 nm. Polarization control will also be available. All of the above, combined with the high burst repetition rate of FLASH, will provide the user community with a unique lightsource in the VUV soft-X-ray wavelength range.

In Fig. 1, the envisioned FLASH footprint at the end of the upgrade project FLASH2020+ [1] is shown. The machine operation concept will rely on the a single superconducting linac feeding both FEL beamlines in parallel. The bunch properties will need to be compatible both with seeded and SASE operation on FLASH2. To achieve this, a large linear energy chirp will be present for FLASH1 in order to allow for further compression in FLASH2, as well as downstream FLASH1 for THz production. Such operational mode was already successfully demonstrated last year [2].

SIMULATIONS

An extensive series of numerical simulations have been performed for optimizing the setup, using different numerical codes. For the electron part we used a combination of elegant [5] and selav [6], that provide fast exploration of the electron beam properties considering collective effects along the linac. Up to now the input beam distribution has been self-generated, but we plan in the next few months to start using realistic beam distributions generated via ASTRA [7]. For the FEL process we use GENESIS1.3v4 code [8]. The seed laser is also fully simulated using [9].

Three different working points, with electron beam energies of 750, 950 and 1350 MeV, represent our baseline. We plan to have full start-to-end simulations for the linac and FLASH1 beamline soon. For this, we developed a comprehensive toolkit with handshaking between the different codes [10]. Such an approach allows for investigating the impact on the FEL output of different machine parameters. As an example, we evaluated the impact of the large residual linear energy chirp needed for parallel operation on the performance of both HGHG and EEHG. By proper tuning of the resonances, we were able to recover similar FEL pulses as in the case when the beam is flat. We also investigated the power jitter variations of the two seed lasers on the EEHG scheme [11]. We also benchmarked EEHG performance using elegant, in particular to investigate the impact of collective effects, e.g. CSR, on the output radiation properties [12]. Concerning the choice of seeding technique to utilize around the transition in efficiency, see Fig. 2, we performed simula-

* eugenio.ferrari@desy.de

HIGH REPETITION RATE, LOW NOISE AND WAVELENGTH STABLE OPCPA LASER SYSTEM WITH HIGHLY EFFICIENT BROADLY TUNABLE UV CONVERSION FOR FEL SEEDING

T. Lang[†], M. M. Kazemi, J. Zheng, S. Hartwell, N. Hoang, E. Ferrari,
L. Schaper, I. Hartl

Deutsches Elektronen Synchrotron DESY, Hamburg, Germany

E. Allaria, Elettra-Sincrotrone Trieste S.C.p.A., Basovizza, Italy

Abstract

We present the concept and first results of new seed laser system for the FLASH2020+ project at the FLASH VUV/XUV FEL facility at DESY (Hamburg, Germany). One goal of the project is to build the first high repetition rate, fully coherent FEL light source worldwide ready for user operation in 2025 [1]. The novel optical parametric chirped pulse amplification seed laser system with highly-efficient, broadly-tunable UV conversion is designed to deliver UV pulse energies up to 100 μJ in two seed beams in order to allow for the Echo-Enhanced Harmonic Generation (EEHG) seeding scheme [2]. The temporal structure will match the burst pulse structure of FLASH which can operate with up to 6000 pulses in one second (1 MHz pulse train in 600 μs - 10 Hz bursts). We compare the first experimental results to a start-to-end simulation allowing to predict the system performance regarding tunability, beam quality, stability and pointing, depending on the measured input parameters and fluctuations of the high-power chirped pulse amplification is a pump laser.

INTRODUCTION

FLASH is up-to-date the only free electron laser facility worldwide delivering highly brilliant and spatially coherent VUV laser pulses with high repetition rates for user experiments in two parallel operating FEL beamlines FLASH1 and FLASH2. The facility is currently undergoing a major upgrade in which FLASH1 will be rebuild in order to support a fully spatially and temporally coherent FEL operation utilizing EEHG for gap-free wavelength tuning down to 4 nm and high gain harmonic generation (HG) for longer wavelengths between 20 nm to 60 nm.

For both HG and EEHG operation the seed laser system needs to provide high power, broadly wavelength tunable UV seeding pulses with excellent stability and beam quality. As illustrated in Fig. 1, the new concept uses two seed laser beams with fixed wavelength at 343 nm (Seed1) and wavelength tunable between 297 nm to 317 nm (Seed2) respectively for EEHG seeding. The HG seeding is planned to be operated with the wavelength tunable Seed2 only. The two laser beams will be spatially and temporally overlapped in two modulation undulators. In our

design we use three different operational electron energies: 750, 950 and 1350 MeV. In order to imprint sufficient electron energy modulation, the seed laser system is designed to deliver UV pulse energies $> 100 \mu\text{J}$ and $> 50 \mu\text{J}$ for Seed1 and Seed2, respectively, while maintaining the high repetition rates of up-to 1 MHz (in-burst) of FLASH. In order to exploit the full capabilities of the narrow-band fully coherent FEL pulses for 24/7 scientific user experiments, the seed laser needs to provide widely tunable, high power UV laser pulses with pulse durations of 50 fs, excellent beam quality and exceptional high short and long-term stability in respect to the seeding wavelength ($< 2 \cdot 10^{-4}$), pulse-to-pulse energy ($< 2\%$) and pointing jitter ($< 20 \mu\text{rad}$). Altogether, the requirements on the laser system are beyond state-of-the-art.

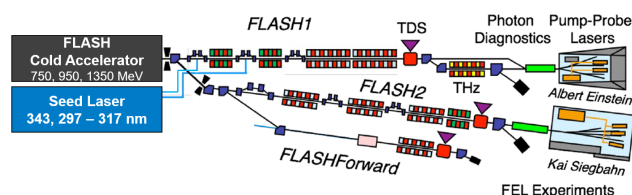


Figure 1: Layout of FLASH VUV/XUV FEL Facility.

Laser Concept

For a successful seeded FEL operation, the laser concept needs to provide stable high energetic, ultra-short UV pulses in combination with high repetition rates and ultra-broad wavelength tunability. Figure 2 shows a schematic of the concept and the power budget of the Seed2 optical chirped pulsed parametric amplification system (OPCPA). The OPCPA is pumped by a commercial Yb:YAG high-power chirped pulse amplifier (CPA, Trumpf/Amphos) and is followed by highly efficient broadband nonlinear UV conversion stages. The amplifier operates under non-thermal equilibrium condition. The 10 Hz pulsed operation with 600 μs long bursts at an in-burst repetition rate of 1 MHz allows for exceptional high in-burst average powers of up-to 5kW. The seed laser oscillator and the Ytterbium fiber laser front-end (FE, NKT-Photonics) provides two outputs. A first output providing 2 W average power is used for seeding the high-power CPA system. Its spectral bandwidth of 2 nm centred at 1030 nm is matched to the amplification bandwidth of the CPA system.

[†] tino.lang@desy.de

PHASE-LOCKED HARD X-RAY SELF-SEEDING FEL STUDY FOR THE EUROPEAN XFEL

T. Long¹, S. Huang, K. Liu

State Key Laboratory of Nuclear Physics and Technology, Peking University, Beijing, China

Y. Chen, W. Decking, S. Liu*, N. Mirian, W. Qin

Deutsches Elektronen-Synchrotron (DESY), Hamburg, Germany

G. Geloni[†], J. Yan, European XFEL, Schenefeld, Germany

¹also at DESY, Hamburg, Germany

Abstract

Phase-locked pulses are important for coherent control experiments. Here we present theoretical analyses and start-to-end simulation results for the generation of phase-locked pulses using the Hard X-ray Self-Seeding (HXRSS) system at the European XFEL. As proposed by Sven Reiche *et al.* in "A perfect X-ray beam splitter and its applications to time-domain interferometry and quantum optics exploiting free-electron lasers", 2022, the method is based on a combination of self-seeding and fresh-slice lasing techniques. However, at variance with this reference, here we exploit different transverse centroid offsets along the electron beam. In this way we may first utilize part of the electron beam to produce SASE radiation, to be filtered as seed and then generate HXRSS pulses from other parts of the beam applying appropriate transverse kicks. The final result consists in coherent radiation pulses with fixed phase difference and tunable time delay within the bunch length. This scheme can be useful for coherent control applications such as coherent x-ray pump-probe experiments.

INTRODUCTION

Phase-locking means a fixed phase relation between successive pulses [1] and phase-locked pulses are important for coherent control experiments [2–4]. Usually a split-and-delay scheme is employed to generate phase-locked pulses in the optical to the extreme ultraviolet wavelengths, while it is challenging to produce phase-locked pulses down to the X-ray regime. X-ray free-electron lasers (FELs) deliver photon pulses with extremely high intensity and show remarkable capabilities for researches in physics, chemistry and biology [5,6]. Self-seeding schemes [7–10] can provide nearly fully coherent x-ray FELs and expand their application to a broader range [11]. Several methods have been proposed to generate coherent phase-locked X-ray pulses from externally seeded FELs [12–15] or using self-seeding techniques [16]. In the first case, the achievable wavelength is limited within the soft x-ray spectral region typical of the high gain harmonic generation configuration, while the second scheme can operate in both soft and hard X-ray regimes by properly choosing the self-seeding monochromators. In Ref. [16], the employed method is based on a combination

of self-seeding and fresh-slice lasing techniques and can offer much higher phase stability than conventional X-ray split-and-delay approaches.

Here we present theoretical analyses and start-to-end simulation results for the generation of phase-locked pulses using the Hard X-ray Self-Seeding (HXRSS) system at the European XFEL. European XFEL is an X-ray FEL facility based on a superconducting linear accelerator [17]. After the collimation section that follows the main linac, there is an arc [18, 19] that bends selected electron beams from a bunch train to the hard x-ray FEL beamline SASE2, where the HXRSS system is built [20]. There are 35 undulator segments of 5 m length interspaced by 1.1 m sections with magnets elements. For the HXRSS system, two single crystal monochromators and chicanes are installed in two positions: one between 8th and 9th segments, the other one between 16th and 17th segments. This configuration provides the flexibility to increase spectrum signal-to-noise ratio by choosing one- or two-chicane scheme according to difference photon energies, and to mitigate crystal heat load effect by using two-chicane scheme for lower photon energies [20].

At variance with Ref. [16], where different lasing parts of the electron beam are defined by the slotted foil in a dispersion section, here we exploit different transverse centroid offsets along the electron beam. This offsets may be induced by collective coherent synchrotron radiation (CSR) effects [21, 22] during the beam transport in the arc upstream of the SASE2 undulators. The method proposed here does not suffer from possible limitation on the beam repetition rate, while the spoiler technique employing slotted foil may do due to radiation losses [23]. In this way we may first utilize part of the electron beam to produce SASE radiation, which is monochromatized as coherent seed to trigger seeded lasing with other parts of the beam that are appropriately kicked on the undulator axis. The final result consists in phase-locked coherent radiation pulses with tunable time delay within the bunch length.

In the following, we will first introduce the slice centroid deviation based scheme to generate phase-locked HXRSS FEL, then CSR effect in the arc before SASE2 at the European XFEL is analysed. Finally the start-to-end simulation is presented.

* shan.liu@desy.de

† gianluca.aldo.geloni@xfel.eu

TOWARDS A SEEDED HIGH REPETITION RATE FEL: CONCEPT OF SEED LASER BEAM TRANSPORT AND INCOUPLING

M. M. Kazemi, T. Lang, L. Winkelmann, S. Hartwell, D. Meissner, E. Ferrari, S. Schreiber, L. Schaper and I. Hartl, Deutsches Elektronen-Synchrotron DESY, Hamburg, Germany
E. Allaria, Elettra-Sincrotrone Trieste S.C.p.A., Basovizza, Italy

Abstract

In this contribution we report the concept of seed laser beam transport and incoupling into the electron beamline to achieve the required seeding parameters for FLASH2020+ project. In our concept a defined source point inside the laser lab is imaged to the center of the modulator. This provides the possibility of controlling the delivered seed parameters at the modulators by actuators within the laser system. We illustrate how the total energy transmission is maximized while the risk of laser induced damage of optics is mitigated. The nonlinear effects of high peak power pulse propagation are studied. Considerations for the incoupling of the seed laser into the electron beamline and the concept for laser-electron timing stabilization are presented.

INTRODUCTION

FLASH2020+ is an upgrade project of the FLASH facility at Hamburg. A main goal of the project is to generate fully coherent soft X-ray FEL radiation at a high repetition rate (MHz) [1]. This will be accomplished by utilizing the well-known seeding techniques High Gain Harmonic Generation (HG) and Echo-Enhanced Harmonic Generation (EEHG), hence it requires two external seed lasers. The combination will provide seeded FEL radiation with tunable wavelength from 4 to 60 nm.

For HG, a tunable UV laser system (Seed2: 297 – 317 nm, 50 fs, < 16 μ J) will modulate the electrons inside the second modulator (Mod2). For EEHG, fixed wavelength (Seed1: 343 nm, 500 fs, < 50 μ J) laser pulses interact with the electrons inside the first modulator (Mod1) which is followed by the interaction of Seed2 and electrons inside the second modulator [2].

Details of the high energy and high repetition rate laser system for seeding are described in [3]. The laser system operates at 10 Hz burst mode with a pulse train of 6000 pulses per second with 1 MHz in a 600 μ s long pulse trains. This matches the electron bunch repetition rate structure.

The femtosecond laser pulses will be transported about 28 and 35 m to the first and second modulators, respectively using dedicated transport laser beamlines and incoupling. The laser beamlines pass mainly through radiation protected area. Figure 1 illustrates the overview of the FLASH accelerator, seeding laser lab and the laser beam transport.

FLASH operates 24/7, with limited access (4 – 8 hours per month) for the maintenance and repair of components inside accelerator tunnel. Therefore, our design has to provide proper means to monitor and control the beam

parameters and at the same time. minimize the required time and expenses for repair and maintenance.

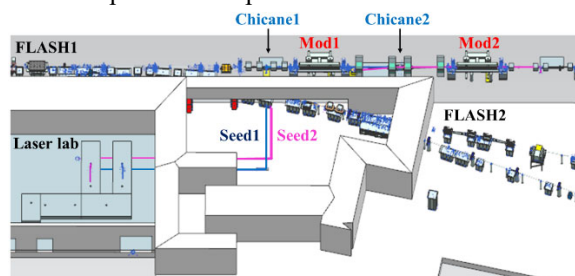


Figure 1: Overview of laser beam transport. Seed1 and Seed2 are coupled into first and second modulators via mirrors installed at the chicanes, where a transversal offset between the laser path and the electrons is presented.

Table 1: Required Seed Laser Beam Parameters Inside Modulators, Mod1 and Mod2

Parameter	Seed1	Seed2
Wavelength (nm)	343	297 – 317
Pulse duration (fs)	500	50
Pulse energy (μ J)	50	16
Peak power (MW)	1 – 100	5 – 300
Polarization	s (perpendicular)	
Beam radius (μ m, $1/e^2$)	600	
Beam quality	$M^2 < 1.5$	
Position control (μ m)	± 500 , 20 μ m resolution	
Pointing (angle) control (μ rad)	± 80 , 3 μ rad resolution	
Position / pointing stability (μ m, rms) / (μ rad)	50 / 40	
Temporal jitter (fs, rms)	Seed1 to e-beam < 50 Seed2 to Seed1 < 50	

SEED LASER BEAM TRANSPORT

Required Parameters for Seeding

Stable overlap in time and space between seed laser and electron beam inside Mod1 and Mod2 is required to imprint an energy modulation onto the electron bunches. Each of the modulator undulators are about 2.5 m long, the electron beam size is between 100 μ m and 200 μ m ($1/e^2$, radius) along the modulator and the laser beam size is ~ 600 μ m ($1/e^2$, radius). This beam size ratio ensures that the electron beam is modulated by the uniform pulse energy distribution of the laser beam and providing most stable modulation.

Table 1 summarizes some of the most relevant parameters of the Seed1 and Seed2 laser pulses inside

IMPACT OF ELECTRON BEAM ENERGY CHIRP ON OPTICAL-KLYSTRON-BASED HIGH GAIN HARMONIC GENERATION

G. Paraskaki*, E. Ferrari, L. Schaper, E. Schneidmiller
Deutsches Elektronen-Synchrotron DESY,
Hamburg, Germany

E. Allaria, Elettra-Sincrotrone Trieste S.C.p.A., Trieste, Italy

Abstract

External seeding schemes allow the generation of stable and fully coherent free electron laser (FEL) radiation but are limited in repetition rates in the order of tens of Hz. This limitation is mainly posed by the limited average power of the seed lasers required to provide hundreds of MW peak power to modulate the electron bunches. An optical-klystron-based high gain harmonic generation (HG) scheme, which can be implemented in several existing and upcoming seeded FEL beamlines with minimal to no additional installations, overcomes this limitation by greatly reducing the required seed laser power. In this work, we carefully study the scheme with detailed simulations that include imperfections of electron beam properties such as a quadratic electron beam energy chirp that characterizes existing FEL facilities. We discuss the optimization steps that in these conditions ensure successful operation, opening the path towards exciting science at FELs with fully coherent and high repetition rate FEL radiation.

INTRODUCTION

High-gain Free electron lasers (FELs) generate pulses of high peak power, short duration, high brightness and transverse coherence down to wavelengths in the hard x-ray regime. These unique properties have allowed several state of the art experiments [1, 2]. However, the temporal coherence of FEL pulses is not guaranteed: the original and well-established mode of operation of high-gain FELs self-amplified spontaneous emission (SASE) [3, 4] is initiated by the spontaneous undulator emission that is naturally chaotic and leads to several individual longitudinal modes being amplified.

To improve the temporal coherence, several proposals have come forward with self-seeding [5, 6] being a promising method to obtain a single-spike spectrum, however, still suffering from SASE intensity fluctuations. A well-established method to achieve not only near transform-limited pulses but also of unprecedented stability is the external seeding [7, 8]. This family of techniques depends on an external seed laser source that imposes both its coherence and its stability onto the output FEL radiation that is a harmonic of the seed laser wavelength.

While seeded FEL radiation has proven very important for several experiments due to its unique pulse properties,

it is limited in terms of repetition rate and shortest output wavelength. Despite the fast progress of lasers, it is still not possible to access lasers that provide sufficient peak power for successful seeded operation at repetition rates exceeding hundreds of Hz. At the same time, there is currently an increasing trend on FELs providing electron bunches at much higher repetition rates of MHz, with FLASH [9] doing this since 2005, European XFEL [10] since 2017 and SHINE [11] together with LCLS-II [12] coming into operation in the near future as continuous-wave-based machines. External seeding cannot keep up with these repetition rates with the currently used seed lasers.

To relax the requirements put on the seed laser systems and therefore increase their repetition rate at a much lower peak power, an alternative seeding scheme has been proposed, the optical-klystron based high gain harmonic generation (OK HG) [13, 14]. This scheme combines the already known optical klystron (OK) [15] and high gain harmonic generation (HG) [7, 16] schemes with the goal to replicate the properties of seeded radiation but with a much lower seed laser power, which in some cases is up to three orders of magnitude smaller [14]. With such a lower power, the repetition rate of the seed laser system can be increased or shorter-wavelength seed laser sources can be used to achieve shorter output wavelengths.

In the following, we take a closer look into this scheme and we study its response to an electron beam energy chirp. While a linear electron beam energy chirp is necessary for compressing the electron bunch and achieving sufficient peak current to drive the FEL amplification in high-gain, higher order terms in longitudinal phase space are typically undesired, but unavoidable. Several factors along the linear accelerator contribute to those high order terms effects with wakefields, space charge and non-linearities in compression being a few of them. In this paper, we isolate a purely quadratic energy chirp and we study its effect on the output FEL pulses of a standard HG and an OK-HG scheme. We study the 15th harmonic of a 300 nm seed laser wavelength, resulting in 20 nm as output wavelength.

THE LAYOUT

In this section, we briefly review the standard HG scheme and the modifications needed for an OK-HG scheme. In standard HG, we take advantage of a powerful seed laser that modulates the energy of the electrons via

* georgia.paraskaki@desy.de

AN XFELO DEMONSTRATOR SETUP AT THE EUROPEAN XFEL*

P. Rauer[†], W. Decking, Deutsches Elektronen-Synchrotron DESY, Hamburg, Germany
 I. Bahns, D. La Civita, J. Gruenert, M. Di Felice, A. Koch,
 L. Samoylova, H. Sinn, M. Vannoni, European XFEL GmbH, Schenefeld, Germany
 J. Rossbach, Universitaet Hamburg, Hamburg, Germany

Abstract

An X-ray free-electron laser oscillator (XFELO) is a next generation X-ray source promising radiation with full three-dimensional coherence, nearly constant pulse to pulse stability and more than an order of magnitude higher spectral flux compared to SASE FELs. In this contribution the concept of an R&D project for installation of an *XFELO* demonstrator experiment at the European XFEL facility is conceptually presented. It is composed of an X-ray cavity design in backscattering geometry of 133 m round trip length with four undulator sections of 20 m total length producing the FEL radiation. It uses cryocooled diamond crystals and employs the concept of retroreflection to reduce the sensitivity to vibrations. Start to end simulations were carried out which account for realistic electron bunch distributions, inter RF-pulse bunch fluctuations, various possible errors of the X-ray optics as well as the impact of heat load on the diamond crystals. The estimated performance and stability derived from these simulations shall be reported and foreseen issues shall be discussed.

INTRODUCTION

In order to overcome one of the major flaws of SASE based FEL radiation in the hard X-ray regime, which is the low degree of monochromaticity and the lack of longitudinal coherence, multiple schemes have been proposed and partly realized over the recent years. Promising schemes are the *X-ray Regenerative Amplifier FEL* (XRAFEL) proposed by Z. Huang in 2006 [1] and the *X-ray Free Electron Laser Oscillator* (XFELO) proposed by K.J. Kim in 2008 [2]. Both schemes are based on trapping FEL radiation inside a X-ray optical cavity, using monochromatizing crystals based on Bragg reflection instead of total reflecting optical mirrors [1, 3]. While the XFELO is closely related to the low gain FEL scheme, the XRAFEL is based on the strong gain FEL amplifier scheme. In the following, both schemes will be summarized under the term *XFELO*. Due the promise of delivering outstanding radiation properties, *XFELOs* have received growing interest in the recent years [3–14]. European XFEL is developing an *XFELO* demonstrator to be installed at the end of one of the hard X-ray undulator lines (SASE1) in the first quarter of 2024. The principal goal of the demonstrator is to prove the working concept - meaning seeding and increasing longitudinal coherence by several orders of magnitude over subsequent round trips, from synchrotron radiation to almost monochromatic FEL amplifier

radiation. It is not primarily meant for user-operation, and therefore not optimized to this end.

In this proceeding, the fundamentals of the experimental setup as well as the expected output characteristics shall be sketched. More detailed information will be given in a separate publication [15] or can be looked up in ref. [16].

A PROOF-OF-CONCEPT XFELO EXPERIMENT

The X-ray cavity is designed in a simple two crystal backscattering geometry, following the principle of maximum simplicity to avoid mechanical complications. Hence, features like wavelength tunability [3, 7] are omitted. The crystals are two optically thick ($t_C \approx 250 \mu\text{m}$) diamond crystals. This increases the robustness of the setup against thermal load, which is further improved by cooling the diamonds to a temperature of $T = 77 \text{ K}$ [10, 11, 17–19]. In between the crystals, four 5 m long variable gap undulator sections are positioned and two chicanes are used to in- and out-couple the electrons. The crystal to crystal distance is fixed to $L_{C-C} \approx 66.42 \text{ m}$, which matches an electron bunch repetition rate of $f_{\text{rep}}^{\text{el}} = 2.25 \text{ MHz}$, being a common repetition rate at the European XFEL accelerator. Each reflecting crystals is combined with two grazing incidence mirrors aligned orthogonally with respect to each other and the crystal. This forms a so called retroreflector, which may decouple the setup from outer vibrations (see [15] or [16] for reference). Additionally, by applying a slight meridional curvature $R_m \approx 20 \text{ km}$ on the total reflecting mirrors, focusing of the X-ray pulses can be achieved.

In Fig. 1 the evolution of the pulse energy of the *XFELO* demonstrator for a photon energy of $E_c = 9.05 \text{ keV}$ is displayed. The different curves correspond to the X-ray pulse directly after the undulator (blue), reentering the undulator as seed for the subsequent round trip (red) and the transmitted pulse (yellow). The simulations include various different error sources, such as statistical electron beam shot to shot fluctuations common for the European XFEL accelerator [20], crystal misalignment and mirror surface profile error of $h_{\text{rms}} = 1.5 \text{ nm}$. Figure 1(a), which neglects the impact of heat load on the crystals, shows that the pulse energy trapped inside the X-ray cavity reaches up to very high value, which corresponds in combination with a very small bandwidth of only $\sigma_{E_{\text{ph}}} = 20.4(5) \text{ meV}$ to unparalleled peak spectral densities. Owing to the simplistic transmission through a thick crystal, only the spectral side lobes regenerated at every round trip are transmitted. This leads to much lower trans-

* Work supported by (FKZ 05K16GU4)

[†] patrick.rauer@desy.de

FLASH2020+ PROJECT PROGRESS: CURRENT INSTALLATIONS AND FUTURE PLANS

L. Schaper[†], Ph. Amstutz, N. Baboi, K. Baev, M. Beye, Ch. Gerth, I. Hartl, K. Honkavaara, J. Müller-Dieckmann, R. Pan, E. Plönjes-Palm, O. Rasmussen, J. Rönsch-Schulenburg, E. Schneidmiller, S. Schreiber, K. Tiedtke, M. Tischer, S. Toleikis, R. Treusch, M. Vogt, L. Winkelmann, M. Yurkov, J. Zemella
Deutsches Elektronen Synchrotron DESY, Hamburg, Germany

Abstract

The FLASH2020+ project has started to transform the FLASH facility to broaden the facility profile and meet demands of future user experiments. In a nine-month lasting shutdown until August 2022 the linear accelerator of the FLASH facility has, among others, been upgraded with a laser heater, new bunch compressors and new modules. The latter results in an energy upgrade to 1.35 GeV allowing to reach sub 4 nm wavelength. In the following 14-month lasting shutdown starting mid 2024 the FLASH1 FEL beamline will be completely rebuild. The design is based on external seeding at MHz repetition rate in burst mode allowing for coherent tuneable FEL radiation in wavelength and polarization by installation new APPLE-III undulators. Post compression of the beam downstream of the radiators will allow for high quality THz generation and together with the new experimental end stations and pump probe lasers provide a unique portfolio for next generation user experiments.

INTRODUCTION

The FLASH facility [1-3], housed at DESY, Hamburg, currently consists of a superconducting linac powering two FEL beamlines (FLASH1 and FLASH2). These beamlines provide extreme ultraviolet to soft x-ray radiation generated via self-amplified spontaneous emission (SASE) to facilitate various kinds of user experiments. In addition, a

significant share of the FLASH operation time is committed to research and development, which e.g. led to developments like the gas monitor detector for FEL beam position and intensity diagnostics [4]. The developed components in R&D also contributed significantly to upgrades and improvements the facility has undergone since it was built in 2003/2004, at that time named VUV-FEL at TTF2 [5]. To increase the available parameter range and enable next generation user experiments the current facility upgrade, coordinated in the FLASH2020+ project, has already been started. One of the main goals is to provide coherent and spectro-temporally stable beams while also extending the wavelength range even further into the water window.

The individual updates required to achieve the project milestones are grouped in a two-stage process: During a nine-month shutdown which finished in mid-August 2022 the linac has been in focus with upgrades targeting the beam quality and energy, described in detail in the following. The second stage will target the current FLASH1 FEL beamline, removing all of its components and replacing it by an externally seeded beamline. The latter includes an upgrade of the existing photon diagnostics and photon beam transport to allow for most efficient use of beamtime by users with fully characterised beams for every shot at highest possible intensities.

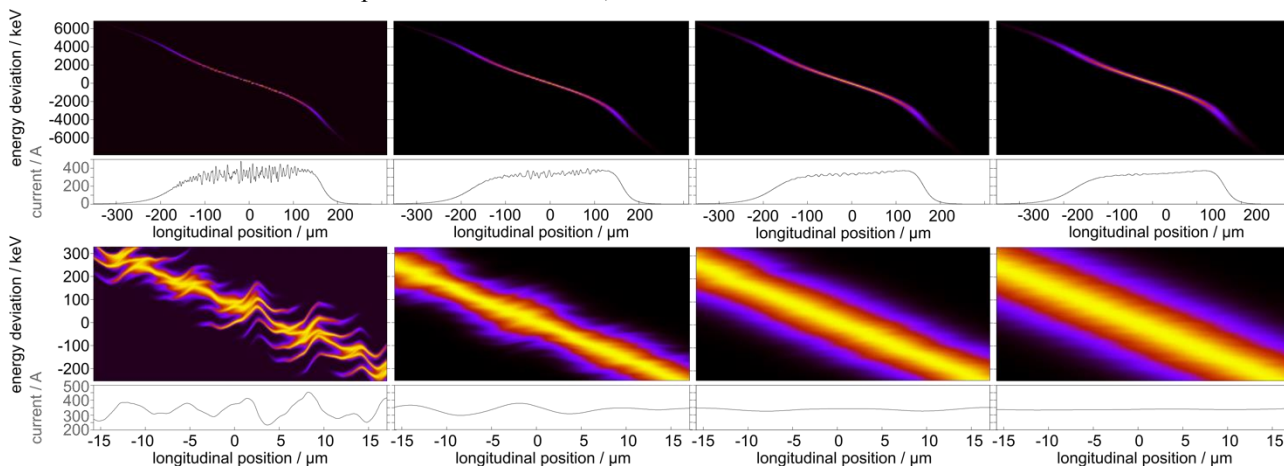


Figure 1: Numerical simulation of the phase space of the full electron beam (top) and the central slice (bottom) together with the current profile at the end of the linac using a recently developed semi-Lagrangian Vlasov simulation code [6]. The images on the left display the situation with the laser heater at zero laser power resulting in an initial sliced energy spread of 3 keV before compression. Towards the right the laser power is increased to reach sliced energy spreads of 5

[†]URS.schaper@desy.de

THE NEW FLASH1 UNDULATOR BEAMLINE FOR THE FLASH2020+ PROJECT

Johann Zemella, Mathias Vogt*
Deutsches Elektronen-Synchrotron DESY, Hamburg, Germany

Abstract

The 2nd stage of the FLASH2020+ project at DESY will be an upgrade of the FLASH1 beamline to enable HGHG and EEHG seeding with two modulator-chicane stages, and a radiator section with 11 APPLE-III undulators to enable FEL radiation with controllable polarization. A key feature of FLASH, namely the capability of providing several thousand FEL pulses in the extreme UV and soft X-ray must not be compromised. Downstream of the radiator the beamline houses longitudinal diagnostics, a double bend (quasi-)achromat to separate the electrons from the photons and divert the electron beamline from the photon diagnostics, a post-compressor, a THz-Undulator (requires an electron beam that is compressed more strongly than for seeding), and finally the dumpline, capable of safely aborting up to 100 kW electron beam power.

This article describes the conceptional and some technical details of the beamline with emphasis on the upstream part (modulators and radiator) designed for seeding.

INTRODUCTION

FLASH the XUV- and soft X-ray user facility at DESY in Hamburg [1–7] is currently undergoing a substantial upgrade and refurbishment project, FLASH2020+ [8–10]. The FLASH accelerator consists of four functionally distinct sections: the common part (injector, linac), called FLASH0, which is upgraded and refurbished in the current shutdown [3, 5], the two independently operated undulator beamlines FLASH1 & FLASH2 [11, 12], and the experimental beamline FLASH3. The superconducting linac supplies long RF pulses with a flat top usable for beam operation of up to 800 μ s). This flat top can be split with a transition time of typically 70 μ s, so that both beamlines can be served with sub-trains of up to several hundred bunches at bunch frequencies of up to 1 MHz at every RF-pulse. The RF pulse repetition frequency is 10 Hz. FLASH1 will be basically completely rebuilt in 2024/25 which is the topic of this contribution.

Conceptual Overview of the Beamline

In the past both FLASH1/2 were dedicated SASE (Self-Amplified Spontaneous Emission) FELs (Free-Electron Lasers). In the future the new FLASH1 beamline, however will be optimized for high repetition rate HGHG (High Gain Harmonic Generation) and EEHG (Echo-Enabled Harmonic Generation) external seeding [9] within the FLASH2020+ project.

SASE has proven to be an extremely powerful and robust FEL mechanism, but external seeding potentially enhances the control over properties of the produced FEL radiation, i.p. the longitudinal coherence, substantially [9].

The incoming bunch is overlaid in the first undulator (modulator UM1) with the first seed laser beam (L1). Thereby an energy modulation is impregnated on the bunch PSD. Next the energy modulation from L1 and UM1 is strongly over-sheared in the first magnetic chicane (CH1). Then the bunch is overlaid in the second undulator (modulator UM2) with the second seed laser beam (L2). Finally bunch is moderately sheared in the second magnetic chicane (CH2) so that its sinusoidally modulated fine structure generates bunching whose higher order Fourier harmonics will seed the FEL process in the radiator.

Downstream of the radiator the electron beam passes through a longitudinal diagnostic section before it is separated from the FEL beam, post-compressed, sent through an electromagnetic undulator for THz radiation used for highly synchronized pump-probe experiments [13] before it is finally dumped.

Here we give an overview of the FLASH1 beamline with emphasis on the FEL sections, namely the two modulator sections with their chicanes and the radiator section. The other sections of the beamline, collimation, matching, longitudinal diagnostics, horizontal separation from the FEL beam, post-compression, THz undulator and the dump beamline have been described in greater detail in [14].

BEAMLINE DETAILS

The undulator beamline is split into several functional sections as is shown in Fig. 1

A section for diagnostic collimation and matching will be installed upstream of the modulator section immediately following the FLASH1/FLASH2 switch yard.

The modulator sections FL1MOD1/2 contain the 2.5 m long planar modulator undulators UM1 and UM2. The magnetic structure of the undulators is not yet fixed but will soon be finalized. Each modulator is surrounded by two 0.6 m long intersections (see Fig. 2 left) equipped with a beam position monitor (BPM), a quadrupole with x/y -mover, a screen station, 2 beam loss monitors (BLMs) and x/y -steering using air-coils or small ferrite coils. The modulator sections also contain the two vertical C-chicanes CH1 and CH2 needed for the EEHG external seeding process as briefly explained in subsection . An additional chicane InC (Fig. 3) is needed upstream of modulator UM1 for in-coupling of the first seed laser L1. The seed laser L2 is coupled in through CH1 (Fig. 4) upstream UM2. The laser beams are coupled out

* vogtm@mail.desy.de

FUTURE UPGRADE STRATEGY OF THE FERMI SEEDED FEL FACILITY

E. Allaria, L. Badano, F. Bencivenga, C. Callegari, F. Capotondi, D. Castronovo, P. Cinquegrana, M. Coreno, M. B. Danailov, A. Demidovich, G. De Ninno, P. Del Giusto, S. Di Mitri, B. Diviaco, W. M. Fawley, M. Ferianis, G. Gaio, F. Gelmetti, L. Giannessi, G. Kurdi, M. Lonza, M. Malvestuto, M. Manfredda, C. Masciovecchio, I. Nikolov, G. Penco, K. C. Prince, E. Principi, P. R. Rebernik, C. Scafuri, N. Shafqat, P. Sigalotti, A. Simoncig, S. Spampinati, C. Spezzani, L. Sturari, M. Trovò, M. Veronese, R. Visintini, M. Zangrando, Elettra-Sincrotrone Trieste S.C.p.A, Basovizza, Italy.

T. Tanaka, RIKEN SPring-8 Center, Hyogo, Japan.

G. Penn, Lawrence Berkeley National Laboratory, USA

G. Perosa, F. Sottocorona, Università degli Studi di Trieste, Trieste, Italy

Abstract

FERMI is undergoing a series of upgrades to keep the facility in a world-leading position. The ultimate goal of the development plan consists in extending the facility spectral range to cover the water window and above and to reduce the minimum pulse duration below the characteristic lifetime of core holes electrons of light elements. We present here the main elements of this upgrade strategy.

INTRODUCTION

The upgrade involves deep modifications of the linac and of the two FERMI FELs with the ambition of extending the FEL performances and the control of the light produced to include the K-edges of N and O, and the L_{23} -edges of elements of the first two periods. One of the main requisites of this upgrade is the preservation of the uniqueness of FERMI: the possibility to control the properties of the radiation by seeding the FEL with an external laser system. Through the control of the microbunching formation in the electron beam the seed allows amplification of almost Fourier transform-limited pulses [1–3], to synchronize the FEL pulses with unprecedented precision to an external laser [4] and to control many pulse properties as phase and coherence [5, 6]. The extended photon energy range will allow resonant experiments (XANES, XMCD, SAXS, CDI,...) exploiting several important edges (life-time in the range of few fs), larger wave-vector (non-linear Optics), ultrafast chemistry (conical intersections lifetime 0.5 – 10 fs) [7]. Presently, the spectral range up to 310 eV is covered by the two FELs: FEL-1 and FEL-2; the first provide photons in the range 20 – 65 eV, the second in the range 65 – 310 eV. In view of the upgrade, the photon energy distribution between the two FELs has to be adapted to the upgraded scenario, with FEL-1 still covering the low photon energy range, but extended to reach a photon energy of 100 eV [8], and FEL-2 dedicated to the high energy range, from 100 eV to about 550 eV.

FEL-2 UPGRADE

To extend the FEL-2 spectral range to the oxygen K-edge, two options were considered, either by using EEHG directly, or with a cascade employing both EEHG and HGHG techniques in the “fresh-bunch” injection technique now used on FEL-2. The implementation of EEHG first solution requires a first large dispersion chicane of up to 15 mm for optimized EEHG operation. This makes the scheme prone to a number of effects which may result in a degradation of the FEL spectral purity and of the FEL gain in the final radiator [9, 10]. The large chicane is indeed an amplifier of microbunching instability (MBI). A second issue is the emission of incoherent synchrotron radiation (ISR) and the intra-beam scattering (IBS) along the chicane. These two effects are the source of mixing of the filamented phase space that produces the high harmonic bunching in EEHG after the second chicane, a factor reducing the bunching at the entrance of the amplifier.

All these effects would be mitigated in a scheme where the chicanes have a lower dispersion. This is the reason why we considered the second option, where the EEHG generates a seed that is then used in fresh-bunch to seed a second HGHG stage, similarly to what is done in the present FEL-2 configuration. The present double-stage HGHG with fresh-bunch scheme, can be upgraded by converting the first stage to an EEHG configuration aimed at reaching harmonics of the order of 30. The second stage would then up-convert the output of the first stage to harmonics of the order 120 – 130 as required.

This configuration needs a much lower dispersion, of the order of 4-5 mm, which is only a factor two larger than the one used in the FERMI EEHG experiment. We analysed the four different configurations of seeded FELs shown in Fig. 1 and selected the most promising one with the aim of extending the seed coherence to the highest harmonic orders.

CHIRPED PULSE AMPLIFICATION IN A SEEDED FEL: TOWARDS THE GENERATION OF HIGH-POWER FEW-FEMTOSECOND PULSES BELOW 10 nm

D. Garzella*, G. De Ninno¹, E. Allaria, A. Brynes, C. Callegari, P. Cinquegrana, M. Coreno, I. Cudin, M.B. Danailov, A. Demidovich, S. Di Mitri, B. Diviacco, L. Giannessi, L. Novinec¹, G. Penco, G. Perosa, P. Rebernik, A. Simoncig, F. Sottocorona, L. Sturari, M. Trovò, M. Zangrando, Elettra-Sincrotrone Trieste, Basovizza, Italy
F. Frassetto, L. Poletto, CNR IFN-Padova, Padua, Italy
P. Zeitoun, Laboratoire d'Optique Appliquée, Palaiseau, France
¹also at University of Nova Gorica, Nova Gorica, Slovenia

Abstract

In this contribution we report the successful implementation of CPA in a seeded XUV FEL. After the first unique result, the FERMI CPA collaboration team (open entity to which interested colleagues from abroad can participate) has set-up a second experiment for demonstrating and implementing a two-stage harmonic generation scheme on the FERMI FEL-2 branch, aiming at generating coherent and phase-tailored few-femtosecond FEL pulses, with gigawatt peak power in the sub-10 nm spectral range. The set-up of the second experiment is still undergoing. Here we discuss the work in progress, together with the main scientific and technical bottlenecks and their implications.

INTRODUCTION

In optical conventional lasers, chirped pulse amplification (CPA) revealed to be, in the early 80's, a revolutionary technique, allowing the generation of extremely powerful femtosecond pulses in the infrared and visible spectral ranges, taking advantage of their emission broadband (10's of nm). Nowadays, CPA is the basis for the worldwide operation of laser systems delivering very ultrashort pulses, in the few femtosecond (quasi single cycle) regime, and carrying peak powers up to the Petawatt scale. The experimental implementation of CPA on a seeded FEL in the extreme-ultraviolet, successfully achieved on FERMI in last recent years, has been driven by the following considerations : for any given FEL configuration, a limit presently exists in the generation of ultra-short pulses, as the output pulse energy is limited by the reduced number of electrons participating in the amplification process. Moreover, the pulse shortening is constrained by the FEL gain bandwidth. Eventually, stretching the seed pulse allows one to extract energy from the whole electron bunch, substantially enhancing the FEL pulse energy at saturation. In seeded FELs the bandwidth of the output emission can be significantly larger than that of the seed. This allows at obtaining, after compression, a FEL pulse shorter than the one generated when the FEL is operated in standard (i.e., no-CPA) mode.

* david.garzella@elettra.eu

CHIRPED PULSE AMPLIFICATION

CPA General Setup

CPA lasers [1] show four major stages : the oscillator and preamplifier (also called "the front end"); the stretcher, aiming at dispersing the laser broad spectrum through a dispersive element, like a prism or a diffraction grating ; the main amplifier, where the CPA main feature takes place : to achieve very high energies (with a net gain up to 6 orders of magnitude). Stretching the pulse allows at keeping constant the laser fluence while reducing the intensity, which mitigates the occurrence of phase distortion issues and prevent from damage on optics during the pulse propagation; finally the compressor, another dispersing element similar to the first one, where the previously induced group delay dispersion is fully compensated, and the laser pulse duration is set back to the original value, typically in the Fourier-Transform limit (TF) regime. In a seeded FEL the setup is quite similar [2]. The seed laser is chirped, stretched and co-linearly injected in the undulator. Thanks to the time- energy correlation, the resonance condition is also dispersed on a longer temporal scale, inducing the broadening of the gain bandwidth, thus experiencing a different electron bunching pattern. Higher amplification occurs and the FEL phase pattern reproduces the seed laser, scaled by the harmonic bunch number [3]. Finally, thanks to a XUV compressor, typically composed of two gratings in classical mount configuration [4], the FEL pulse duration results shorter by a higher factor than the one reckoned by Stupakov's law [3].

Theoretical Background

In order to numerically compare the obtained results and the expected pulse duration under the actual experimental conditions, here is a brief summary and the main outcomes of the CPA FEL theory. In the following the considered seed laser pulse has a gaussian spectral shape . The corresponding electric field in the frequency domain is $\hat{E}(\omega) \sim e^{-\omega^2/(2\sigma_\omega^2)} e^{-i\beta\omega^2/4}$, where σ_ω is the (rms) laser bandwidth and β is the so-called group delay dispersion (GDD) [5]. The Inverse Fourier Transform $E(t)$ of $\hat{E}(\omega)$ is $E(t) \sim e^{-t^2/(2\sigma_t^2)} e^{i\Gamma t^2}$. In presence of strong chirp, for $\beta \gg 2/\sigma_\omega^2$, the coefficient of the quadratic temporal phase,

NON-LINEAR HARMONICS OF A SEEDED FEL AT THE WATER WINDOW AND BEYOND

G. Penco[†], E. Allaria, L. Badano, F. Bencivenga, A. Brynes, C. Callegari, F. Capotondi, A. Caretta, P. Cinquegrana, M.B. Danailov, D. De Angelis, A. Demidovich, S. Di Mitri, L. Foglia, G. Gaio, A. Gessini, L. Giannessi, G. Kurdi, M. Manfreda, M. Malvestuto, C. Masciovecchio, R. Mincigrucci, I. Nikolov, E. Pedersoli, S. Pelli Cresi, E. Principi, P. Rebernik, A. Simoncig, S. Spampinati, C. Spezzani, M. Trovò, M. Zangrando, G. De Ninno
Elettra – Sincrotrone Trieste SCpA, Basovizza, Italy
G. Perosa, F. Sottocorona, Università degli Studi di Trieste, Trieste, Italy
S. Dal Zilio, Istituto Officina dei Materiali, Consiglio Nazionale delle Ricerche, Trieste, Italy
V. Chardonnet, M. Hennes, B. Vodungbo, E. Jal, Sorbonne Université, CNRS, Laboratoire de Chimie Physique-Matière et Rayonnement, France
J. Lüning Helmholtz-Zentrum Berlin für Materialien und Energie GmbH, Berlin, Germany
P. Bougiatioti, C. David, B. Roesner, Paul Scherrer Institut, Villigen PSI, Switzerland
M. Sacchi, Institut des NanoSciences de Paris, CNRS, Sorbonne Université, Paris, France and Synchrotron SOLEIL, L'Orme des Merisiers, Saint-Aubin, Gif-sur-Yvette, France
E. Roussel, PhLAM/CERLA, Villeneuve d'Ascq

Abstract

The advent of free electron lasers (FELs) in the soft and hard X-ray spectral region has opened the possibility to probe electronic, magnetic and structural dynamics, in both diluted and condensed matter samples, with femtosecond time resolution. In particular, FELs have strongly enhanced the capabilities of several analytical techniques, which take advantage of the high degree of transverse coherence provided. FELs based on the harmonic up-conversion of an external seed laser are also characterised also by a high degree of longitudinal coherence, since electrons inherit the coherence properties of the seed. At the present state of the art, the shortest wavelength delivered to user experiments by an externally seeded FEL light source is about 4 nm. We show here that pulses with a high longitudinal degree of coherence (first and second order) covering the water window and with photon energy extending up to 790 eV can be generated by exploiting the so-called nonlinear harmonic regime, which allows generation of radiation at harmonics of the resonant FEL wavelength.

Moreover, we report the results of two proof-of-principle experiments: one measuring the oxygen K-edge absorption in water (~ 530 eV), the other analysing the spin dynamics of Fe and Co through magnetic small angle x-ray scattering at their L-edges (707 eV and 780 eV).

INTRODUCTION

The high degree of transverse coherence of the FELs pulses has been exploited by several techniques, including Fourier transform holography, coherent diffraction imaging, and ptychography. In the case of a seeded FEL, the output radiation has been proven to have also a high degree of longitudinal coherence [1-3] that is of crucial

importance for techniques such as linear and nonlinear spectroscopies and coherent control, requiring both phase and wavelength manipulation within a given pulse. In a seeded FEL operating in High Gain Harmonic Generation (HG) mode [4] an external seed laser imprints an energy modulation on an electron beam passing through an undulator (called modulator). Then, the electrons are sent through a magnetic dispersive section that converts this energy modulation into a density modulation, known as bunching, whose spectral content includes higher harmonics of the seed, with a progressively fading coefficient [5]. The electron beam is then injected into an undulator tuned to be resonant to a given harmonic of the seed: since the process is stimulated by the seed laser, all electrons emit in phase, resulting in the generation of nearly Fourier-transform-limited pulses. The reduction of the bunching with the increase of the harmonic order sets a limit on the shortest wavelength that can be generated. In fact, the bunching level at the desired harmonic has to be substantially larger than the shot noise, in order to avoid the Self Amplified Spontaneous Emission (SASE) process becoming dominant, thereby spoiling the longitudinal coherence of the FEL output.

The HG scheme has been implemented at FERMI in a two-stage cascade, using the emission from the first stage to seed the second one. In this configuration the shortest wavelength delivered to users for experiments is about 4nm [6-8], corresponding to the 65th harmonic of an ultraviolet laser. The possibility to reach a similar spectral regime in a single stage FEL by adopting the echo-enabled harmonic generation (EEHG) scheme [9] has been recently proven. Moreover, coherent and stable emission at 2.6 nm (~474 eV) was observed [10], although the parameters used for the experiment allowed only a feeble intensity, comparable to the broadband spontaneous emission coming from the whole electron bunch.

[†] giuseppe.penco@elettra.eu

FREQUENCY PULLING IN A SUPERRADIANT FEL AMPLIFIER

Najmeh S. Mirian, DESY, Hamburg, Germany

Michele Di Fraia, Simone Spampinati, Filippo Sottocorona¹, Enrico Allaria, Laura Badano, Miltcho B. Danailov, Alexander Demidovich, Giovanni De Ninno², Simone Di Mitri, Giuseppe Penco, Primož Rebernik Ribič², Carlo Spezzani, Giulio Gaio, Mauro Trovó, Nicola Mahne, Michele Manfreda, Lorenzo Raimondi, Marco Zangrando, Oksana Plekan, Kevin C. Prince³, Carlo Callegari and Luca Giannessi⁴, Elettra Sincrotrone Trieste, Basovizza, Italy

Richard J. Squibb, University of Gothenburg, Gothenburg, Sweden

Xi Yang, National Synchrotron Light Source II, Brookhaven National Laboratory, Upton, NY, USA

¹ also at Università degli Studi di Trieste, Trieste

² also at Laboratory of Quantum Optics, University of Nova Gorica, Nova Gorica, Slovenia

³ also at Centre for Translational Atomaterials, Swinburne University of Technology, Melbourne, Victoria, Australia

⁴ also at Istituto Nazionale di Fisica Nucleare, Laboratori Nazionali di Frascati, Frascati, Italy

Abstract

A superradiant cascade is a method proposed to shorten the pulse duration in seeded FEL. Pulses shorter than the typical duration supported by the FEL gain bandwidth of the FEL amplifier in the linear regime were measured at FERMI, user FEL facility in Italy. In these conditions we observed a strong frequency pulling phenomenon that will be discussed in this contribution. Finally, we report the most recent measurements carried on FEL-2 set-up in what we label “superradiant mode” of operation.

INTRODUCTION

Ultrashort pulses can probe terahertz-driven dynamics such as coherent phonons or collective excitations in condensed matter, opening the way to the observation of field-dependent, coherently driven phenomena [1-3]. Most pump-probe experiments with FELs must cope with the many complications of poor synchronization and large intensity fluctuations: the need for post-processing, the rejection of outliers reducing the efficiency of data collection, and rogue pulses that may be the cause of premature sample damage. Externally seeded FELs, currently based on high gain harmonic generation (HG), are ideal in terms of synchronization (a few femtoseconds (ref. [4]) and control of pulse properties, which are inherited from the seed source [5-7]. The typical pulse duration, in a seeded HG FEL, is a function of the seed duration and decreases with harmonic order [8]; at the FERMI machine used in this study, two HG FELs cover the range from 100 to 4 nm (refs. [5-9]), with pulses from 90 fs down to 20 fs (for a 70 fs seed). An alternative, which exploits the FEL dynamic process itself to beat the gain bandwidth limit, was proposed in refs. [10-14]: driving the FEL amplifier into saturation and superradiance, along a cascade of undulators resonant at progressively higher harmonics of

an initial seed. This is the practical realization of an idealized condition under which a radiation pulse at the onset of saturation in a FEL amplifier propagates and grows as a self-similar solitary wave, undergoing longitudinal compression [15,16]. After saturation, the peak power of an isolated spike moving along a uniform electron beam grows proportionally to the square of the distance covered along the undulator and its duration becomes shorter than the duration supported by the FEL gain bandwidth at the Fourier transform limit (FTL) [17]. A few experiments carried out at visible wavelengths have demonstrated several of the key elements of the scheme [18-20]. In the experiment reported in ref. [1] a few steps forward in the comprehension and characterization of the extreme-ultraviolet (EUV) X-ray superradiant pulses resulting from a cascaded FEL were achieved. A three-stage superradiant cascade (SRC) starting from an ultraviolet (UV) seed pulse and reaching the EUV spectral range was realized at FERMI, according to the scheme proposed in ref. [21].

EXPERIMENT

The experiments were carried out at the FERMI FEL-2 line during three experimental sessions labelled A, B and C.

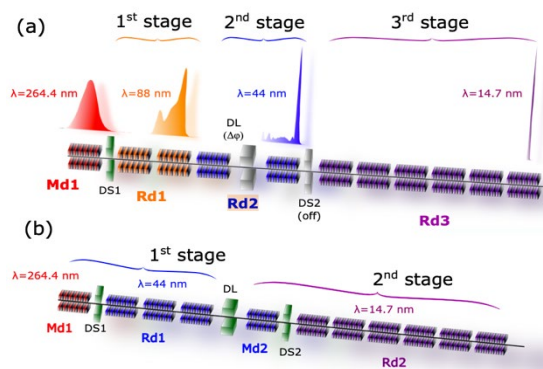


Figure 1: FEL layout (a) FEL-2 in SRC, (b) FEL-2 in HG.

STUDIES OF WAVELENGTH CONTROL AT FERMI

F. Sottocorona, G. Perosa, Università degli Studi di Trieste, Italy
 L. Giannessi¹, E. Allaria, S. Di Mitri, M. B. Danailov., Elettra-Sincrotrone Trieste S.C.p.A,
 Basovizza, Italy

¹also at INFN LFN, Frascati, Roma, Italy

Abstract

FEL basic theory indicates that the output wavelength of a seeded FEL operated in the HGHG configuration is determined by the wavelength of the seed laser and light is emitted when undulators are tuned to an exact harmonics of the seed laser. In a realistic case, when taking into account the electron beam imperfections and the finite bandwidths of the seed and of the amplification process, the output wavelength is influenced by these factors and can deviate from the exact harmonic giving some flexibility to control the FEL wavelength without the need to change the seed laser wavelength. In this work, we consider the effects of the dispersive section, the curvature of the electron beam longitudinal phase-space and the frequency pulling as major contributors. We show how these quantities influence the effective final FEL wavelength. Furthermore, we show how one can reconstruct the electron beam longitudinal phase-space from the analysis of the FEL wavelength sensitivity to the seed laser delay with respect to the beam arrival time.

INTRODUCTION

In a Self-Amplified Spontaneous Emission FEL, the output wavelength is governed by the resonance condition in the amplifier [1]. Operations of seeded FEL such as High Gain Harmonic Generation [2] require the resonance condition to be set at one of the higher harmonics of the seed used to modulate the beam, undulator tuning is no longer a free parameter and wavelength is determined by the seed laser. This condition is the result of the interference process of the emission of the density modulated beam and contributes to the superior wavelength stability of the FEL that is not dominated by the beam energy jitter [3]. In practice, there are different phenomena in the HGHG harmonic conversion process that can shift the output wavelength from this condition, such as the effect of the dispersive element in the undulator chain or the frequency pulling phenomenon shifting the wavelength when the undulator resonance does not coincide with the one of density modulation. In order to control the properties of the FEL light and understanding of the various elements of the machine involved in the process is required for an accurate tuning of the FEL.

THEORETICAL BACKGROUND

It is well known from literature that the FEL emission is based on the coherent radiation emitted by a high-brightness, relativistic electron beam passing through the periodic field of an undulator. The interaction between the

undulator magnetic field and the transverse motion of the wiggling electrons leads to an energy exchange from the e-beam into the electromagnetic radiation. The output wavelength of this process can be calculated by the relation

$$\lambda_{res} = \frac{\lambda_u}{2\gamma^2} (1 + a_w^2) \quad (1)$$

where λ_u is the undulator period, a_w is equal to the undulator strength parameter K , for circular polarizations, and $K/\sqrt{2}$ for linear polarizations, and γ_0 is the energy of the beam (in mc^2 units). Normally, for small adjustments of the FEL wavelength, the energy of the e-beam can be kept constant, and the parameter a_w is varied by varying the undulator gaps. FEL amplification occurs only within the gain bandwidth that can be estimated from the Pierce parameter ρ [2]. In the case of FERMI ρ is of the order of 10^{-3} . The range of the wavelength tuning, with fixed gap, is therefore pretty small. In terms of beam energy, the corresponding accuracy to stay within the gain bandwidth is of about a MeV, at a beam energy of 1 GeV. In a seeded FEL like FERMI, the generation of coherent FEL pulses is the result of few processes. First, as a result of the interaction between the electrons and the external seed, inside a modulator, the beam is modulated in energy, with the period of the modulation being equal to the wavelength λ of the seed. In a second step, this energy modulation is converted into density modulation by a dispersive chicane. As a result, the electron beam is subdivided into micro-bunches that can emit in phase, producing coherent emission at the fundamental wavelength. Because bunching can have strong harmonic components, coherent emission can also be produced at the harmonics of the resonant wavelength. In the third phase, bunched electrons passes through undulator tuned to a specific harmonic n of the seed and emit coherently. Finally, FEL amplification occurs leading to generation of high power pulses at λ/n .

The dispersive section has the main role of energy-density conversion, but, in combination of an energy chirp into the electron beam has also the effect of compressing (or decompressing) the bunch, because electrons at different energies travel on different paths. Since the seeding process is done before the dispersive element, the wavelength impressed by the seed is also slightly compressed by the dispersive element. This effect is present when the e-beam has not a flat longitudinal phase-space. In particular, linear compression of the beam is determined by the linear chirp. Therefore, the harmonic coherent emission will no longer occur at λ_{seed}/n , but rather at the compressed wavelength. This new wavelength can be calculated by the relation

CONTROL OF THE LONGITUDINAL PHASE AND BENCHMARKING TO HBSASE

Saeid Pirani, Francesca Curbis, Mihai Pop, Sverker Werin*
Department of Physics, Lund University, P.O. Box 118, SE-22100 Lund, Sweden

Abstract

Improvement of the longitudinal coherence in the proposed Soft X-ray FEL, the SXL, for the MAX IV Laboratory is an important design aspect to enhance the user case. One of the main considered methods is HBSASE. However the final compression in the MAX IV accelerator is done at full energy, and thus leaving an energy chirp in the electron pulse. This chirp in longitudinal phase space has to be removed for an efficient implementation of HBSASE. In this paper we show in simulations how the phase space is improved by first overcompressing the pulse, and then correct it by a two-plate wakefield de-chirper. The resulting pulse is then shown to have qualities such that, by HBSASE, a significant narrowing of the FEL bandwidth is achieved at 1 nm.

INTRODUCTION

Free Electron Lasers (FEL) driven by linear accelerators can provide high power photon pulses with short duration, narrow bandwidth and high brilliance. The transverse coherence is excellent, while the longitudinal coherence in a SASE FEL is limited. To improve the longitudinal coherence, intensity and wavelength stability different seeding techniques can be implemented. While longer wavelength FELs can make use of external lasers for directly seeding, this is not easily achieved in the X-ray range. Thus other techniques have to be used, such as EEHG (Echo Enhanced Harmonic Generation) [1], Self-seeding [2] or HBSASE (High Brightness SASE) [3]. All these techniques put additional requirements on the electron beam quality and provide different enhancement of the fundamental properties.

One critical parameter is the flatness of the longitudinal phase space. The compression of the pulse, wakefields and CSR will influence the energy distribution along the pulse. Wakefields are also commonly used to adjust and correct the longitudinal phase space. A limitation is that the wakefields normally reduce the energy of the tail of the electron pulse, and thus pulses with lower energy in the tail cannot easily be adjusted. This is the situation in the MAX IV linear accelerator using achromat bunch compressors and final compression at full energy.

In this paper we discuss how the sign of the chirp can be flipped through over-compression. The flipped chirp is then removed by standard de-chirper, using parallel metallic plates with a corrugated surface. Finally, by simulations we show a proof of concept of the beam being used in a HBSASE mode at 1 nm with improved spectral properties and reduced jitter.

MAX IV ACCELERATOR AND THE SXL PROJECT

The MAX IV Laboratory is a synchrotron radiation facility operating two storage rings, at 3 and 1.5 GeV respectively, and a full energy linear accelerator injector. Around the facility 16 beamlines (2022) provides a palette of performance including one beamline placed directly on the linear accelerator in the Short Pulse Facility operating with pulses compressed down to 100 fs.

A Soft X-ray FEL (the SXL project) [4] is being designed and consists of a FEL placed on the 3 GeV linac targeting the 1–5 nm wavelength range. The FEL will start in SASE mode with pulses of intermediate, 15 fs, and short, 1 fs, pulse length. Following on SASE operation seeding is requested and suitable methods are studied.

The MAX IV linear accelerator (Fig. 1) is based on normal conducting S-band linac structures. At 256 MeV the first bunch compressor (BC1) is placed. The main linac consists of 36 structures which are followed by another bunch compressor (BC2) at full energy, 3 GeV. This implies that there will be a remaining energy chirp in the electron beam when it enters the FEL. While this is not an issue for ordinary SASE operation, HBSASE operation will be negatively affected.

The longitudinal wakefields in a linac accelerating structure increase the chirp used for compression. Thus a smaller off-crest RF-phase for a specified compression is required.

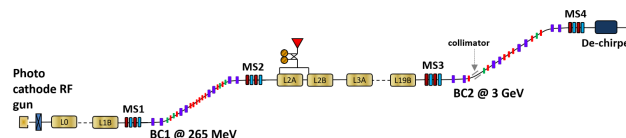


Figure 1: The MAX IV linac.

The linac and SXL has a standard operation mode called high charge long pulse mode [4]. The different modes have been studied by start-to-end simulation using Astra [5], Elegant [6] and Genesis [7], for the FEL. In Fig. 2 the longitudinal phase space and beam current after the second bunch compressor (BC2) is shown. The RF phases in the linacs before and after BC1 are set on 26.3 and zero degree, respectively.

REVERSING THE LONGITUDINAL CHIRP BY OVER COMPRESSION

Since the compression in the MAX IV linac requires a negative chirp in energy, over-compression can be implemented to reverse the chirp. This allow to use a standard de-chirper

* sverker.werin@maxiv.lu.se

EEHG SEEDING SCHEME AT SwissFEL ATHOS FEL

R. Ganter[†], G. Aeppli¹, C. Arrell, H.-H. Braun, M. Calvi, A. Cavalieri, A. Dax, P. Dijkstal, E. Ferrari², N. Hiller, M. Huppert, P. Juranic, C. Kittel, X. Liang, S. Neppl, E. Prat, S. Reiche, A. Trisorio, C. Vicario, D. Voulot,
Paul Scherrer Institut, Villigen, Switzerland
¹also at ETH, Zürich and EPFL, Lausanne, Switzerland
²also at DESY, Hamburg, Germany

Abstract

In order to improve the brightness and coherence of the soft x-ray FEL line of SwissFEL (Athos), components for an Echo Enabled Harmonic Generation (EEHG) scheme are currently being installed. The first components have been installed to allow ESASE operation test in spring 2022. This first stage consists in a 10 mJ class seed laser, a U200 modulator with individual control of each half period gap and a four electromagnet dipole chicane ($R_{56} \sim 850 \mu\text{m}$). The large magnetic chicane and the second modulator are still in preparation for an installation by the end of 2022. This paper describes the different components as well as preliminary results of the commissioning with beam.

ATHOS MODES OF OPERATION

Athos is the second Free Electron Laser (FEL) of SwissFEL which had its first lasing in December 2019 [2-4]. It covers the soft x-ray wavelength range extending from 0.65 nm to 5 nm. It is complementary to Aramis, the FEL already in operation since 2016, which operates in the hard x-ray wavelength range from 0.1 to 0.7 nm. Both FELs share the same photoinjector and linac in which two electron bunches are accelerated with only 28 ns time separation at a repetition rate of 100 Hz [5]. A series of fast kicker magnets followed by a DC septum magnet situated about 300 m downstream the photocathode are deflecting the second bunch towards Athos as the first bunch continues towards the Aramis FEL (Fig. 1). Being the second FEL of SwissFEL, the design of Athos was more ambitious than Aramis and the choice was made at the very early stage to have a very versatile FEL line with different operation modes to control as many parameters as possible of the generated FEL pulses. The ultimate goal is to offer the users a full control of the main light parameters and to push the performances beyond the state of the art. To achieve these goals a few key technologies and design choices had to be made [3]. From day one, Athos has been equipped with small chicanes (CHIC chicanes) between subsequent undulator segments (Fig. 1, top) speeding up the SASE process by about 20 % (optical klystron mode of operation [6]). The undulator design is a so-called APPLE X design [7] where the four magnet arrays can move radially and independently such that a transverse magnetic field gradient can be obtained [8]. Recently a seed laser has been com-

missioned and is the main ingredient required to do enhanced SASE (ESASE) [9], mode-locked lasing [10] or Echo Enabled Harmonic Generation (EEHG) [11].

With the introduction of an external seed laser, it becomes possible to manipulate the time structure of the generated FEL pulse. For example in the ESASE scheme, a train of attosecond pulses can be generated. Overlapping the seed laser and the electron bunch in a modulator (U200) introduces an energy modulation in the electron bunch, this energy modulation is converted in a density modulation when the bunch passes through an electromagnetic chicane. The obtained electron density peaks will dominate the lasing and generate a train of sub-femtoseconds pulses with a regular periodicity. These peaks are not phase locked but phase locking can be obtained with the mode locking scheme which requires to use the small chicanes situated between every undulator segment. In fact, when the sum of the chicane delay and the radiation phase slippage after one undulator segment is exactly equal to the seed laser period, then it becomes possible to reduce the bandwidth of individual pulses and to propagate the phase information over many pulses of the train. The pulses are then phase locked.

With the EEHG scheme very high harmonics of the seed laser wavelength can be amplified and the bandwidth of the radiated pulses is further reduced close to the Fourier Transform limit. Also, the shot to shot wavelength jitter is reduced which is a very important parameter for experiments. The produced pulses are then almost fully coherent, both transversally and longitudinally.

EEHG COMPONENTS

Layout

ESASE and mode-locking modes of operation are using half of the components required for EEHG. Logically the project was then split in two phases. In the first phase, a completely new laser room with controlled air temperature, humidity and cleanness has been installed in a building room next to Athos. The seed laser was installed together with an UHV vacuum line to transfer the laser pulses over about 13 m from seed laser room to a laser table near the incoupling electromagnet dipole (Fig. 1-Bottom). This dipole is in fact the last dipole of the SwissFEL dogleg allowing easy incoupling onto Athos axis. About two meters downstream from the in-coupling window, a modulator U200 has been installed where the electron bunches and the seed laser pulses should overlap.

[†] romain.ganter@psi.ch.

LASER-BASED SEEDING OF SwissFEL ATHOS

A. Trisorio, S. Reiche, C. Arrell, A. L. Cavalieri¹, A. Dax, C. M. Deutschendorf, P. Dijkstal, E. Divall, R. Ganter, R. Ischebeck, N. Hiller, M. Huppert, P. Juranic, S. Neppl, E. Prat, C. Sydlo, C. Vicario, D. Voulot, G. Aeppli²

Paul Scherrer Institute, Villigen PSI, Switzerland

E. Ferrari, DESY, Hamburg, Germany

¹also at University of Bern, Bern, Switzerland

²also at ETH Zürich, Zürich, Switzerland

Abstract

We are implementing a laser-based seeding scheme at the SwissFEL soft X-ray Athos beamline. The project has two phases. In the first phase (funded via the HERO ERC project [1]) trains of attosecond pulses having a phase relation in between will be generated. In the second phase, an Echo Enabled Harmonic Generation (EEHG) scheme will be implemented and allow the generation of fully coherent X-ray Free Electron Laser (FEL) pulses down to 1 nm photon wavelength. In this proceeding, the laser facility for phase 1 as well as its features and performance are presented in details. Finally, some first commissioning results with electron beam and E-SASE FEL mode of operation obtained in June 2022 are also shown.

INTRODUCTION

FELs are the newest generation of large scale research facilities. They have been developed over the last fifteen years, especially in soft and hard X-ray spectral range. Since the lasing process of these machines is based on the self-amplified spontaneous emission (SASE) mechanism, the emitted FEL radiation suffers from large shot-to-shot intensity and photon-energy fluctuations and the limited longitudinal coherence inherent in the SASE mechanism. One possibility to overcome such limitations, is to use another (coherent) source as a trigger for the FEL process. A source of choice is an optical laser system, synchronized with the FEL accelerator and with appropriate pulse duration, wavelength and intensity. In 2012, direct seeding of the Fermi FEL facility demonstrated tunable emission throughout the 65 to 20 nm wavelength range, with unprecedented shot-to-shot wavelength stability, low-intensity fluctuations, close to transform-limited bandwidth, transverse and longitudinal coherence and full control of polarization [2]. As an upgrade of SwissFEL Athos towards fully coherent soft X-ray facility, a laser-based, two stage seeding facility following an Echo Enable Harmonic Generation (EEHG) scheme [3] is being implemented. Taking profit of the unique available CHIC chicane scheme [4], and using the mode locking approach [5], we target to produce trains of phase-locked attosecond pulses and fully coherent radiation down to 1 nm wavelength at Athos using the EEHG scheme.

SEED LASER FACILITY AT SwissFEL ATHOS

As depicted in Figure 1, the SwissFEL Athos beamline is hosting the laser-based seeding facility. A laser laboratory hosts two Ti:Sa laser amplifiers. The first phase of the project (HERO) started in January 2020 and finished in April 2022 with the first commissioning results shown here. The second phase, so-called EEHG started in May 2022 and is supposed to be ready for first commissioning in May 2023. For each phase, the seed laser facility consists of the laser itself, the transport towards the interaction point (modulator) through a vacuum transfer line and launching optics, and as well diagnostics placed before and after the modulator to ensure spatial and temporal overlap between the seed laser pulse and the electron bunch.

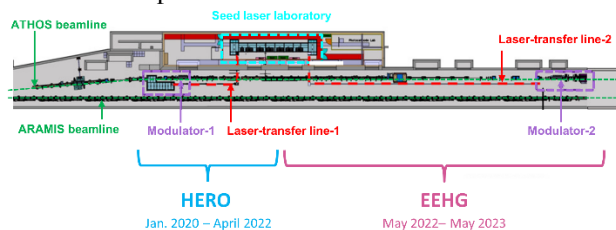


Figure 1: Overview of the project phases and the seed laser facility at the ATHOS beamline. The seed laser laboratory (cyan), the laser transfer lines (red) as well as the launching optical setups into the modulators (violet) where the seed laser pulse interacts with the electron bunch are integrated in the accelerator facility.

Seed Laser System

The seed laser system is a dual output, terawatt-class, femtosecond laser system based on Titanium Sapphire (Ti:Sa) technology with wavelength tuning capability. A detailed layout is shown in Figure 2. As one can see, it consists of two Chirped Pulse Amplifiers (Pulsar - Amplitude) seeded with a common laser oscillator (Gecco - Laser Quantum). The repetition rate of the laser oscillator is locked to the FEL Optical Master Oscillator (OMO). Using a common oscillator to seed both amplifiers reduces drastically the timing jitter between the two compressed outputs of the two amplifier chains. This is crucial to ensure the stability of the overall seeded FEL operation mode.

HIGH REPETITION RATE SEEDED FREE-ELECTRON LASER WITH A HARMONIC OPTICAL KLYSTRON IN HIGH-GAIN HARMONIC GENERATION

H. Sun, Shanghai Institute of Applied Physics, Shanghai, China
 University of Chinese Academy of Sciences, Beijing, China
 G. Paraskaki, DESY, Hamburg, Germany

B. Faatz, C. Feng*, B. Liu†, Shanghai Advanced Research Institute, Shanghai, China

Abstract

External seeding techniques like high-gain harmonic generation (HG) and echo-enabled harmonic generation (EEHG) have been proven to be able to generate fully coherent radiation in the EUV and X-ray range. However, towards seeding at a high repetition rate, the repetition rate of current laser systems with sufficient power for seeding is limited to the kilohertz range. One attractive solution to this limitation is to reduce the required seed laser power. In this contribution, we will present a harmonic optical klystron scheme with high gain harmonic generation. With the harmonic optical klystron scheme as the seeding technique, the required seed laser power is decreased, and higher harmonics than in a standard single-stage HG can be achieved.

INTRODUCTION

External seeding techniques have been proposed and proven to be able to generate widely tunable, fully temporally and spatially coherent radiation [1, 2]. These seeding schemes are triggered by stable, coherent external lasers, and thus their output radiation can be stable and coherent. However, the repetition rate of current laser systems with sufficient power to modulate the electron beam is limited to the kilohertz range.

To relax the power requirements of external seeding lasers in high repetition rate FELs, some methods, such as self-amplification of coherent energy modulation (Optical Klystron) [3, 4] and direct amplification enabled harmonic generation (DEHG) [5] were proposed. For seeding at a high repetition rate, optical cavity-based FEL schemes [6–10] have been introduced to recirculate the radiation in the modulator to seed the high repetition rate electron bunches. This scheme overcomes the limitation of requiring high repetition rate seed laser systems.

In this contribution, a harmonic optical klystron HG (HOK HG) configuration is studied for seeding at a high repetition rate. The harmonic optical klystron concept was studied in Ref. [11] to enhance self-amplified spontaneous emission or introduced as a harmonic cascade method in Ref. [12]. Similar to Ref. [12], instead of using a single modulator, the modulator is divided into two parts separated by a chicane as shown in Fig. 1. Here, we present the HOK HG simulation results for a single pass. In Ref. [9],

more information about the resonator seeding based on HOK HG is presented.

SIMULATIONS

Layouts for HOK HG configuration is shown in Fig. 1. In this setup, the first modulator is resonant at the fundamental wavelength of the seed laser and the second modulator is tuned to a harmonic of the first modulator. In the first modulator, a small energy modulation of the electron beam is induced and it is transformed into a density modulation after traversing through the first chicane with a longitudinal dispersion $R_{56,1}$. Then the electron beam is modulated at the harmonic of the seed laser wavelength in the second modulator. A density modulation will occur at a harmonic of the seed laser wavelength when the electron beam traverses through the second chicane with a longitudinal dispersion $R_{56,2}$. Finally, the FEL amplification of a harmonic of the seed laser wavelength is taking place in the radiator. In the next simulations, we use the typical parameters of a soft X-ray FEL. The electron beam parameters are summarized in Table 1. The simulations are performed with Genesis 1.3 [13].

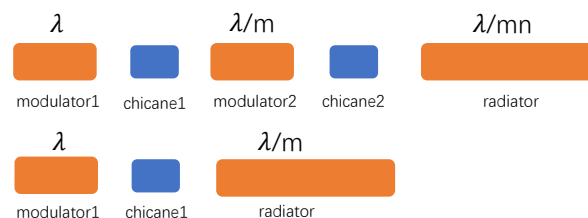


Figure 1: The layouts of the HOK HG scheme (top) and the standard single-stage HG scheme (bottom).

In our simulations, to generate fully coherent x-rays in the water window range, we use a 50 nm seed laser from the high harmonic generation (HHG) source. In fact, in the current laser system, the repetition rate of an HHG source cannot reach 1 MHz. Our concern is to reduce the required seed laser power as much as possible. It should be noted that the advantages of this scheme in terms of reducing required seed laser power still apply to longer wavelengths. To generate coherent radiation in the water window range, here we tuned the second modulator to the 4th harmonic ($m=4$) of the seed laser and the radiator is tuned to the 5th ($n=5$) harmonic of

* fengchao@zjlab.org.cn

† liubo@zjlab.org.cn

PREPARATORY EXPERIMENTAL INVESTIGATIONS IN VIEW OF EEHG AT THE DELTA STORAGE RING *

B. Büsing [†], A. Held, S. Khan, C. Mai, A. Radha Krishnan, Z. Usfoor, V. Vijayan
Zentrum für Synchrotronstrahlung (DELTA), TU Dortmund, 44227 Dortmund, Germany

Abstract

At DELTA, a 1.5-GeV electron storage ring operated by the TU Dortmund University, the seeding scheme CHG (coherent harmonic generation), the counterpart to HGHG (high-gain harmonic generation) without FEL gain, is used to provide ultrashort pulses in the femtosecond regime at harmonics of the seedlaser wavelength. To provide higher harmonics and thus shorter wavelengths, it is planned to upgrade the short-pulse facility to the EEHG (echo-enabled harmonic generation) scheme, which has yet not been implemented at any storage ring. To install the needed three undulators and two chicanes, about a quarter of the storage ring needs to be modified. The paper presents the layout of the envisaged EEHG facility and the demo project SPEED (Short-Pulse Emission via Echo at DELTA) where all components are realized in a single undulator.

ECHO-ENABLED HARMONIC GENERATION

The seeding scheme echo-enabled harmonic generation (EEHG) [1, 2] makes use of a two-fold laser-induced modulation of the electron energy to generate a complex density modulation. As shown in Fig. 1, the interaction of an ultrashort laser pulse and an electron bunch in an undulator (modulator) tuned to the laser wavelength results in a sinusoidal energy modulation. A strong first chicane after the first modulation leads to thin stripes in the longitudinal phase space due to the energy-dependent path length. With an additional modulator and a second weaker chicane in front of a third undulator (radiator), a periodic density modulation is generated, so-called microbunches. In the radiator, which is tuned to a harmonic of the laser wavelength, these microbunches lead to coherent emission of radiation.

EEHG was proposed and successfully demonstrated as seeding scheme for free-electron lasers (FELs) [3–5] to trigger the microbunching process. Adopted in storage rings, this seeding scheme is a promising candidate to generate ultrashort synchrotron radiation pulses in the extreme ultraviolet regime.

SEEDING AT DELTA

Since 2011, the short-pulse facility at DELTA, a 1.5-GeV electron storage ring operated by the TU Dortmund University, based on the seeding scheme coherent harmonic generation (CHG) [6, 7] provides ultrashort synchrotron radiation pulses. This seeding scheme is based on a single

* Work supported by the BMBF under contract 05K16PEB and 05K19PEB, Forschungszentrum Jülich and by the Federal State NRW

[†] benedikt.buesing@tu-dortmund.de

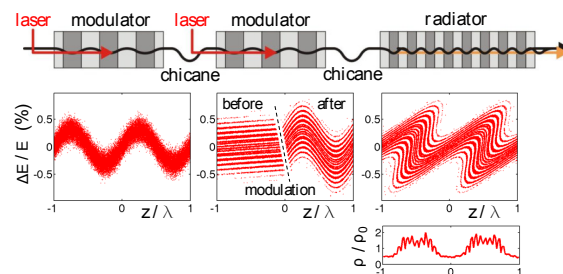


Figure 1: Magnetic setup for EEHG, corresponding longitudinal phase space distributions, and the final longitudinal electron density.

laser-electron interaction and is limited to low harmonics of the laser wavelength. The seeding experiments take place in a single undulator acting as one modulator, one chicane and the radiator. Seeding is performed by 800-nm pulses of a Ti:sapphire laser system or their second harmonic. In addition, radiation in the terahertz regime is coherently emitted in a subsequent dipole magnet. The present setup is depicted in Fig. 2 (top).

Storage Ring Optics for EEHG

To realize an EEHG-based short-pulse facility at DELTA, it is necessary to remodel a quarter of the storage ring so that all three undulators and the two chicanes can be placed in a single straight section, see Fig. 2 (bottom). The beam optics is optimized using the simulation code *elegant* [8] to fulfill all boundary conditions such as an achromatic straight section to not influence the longitudinal phase space while conserving the optics for the rest of the ring and not changing the source point of the other beamlines [9]. The resulting beta functions are shown in Fig. 3 and the main parameters of the present CHG and the future EEHG optics are listed in Tab. 1.

Table 1: Main Parameters of the DELTA Storage Ring

Parameter	Present	EEHG
electron beam energy	1.5 GeV	1.5 GeV
circumference	115.20 m	115.21 m
hor. tune	9.19	8.59
vert. tune	3.28	3.55
mom. comp. factor	$4.9 \cdot 10^{-3}$	$4.7 \cdot 10^{-3}$
rel. energy spread	$7 \cdot 10^{-4}$	$7 \cdot 10^{-4}$
hor. emittance	16 nm rad	22 nm rad
max. hor. beta function	45 m	22 m
max. vert. beta function	51 m	25 m

SPECTRO-TEMPORAL PROPERTIES OF COHERENTLY EMITTED ULTRASHORT RADIATION PULSES AT DELTA *

A. Radha Krishnan[†], B. Büsing, A. Held, S. Khan, C. Mai, Z. Usfoor, V. Vijayan
Center for Synchrotron Radiation (DELTA), TU Dortmund, Dortmund, Germany

Abstract

At the 1.5 GeV synchrotron light source DELTA operated by the TU Dortmund University, the short-pulse facility employs the seeding scheme coherent harmonic generation (CHG) to produce ultrashort pulses in the vacuum ultraviolet and terahertz regime. This is achieved via a laser-induced electron energy modulation and a subsequent microbunching in a dispersive section. The spectro-temporal properties of the CHG pulses as well as the coherently emitted terahertz radiation are influenced by the seed laser parameters and can be manipulated by varying the laser pulse shape and the strength of the dispersive section. CHG spectra for different parameter sets were recorded and compared with the results of numerical simulations to reconstruct the spectra. A convolutional neural network was employed to extract the spectral phase information of the seed laser from the recorded spectra. In addition, the shaping of the coherently emitted THz pulses by controlling the seed pulse spectral phase using a spatial light modulator was also demonstrated.

INTRODUCTION

Synchrotron radiation is proven vital for the study of properties of matter in a variety of experiments due to its characteristics such as high intensity, collimation and tunable wavelength. However, a lower limit to the achievable pulse duration is given by the electron bunch length which is usually in the order of several tens of picoseconds. These pulses lack the temporal resolution to probe the atomic processes taking place on the sub-picosecond scale. On the other hand, conventional mode-locked lasers can produce light pulses in the femtosecond regime but are in the visible and infrared wavelength range. Coherent harmonic generation (CHG) [1] is a technique that combines the advantages of these two radiation sources to produce coherent femtosecond light pulses of short wavelength.

CHG in storage rings is similar to the high-gain harmonic-generation (HGHG) seeding scheme used for free-electron lasers (FEL) but without the FEL gain [2–4]. As depicted in Fig. 1, CHG is based on a laser-electron interaction in an undulator that is tuned to the seed laser wavelength (modulator). The laser-electron interaction induces a sinusoidal modulation of the electron energy, which is then transformed into a density modulation (microbunches) via a dispersive section (chicane). These microbunches results in coherent emission in a subsequent undulator that is tuned to a target

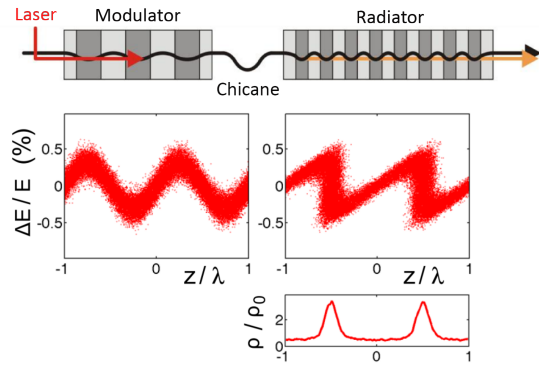


Figure 1: Magnetic setup for CHG, corresponding longitudinal phase space distributions and final longitudinal electron density.

harmonic of the seed laser wavelength (radiator). Since the laser pulse only modulates a very thin slice of the electron bunch, the resulting coherently emitted pulse will also have a pulse length comparable to that of the laser pulse.

The power of the CHG radiation at the n^{th} harmonic of the laser wavelength λ is given by

$$P(\lambda/n) \sim N_e^2 b_n^2 \quad (1)$$

where b_n is the bunching factor and N_e is the number of modulated electrons. For the CHG scheme, the bunching factor is given by [5],

$$b_n = |J_n(nAB)| e^{-\frac{n^2 B^2}{2}} \quad (2)$$

where $A = \Delta E_{\text{max}}/\sigma_E$ is the relative energy modulation amplitude and $B = R_{56} k \sigma_E / E_0$ is the dimensionless chicane parameter. Here, R_{56} is the matrix element of the chicane describing its longitudinal dispersion which quantifies the strength of the chicane, E_0 is the nominal beam energy, σ_E is the rms energy spread and $k = 2\pi/\lambda$. When seeded with a Gaussian laser pulse, the energy modulation amplitude A varies longitudinally following the pulse shape of the laser. Since the amplitude of the energy modulation along the bunch is proportional to the electric field of the laser, the Gaussian distribution of the modulation follows a length larger than that of the seed pulse by a factor of $\sqrt{2}$. Due to this non-uniform energy modulation, the optimum R_{56} required will be different along the longitudinal position of the bunch. This allows one to manipulate the pulse shape of the CHG radiation by controlling the chicane strength. As can be seen in Fig. 2, the CHG radiation will be a single bell-shaped pulse for $R_{56} = 50 \mu\text{m}$ (green line) where

* Work supported by BMBF (05K16PEA, 05K16PEB, 05K19PEB, 05K19PEC), DFG (INST 212/236-1 FUGG) and the federal state of NRW.

[†] arjun.krishnan@tu-dortmund.de

SENSITIVITY OF ECHO-ENABLED HARMONIC GENERATION TO SEED POWER VARIATIONS

F. Pannek*, W. Hillert, University of Hamburg, Hamburg, Germany

S. Ackermann, E. Ferrari, L. Schaper, Deutsches Elektronen-Synchrotron DESY, Hamburg, Germany

Abstract

The external seeding technique Echo-Enabled Harmonic Generation consists of two undulators which are used to imprint energy modulations to an electron bunch via interaction with a seed laser. Each of these so-called modulators is followed by a chicane which introduces longitudinal dispersion. Proper adjustment of the amplitudes of the energy modulations and dispersive strengths allows to achieve bunching at high harmonics of the seed laser wavelength. In the near future, this seeding scheme will be utilized in one of the beamlines of the free-electron laser (FEL) user facility FLASH at DESY to provide stable seeded radiation down to the soft X-ray regime at high repetition rate. Dedicated numerical simulations are carried out within the foreseen parameter space to investigate how variations of the energy modulations due to power fluctuations of the two seed lasers affect the bunching properties and the stability of the generated FEL radiation.

INTRODUCTION

Echo-Enabled Harmonic Generation (EEHG) [1, 2] is an external seeding scheme which makes use of two undulators, so-called modulators, each followed by a chicane. In the first modulator the electron bunch interacts with a seed laser and is modulated in energy. The large longitudinal dispersion of the first chicane transfers the energy modulation in multiple energy bands in the longitudinal phase space. By interaction with another seed laser in the subsequent second modulator, an energy modulation is imprinted on these energy bands, which is finally converted to a density modulation with high harmonic content in the second chicane. Since this scheme relies on two seed lasers, it is indispensable to investigate the influence of variations in the seed laser power on the stability of the free-electron laser (FEL) radiation generated in the subsequent undulator radiator. Numerical modeling and simulations are performed within the parameter range of the future FLASH2020+ upgrade [3, 4].

THEORY

The energy modulation amplitudes $\Delta E_{1,2}$ imprinted on the electron bunch in the first and second modulator are proportional to the square root of the peak power $P_{1,2}$ of the first and second seed laser [5]. In EEHG, the energy modulation amplitudes $A_{1,2}$ are commonly described in terms of the rms beam energy spread σ_E , such that

$$A_{1,2} = \frac{\Delta E_{1,2}}{\sigma_E} \propto \sqrt{P_{1,2}}. \quad (1)$$

* fabian.pannek@desy.de

The dispersive strengths of the two chicanes are described by the parameters $B_{1,2} = R_{56}^{(1,2)} k_1 \sigma_E / E$, where $R_{56}^{(1,2)}$ is the longitudinal dispersion, k_1 the wavenumber of the first seed laser and E the electron beam energy.

The EEHG bunching around the harmonic wavenumber $k_E = a_E k_1$ can be calculated according to [6]

$$b(k) = e^{-\frac{1}{2} \left(\xi_E + \frac{k - k_E}{k_1} B \right)^2} \int_{-\infty}^{\infty} J_m \left(-\frac{k}{k_1} B_2 A_2(t) \right) \cdot J_n \left(-\left[\xi_E + \frac{k - k_E}{k_1} B \right] A_1(t) \right) \cdot e^{-i(k - k_E)ct} c dt, \quad (2)$$

with the EEHG scaling factor $\xi_E = n B_1 + a_E B_2$, the harmonic number $a_E = n + m k_2 / k_1$, n and m being two integers, $B = B_1 + B_2$, the Bessel functions $J_{n,m}$ of the first kind of order n and m , respectively, and the speed of light c . In this study, the time-dependent energy modulation amplitudes $A_{1,2}(t)$ are based on Gaussian seed laser envelopes and have the peak values $A_{1,2}$. Applying a Fourier transform to $b(k)$ results in the temporal description $b(t)$ of the bunching.

SEED LASER POWER VARIATIONS

In the following, the effect of power variations of both seed lasers is investigated at the 15th and the 75th harmonic at $n = -1$ working points. For simplicity, the wavelengths of the two seed lasers are set to $\lambda_{1,2} = 300$ nm, the full width at half maximum (FWHM) pulse durations of the first and second seed are $\tau_1 = 150$ fs and $\tau_2 = 50$ fs. The 15th harmonic corresponds to 20 nm and is achieved with a 950 MeV electron bunch with an rms energy spread of 105 keV, whereas, the 75th harmonic corresponds to 4 nm and is achieved with an electron energy of 1.35 GeV with 150 keV rms energy spread.

First, power variations of the two seed lasers are explored by utilizing Eq. (2) and the proportionality in Eq. (1). The FWHM pulse duration $\Delta\tau$ and bandwidth $\Delta\nu$ are estimated from $|b(t)|^2$ and $|b(k)|^2$, respectively. The time-bandwidth product (TBP) is calculated as $TBP = \Delta\tau \cdot \Delta\nu$.

The results of the bunching equation are finally compared to numerical simulations of the EEHG and radiator beamline with the FEL code GENESIS 1.3, version 4 [7, 8]. Here, a Gaussian electron bunch of $\sigma_z = 100$ μm rms length with $I_p = 500$ A peak current and a normalized emittance of $\varepsilon_n = 0.6$ mm mrad is assumed. The seed lasers are focused at the center of the respective modulator and have a beam waist much larger than the transverse electron beam size. The radiator beamline consists of helical undulator modules with 76 periods of $\lambda_u = 33$ mm length.

CALCULATION OF THE CSR EFFECT ON EEHG PERFORMANCE

D. Samoilenko*, W. Hillert

Institute for Experimental Physics University of Hamburg 20148 Hamburg, Germany
 N. Mirian†, P. Niknejadi, L. Schaper, Deutsches Elektronen-Synchrotron DESY, Hamburg, Germany
 D. Zhou, KEK, Ibaraki, Japan

Abstract

Externally seeded FELs can produce fully coherent short-wavelength pulses with the advantage of higher shot-to-shot stability and spectral intensity than SASE radiation. For the FLASH2020+ project, the Echo-Enabled Harmonic Generation (EEHG) seeding technique achieves seeded FEL radiation in the XUV and soft X-ray range down to wavelengths of 4 nm. The implementation of the EEHG requires precise phase space manipulations in the seeding section of the beamline, which would make the performance of the EEHG sensitive to the collective effects, such as Coherent Synchrotron Radiation (CSR) in some working range. Therefore, it is essential to consider the CSR in EEHG simulations and to understand its impact on the electron beam properties. In this work, we compare different methods for calculating CSR and investigate the mechanism of its effect on the EEHG performance.

INTRODUCTION

Echo-Enabled Harmonic Generation (EEHG) [1] is an external seeding technique for Free Electron Lasers (FEL). Implementation of EEHG gives a number of advantages as compared to Self Amplified Spontaneous Emission (SASE) mode. These advantages include shot-to-shot stability, increased longitudinal coherence and narrow-bandwidth spectrum. The choice of EEHG above other seeding techniques also allows to reach higher harmonics of the seed laser wavelength [2]. Currently FLASH facility is undergoing a major upgrade to implement EEHG technique in one of the beamlines to allow for FEL radiation at wavelengths down to 4 nm [3]. The challenge here is that EEHG requires creation of fine structures in the electron beam phase space achieve such wavelengths. These structures also have to be transported through the seeding section without significant distortions. The distortions can be created, for example, by collective effects. In the strong EEHG chicane the Coherent Synchrotron Radiation (CSR) is particularly concerning. In our previous work we already addressed the effect of CSR in the strong EEHG chicane and showed, that it can have an effect on EEHG performance [4, 5]. In this work we focus on the analytical treatment of EEHG, introduced in [6] to get a better understanding of the mechanism behind this effect. We show how this mechanism connects the EEHG bunching spectrum to the impedance in chicane 1. We also compare different models for the calculation of the impedance to discuss the effect of the chicane chamber. We show how the

difference in the impedance for the two models translates into the properties of the electron beam with particle-tracking simulations and find the results to be consistent with the analytical consideration.

METHODS

Schematic representation of the EEHG setup is given in Fig. 1. The most relevant parameters are listed in Table 1. The simulations are done by ELEGANT simulation code [7]. For the analytical treatment we follow the method presented

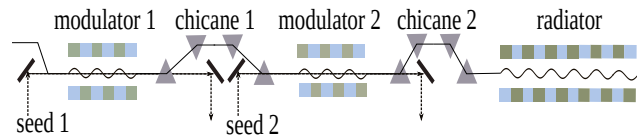


Figure 1: EEHG setup.

Table 1: Simulation Parameters

Initial beam parameters	
Central energy	1350 MeV
Slice energy spread	150 keV
Bunch length rms (σ_z)	96 μm
Peak current	500 A
Normalized emittance	0.6 mm · mrad
Seeding section parameters	
Seed lasers wavelength	300 nm
A_1	3.10
$R_{56}^{(1)}$	7.05 mm
$L_D^{(1)}$	42 cm
A_2	5.18
$R_{56}^{(2)}$	81.25 μm

in [8]. The evolution of the electron beam phase space is described by the set of equations:

$$\begin{aligned}
 P_1 &= P + A_1(z) \sin(k_1 z) \\
 z_1 &= z + B_1 P_1 / k_1 \\
 P_2 &= P_1 + A_2(z_1) \sin(k_2 z_1) + \Delta p_2(z_1) \\
 z_2 &= z_1 + B_2 P_2 / k_2,
 \end{aligned} \tag{1}$$

where $P = \Delta E / \sigma_E$ is the normalized energy, $A_{1,2}(z) = \Delta E_{1,2}(z) / \sigma_E$ is the normalized energy modulation induced in the first and the second modulator respectively, $k_{1,2}$ is the wavenumber of the first and the second seed laser respectively, $B_{1,2} = k_{1,2} R_{56}^{(1,2)} \sigma_e / E$ is the normalized dispersion in

* dmitrii.samoilenko@desy.de

† najmeh.mirian@desy.de

ARIA, A VUV BEAMLINE FOR EUPRAXIA@SPARC_LAB

M. Opromolla*¹, V. Petrillo¹, University of Milan, Milan, Italy

F. Nguyen, A. Petralia, A. Selce, ENEA-Frascati, Frascati, Italy

F. Stellato, University of Rome Tor Vergata and INFN-Rome Tor Vergata, Rome, Italy

M. Coreno^{2,3}, Z. Ebrahimpour, M. Ferrario, A. Ghigo, L. Giannessi³, A. Marcelli^{2,4}, F. Villa,
INFN-LNF, Frascati, Italy

¹ also at INFN-Milan, Milan and LASA, Segrate, Italy

² also at CNR-ISM, Trieste, Italy

³ also at Elettra-Sincrotrone Trieste, Trieste, Italy

⁴ also at RICMASS-International Centre for Material Science Superstripes, Rome, Italy

Abstract

EuPRAXIA@SPARC_LAB is a new Free Electron Laser (FEL) facility currently under construction at the Laboratori Nazionali di Frascati of the INFN. The electron beam driving the FEL will be delivered by an X-band normal conducting LINAC followed by a plasma wakefield acceleration stage. It will be characterized by a small footprint and include two different plasma-driven photon beamlines. In addition to the soft-X-ray beamline, named AQUA and delivering to the user community ultra-bright photon pulses for experiments in the water window, a second beamline, named ARIA, has been recently proposed and included in the project. ARIA is a seeded FEL beamline in the High Gain Harmonic Generation configuration and generates coherent and tunable photon pulses in the range between 50 and 180 nm. Here we present the potentiality of the FEL radiation source in this low energy range, by illustrating both the layout of the FEL generation scheme and simulations of its performances.

INTRODUCTION

Free Electron Laser (FEL) light sources are capable of generating high quality and tunable pulses in the VUV-X-ray energy range, characterized by a peak brilliance larger than 10^{30} photons $s^{-1} \text{ mrad}^{-2} \text{ mm}^{-2}$, 0.1 % bandwidth and a short pulse duration, of the order of tens of femtoseconds or even less, which are needed for a wide class of experiments [1–7]. Thanks to such output pulse properties, FELs allow ultrafast time-resolved measurements and provide a high signal-to-noise ratio [8–10]. Due to the required space for electron acceleration, undulators and photon beamlines (in the order of many hundreds of meters up to few km), the present X-ray FEL facilities can only be realized in large scale laboratories and few of them are currently in operation.

Plasma Wakefield Acceleration, either laser- or particle-driven, is recognized as one of the most promising techniques for novel high-gradient accelerating structures: very high accelerating gradients beyond 1 GV/m can be achieved [11–17], *i.e.* about one order of magnitude larger than the ones of a normal-conducting LINAC structure, thus leading to an essential footprint and cost reduction for the whole facility. The EuPRAXIA Design Study [18] aims

at realizing a new FEL facility driven by plasma acceleration. In this framework, the INFN Frascati National Laboratories, as a part of the EuPRAXIA project, will host EuPRAXIA@SPARC_LAB [19], a compact facility based upon a high brightness X-band LINAC, a particle-driven plasma acceleration stage and a FEL. The layout of its acceleration stage and FEL undulator lines is shown in Fig. 1. Before being matched and injected into the undulator line, the electrons are accelerated in two pairs of eight X-band accelerating cavities, separated by a magnetic bunch compressor (BC in Fig. 1) and followed by the plasma module.

This facility is able to fulfill the 1 GeV beam energy foreseen by EuPRAXIA in a low charge configuration by using particle- or laser- driven plasma acceleration, but it also can achieve the same energy at an higher charge from the X-band RF LINAC without the plasma module. The electron beam parameters at 1 GeV for FEL operation in both beam modes are reported in Table 1.

Table 1: EuPRAXIA@SPARC_LAB Electron Beam Parameters. The Normalized Emittance Is Here Reported

	LINAC	LINAC+PWA
Charge (pC)	200	30
Bunch length (rms, μm)	34	2
Energy (GeV)	1	1
Peak current (kA)	0.7	1.8
Slice energy spread (%)	0.01	0.05
Slice emittance (mm mrad)	0.5	0.8

As required by the EuPRAXIA Design Study, a first FEL beamline called AQUA [20–22], operating in the water window at 3–4 nm, was funded and included in the project baseline. It will use the full undulator length available to the project and requires very high quality electron beams.

A second lower photon energy FEL beamline in the VUV range (around 50–180 nm), called ARIA [23], has been recently considered and included in the project baseline, although not yet fully funded. In comparison with AQUA, such VUV beamline is highly flexible, with a larger input parameter acceptance, and requires a shorter magnetic length to lase.

* michele.opromolla@mi.infn.it

TRANSVERSALLY SEPARATED CROSSED POLARIZED FEL SUBPULSES

G. Perosa*, F. Sottocorona, Università degli Studi di Trieste, Trieste, Italy
 E. Allaria, F. Bencivenga, A. Caretta, G. De Nino², L. Foglia, S. Di Mitri, D. Garzella,
 L. Giannessi¹, S. Laterza, R. Mincigrucci, G. Penco, C. Spezzani, P. Rebernik Ribic, M. Trovò,
 Elettra-Sincrotrone Trieste S.C.p.A., Basovizza, Italy
 S. Khan, Center for Synchrotron Radiation, TU Dortmund University, Dortmund, Germany
¹also at Laboratori Nazionali di Frascati, INFN, Frascati, Italy
²also at University of Nova Gorica, Nova Gorica, Slovenia

Abstract

The extension of four-wave mixing (FWM) technique to the extreme ultraviolet and soft X-ray ranges allows to monitor the dynamics of coherent excitations of matter, when realized with the exquisite coherent property of bright FEL pulses. We show for the first time a scheme to provide transversally separated pulses with parallel or crossed linear polarizations, realized at FERMI FEL. This configuration paves the way to explore additional features of pump and probe and FWM techniques, and, in particular, the possibility to excite a transient polarization grating on the sample. For this reason, such a technique is important for the detection of circular dichroism and chiral properties of matter and the characterization of spin waves and magnons. By tailoring the electrons trajectory along the undulator line, we demonstrate the possibility of deliver balanced and stable couple of pulses with an horizontal separation of the order of millimeters at the focusing mirror of the experimental station.

INTRODUCTION

Modern science advancement relies on the possibility to produce short laser-like coherent pulses in the XUV regime and in the X-rays to probe electronic structure in atoms, molecules and solid state matter [1]. In this scenario, free-electron lasers (FELs) are invaluable tools for research. In particular, the versatility of seeded FELs scheme is paving the way towards the tailoring of coherent light and its exploitation in novel experimental schemes [2–4]. One of the most known example of the FEL-based experiment is the four-wave mixing (FWM) technique in the extreme ultraviolet and soft X-ray ranges [5]. It is well established that the interference of two pulses with linear parallel polarizations will result in a modulation of the light intensity, translated into a density grating at the sample position. On the contrary, when the polarizations are crossed, a sinusoidal oscillation of the light chirality is obtained and, consequently, a polarization grating is induced in the sample. Although the principle of this technique has been already demonstrated in the optical regime [6], FEL radiation can provide the proper wavelength range to investigate the chiral features of a sample down to nanometer scale. In this work we demonstrate that FERMI FEL1 [7] can provide the kind of light required for this type of experiment, by delivering spatially separated

crossed polarized pulses, preserving the good spectral properties of seeded FELs.

EXPERIMENTAL REALIZATION

From now on we are going to refer to the FEL scheme with transversally separated subpulses with crossed or parallel polarizations as TSXPU or TSPPU respectively. As already explained and as the name underlines there are two main ingredients that are crucial. In [8], a possible solution to get crossed polarized beams is proposed and consists of splitting the undulator line into two sections. Following this prescription, the overall setup for FEL1 used for the experiment is shown in Fig. 1.

Table 1: FEL and Electrons Parameters

Parameters	Values
Electron beam energy	1.3 GeV
Seed laser wavelength	249.6 nm
Seed laser energy	26 μ J
FEL harmonic	12
FEL wavelength	20.8 nm
FEL polarization	LV+LH, LV+LV
FEL energy pulse	8 μ J per pulse

The possibility to generate crossed or parallel polarized pulses that are also separated in the horizontal plane is given instead by the careful design of the electrons' trajectory [9, 10]. In fact, the introduction of an angle θ between the directions followed along each section results in a separation d which is proportional approximately to $d \approx \theta L$ (for small θ), where L is the distance from the diagnostic or experimental station. The general idea is shown in Fig. 2.

However, it becomes mandatory to balance the reduction of FEL gain given by the off-axis trajectory, the increase of the separation given by the tilt and the relative energy pulse of the two beams. To do so, we tested a trajectory given by two line segments, one for each three-undulators section, both off-axis with respect to the undulator line. This strategy resulted successful to overcome the aforementioned issues and is summarized in Fig. 3. Another possible origin for the reduction of the signal could be a imperfect microbunches rotation given by the kicks in the trajectory [10]. From the practical point of view, we exploit the correctors along the undulator line, determining an increasing kick to the left for

* giovanni.perosa@elettra.eu

REVIEW OF RECENT PHOTOCATHODE ADVANCEMENTS

L. Monaco* and D. Sertore, INFN Milano - LASA, Segrate, Italy

Abstract

Photocathodes are routinely used as a source of electrons in high brightness beam photoinjectors. The properties of the photocathode have a significant influence on the parameters of the electron beams and on the operation of the machines. The choice of photocathode materials is an important step in reaching the challenging requirements of modern accelerators. Recent advancements towards more performing photocathodes are here presented and discussed.

INTRODUCTION

Photocathodes are key components of modern and advanced high brightness electron sources [1]. Illuminated by a laser beam, photocathodes emit electrons at proper phases in a high electric field region, necessary to accelerate the electron bunch to high energy to compensate for space charge forces and optimize beam emittances.

To generate the required electric field, the most common solutions are DC and RF guns. The solution adopted by different labs is mainly related to the kind of application of the specific machine. Indeed, polarized electron sources typically use DC guns due the extreme requirements of vacuum necessary for the operation of these kind of photocathodes (i.e. GaAs/Cs). Nearly the same vacuum conditions are necessary for the operation of alkali antimonide photocathodes due to their sensitiveness to vacuum level and composition. Recently, antimonide photocathodes have been used also in RF guns with limited performances due to dark current and limited operative lifetime. RF guns are instead routinely used with metallic photocathodes and, in case of high QE (Quantum Efficiency) materials, with cesium telluride (Cs₂Te).

Photocathodes properties determine also the minimal electron beam emittance through the so called thermal emittance. This property depends on the electron transverse velocity and hence on many parameters like photocathode surface roughness, distribution of work function on the surface, etc. This has motivated, in the present years, a strong activity based on solid state physics, surface science and material engineering to improve and optimize present photocathodes and explore new materials.

This paper presents the recent photocathode advancements with emphases on semiconductor photocathodes and their application in user dedicated accelerators. These materials are nowadays used in the main FEL user facilities and they are the best candidates for the coming new advanced CW FEL machines (see LCLS-II, SHINE, ..) and very high current electron source for ERLs or for the beam cooling of the Electron Beam Collider (EIC).

* laura.monaco@mi.infn.it

PHOTOCATHODE REQUIREMENTS

Photocathodes requirements are specific to their applications and a simple classification is not easily achievable.

However, it is possible to identify a common set of properties that are a minimal requirement for application of photocathode in modern accelerator machines [2]. They can be summarized in the following points:

- Long operative lifetime. This is important for photocathode operation in user facility based machine. Long operative lifetime implies also stable photocathodes properties in particular for operation in RF guns.
- Low dark current. Activation of components along the accelerators must be avoided and, hence, it is important to limit field emitters both from the photocathode and from the gun. In DC gun operation where the electric field is static, this is even detrimental for the photocathode itself since it generates ion back bombardment that damages the photoemissive film.
- Fast response time. Prompt response of the photocathode material to laser illumination is mandatory to guarantee proper phasing between laser and electric field (in particular for the RF gun operation). Moreover, the emitted electron bunch needs to be as similar as possible to the laser beam profile in order to minimize the effect induced by the space charge on the electron beam emittance.
- High QE. This parameter is extremely important for high repetition rate or CW applications. Lower repetition rate electron sources usually use metal photocathodes with QE in the 1×10^{-6} range.

Besides the previous presented parameters, electron polarization is a very specific requirement that only a family of photocathode is able to satisfy, i.e. III-V materials. This class of photocathodes is the subject of many studies towards improving the polarization ratio and the lifetime. Indeed these are Negative Electron Affinity (NEA) photocathodes and they need usually an atomic layer of Cesium on the surface to preserve the electron polarization. Consequently, the specification for vacuum level and composition are very demanding and require specific vacuum system. It is then clear that polarized photocathode are a class of photocathodes by itself and, given the limited space here available, they will not be addressed it here but recent updates have been presented at the Snowmass2021 Electron Workshop [3].

METAL

Metal photocathodes are widely used in low repetition rate electron sources and where fast response time and very low emittance are required.

The most common material is copper (see LCLS for example) but, recently, magnesium has been used in SRF gun at HZDR Elbe [4–6]. Given the “simplicity” of the mate-

CHIRPED PULSE LASER SHAPING FOR HIGH BRIGHTNESS PHOTOINJECTORS

C. Koschitzki, H. Qian, Z. Aboulbanine, G. Adhikari, N. Aftab, P. Boonpornprasert, G. Georgiev, J.D. Good, M. Gross, A. Hoffmann, M. Krasilnikov, X. Li, O. Lishilin, A. Lueangaramwong, G. Loisch, R. Niemczyk, A. Oppelt, G. Vashchenko, T. Weilbach, F. Stephan, DESY Zeuthen, Germany
I. Hartl, DESY Hamburg, Germany

Abstract

In this publication we show the current status on spectral-spatial shaping at the Photo Injector Test Facility at DESY in Zeuthen (PITZ). The laser pulse shaper presented here is based on spectral amplitude modulation of chirped laser pulses. In this unique approach one can modulate the spatial profile of individual time slices in density and diameter. The photoinjector requires a wavelength of 257.5 nm, but the laser shaping applies at a wavelength at least greater than 400 nm, in this paper, at 1030 nm. Both the shape preservation and fourth harmonic generation efficiency of the chirped laser pulses are discussed.

INTRODUCTION

The free electron laser (FEL) is currently the most powerful source for coherent X-rays. It is typically based on linear electron accelerators, which rely on a low transverse emittance electron source, to allow X-ray lasing in the undulator. As the emittance in modern FELs is limited by the source emittance, it is intuitive to also optimize the photoemission laser shape to control the emittance growth due to nonlinear space charge forces during the low energy transportation. For electron beams, dominated by space charge effects, it was shown that shaping of the extracting laser pulse can reduce the space charge induced emittance growth [1] [2]. Another study shows, that slice mismatch of a triangular driver beam for high efficiency beam based plasma acceleration can be reduced [3], if the extraction laser allows for independent control of slice charge and charge density. A Spatial Light Modulator (SLM) based laser pulse shaper with such a capability has been proposed by Mironov [4] and a variation of such a shaper has been used to shape the output of an infrared (IR) laser amplifier at 1030 nm. The photo injector cathode requires a UV pulse to extract electrons, thus the fourth harmonic was obtained from two consecutive second harmonic generation (SHG) stages. A high quality laser pulse shaping was demonstrated for the IR pulses.

SLM SHAPER

The shaper is an imaging zero compressor or Martinez system as shown in Fig. 1, where a 4f-telescope with two identical lenses images the surface of one grating to another grating and ultimately path length differences of different wavelengths add up to zero. The SLM is then placed at the Fourier plane in between the two lenses, where a collimated

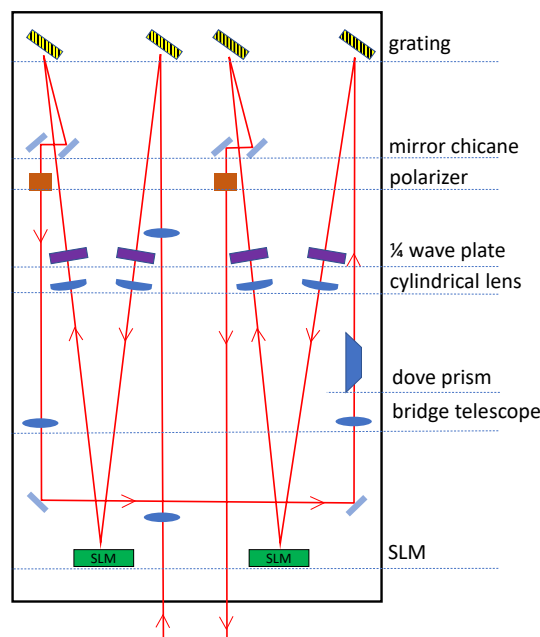


Figure 1: Schematic of a double SLM Shaper.

beam in absence of the gratings would be focused. Due to the grating dispersion the intensity distribution at the SLM plane parallel to the table corresponds to the spectral amplitude distribution. This is still true, if cylindrical lenses are used and the lens rotation is aligned with the grating rotation. But since neither the grating nor the lenses act on the transverse vertical axis, the optical transfer is identical to a free drift for the transverse vertical axis. Thus in the vertical plane an image of the SLM can be transported, if the lens is placed outside the shaper, i.e. after the second grating. Then of the two axis of our two dimensional SLM, one axis corresponds to spectrum, while the other corresponds to a spatial axis like in a typical spectrograph setup. The liquid crystals in an SLM act as polarization dependent phase shifters and a setup like this could be operated as a digital prism. In order to turn it into an attenuator we can use two quarter wave plates at 45 degrees, before and after the SLM. This turns the phase shift into a polarization rotation and thus 180 degrees of phase shift become an attenuation between 0 and 100% after a subsequent polarizer. As only one spatial dimension is accessible in a single shaper, the laser beam is rotated by 90 degree using a Dove Prism and sent through a

COMPARISON OF EULERIAN, LAGRANGIAN AND SEMI-LAGRANGIAN SIMULATIONS OF PHASE-SPACE DENSITY EVOLUTION

Ph. Amstutz*

Deutsches Elektronen-Synchrotron DESY, Hamburg, Germany

Abstract

Good understanding of the underlying beam dynamics is mandatory for the successful design and operation of Free-Electron Lasers. In particular, it is important that all physically relevant collective effects are adequately represented in simulation codes so that their influence on the phase-space evolution of the bunch can be calculated with sufficient accuracy at all relevant length scales. Besides coherent collective effects such as space charge or coherent radiative interaction also incoherent effects such as intra-beam scattering are suspected to have a significant impact on the efficacy of sophisticated lasing techniques.

Most of the well-known and widely-used beam dynamics codes employ the Lagrangian approach, in which the particle bunch is represented by discrete points in phase-space and track the solutions of their equations of motion. In contrast to that, in the Eulerian and semi-Lagrangian approach, the bunch is described by a numerical representation of its phase-space density function.

This contribution discusses the working principles of the three classes of simulation methods Lagrangian, Eulerian, and semi-Lagrangian and highlights their respective advantages and short-comings, when applied to the simulation of collective beam dynamics in FELs.

INTRODUCTION

Many applications of particle accelerators and in particular FELs require a high particle density, so that the number of particles contained in a bunch is typically very large. If the particles can be assumed to be initially independent and identically distributed (IID), then the entire bunch can be represented by a function of one set of single-particle phase-space coordinates, describing the probability of any one particle to occupy a certain position in phase-space — the single-particle phase-space density (PSD). In practice, this PSD can usually be obtained either based on experimental data or from a theoretical model of the generation process. As this macroscopic PSD depends only on one set of phase-space coordinates, instead of the phase-space coordinates of all individual particles, it is more likely that the evolution of the PSD can actually be simulated numerically. In the following we will present an overview of the various kinetic equations frequently encountered in beam dynamics, which describe the evolution of PSDs and outline the three principle families of methods to solve them numerically: Eulerian, Lagrangian, and Semi-Lagrangian methods.

* philipp.amstutz@desy.de

KINETIC EQUATIONS

In the following we will briefly recap how an evolution equation of a PSD of a non-interacting particles is derived starting from Hamiltonian mechanics and then show how it can be extended to describe interaction between the particles and stochastic motion of the particles, yielding a set of well-known kinetic equations.

Consider a Hamiltonian dynamical system with a non-collective Hamiltonian $H(t, z)$, $H: \mathbb{R} \times \mathbb{R}^{2d} \rightarrow \mathbb{R}$ and d degrees of freedom, so that the dimension of its phase-space is $2d$. Using the Poisson bracket $\{f, g\} \equiv \nabla_z f^T J \nabla_z g$ the equations of motion (EOM) of the phase-space coordinates $z \equiv (q_1, \dots, q_d, p_1, \dots, p_d)^T$

$$d_t z = \{z, H\} \equiv J \nabla_z H, \quad J = \begin{pmatrix} 0 & \mathbb{I}_d \\ -\mathbb{I}_d & 0 \end{pmatrix} \quad (1)$$

are solved by the flow $\phi_{t \leftarrow t_0}: \mathbb{R}^{2d} \rightarrow \mathbb{R}^{2d}$

$$z(t) = \phi_{t \leftarrow t_0}(z(t_0)) \quad (2)$$

where $z(t_0)$ are the known initial conditions [1, 2]. Stochastic terms may be added to the EOM to describe random processes affecting the trajectory of a particle.

For a phase-space density $\Psi(t, z)$, i.e. a function describing the probability of finding any particle in a certain position in phase-space, from the conservation of probability it can be seen that its total time-derivative vanishes

$$d_t \Psi = \partial_t \Psi + d_t z^T \nabla_z \Psi = 0, \quad (3)$$

which is known as the *Liouville equation* [3, 4].

Liouville Equation

It can be seen that the Liouville equation is a linear, first-order PDE, taking the form of a continuity or advection equation, with the velocity field $(J \nabla_z H)^T$:

$$\partial_t \Psi - \{H, \Psi\} = \partial_t \Psi + (J \nabla_z H)^T \nabla_z \Psi = 0. \quad (4)$$

Hence the time evolution of a PSD of non-interacting particles in a Hamiltonian system can be interpreted as an incompressible fluid being transported along the vector field of the Hamiltonian. In the next section it will be shown how the *method of characteristics* can be employed to derive an closed-form solution of the Liouville equation, which is known as *Liouville's theorem*.

Boltzmann Equation

While the Liouville equation describes the case of non-interacting particles, it can be extended to also capture interaction between the particles. In many systems of interest, the

DESIGN OF A NEW BEAMLINE FOR THE ORGAD HYBRID RF-GUN AT ARIEL UNIVERSITY

A. Weinberg*, A. Nause†, Ariel University, Ariel, Israel

Abstract

The ORGAD Hybrid RF-gun was commissioned in Ariel University. The main beamline of the hybrid S-band (2856 MHz) photo injector is currently driving a 150 kW, short pulse THz-FEL. In order to use the RF gun for other applications, a new and independent beam line is required. A secondary beamline is only feasible with the design of a dispersive beam-line dogleg section. High quality beam is crucial for the designated applications such as Ultra-fast Electron Diffraction (UED). The design is based on transfer matrices analytical model followed by simulations. Full 3D GPT (General Particle Tracer) simulations were done on this secondary beamline in which we manipulate and compress the beam to maintain beam emittance and pulse duration. An optimization procedure of the design using realistic field-maps and fringe fields of the quadrupoles was performed to reconstruct the electron beam quality parameters after passing through the dispersive dogleg section. The optimization results demonstrate improved beam quality are presented.

INTRODUCTION

The main beamline of the hybrid S-band (2856 MHz) photo injector [1] ORGAD accelerator is currently used to drive a 150 kW, short-pulse THz-FEL. Using a 90 cm Undulator the THz-FEL is emitting super-radiantly (radiation emitted coherently from all the electrons within the pulse [2]) at 1–3 THz. In order for the electrons to emit coherently in the super-radiant regime, the emitting electron bunch must be shorter than the wavelength of the emitted radiation, in this case less than 100 μm .

A new and independent beam line is required for additional e-beam emission based experiments such as MeV-UED, Compton scattering, noise suppression and enhancement schemes, sub-radiant emission, etc. This secondary beamline is feasible with the design of a dogleg section [3]. A dogleg is constructed of two dipole sections, with higher-order magnetic electron-optics such as quads and sextupoles, added to prevent dispersion. The construction of a dogleg requires a full 3D start-to-end simulations of the entire RF GUN and beamlines. In this work, simulations were carried out using the General Particle Tracer code (GPT), and optimization procedure [4] was performed on these simulations using realistic field-maps. Figure 1 shows the two beamlines and the beam-optics elements. The major challenge in the design was maintaining beam parameters at optimal values for the additional e-beam emission based experiments.

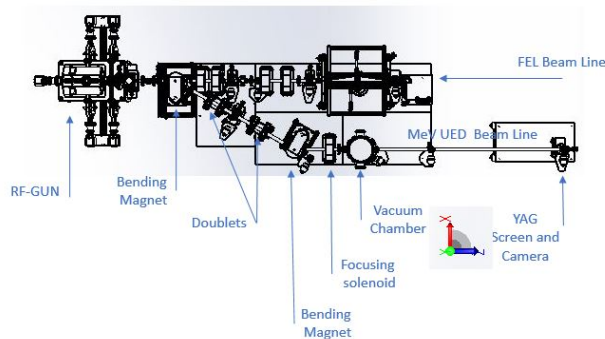


Figure 1: Ariel University's Hybrid Gun. The top beamline is the superradiant THz FEL. The lower beamline is designed for different experiments such as MeV-UED.

DESIGN

The hybrid gun was designed to produce an extremely short pulse in order to emit THz super-radiantly. For this reason, the traveling-wave section of the gun is used to apply a negative chirp on the beam. This is achieved by setting a phase difference of $-\frac{\pi}{2}$ between the standing wave and the traveling-wave sections. However, if required, this phase difference can be varied, resulting with a higher beam energy, or a positive chirp. A dogleg section is designed as a bunch compressor and a positive chirp at the entrance is essential. The planned oblique section of the dogleg design is symmetric around its center and consists of two doublets (focusing and defocusing quadrupoles), with the defocusing quadrupoles facing the center of the section. Sextupole magnets are located on the top of, or next to, the focusing quadrupoles to decrease second order longitudinal dispersion (Fig. 2).

This symmetric configuration of the dogleg electron-optics suggests a preferred beam transport design in which the longitudinal waist is located at the center of the section. Thus, the beam arrives to the center with a positive chirp and emerges with a negative chirp. We begin with an analytical model based on transfer matrices [3] before starting the numerical simulation and optimization procedure. We calculate the transport matrix of the entire dogleg system as the product of the thin lens first order (see Eq. (1)) and second order matrices of the electron optical elements [3].

We find out the value of the longitudinal dispersion parameter at the center of the dogleg, for our given electron optics configuration using the analytical expression (Eq. (2)) to be $R_{56} = -0.0297$ m. The second order matrices were solved analytically using a MATLAB script. The second order dispersion element T_{566} obtained is -0.63 m with no

* amirwe@ariel.ac.il

† arieln@ariel.ac.il

DESIGN CONSIDERATIONS FOR A NEW EXTRACTION ARC AT THE EUROPEAN X-RAY FREE ELECTRON LASER

S. D. Walker*

Deutsches Elektronen-Synchrotron DESY, Hamburg, Germany

Abstract

It has been proposed that a new arc, called T20, should be installed for a third fan of undulators at the European X-ray Free Electron Laser (EuXFEL) in the next decade. Due to geometric constraints this arc will need to be at a much larger angle than for the existing arc, called T1. It is expected therefore that coherent synchrotron radiation effects (CSR) in T20 on the bunch emittances will be considerable. To preserve the x-ray beam qualities in any downstream undulators, this effect will need to be understood and ideally mitigated. In this paper the status of the T20 beamline design is discussed, the expected downstream beam properties are shown and possible strategies for improving the beam quality are outlined.

INTRODUCTION

X-ray free electron lasers (XFELs) require ultra-bright electron beams to achieve the desired photon beam characteristics. This means that ultra-short (high peak current) electron bunches with small transverse emittances and energy spread are necessary. However, the impact of coherent synchrotron radiation (CSR), in which radiation from the bunch's tail interacts with its head and subsequently dilutes the bunch's emittance, mandates linear machines. Running counter to this is the desire for multiple undulator beamlines and user experiments. For this reason, XFEL facilities around the world typically branch at relatively small angles (a few degrees with respect to the linac) after acceleration to two or more undulator lines. Still, the effects of CSR on the beam when diverting to these separate lines must be accounted to maintain performance in the downstream undulators.

The EuXFEL [1, 2] splits into three beamlines (T1, T2 and TLD) after the collimation section at the *switchyard*. Directly ahead of the switchyard lies T2, where SASE1 and SASE3 are situated. To the left lies T1 and SASE2, and downwards lies TLD and a beam dump. An additional beamline that branches to the right, called T20, and with it a new set of undulators is planned for the end of the decade. The switchyard and the beam distribution system, including the proposed T20 beamline, were mostly developed during the initial EuXFEL design process [3–5]. The use of CSR mitigation techniques was limited in the T1 arc design due to its small total bending angle (2.3°) rendering them less necessary. Whilst the T20 arc is much larger at 6° to 7° , the T20 design was frozen after considering only the linear optics, without studying collective or non-linear effects. For this reason the impact of CSR on bunches passing through

the T20 arc must be investigated, and possible mitigation strategies developed and implemented. In this paper design considerations for transporting ultra-bright bunches in the T20 beamline to new sets of undulators are discussed.

THE T20 BEAMLINE AND COHERENT SYNCHROTRON RADIATION EFFECTS

The T20 arc design mostly developed during the EuXFEL design process outlined in Refs. [3–6] forms a baseline for the performance of subsequent T20 arc designs, as it meets the most fundamental constraints on any such arc—it bends the bunch sufficiently, it matches the upstream optics, and it doesn't overlap with any of the existing magnets, tunnel walls or infrastructure.

To understand the design's performance with regards CSR I tracked 14 GeV, 250 pC Gaussian bunches with initial transverse emittances of 0.6 mm mrad and consisting of two hundred thousand macroparticles with peak currents of 3 kA, 5 kA and 7 kA using OCELOT [7] and its 1D CSR model. I justified the use of the 1D CSR model by evaluating the Derbenev criterion [8] along the entire arc and found that it was satisfied everywhere. The result from this peak current scan is shown in Fig. 1. The local linear dispersion's effect on the emittance at each observation point is accounted for by tracking, without collective effects, each bunch to the end of the arc (where $\eta = \eta' = 0$) before calculating the emittance. The changes in the emittance, $\Delta \varepsilon_x$, are 0.37 mm mrad, 1.3 mm mrad and 3.7 mm mrad at 3 kA, 5 kA and 7 kA, respectively. As expected, this is worse than the simulated impact of CSR on the smaller-angled T1 arc [9], where the simulated projected emittance growth is on order of 1.1 mm mrad in the 7 kA case. The vertical emittances are not discussed here as $\theta_x \gg \theta_y$ for the T20 arc.

The development of the emittance growth can be broadly split into three regions, first the Lambertson kicker-septum scheme up to the 30 m point, the middle six dipoles centred at 50 m and the final three dipoles centred at 70 m (the last two dipoles are vertical). Whilst the emittance growth is clearly dominated by the second two set of dipoles, the impact of the extraction system cannot be neglected, causing the emittance to grow by 0.6 mm mrad to 0.9 mm mrad in the 3 kA to 7 kA range.

The beamline layout, the switchyard, and its position within the tunnel and hall are shown in Fig. 2 and demonstrates the spatial constraints imposed upon the T20 lattice design. The railing at $(z, x) = (2120 \text{ m}, -3.5 \text{ m})$ is 16.3 m from the upstream wall and is angled at 6.6° with respect to the straight ahead (i.e., T2) direction. The angle of this wall

* stuart.walker@desy.de

UPGRADE TO THE TRANSVERSE OPTICS MATCHING STRATEGY FOR THE FERMI FEL

A. D. Brynes*, E. Allaria, S. Di Mitri, L. Giannessi, G. Penco, G. Perosa, S. Spampinati, M. Trovò
Elettra-Sincrotrone Trieste S.C.p.A., Trieste, Italy

Abstract

Good control over the transverse distribution of an electron bunch is crucial for optimising the beam transport through a linear accelerator, and for improving the energy transfer of electrons to photons within the undulators of a free-electron laser (FEL). In order to achieve this, it is necessary to match, as closely as possible, the Twiss parameters of the electron bunch to the design values. This is done, in the case of the FERMI FEL, by finding the optimal quadrupole strengths in various matching sections using a particle tracking code. This contribution reports an upgrade to the matching tools in use in the FERMI control room: the functionalities of two existing programs have been merged into a single tool; and some new options are available in order to provide more flexibility when performing transverse optics matching.

INTRODUCTION

Transverse optics matching is a procedure which aims to modify the beam distribution of a particle bunch such that the measured Twiss parameters match the design values [1]. This is an important aspect of accelerator operations and the optimisation of the performance of the machine; in the case of free-electron lasers (FELs), control (and therefore knowledge) of the transverse beam distribution is also important in order to maximise the efficiency of the FEL process and to minimise losses. In general, matching requires a measurement of the Twiss parameters at a dedicated location and an optimisation algorithm which uses a simulation code to take in the measured values and change some elements of the machine, with the goal of minimising the mismatch between the design and measured Twiss parameters.

In the case of the FERMI FEL [2], matching is performed at five locations, consisting of at least one measurement screen and four quadrupole magnets: three along the linac (at the entrance of the laser heater, the exit of the first bunch compressor, and at the end of the linac), and two at the entrance to each of the FEL lines. Matching is routinely done in the FERMI control room using two different programs for the linac and the FEL (refs. [3] and [4] respectively) – this contribution describes an upgrade which combines the functionality of both of these applications into one tool, and includes some new features.

MATCHING PROCEDURE

In order to perform accurate beam matching, a measurement of the transverse beam emittance and Twiss parameters

is required. This is typically done at FERMI using the single quad-scan technique [5] at various dedicated matching stations along the machine, and the results of the measurement are written to a dedicated TANGO server [6]. In the process of the upgrade to the matching tools, the program to measure the Twiss parameters has also been updated. The MATLAB-based code that performs the quadrupole scan was migrated to Python in order to make it more robust and faster, and also some new features have been introduced. The previous iteration of the program selected the quadrupole scan range in order to achieve a phase advance variation of $4\pi/3$ during the scan, leaving a certain degree of freedom to the operator. To make the program results less dependent on the operator, the current range of the quadrupole scan and the fitting range can be determined automatically such that it is symmetric with respect to the minimum beam size, and ensuring a phase advance in both planes of $4\pi/3$. The study of an alternative method to measure the transverse beam parameters, based on measurements of the transverse beam size on three or more screens [7], has also recently been started. The method has been tested on the FEL-1 line to derive the beam emittance and the Twiss parameters at matching quadrupole used for the single quadrupole scan method, using measurements of the transverse beam envelope along the undulators. With more measurements (of which seven are, in principle, available along the undulator), the system is overdetermined and a factorization of the matrix [8] or least squares method has to be used to obtain a solution. In a first test, we obtained – in the vertical plane – values of the initial Twiss parameters which were very close to those measured with the single quadrupole scan method. The horizontal Twiss parameters derived from this method, however, were larger by around 50% than those obtained with the standard emittance measurement. The Twiss parameters are then used as an input to the matching algorithm, which runs as follows:

1. Read in the measured Twiss parameters at the quadrupole entrance, measured beam energy and quadrupole strengths upstream of the measurement screen.
2. Reverse the values of $\alpha_{x,y}$ and back-track along the line to a pre-defined location (consisting of at least four quadrupoles).
3. Take the back-tracked Twiss parameters (again reversing the values of $\alpha_{x,y}$) and forward-track using an optimisation procedure in order to reach the design Twiss parameters at the measurement location.
4. The matching procedures then run as follows:

* alexander.brynes@elettra.eu

WAKEFIELD CALCULATIONS OF THE UNDULATOR SECTION IN FEL-I AT THE SHINE

H. Liu¹, Shanghai Institute of Applied Physics, Chinese Academy of Sciences, Shanghai, China

J. W. Yan, European XFEL, Schenefeld, Germany

J. J. Guo, Zhangjiang Laboratory, Shanghai, China

T. Liu, H. X. Deng, B. Liu,

Shanghai Advanced Research Institute, Chinese Academy of Sciences,
Shanghai, China

¹also at University of Chinese Academy of Sciences, Beijing, China

Abstract

The wakefield is an important issue in free electron laser (FEL) facilities. It could be extremely strong when the electron bunch is ultra short. Wakefields are generated by the electron bunch and affect the electron bunch in turn which possibly destroy the FEL lasing. Wakefield study of the undulator section in FEL-I at the Shanghai high-repetition-rate XFEL and extreme light facility (SHINE) has been carried on in our work before. It shows that the wakefield has a critical impact on lasing performance. In order to diminish the impact of the wakefield, four different pipe schemes were presented. Based on sufficient calculations of resistive wall wakefields and geometry wakefields, we compare the results of these schemes and choose the optimal one for designation of the FEL-I.

INTRODUCTION

In FEL facilities the accumulative effects of wakefields always lead to critical impacts on the electron bunch, resulting in the energy spread and the deviation of transverse position. Thus the lasing performance will be decreased. The SHINE is under construction and the wakefield estimations are required. The SHINE contains three different undulator lines (FEL-I, FEL-II and FEL-III) designed for different functions. The wakefields of FEL-I undulator section have been studied in our work before [1]. However the wakefields of inner segments between undulators were calculated simply. In this paper, we calculate the wakefields of inner segments considering more exquisite structures in FEL-I. We consider gradual changed connections between beam pipes of different diameters and corrugated pipes. We compare wakefields of different schemes of inner segments. In order to estimate the roughness wakefields, we develop the original theory to make it reliable in our cases. Based on the results, we give some suggestions for the designation of the inner segments in FEL-I.

FEL-I PIPE SCHEMES

In our work before, the diameter of the vacuum chamber is 16mm and the corrugated pipes are shielded. The wakefields of the undulator section in FEL-I were studied and showed a critical impact on lasing performance. It is worth noting that the sum of geometry wakefields of the

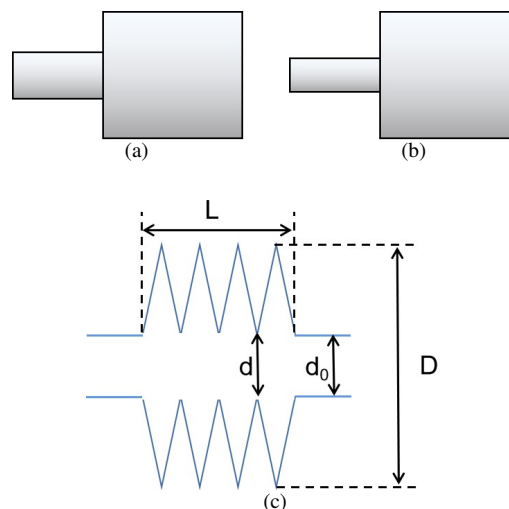


Figure 1: (a) and (b) are the diagram of two kinds of step-outs. (c) shows the geometry of the corrugated pipe.

step-outs (discontinuous connections of pipes with different diameters, Figure 1) is one of the main parts of the total wakefield. Thus we consider a new scheme to diminish this part of wakefield through narrowing the aperture variation of step-outs. Since the apertures of the vacuum chambers in undulators and the gap of photon absorbers are fixed, the only changeable pipe is the vacuum chamber in the inner segment. In order to narrow the aperture variation, smaller diameter vacuum chambers should be adopted. However a smaller diameter means a larger resistive wall wakefield [2, 3] and further more, the wakefields of corrugated pipes [4–6] may be introduced because of unshielding. In addition, different materials could lead to different results.

Table 1: Parameters of Four Pipe Schemes

d_0	d	D
12	shielded	shielded
10	12	23
8	10	20
6	8	18

On the foundation that synthesize the above considerations, we proposed four different pipe schemes with three kinds of materials, copper, aluminum and stainless steel 304. The detailed parameters of the four pipe schemes are shown in Table 1. The differences of these schemes are the diame-

LASER PLASMA ACCELERATOR BASED SEEDED FEL COMMISSIONING ON COXINEL AT HZDR

A. Ghaith*, J. P. Couperus, U. Shramm, A. Irman, HZDR, Dresden, Germany
M. Labat, A. Loulergue, M. E. Couprie, Synchrotron SOLEIL, L'Orme des Merisiers, France
E. Roussel, PhLAM–Physique des Lasers Atomes et Molécules, Lille, France

Abstract

The tremendous developments on Laser Plasma Accelerators (LPAs) have significantly improved the electron beam properties and stability making it possible to drive a Free Electron Laser (FEL). We report on the electron beam transport and manipulation using the COXINEL beamline implemented at HZDR that has recently led to the first measurements of an LPA-based seeded FEL in the UV region. Our experiment, cross-checked with Elegant simulations, shows that the beamline enables the handling of the large divergence via high gradient quadrupoles, reducing the slice energy spread with the help of a chicane, controlling the position and dispersion in both transverse planes using beam pointing alignment compensation and implementing the super matching optics. We also show that the beamline properly allows for the spectral tuning and spatial overlap between the electron beam and the seed.

INTRODUCTION

A Free Electron Laser (FEL) consists of a relativistic electron beam traversing a sinusoidal magnetic field generated by an undulator. The electrons interact with the emitted radiation leading to a gain of the FEL wave at the resonant wavelength λ_r [1]:

$$\lambda_r = \frac{\lambda_u}{2\gamma^2} \left(1 + \frac{K_u}{2} \right) \quad (1)$$

where λ_u is the undulator period, γ the relativistic factor, K_u the undulator parameter. The FEL wavelength can be varied by changing the electron beam energy or/and undulator magnetic field. In case of a long undulator, the energy modulation in the electron beam transforms to a density modulation leading to a micro-bunching mechanism. In consequence, a positive feedback is attained between the coherence level and the bunching process, where the FEL wave experiences an exponential gain until saturation. The FEL efficiency can be reinforced by applying an external laser tuned at λ_r to enhance the micro-bunching process. The FEL systems typically operate using conventional Linacs, which are limited to tens to hundreds of MeV/m accelerating gradient, and the pursue for shorter wavelength FEL requires a large accelerator scale and costly infrastructure. Following the advancement on chirped pulse lasers, Laser Plasma Accelerator (LPA) can now generate high energy electron beams within a very short accelerating distance [2–8]. Several experiments have been trying to demonstrate FEL using

an LPA the past decade [9–11], and recently amplification has been reported in the self-amplified spontaneous emission configuration at 27 nm wavelength [12].

We report here on the COXINEL beamline design [13, 14] that aims at demonstrating FEL in the seeded configuration at 270 nm. The electron beam transport is discussed along side measurements compared to simulations using Elegant [15].

COXINEL BEAMLINE DESCRIPTION

The COXINEL transport line [16–18], as shown in Fig. 1, starts with a triplet of high gradient permanent magnet based quadrupoles with variable gradient that strongly focuses the LPA electron beam and permits the handling of the divergence. The electron beam is then sent through a four-dipole-magnet chicane enabling to reduce the slice energy spread and lengthening the electron bunch. A second set of quadrupoles placed after the chicane allow for the implementation of the supermatching optics [14]. The commissioned undulator is a hybrid in-vacuum 2 meter long undulator with adjustable magnetic gap. Finally a dipole dump is placed at the end of the line allowing for photon diagnostics.

QUAPEVAS

In order to achieve FEL amplification, one crucial requirement has to be satisfied $\varepsilon_n < \frac{\gamma\lambda_r}{4\pi}$, where ε_n is the normalized emittance. The typical ε_n of electron beams generated by LPA is around 1 mm.mrad, however the chromatic term, in the following expression,

$$\varepsilon_n^2(s) \approx \varepsilon_{n0}^2 + \gamma^2 \sigma_\gamma^2 \sigma_{x,z}'^4 s^2$$

increases significantly after a drift s , where σ_γ is the energy spread and $\sigma_{x,z}'$ the divergence. For example, a typical LPA electron beam of 1 mrad divergence, 200 MeV energy and 5% spread: ε_n increases by a factor of 8 after 20 cm drift. Hence the need for high gradient quadrupoles placed very close to the generation source point to mitigate the emittance growth. At COXINEL, a triplet of QUAPEVAs [19, 20] is placed ≈ 4.2 cm from the gas jet (see Fig.2). The QUAPEVA is composed of two concentric quadrupoles, the one at the center has a Halbach hybrid structure, surrounded by the other one that consists of four rotating cylindrical magnets to provide the gradient tunability. It is also mounted on a translation table allowing for horizontal and vertical displacement.

* a.ghaith@hzdr.de

SIMULATION STUDY OF A DIELECTRIC BEAM ENERGY DECHIRPER FOR THE PROPOSED NSRRC EUV FEL FACILITY

C.K. Liu, S.H. Chen, S.Y. Teng, Department of Physics, NCU, Taoyuan, Taiwan
W.Y. Chiang[†], W.K. Lau, NSRRC, Hsinchu, Taiwan

Abstract

In this report, we present a simulation study of dielectric beam energy dechirper designed for the proposed NSRRC EUV FEL (National Synchrotron Radiation Research Center Extreme UltraViolet Free Electron Laser) facility. As revealed from ELEGANT (ELEctron Generation AND Tracking) [1] simulation of the high brightness driver linac system, a residual correlated energy spread of about $42 \text{ keV}/\mu\text{m}$ is left over after bunch compression. To maximize radiation output pulse energy, this energy chirp is removed by a capacitive dechirper structure when the bunch is slightly over-compressed. We successfully used a 1-m long corrugated pipe to remove the residual energy chirp in the simulation study. However, to save space and for a simplified mechanical design, we also consider the usage of two orthogonally oriented planar dielectric-lined waveguide (DLW) structures for removal of residual energy chirp after bunch compression. Both longitudinal and transverse wake fields due to this DLW dechirper at various gap heights, dielectric layer thickness and dielectric constants have been calculated by Computer Simulation Technology (CST) [2] code for evaluation purposes. Longitudinal wake functions can be deduced for ELEGANT simulation.

INTRODUCTION

A 66.5-200 nm FEL facility driven by a 250 MeV high brightness electron beam has been proposed in NSRRC. The baseline design is a 4th harmonic HGHG FEL that utilize 266-800 nm optical parametric amplifier (OPA) as seed [3-4]. The 200-250 pC drive beam is delivered by a high brightness linac system equipped with a 60 MeV photoinjector and a 100 MeV magnetic bunch compression system using nonlinear optics. A pair of 5.2-m constant-gradient traveling-wave rf linac structures energized by a single 35 MW pulsed klystron/SLED system are used to boost the compressed beam to nominal energy in an efficient way. It is worth noting that the photoinjector has now been operational for generation of THz super-radiant spontaneous undulator radiation (THz SSUR) for some pilot experiments. In previous simulation study, a 1-m corrugated pipe had been used to reduce correlated energy spread of the drive beam [5]. The structure parameters of the corrugated pipe used are recalled in the Table 1 and Fig. 1.

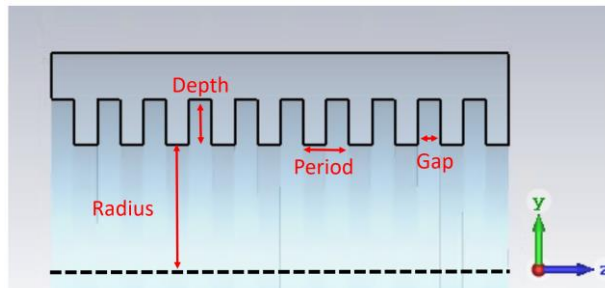


Figure 1: Corrugated beam pipe 2D structure.

Table 1: Dimensions of the Corrugated pipe Dechirper Used in Previous ELEGANT Simulation Study [2].

Parameter	Values
Pipe radius [mm]	1.25
Depth [mm]	0.5
Period [mm]	0.5
Gap [mm]	0.25
Total length [m]	1.0

Figure 2 depicts the electron distribution of the drive beam in longitudinal phase space when the compressed beam passes through such corrugated pipe dechirper. The expected performance of the dechirper has been achieved according to ELEGANT simulation. However, besides relatively large construction cost, the space occupied by the dechirper too long to fit into the 38-m bunker at the NSRRC Accelerator Test Area (ATA). Furthermore, such configuration is not practical because of its unchangeable beam aperture.

In this study, the possibility of using a rectangular dielectric-lined waveguide (DLW) structure for removal of correlated energy spread is under consideration. Longitudinal and transverse wake fields due to this DLW dechirper at various gap heights, dielectric constants and dielectric layer thickness have been calculated by CST code for evaluation purposes. Rectangular DLW structure is considered because it allows a changeable beam gap for wake field amplitude control.

[†] chiang.wy@nsrrc.org.tw

DESIGN CONSIDERATIONS FOR THE EXTRACTION LINE OF THE PROPOSED THIRD BEAMLINE PORTHOS AT SwissFEL

S. Reiche*, P. Craievich, M. Schär, T. Schietinger
Paul Scherrer Institut, Villigen PSI, Switzerland

Abstract

It is planned to extend SwissFEL by a third beamline, named Porthos, operating in the hard X-ray regime. Three bunches will be accelerated within one RF pulse and distributed into the different beamlines with resonant kickers operating at the bunch spacing of a few tens of nanoseconds. While the full extent of Porthos will not be realized before the end of this decade, the extraction line from the main linac will also serve the P^3 (PSI Positron Production) experiment for the demonstration of a possible positron source for the FCC-ee project at CERN. We present the design of the switchyard, which will serve both purposes with only minimal changes.

INTRODUCTION

The free-electron laser (FEL) facility SwissFEL [1] at the Paul Scherrer Institute drives the two independent undulator beamlines Athos and Aramis for the soft and hard X-ray range, respectively. Two electron bunches are generated in the SwissFEL RF photogun within the same RF pulse, accelerated up to the GeV range and compressed in two stages. At 3.2 GeV the second bunch is extracted from the main linac and transported to the Athos undulator, while the other bunch is accelerated further to reach beam energies of up to 6 GeV. Since SwissFEL has demonstrated that multiple beamlines can be operated at the same repetition rate as the RF system, it is planned to extend the facility by a third beamline, called Porthos. Its extraction shares many similarities with the Athos extraction but is placed at the end of the existing linac, putting the operation range of Porthos into the hard X-ray regime. A schematic layout of SwissFEL with the planned third beamline is shown in Fig. 1.

In this contribution we describe the design strategies for the extraction line and its synergy with a planned experiment, named P^3 for “PSI Positron Production” [2], to demonstrate the positron yield for a possible positron source for the FCC project [3].

EXPERIENCE FROM THE ATHOS EXTRACTION LINE

Since the extraction lines for Porthos and Athos share the same purpose they follow the same design guideline. Since we already gained some experience with the operation of the Athos line, we may apply this knowledge to improve upon the design and to eliminate potential bottlenecks in performance and operation.

Design Principle

In SwissFEL two electron bunches are generated and accelerated within a single RF pulse. At an energy of about 3.2 GeV and after two stages of bunch compression a resonant kicker system operating at 17.8 MHz [4] extracts the second bunch from the main linac and sends it into the Athos extraction line. Since the time separation between the two bunches is only 28 ns the combination of a kick in the vertical direction for an offset of 10 mm and a Lambertson septum [5], which steers the beam horizontally, offers optimal performance. The other bunch travels on a straight path, passing through a hole in the lower yoke of the septum magnet.

The extraction line provides an offset of 3.75 m for the Athos beamline with respect to the main linac and Aramis beamline. The transport consists of two sections with a total bending angle of 5° and -5° , respectively, and a straight middle section with its length matched to the overall offset. The dispersion function should be closed in the middle section for reducing constraints on the Twiss function between the two bending sections.

The design [6] solves three problems to preserve the beam quality needed to drive the soft X-ray beamline Athos. The first problem is the closure of the vertical dispersion, originating at the resonant kicker. Since it is impractical to generate an offset without dispersion in a short distance before the Lambertson septum, the vertical dispersion leaks through the first bending section and is then caught by a downward dogleg. Two quadrupoles within the dogleg close the vertical dispersion function after the second dogleg dipole. The tunability is limited and requires values for the dispersion functions η_y and η'_y close to those at the Lambertson septum entrance.

The second problem is the residual R_{56} for the simplest solution of a double-bend system—two bending dipoles and a center quadrupole with a focal length half the distance between the bending magnets. It decompresses any bunch with a residual energy chirp from the last compression stage. Without compensating this intrinsic R_{56} of the double-bend system, the electron bunch needs to be compressed stronger to compensate for the elongation by the extraction line. The coherent synchrotron radiation (CSR) [7] effects are unnecessarily stronger and the risk of electron beam quality degradation is high. The Athos extraction design compensates it by a weak center dipole and a total bending of 2° by the Lambertson magnet, 1° by the center dipole and again 2° by the last bending magnet of the first section. The beam transport ensures that the sign of the dispersion function η_x changes for the center dipole and is inverted back for a

* sven.reiche@psi.ch

ORBIT JITTER ANALYSIS AT SwissFEL

S. Reiche*, Paul Scherrer Institut, Villigen PSI, Switzerland

E. Ferrari, Deutsches Elektronen-Synchrotron DESY, Hamburg, Germany

Abstract

We use the beam-synchronous readout of the beam position measurement at the hard X-ray FEL beamline Aramis at SwissFEL to analyze the intrinsic orbit jitter, applying a classification algorithm and principal component analysis (PCA). The method sorts the jitter in a set of eigenvectors and $-$ values. With the magnitude of the eigenvalues the impact of the different jitter sources can be estimated. From the purely stochastic results we derive also a physical interpretation by matching the linear transport functions to the eigenvectors, reconstructing the orbit jitter in terms of the center of mass jitter of the electron bunch in the transverse positions, momenta, and the mean energy. Any deviation from the theoretical prediction indicates possible wrong set values of the transport magnets or errors in the BPM calibration (sign flip or faulty amplitude calibration). We present the results and give an outlook on extending the analysis to additional channels such as charge, compression and arrival time monitors as well as the FEL output signal.

INTRODUCTION

SwissFEL [1] is an X-ray free-electron laser (FEL) facility at the Paul Scherrer Institute, where the energy of an relativistic electron beam is transferred to an intense, transversely coherent X-ray pulse with femtosecond pulse durations and gigawatt peak powers. For the optimum performance of the hard X-ray branch Aramis with a tuning range between 1 to 7 Å, the orbit within the periodic magnetic field of the undulator [2] needs to be straight within a few microns. Unfortunately, machine jitters add shot-to-shot variations in beam parameters, for instance orbit but also beam charge and bunch length, among many others, which affect the FEL operation. To quantify these jitter sources and their source locations a statistical analysis of the machine data can give valuable insight. We present such an analysis for the hard X-ray branch Aramis at SwissFEL.

PRINCIPAL COMPONENT ANALYSIS

While many of the SwissFEL sensor readings exhibit fluctuations on a shot-to-shot basis, they are typically strongly correlated among each other. The number of actual independent sources is significantly smaller. The process of finding collective jitter sources from the sensor readings is called principal component analysis (PCA) [3]. Its application to the orbit jitter in the hard X-ray beamline Aramis at SwissFEL is described in the following sections.

Data Preparation

The data are taken from the beam position monitors (BPMs) [4] along the hard X-ray beamline Aramis. The beamline starts at the exit of the linear accelerator and takes all BPMs up to the beam dump after the undulator. There are in total 39 BPMs with two channels each for the position in x - and y . The data acquisition uses the beam-synchronous stream [5], ensuring that a single record of all channels belongs to the same shot in the machine. The acquisition rate is 100 Hz. During the data acquisition the orbit feedback system remains enabled.

The rms orbit jitters are overall small, with the largest jitter occurring in the dispersive section of the energy collimator and reaching about 30 μm . Within the undulator beamline it is less than 5 μm . Therefore we assume that the observed jitter is a linear superposition of different jitter sources such as energy deviation or jitter in the transverse position. The former will manifest itself only in BPM readings of dispersive sections of the beamline.

The BPM readings represent the absolute orbit position but since we are analyzing the relative orbit jitter, we subtract a reference orbit to convert the data. For the sake of simplicity this is the first record of the acquired data records. The observed relative orbit can be described by a general transport matrix $\tilde{\mathbf{R}}$ and an input vector \vec{r} . The naming reflects a generalizing approach of the linear transport matrix in beam optics with $\vec{r}(s_1) = \mathbf{R}(s_0 \rightarrow s_1)\vec{r}(s_0)$. The six components of \vec{r} consist of the two transverse positions x and y , two transverse momenta x' and y' , longitudinal position t and relative energy deviation $\delta = \Delta E/E$. The analogy to the PCA becomes obvious, since a jitter in one of the input parameters (e.g., in x) can be regarded as the jitter source. The response of the transport matrix to a change in x describes the principal component of this jitter source. In practice there might be other jitter sources (e.g., coherent synchrotron radiation kicks from a jitter in the bunch charge or length). The model for the linear transport is a subset of the more general description by PCA.

The PCA becomes simpler in the linear regime and can be expressed by a set of eigenvectors. Figure 1 illustrates the case for two observed BPM readings. Note that the eigenvectors are evaluated from the ‘center of mass’ position of the distribution and not from the origin. Therefore we prepare our records by subtracting as a second step the mean value for each channel. Since the mean orbit is a superposition of valid orbits, the subtraction preserves the validity of the measured orbit as part of a linear transport system. It turns out that the first step of subtracting the first measured orbit from all others is actually not needed and that the subtraction of the mean BPM readings can be applied directly.

* sven.reiche@psi.ch

MEASUREMENT OF ORBIT COUPLING BY THE APPLE-X UNDULATOR MODULES IN THE SOFT X-RAY BEAMLINE ATHOS AT SwissFEL

S. Reiche*, M. Calvi, R. Ganter, Paul Scherrer Institut, Villigen PSI, Switzerland
E. Ferrari, DESY, Hamburg, Germany

Abstract

Orbit response measurements in the soft X-ray beamline of Athos have shown coupling of the beam transport between the transverse planes, which is influenced by the on-axis field strength of the APPLE-X undulator modules. A model reproduces this observation if a coupling term is included in the transport matrix of the undulator module. The presentation shows the estimate of the coupling strength as a function of beam energy, undulator field strength and orbit excitation.

INTRODUCTION

SwissFEL [1] is a free-electron laser (FEL) facility delivering coherent hard and soft X-rays to users from Switzerland and worldwide. The soft X-ray beamline Athos [2] uses the novel APPLE-X undulator type [3] to allow for an independent control on polarization and field strength without the broken symmetry of a APPLE-II or III configuration. The chosen undulator type has proven its high effectiveness during commissioning and user operation of Athos, but we observed a strong coupling between the orbits of the x - and y -plane. In this paper we describe the investigation on the possible sources and their quantification. While the effect is undesired, it can be accounted for (e.g., in the orbit feedback system) by means of an improved model of the beam transport.

POSSIBLE SOURCES FOR COUPLING

We observed early during the commissioning of the Athos undulator beamline that the orbits in both planes were coupled. Given the symmetry of the involved magnets (undulator, phase shifters and quadrupole magnets) this was unexpected. We explored possible sources and checked them systematically.

Coupling can be generated by quadrupoles that have a non-zero roll angle, effectively converting parts of the field to that of a skew quadrupole. Since the coupling strength is roughly at the percent level of the normal quadrupole field, the roll would be on the order of 10 mrad. However, to explain the observed resonant growth in the betatron amplitude, the roll angles need to have the same signs as the quadrupole field gradient in the FODO lattice of the Athos beamline. This is highly unlikely if the effect is caused by a systematic misalignment. Neither did field measurements for the quadrupole type indicate a skew quadrupole component nor can a systematic tilt in the support structure reproduce an alternation in the roll angle. Similar exclusion applies to the

delaying chicanes between the undulator modules. They are planar by design and the coupling is not influenced by the strength of the chicanes.

We also tested for possible transverse wakefields, e.g., when the beam passes close to the vacuum chamber wall. In the case where the chamber is slanted at that position (e.g., in the upper left region of a round vacuum chamber), a steering in one plane causes a kick in the perpendicular plane. However this effect is highly asymmetric and non-linear, contrary to our observation. Alternative trajectories through the undulator vacuum chamber didn't change the coupling either.

On the other hand changing the magnetic field of the undulator field itself has an impact on the coupling strength. Thus we conclude that the primary reason for the coupling lies in the magnetic field of the APPLE-X undulators. Our studies of this effect are described in the following section.

MODELING OF COUPLING TERMS

For the analysis of the orbit response in the Athos undulator beamline we developed a simple model for a possible coupling of the undulator field. For the helical configuration the magnetic field is symmetric against swapping the x and y coordinate. Thus the transport matrix should also be symmetric. Instead of an explicit solution for the transport matrix, we approximate each undulator module with a series of thin lenses and drifts. We express the effective quadrupole strength of the natural focusing with k_n , which occurs in the matrix element R_{21} and R_{43} of the thin-length approximation. In analogy we define the skew quadrupole strength with k_s for the R_{23} and R_{41} coefficient. We allow for different values of k_n and k_s .

The complete expression for the transport matrix is then

$$M = \left[\begin{pmatrix} 1 & 0 & 0 & 0 \\ -k_n \frac{L_u}{m} & 1 & -k_s \frac{L_u}{m} & 0 \\ 0 & 0 & 1 & 0 \\ -k_s \frac{L_u}{m} & 0 & -k_n \frac{L_u}{m} & 1 \end{pmatrix} \cdot \begin{pmatrix} 1 & \frac{L_u}{m} & 0 & 0 \\ 0 & 1 & 0 & 0 \\ 0 & 0 & 1 & \frac{L_u}{m} \\ 0 & 0 & 0 & 1 \end{pmatrix} \right]^m, \quad (1)$$

with the value m as the number of subdivisions to be chosen sufficiently large. For the fitting of the orbit response we use $m = 100$.

The total transport channel is quasi a FODO lattice, transporting the beam from the first beam position monitor (BPM) stepwise to the succeeding BPMs. After each BPM there is a quadrupole and—for most of the sections—an undulator module, except for the first five sections, which are reserved

* sven.reiche@psi.ch

APPLICATION OF MACHINE LEARNING IN LONGITUDINAL PHASE SPACE PREDICTION AT THE EUROPEAN XFEL

Z. H. Zhu^{1,2*}

Shanghai Institute of Applied Physics, Chinese Academy of Sciences, Shanghai, China

¹also at University of Chinese Academy of Sciences, Beijing, China

²also at Deutsches Elektronen-Synchrotron DESY, Hamburg, Germany

S. Tomin, J. Kaiser

Deutsches Elektronen-Synchrotron DESY, Hamburg, Germany

Abstract

Beam longitudinal phase space (LPS) distribution is the crucial property to driving the high-brightness free-electron laser. However, the beam LPS diagnostics is often destructive and the relevant physical simulation is too time-consuming to be involved in the control room. Therefore, we explored applying the machine learning models to facilitate the virtual diagnostic of the LPS distribution at European XFEL. Two different model designs are proposed and the performance demonstrates its feasibility based on the simulations. This work lays the further investigation of the real-time virtual diagnostics in the operational machine.

INTRODUCTION

In the past decade, The X-ray free-electron laser (XFEL) facilities around the world provide coherent and ultra-short X-ray radiation with tunable wavelength and high-brightness [1], facilitating the ultra-fast scientific research and discovery with atomic spatial resolution [2–4]. In the daily operation of the facility, the electron beam with high quality is indispensable to the desirable lasing performance in the undulator sections, especially the beam longitudinal properties, such as the charge distribution and slice energy spread distribution along the beam. The acquirement of these essential beam properties requires the measurement of the entire beam longitudinal phase space (LPS) with a diagnostic instrument such as transverse deflecting structure (TDS). However, this measurement is conducted in an interceptive manner, which makes it impossible to be taken during the photon delivery to the experimental stations unless it is implemented downstream of the undulator section. In addition to that, the LPS measurement is subject to the resolution limitations from the TDS. One potential approach is beam physical simulation in which the collective effects are modeled and the beam dynamics results are well matched with experimental measurement [5]. Unfortunately, it is too computationally expensive to be applicable in the control room.

To overcome these difficulties, machine learning (ML), especially the deep neural network, has the potential to cope with system modeling in the accelerator community as a result of the rapid development of computer science. Based

on it, we are enabled to construct the surrogate model with the fast-execution speed with ML, which has demonstrated its data processing capabilities in many industrial fields. With this powerful tool introduced, some ML applications in accelerators have been explored and studied in the past few years. Based on the built surrogate model with fast execution and reliable accuracy, some beam dynamics optimization projects can benefit from the orders of magnitude increase in speed [6, 7]. In addition to that, it can also facilitate the automatic online tuning and beam phase space control in FEL facility [8, 9].

Because of the powerful capability of interpreting images, there has been some recent research about neural network-based virtual diagnostic of 2D beam LPS distribution in the accelerator community [10–13]. In this paper, we propose an alternative manner to predict the beam LPS distribution. This surrogate model is built to provide the prediction of the slice beam properties distributions and its corresponding LPS is reconstructed based on them. Furthermore, Convolutional neural networks (CNN) have been implemented as the second method. We compare the results from these two approaches and the preliminary study paves the path for further investigation on the online virtual diagnostic in the operational machine.

METHODOLOGY AND RESULTS

Here we demonstrate the feasibility of the machine learning-based beam LPS reconstruction with beam dynamics simulations from European X-ray Free-Electron Laser [14]. The schematic layout of the European XFEL accelerator is shown in Fig. 1. In the main linac section, the beam experiences the longitudinal density modulations at three bunch compressor chicanes with the nominated beam energy of 130 MeV, 700 MeV, and 2.4 GeV respectively. The initial beam distribution at the end of the gun cavity is simulated with ASTRA [15]. The remaining physical tracking, which simulates the beam dynamics from the gun cavity exit to the collimator section at the entrance of the undulator, is conducted with OCELOT code [16].

In the simulations, the momentum compaction factor in each dispersive section is kept as their initial values. We tune the upstream RF parameters to adjust the energy chirp at the entrance of each dispersive section to change the com-

* zihan.zhu@desy.de

DEMONSTRATION OF HARD X-RAY MULTIPLEXING USING MICROBUNCH ROTATION THROUGH AN ACHROMATIC BEND *

R. A. Margraf^{†1}, J. P. MacArthur, G. Marcus, H.-D. Nuhn, A. Lutman, A. Halavanau, Z. Huang¹
 SLAC National Accelerator Laboratory, Menlo Park, USA
¹also at Stanford University, Stanford, USA

Abstract

Electrons in a X-ray free electron laser (XFEL) develop periodic density fluctuations, known as microbunches, which enable the exponential gain of X-ray power in an XFEL. When an electron beam microbunched at a hard X-ray wavelength is kicked, microbunches are often washed out due to the dispersion and R_{56} of the bend. An achromatic (dispersion-free) bend with small R_{56} , however, can preserve microbunches, which rotate to follow the new trajectory of the electron bunch. Rotated microbunches can subsequently be lased in a repointed undulator to produce a new beam of off-axis X-rays. In this work, we demonstrate hard X-ray multiplexing in the Linac Coherent Light Source (LCLS) Hard X-ray Undulator Line (HXU) using microbunch rotation through a 10 μ rad first-order-achromatic bend created by transversely offsetting quadrupole magnets in the FODO lattice. Quadrupole offsets are determined analytically from beam-matrix theory. We also discuss the application of microbunch rotation to out-coupling a cavity-based XFEL (CBXFEL) [1].

INTRODUCTION

Microbunch rotation using achromatic bends has long been known as an option for for out-coupling infrared FEL oscillators [2], and MacArthur et al. demonstrated a 5 μ rad rotation with a single offset quadrupole for soft x-ray microbunches [3]. However, microbunch rotation with hard X-rays has proved more challenging. Shorter microbunches, separated at the radiation wavelength, λ_r , are more sensitive to bunching factor ($\theta \approx (\frac{2\pi}{\lambda_r} + \frac{2\pi}{\lambda_u})z$) degradation due to changes in the z position of the particles relative to the center of the microbunch.

Cavity-based XFELs, such as the X-ray Regenerative Amplifier FEL (XRAFEL) [4, 5] and X-ray FEL Oscillator (XFEL) [6] typically operate Bragg-reflecting cavities at hard X-ray wavelengths. To extend microbunch rotation as an out-coupling mechanism for these cavities, we need to extend it to hard X-rays, such as the 9.832 keV X-ray energy used by the CBXFEL project [1].

MICROBUNCH ROTATION FROM AN OFFSET QUADRUPOLE TRIPLET

MacArthur et al. [3] proposed a triplet of three offset quadrupoles to perform microbunch rotation at hard X-ray

* This work was supported by the Department of Energy, Laboratory Directed Research and Development program at SLAC National Accelerator Laboratory, under contract DE-AC02-76SF00515.

[†] rmargraf@stanford.edu

wavelengths. Such a scheme is illustrated in Fig. 1, where α is the microbunch rotation angle, f_1 , f_2 , and f_3 are the quadrupole focal lengths, and L_1 , and L_2 , are the distances between the quadrupoles.

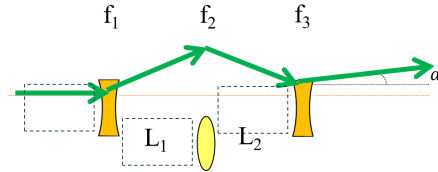


Figure 1: Offset quadrupole triplet for microbunch rotation.

Later work [7, 8] identified microbunch rotation through this triplet is optimized when the kicks from the three quadrupoles form a first-order achromatic bend. To preserve microbunching through a bend, one has to prevent the energy spread of the electron beam from coupling to the longitudinal and transverse dimensions of the beam. In transfer matrix formalism, for a kick in x , these are the R_{16} (Dispersion), R_{26} (Dispersion') and R_{56} elements. An achromatic bend sets the Dispersion and Dispersion' elements to zero. The quadrupole offsets which achieve this can be analytically found. In the thin quadrupole limit, these are [7, 8]:

$$\begin{aligned} o_1 &= \frac{\alpha f_1 f_2}{L_1} \\ o_2 &= \frac{-\alpha f_2 (f_2 L_1 + f_2 L_2 - 2L_1 L_2)}{L_1 L_2} \\ o_3 &= \frac{\alpha (L_2^2 + f_2 f_3)}{L_2}. \end{aligned} \quad (1)$$

If we implement microbunch rotation in a FODO lattice where $f_1 = f_3 = -f_2$, and $L_1 = L_2 = L$, these simplify to:

$$\begin{aligned} o_1 &= \frac{-\alpha f_1^2}{L} \\ o_2 &= -2\alpha f_1 \left(1 + \frac{f_1}{L}\right) \\ o_3 &= \frac{-\alpha (f_1^2 - L^2)}{L}. \end{aligned} \quad (2)$$

A more lengthy analytical solution also exists in the thick quadrupole limit [7], and this was used to determine the quadrupole offsets for this experiment, which differed by a few μ rad from the thin quadrupole values.

To preserve microbunching, we must also keep R_{56} small. An expression for R_{56} through the offset quadrupole triplet

INTRABEAM SCATTERING EFFECTS IN THE ELECTRON INJECTOR OF THE EUROPEAN XFEL

E. Gjonaj*, H. De Gerssem, Technische Universität Darmstadt, TEMF, Darmstadt, Germany
T. Limberg, DESY, Hamburg, Germany

Abstract

A numerical procedure for beam dynamics simulations including IBS effects is presented. The method is implemented in the tracking code Reptil and, furthermore, it is applied in the simulation of the injector section of the E-XFEL. This allows to identify precisely the amount by which IBS contributes to the uncorrelated energy spread growth in the injector. It is found that IBS is responsible for nearly doubling the slice energy spread of the bunch at the central slice. Various aspects related to the IBS-induced growth of the slice energy spread in the injector compared to space-charge related effects are discussed.

INTRODUCTION

The main limitation in the operation of X-Ray Free Electron Lasers (XFEL) is posed by the microbunching instability (MBI) [1, 2]. This is a space-charge induced amplification in the longitudinal phase-space that grows from shot noise. In the European XFEL (E-XFEL), MBI is partially mitigated by means of a laser heater which is placed right after the injector section. The laser heater introduces a small amount of uncorrelated energy spread to the beam, thus, attempting to suppress MBI by the Landau damping mechanism. This process, however, is critical since excessive heating may affect the FEL process. This is why, an accurate estimation of the intrinsic slice energy spread (SES) of the beam in the injector, before laser heating is applied, is crucial for an optimal operation of the facility [2].

In the case of the E-XFEL, tracking simulations for a bunch of 250 pC predict a SES of about 1 keV at the exit of the injector section. However, recent measurements using a transverse deflecting structure indicate that this figure is as high as 6 keV [3]. In the case of SwissFEL, an even higher SES of 15 keV was reported [4], although the operation modes of both machines are quite similar.

These discrepancies are hard to explain. At least partially, they are attributed to intrabeam scattering (IBS) effects [3]. Unfortunately, such measurements do not provide sufficient insight on the cause of SES growth. This could be related to the emission process, wakefields in the gun, IBS or a combination of all. This motivates the present study, where the specific contribution of IBS to the SES growth in the E-XFEL injector is investigated by numerical simulations. A novel IBS modeling approach is introduced that includes in particle tracking simulations the combined effects of the collective, space-charge interaction on the one hand and Coulomb collisions on the other.

* gjonaj@temf.tu-darmstadt.de

The E-XFEL injector section considered in the simulations (see Fig. 1) has a total length of 40 m, it includes the electron gun, a booster module (A1) and a third-harmonic module (AH1). The main injector and beam parameters used in the simulations are summarized in Table 1.

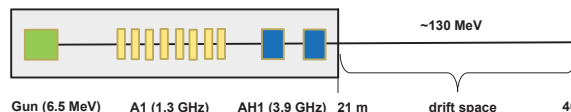


Figure 1: Schematics of the E-XFEL injector beam line.

Table 1: Main Injector Parameters Used in the Simulations

Component	Parameter	Value
Gun (1.3 GHz)	Field gradient	56.3 MV/m
A1 (1.3 GHz)	Field gradient	34.4 MV/m
AH1 (3.9 GHz)	Field gradient	17.3 MV/m
Bunch	Charge	250 pC
Bunch	Duration on cathode	3 ps
Bunch	Spot size on cathode	0.25 mm

SIMULATION METHOD

For the IBS simulations, the tracking code Reptil is extended such that it includes collisional effects in addition to collective interactions. For the IBS modeling, two different Monte-Carlo collision models are considered. These are the Takizuka & Abe's [5] and the Nanbu's [6] models as described below.

The Reptil Code

The **Relativistic Particle Tracker for Injectors and Linacs** (Reptil) is a particle tracking code developed at the TU Darmstadt. The code employs a modified, 4th-order-accurate Adams-Moulton scheme for the integration of particle's equations with an adaptive time step. Various space-charge solvers are implemented in Reptil. These include particle-particle solvers based on the Barnes-Hut and the FMM methods [7], as well as 3D particle-mesh solvers using the integrated Green's function approach [8]. Due to the specifics of IBS modeling, only the particle-mesh approach is used in the following. In addition, Reptil supports various types of accelerating cavities, multipole magnets, and external wakefields. All computations are highly parallelized for shared as well as for distributed memory platforms.

PROTECTION OF THE EUROPEAN XFEL UNDULATORS FROM THE ADDITIONAL BEAM LOSSES CAUSED BY THE INSERTION OF A SLOTTED FOIL

A. Potter, A. Wolski, University of Liverpool, Liverpool, UK
F. Jackson, STFC/ASTeC, Daresbury Laboratory, Daresbury, UK
S. Liu, DESY, Hamburg, Germany

Abstract

The European XFEL undulators are made of permanent magnets that need to be protected from beam losses that could cause demagnetisation. Under current operating conditions, beam losses in the undulators are prevented by a collimation section downstream of the main linac. In the future, a slotted foil may be installed in the European XFEL to reduce the X-ray pulse length; however, particles scattered by the foil could lead to significant radiation dose rates in the undulators. In this paper, we report a study to assess the level of the beam losses in the European XFEL undulators that would be caused by a slotted foil, and to determine the optimal apertures to use in the collimators to minimise the losses. We also assess whether shielding or an additional collimator in front of the undulator could help to reduce the losses.

INTRODUCTION

A potential way of reducing the X-ray pulse length at the European XFEL is to insert a slotted foil in a bunch compressor [1] to scatter electrons at the head and tail of each bunch so that they are either lost downstream of the foil or do not contribute to the lasing process in the SASE sections. Simulations of the electron transport from the slotted foil to the SASE section showed that particles scattered by the slotted foil would cause some radiation dose in the undulator magnets [2].

Beam loss in the undulators at the European XFEL is a problem that has been observed previously. The beamline contains a diagnostic undulator that allows monitoring of radiation dose rates, which can be correlated with demagnetisation of the undulators. To prevent the demagnetisation of the undulators in the SASE section, a total dose limit of 55 Gy over the 10-year lifetime of the undulators was set [3].

An estimate of the dose rates from simulations suggested that if a slotted foil was used to reduce the X-ray pulse length, the 55 Gy dose limit would be quickly exceeded [2]. The simulations showed that some particles scattered by the slotted foil would interact with the collimators downstream of the linac. Particles scraping the surface of a collimator could be further scattered rather than absorbed, and could then perform large betatron oscillations as they continued along the beamline. These particles would generally be lost at a section of the beamline close to the entrance of the SASE section where there is a reduction in the beam-pipe aperture. Particles lost in this way would create a shower of secondary

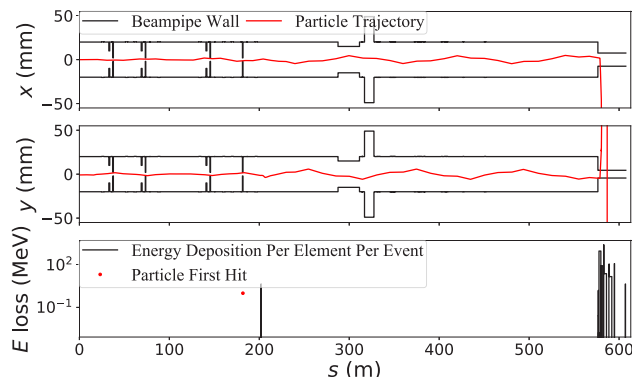


Figure 1: Top and middle plots: trajectory of a particle scattered by a collimator. The particle travels along the following beamline section at large betatron amplitude, before being lost at an aperture reduction near the undulators. Bottom plot: energy deposition by the primary (scattered) particle and by the secondary particles created by the loss of the primary particle.

particles travelling outside the beam-pipe that could be absorbed by the diagnostic undulator and by the first sections of the SASE undulator [2]. Figure 1 shows (in simulation) the trajectory of a primary particle that demonstrates this behaviour. Also shown in the figure is the energy deposited at different locations by this particle or by the secondary particles that it generates. It can be seen that the initial interaction of the primary particle with a beamline component is at the end of the collimation section, and that this results in the loss of the particle at the beam-pipe aperture reduction. The loss of the particle is followed by further energy deposition from a shower of secondary particles.

The study reported here aims to explore ways to reduce the dose caused by a slotted foil to an acceptable level. Two options have been considered. The first is to add shielding after the vacuum chamber transition (where there is a significant reduction in beampipe aperture) to absorb secondary particles generated by the loss of primary beam particles. The second option is to install a collimator upstream of the vacuum chamber transition to absorb primary beam particles that have a high betatron amplitude (as in the example in Fig. 1). Different options and configurations need careful study, because with any components installed to absorb particles there is the risk of creating further particle showers which could increase, rather than reduce the absorbed dose.

INVESTIGATION OF BEAM LOSSES AND RADIATION LOADS FOR THE IMPLEMENTATION OF A SLOTTED FOIL AT THE EUROPEAN XFEL

A. Potter, A. Wolski, University of Liverpool, Liverpool, UK

F. Jackson, STFC/ASTeC, Daresbury Laboratory, Daresbury, UK

B. Beutner, J. Branlard, A. Dehne, S. Liu, N. Walker, DESY, Hamburg, Germany

Abstract

Ultra-short X-ray pulses in an X-ray FEL can be generated by means of a slotted foil inserted into a bunch compressor. There is an ongoing study into whether such a technique could be used at the European XFEL. One important factor that must be considered is whether the additional beam losses and radiation loads caused by the foil are acceptable with a normal operating beam power up to 500 kW. As there is currently no foil installed at the European XFEL, experimental investigations were carried out by inserting a screen in the bunch compressor at the location where a foil would be inserted. Neutron radiation measurements have been compared with simulations using BDSIM to provide validation and calibration of simulations for the case of a slotted foil and also to provide an approximate limit of the number of bunches that should be allowed through the foil to avoid radiation damage.

INTRODUCTION

One of the techniques currently being investigated for producing ultra-short X-ray pulses at the European XFEL is based on the use of a silicon slotted foil in a bunch compressor [1]. The correlation between the transverse and longitudinal position of particles in a bunch in the compressor leads to the scattering of particles by the foil and consequent degradation of the emittance at the head and tail of the bunch. Particles at the centre of the bunch pass through a slot in the foil, and are not scattered. The short section of the bunch where the emittance is preserved will lase as normal in the undulator sections, while the scattered particles will either be lost along the beamline, or will not contribute to lasing.

This study focuses on the particles that are lost along the beamline as a result of use of a slotted foil. Losses can be a problem at the European XFEL because of the high beam power. Previous studies have estimated the effect of a slotted foil for short-pulse generation on heat loads in the collimators [2], and on radiation loads in the undulators [3]. However, radiation resulting from beam losses can affect various accelerator systems and components over the length of the machine, including electronics in the control systems and diagnostics. Losses in European XFEL are routinely monitored using fixed beam loss monitors (BLMs), but losses can also be measured using MARWIN [4], a robot that can move along the beamline tunnel parallel to the machine. MARWIN is equipped with a radiation monitor (LB6419 [5]), and can provide neutron and gamma radiation dose rate as a function of longitudinal position along the accelerator. At the European XFEL, the BLMs are not calibrated, and they

are set to different gains empirically [6]. Also, the insertion of a foil would cause many losses meaning that many of the BLM readings are saturated. For these reasons, the data from MARWIN is better suited for this study.

Currently, there is no slotted foil installed at the European XFEL, so direct measurements of losses caused by the foil cannot be made. It is planned to install the foil at a screen station in the second of three bunch compressors. To reproduce as closely as possible the scattering effects of the foil, we can insert the screen at this location into the beam. Simulations have been performed of the losses caused by the screen and the losses from a slotted foil. Results of simulations in the case of the screen can be compared with the experimental measurements made using MARWIN, to validate and calibrate the simulations. The simulations in the case of the foil can then be used to determine parameter regimes that will allow beam losses and radiation loads to be maintained within safe limits during short-pulse operation.

SIMULATIONS

Simulations were performed using BDSIM [7], a tracking code with the capability to model a range of interactions between beam particles and the beamline components, including the production of secondary particles. For this study, simulations included all electromagnetic and hadronic interactions. A model of the beamline was constructed starting from the first dipole in the bunch compressor (BC1) where the foil would be inserted, through a collimation section (CL) where many losses are expected to occur, and ending at the entrance of one of the undulator beamlines (SASE1). The layout is shown in Fig. 1.

In the first simulation, the beam was tracked with a slotted foil inserted in BC1. The energy deposited per metre of beamline was recorded, and the simulation repeated 10 times. Although the same initial distribution of particles was used for the beam, the random nature of the scattering processes leads to some variation in the energy deposited in the beamline. The mean energy deposition per metre was calculated. The full simulation was repeated with a screen inserted instead of the foil.

The mean energy deposition per tracking run was scaled up to match the bunch charge (250 pC) normally used in operation and converted to a radiation power load by multiplying by the bunch repetition rate. The bunch repetition rate is variable, but for the experimental measurements of the effects of the screen on the dose rates, a bunch rate of 10 Hz was used (limited by the setup of the machine protection system with a screen inserted in the beamline). The simulation

FEASIBILITY OF SINGLE-SHOT MICROBUNCHING DIAGNOSTICS FOR A PRE-BUNCHED BEAM FOR TESSA AT 515 nm*

A. H. Lumpkin^{1†}, Argonne Associate, Argonne National Laboratory, Lemont IL, USA
 D.W. Rule, Silver Spring, Maryland, USA
 P. Musumeci, UCLA, Los Angeles, USA
 A. Murokh, RadiaBeam Technologies, Santa Monica, USA
¹also affiliated at Fermi National Accelerator Laboratory, Batavia, USA

Abstract

The feasibility for microbunching diagnostics of the electron beam after co-propagating it and a high-power laser pulse through a short undulator (modulator) is discussed. This provides an energy modulation that can be converted to a periodic longitudinal density modulation (or microbunching) via the R_{56} term of a chicane. Coherent optical transition radiation (COTR) imaging techniques can be used for beam size, divergence, energy, spectral, alignment, and temporal characterizations on a single shot of this pre-bunched beam for a TESSA experiment at 515 nm.

INTRODUCTION

Co-propagating a relativistic electron beam and a high-power laser pulse through a short undulator (modulator) provides an energy modulation which can be converted to a periodic longitudinal density modulation (or microbunching) via the R_{56} term of a chicane. Such pre-bunching of a beam at the resonant wavelength and the harmonics of a subsequent free-electron laser (FEL) amplifier seeds the process and results in improved gain in a Tapering Enhanced Super-Radiant Stimulated Amplification (TESSA) experiment [1,2]. We describe potential characterizations of the resulting microbunched electron beams after the modulator using coherent optical transition radiation (COTR) imaging techniques for transverse size (50 μm), divergence (sub-mrad), trajectory angle (0.1 mrad), coherence factor, spectrum (few nm), and pulse length (ps). The transverse spatial alignment is provided with near-field imaging and the angular alignment is done with far-field imaging and two-foil COTR interferometry (COTRI). Analytical model results for a 515 nm wavelength COTRI case with a 10% microbunching fraction will be presented. COTR gains of 22 million were calculated for an initial charge of 1000 pC which enables splitting the optical signal for single-shot measurements of all the cited parameters.

EXPERIMENTAL ASPECTS

The TESSA-515 experiments are being staged at the Fermilab Accelerator Science and Technology (FAST) facility where the superconducting TESLA-type linac [3] will generate the driving beam for the FEL experiments. A schematic of the linac is shown in Fig. 1. Also shown are

* Work supported by the U.S. Department of Energy, Office of Science, Office of Basic Energy Sciences, under Contract No. DE-AC02-06CH11357.

† lumpkin@anl.gov

the photocathode rf gun, the two TESLA capture cavities operating at about 20 MV/m gradient, the chicane for bunch compression, the cryomodule (with eight, 9-cell cavities) and the high-energy transport line to the location of the FEL experiment. The nominal electron beam properties are given in Table 1, and the final energy of 220 MeV results in the generation of 515 nm radiation in the tapered undulator at the laser seed wavelength. An Amplitude Magma seed laser generating 5 mJ per pulse at 1030 nm will be used as a seed [4]. We will use the frequency-doubled component from the 10-mm thick beta-BBO crystal.

Past experiments on wakefield effects [5-7] in the cavities, which are correlated with their higher-order mode strength, motivated our instrumenting HOM detectors for all 10 cavities. In the single-bunch phase for the TESSA test, the short-range wakefields would be a concern so proper on-axis steering of the beam through the 10 cavities is warranted. In the oscillator configuration, the submacro-pulse centroid-slewing effects will also be critical to minimize.

Table 1: Electron Beam Parameters.

Parameter	Unit	Value
Charge	nC	0.5-1.0
Emittance	mm mrad	2-5
Gun energy	MeV	4.5
Beam energy	MeV	220

COTR FORMALISM

Microbunching of an electron beam, or a z-dependent density modulation with a period λ , can be generated by several mechanisms [8]. The laser-induced microbunching (LIM) occurs at the modulator resonant wavelength (and harmonics) as the e-beam micropulse co-propagates through the modulator with the seed laser beam. The energy modulation is converted to a longitudinal modulation by the chicane's small R_{56} term. This is a narrow-band effect. The modulator is a helical undulator with 10 periods 3.2-cm period length.

A microbunched beam will radiate coherently as an FEL or by interaction at a vacuum to metal screen interface as COTR. The first microbunching diagnostics station is located after the chicane as schematically shown in Fig. 2. A thin blocking foil for the seed laser also serves as the source of forward COTR, and this is followed 6.3 cm downstream

CONSIDERATIONS ON WAKEFIELD EFFECTS IN A VUV FELO DRIVEN BY A SUPERCONDUCTING TESLA-TYPE LINAC*

Alex H. Lumpkin[†], Fermi National Accelerator Laboratory, Batavia, IL USA

Henry P. Freund¹, University of New Mexico, Albuquerque, NM, USA

Peter Van der Slot, University of Twente, Enschede, the Netherlands

¹also at University of Maryland, College Park, MD, USA

Abstract

The effects on beam dynamics from long-range and short-range wakefields from TESLA-type cavities are considered in regard to a proposed FEL oscillator (FELO) operating at 120 nm. This would be driven by the Fermilab Accelerator Science and Technology (FAST) linac at 300 MeV with a 3-MHz micropulse repetition rate. Our wakefield studies showed measurable effects on submacropulse centroid stability and on submicropulse head-tail kicks that can lead to emittance degradation. In the case of the former, we use MINERVA/OPC to simulate the $\sim 100\text{-}\mu\text{m}$ centroid slew effects on the saturated output power levels of the FELO.

INTRODUCTION

The electron-beam properties needed for successful implementation of a free-electron-laser oscillator (FELO) on a superconducting TESLA-type linac at the Fermilab Accelerator Science and Technology (FAST) facility include the intrinsic normalized emittance and the submacropulse centroid stability [1]. We have demonstrated that short-range wakefields (SRWs) and long-range wakefields (LRWs) including higher-order modes (HOMs) are generated for off-axis beams in the two, 9-cell capture cavities and eight, 9-cell cavities of a cryomodule in the FAST linac [2-4]. The resulting degradation of the emittance and centroid stability would impact the FELO performance. At 300 MeV and with the 4.5-m long, 5-cm period undulator, the saturation of a vacuum ultraviolet (VUV) FELO operating at 120 nm has previously been simulated with GINGER and MEDUSA-OPC using the non-degraded beam parameters [1]. The measured electron-beam dynamics due to the SRWs (submicropulse, 100-micron head-tail kicks) and HOMs (submacropulse centroid slew of up to 100s of microns) will be presented [2-4]. These are mitigated by steering on axis as guided by the minimization of the HOM signals and beam dynamics effects. Simulations using MINERVA/OPC [5-7] of the effects of a submacropulse centroid slew on FELO performance will also be reported for the first time.

EXPERIMENTAL ASPECTS

The Fermilab Accelerator Science and Technology (FAST) facility includes the superconducting TESLA-type linac [8] which could generate the driving beam at 300

MeV. This would enable an FELO operating at 120 nm. A schematic of the linac is shown in Fig. 1, and the photocathode rf gun, the two TESLA capture cavities operating at about 20 MV/m gradient, the first chicane for bunch compression, the cryomodule (with eight, 9-cell cavities) and the high energy transport line to the location of the FEL experiment are shown. The nominal electron beam properties are given in Table 1. The FELO experiments would be based on the U5.0 planar undulator [9,10] in hand with a 5.0-cm period, tunable magnetic gap, and 4.55-m length as summarized in Table 2. A schematic of the resonator cavity positioned in the high energy transport end of the beamline is shown in Fig. 2. In practice, the second 4-magnet chicane could provide e-beam bunch compression as well as access for the upstream mirror and be placed closer to the D600 dipole with the undulator downstream of this dipole. There is a second dipole, D603 (not shown), that would direct the electron beam off the optical axis and to the high-energy absorber. The 50-m optical cavity round-trip time matches the 3-MHz micropulse repetition rate. The downstream mirror was assumed to have about 80% reflectance at 120 nm, and we would use a 1-mm radius hole outcoupling.

Table 1: FAST Electron Beam Parameters

Parameter	Unit	Value
Charge	nC	0.5-1.0
Emittance norm.	mm mrad	2-5
Gun energy	MeV	4.5
Beam energy	MeV	300

Table 2: Summary of the U5.0 Undulator Parameters [7]

Parameter	Unit	Value
Period	cm	5.0
K value	0.45-3.9
Length	m	4.55
Tunable gap	cm	1.4-2.17
Maximum field at 1.4 cm	T	0.89

Past experiments on wakefield effects in the cavities which are correlated with their HOM signal strength motivated our instrumenting detectors on the HOM couplers for

* Work supported by the U.S. Department of Energy, Office of Science, under Contract No. DE-AC02-06CH11359.

[†] lumpkin@fnal.gov

ACHIEVEMENTS AND CHALLENGES FOR SUB-10 fs LONG-TERM ARRIVAL TIME STABILITY AT LARGE-SCALE SASE FEL FACILITIES

B. Lautenschlager*, M. K. Czwalińska, J. Kral, J. Müller, S. Pfeiffer,
H. Schlarb, C. Schmidt, S. Schulz, M. Schütte, B. Steffen

Deutsches Elektronen-Synchrotron DESY, Notkestr. 85, 22607 Hamburg, Germany

Abstract

A high temporal stability of produced photon pulses is a key parameter for some classes of experiments, e.g., those using a pump-probe scheme. A longitudinal intra bunch-train feedback system, that reduces the intra bunch-train and the train-to-train arrival time fluctuations down to the sub-10 fs level was implemented at the European X-ray free electron laser (EuXFEL). The low arrival time jitter of the electron beam is preserved in the generated photon pulses. However, over long measurement periods, additional environmental factors acting on different time scales have to be considered. These factors include the temperature, relative humidity and in case of the European XFEL ground motions due to ocean activities. Mitigation of the residual timing drifts between pump laser and FEL pulses requires additional measures to disentangle the overlaid effects. The latest results and future challenges for the long-term arrival time stabilization will be presented.

INTRODUCTION

The European XFEL (EuXFEL) is a free electron laser facility with a 2 km long superconducting electron accelerator and a total length of 3.4 km. The facility operates in a 10 Hz burst mode with an RF pulse length of 600 μ s. Each RF pulse can accelerate up to 2700 bunches with the maximum repetition rate of 4.5 MHz. The superconducting radio frequency (SRF) cavities accelerate the electron bunch-trains up to an electron beam energy of 17.5 GeV. Three undulator beamlines can be used to provide photon pulses to the different experiments.

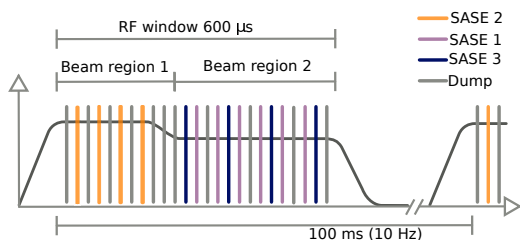


Figure 1: Schematic of the electron bunch distribution to the different SASE beamlines and the dump [1].

A system of slow and fast kickers distributes the electron bunches into the three different undulator beamlines and a dump, see Fig. 1. Photon energies in the range from 0.25 to 25 keV can be provided, using different linac energies

* bjoern.lautenschlager@desy.de

and variable gap undulators. A three stage compression scheme, with the three magnetic chicanes, BC1, BC2, and BC3 can be used to influence the longitudinal parameters, like the compression and arrival time. The RF pulse can be separated into different beam regions, with different RF parameters in amplitude and phase, in order to provide individual compression schemes for the beamlines [2].

A longitudinal intra bunch-train feedback (L-IBFB) adjusts the electron bunch energies in front of a magnetic bunch compression chicane by actuating the preceding accelerator's module amplitude and phase. This introduces an energy dependent path length of the electron bunches through the chicane and thus a change of the arrival time. The bunch arrival time monitors (BAMs) measure the relative arrival time of the electron bunches, with a resolution down to 3 fs [1], against a femtosecond stable optical reference system [3]. The laser based synchronization system is also used to synchronize the lasers in the experimental hutches. An overview of optical reference system can be found in [4].

The low-level radio frequency (LLRF) system controls the 1.3 GHz RF field of the SRF cavities in phase and amplitude. An optical reference module (REFM-OPT) is used to resynchronize the RF phase with respect to the laser pulses, coming from the optical synchronization system, to compensate for drifts in the 1.3 GHz RF reference distribution chain, due to humidity and temperature variations [5]. Different controllers are combined in the LLRF system to achieve the typical RF field stability in amplitude of $\Delta A/A \approx 0.008\%$ and in phase of $\Delta\Phi \approx 0.007$ deg [6, 7]. A second order multiple-input multiple-output controller is used to react within a bunch-train. To minimize repetitive errors from bunch-train to bunch-train a learning feedforward control algorithm is applied. A combination of the measured field information in amplitude and phase and beam-based measurements, e.g., the arrival time, is included in the LLRF control strategy and introduced in [8, 9]. This combination is used by the L-IBFB to stabilize the the electron bunch arrival time below 10 fs (rms) [1].

ARRIVAL TIME MEASUREMENT AND STABILIZATION AT THE EUROPEAN XFEL

A schematic of the EuXFEL facility is shown in Fig. 2. The bunch arrival time monitors provide the arrival time bunch-by-bunch using an electro-optical detection scheme. The electromagnetic field of the electron bunches is captured by four broadband (40 GHz) RF pickups. The induced RF signal is sampled by an ≈ 200 fs laser pulse of the optical ref-

OPTIMIZATION IN THE STRUCTURE OF KLYSTRON DRIVE SIGNAL TO EXTEND RF PULSE FLATTOP LENGTH AT THE EUROPEAN XFEL

V. Vogel, V. Ayvazyan, M. Bousonville, J. Branlard, L. Butkowski, A. Cherepenko, S. Choroba, J. Hartung, S. Goeller, N. Walker and S. Wiesenberg,
Deutsches Elektronen-Synchrotron DESY, Hamburg, Germany

Abstract

Currently 26 RF stations are in operation at the European X-ray Free Electron Laser (XFEL) and all RF stations can deliver sufficient power to reach maximum gradients in the accelerating modules, limited only by cavity and coupler properties. It was demonstrated that by activating a dynamic frequency shift (DFS) of the RF drive signal, the requested klystron power can be reduced by up to 20%, keeping the gradient levels unchanged. Currently, the RF pulse starts when the level of klystron HV reaches 99% of the nominal voltage. If one allows the RF pulse to start at 80% level of the nominal voltage, then the RF pulse length can be increased. The first demonstration of the proposed procedure with the 10MW multi-beam klystrons (MBK) at the klystron test stand and at the XFEL RF stations A10.L3 and A23.L3 will be presented as well. The described procedure can be used both to increase the duration of the RF flat top as well as to shorten the duration of the HV, which could lead to energy savings. In this article we will present a proposal for increasing the XFEL RF pulse flattop length using phase and amplitude compensation during the rise and fall of the HV, as well as applying DFS when filling the cavities of the accelerator.

INTRODUCTION

Currently, XFEL has three laser lines, each of which requires a specific electron beam parameter set for better lasing [1]. The transition between different beam region cannot be done instantly, as it needs some time to change energy and phase in several accelerator modules. At the moment the high voltage (HV) pulse has a length of 1.7 ms and the RF pulse a length of 1.4 ms, out of which only 0.6 ms can be used for the beam acceleration. The level of klystron output power is 15% below the saturated power to provide margin for feedback regulation. The optimization of the klystron drive signal can help increase the length of beam time without touching other accelerator parameters. Keeping the design klystron power level and using DFS can reduce the filling time up to 10%. We can get another 20% if the RF pulse starts at the 80% level and stops at 70% of nominal HV. The phase change and lower power during the rise and fall of the HV need to be compensated. The result is a longer RF pulse flattop which can be used to accelerate a longer beam pulse.

KLYSTRON DYNAMIC FREQUENCY SHIFT

When a cavity is filled with electromagnetic field the cavity surfaces are under pressures known as Lorentz forces. These pressures in the case of standing wave are

proportional to the square of the surface electric and magnetic fields as in [2]:

$$P_{sw} = 0.25 (\epsilon_0 E^2 - \mu_0 H^2). \quad (1)$$

The resulting cavity detuning is therefore proportional to the accelerating field squared:

$$\Delta f = -KE_{acc}^2. \quad (2)$$

For the TESLA type superconducting cavities (SC), the typical Lorentz force detuning constant K is about $0.9 \text{ Hz}/(\text{MV}/\text{m})^2$. To keep the phase and amplitude stable during RF flattop, piezoelectric actuators are used [3][4]. The piezoelectric actuators induce mechanical cavity deformations that compensate the effect of Lorentz detuning during RF flattop. In [5] and [6], a procedure for changing of the klystron frequency during filling time was proposed. This procedure was later named DFS and tested at FLASH. The main idea of DFS is to keep the klystron frequency during filling time matched to the cavity frequency, by modulating the klystron phase:

$$\varphi(t) = \Delta\varphi(G) \left(1 - e^{-\frac{t}{\tau(G)}}\right). \quad (3)$$

where $\Delta\varphi$ is the initial phase offset that depends on cavity gradient, τ is the mechanical time constant that also depends on cavity gradient, and G is cavity gradient.

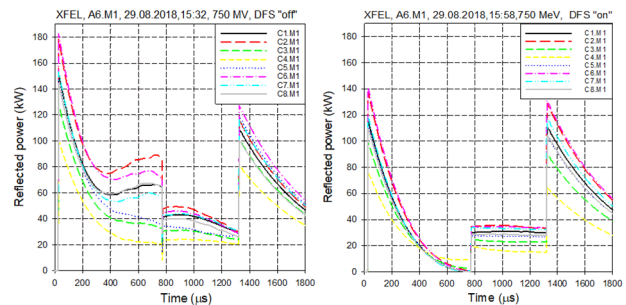


Figure 1: Effect of DFS on reflected power from cavities.

The formula Eq. (3) is not an exact solution for the single cavity, but it gives enough good results for the sum of 32 different cavities fed by one klystron. For the XFEL TESLA type of cavities with filling time of $750 \mu\text{s}$ and gradient about $20 \text{ MV}/\text{m}$, $\Delta\varphi = -55$ degrees, and the time constant is about $230 - 320 \mu\text{s}$. With the optimization of the cavity filling procedure, the reflected power was reduced significantly, allowing the cavity gradient to be increased or the cavity filling time shortened, with the same level of forward RF power. Figure 1 shows the impact of DFS on the reflected power from the cavities.

RF COMMISSIONING AND FIRST BEAM OPERATION OF THE POLARIX TRANSVERSE DEFLECTING STRUCTURES IN THE FLASH2 BEAMLINE

M. Vogt*, J. Rönsch-Schulenburg, S. Schreiber, and F. Christie¹
Deutsches Elektronen-Synchrotron DESY, Hamburg, Germany
¹now at TNG Technology Consulting GmbH, Unterföhring, Germany

Abstract

In January 2021 two X-band (12 GHz) PolariX Transverse Deflecting Structures with variable streak polarization were installed into the FLASH2 beamline at FLASH. Since none of the RF components for the FLASH2-PolariX RF-distribution system nor the two PolariX structures could be pre-conditioned, RF-conditioning was and is quite tedious. Nevertheless, after 6 weeks of conditioning, we have already been able to streak the electron beam enough to start commissioning of the PolariX controls and the software. After 4 months of conditioning in parallel to FLASH2 user operation, we achieved a stable 5.5 MW flat top of 400 ns operation. Next step will be to include RF pulse compression to achieve the design power of 22 MW.

INTRODUCTION

FLASH [1–5] at DESY (Hamburg, Germany) is a free-electron laser (FEL) user facility. FLASH consists of a normal-conducting photo-injector, and a superconducting linac. The superconducting LINAC can accelerate several thousand electron bunches per second in 10 Hz bursts of up to 800 μ s length. The long bunch trains are split in two parts and are shared between two undulator beamlines. FEL radiation can be generated with the SASE (Self Amplified Spontaneous Emission) process and fundamental wavelengths ranging from 4 nm to 90 nm. In addition, FLASH hosts a seeding experiment Xseed [6], and a plasma wakefield acceleration experiment FLASHForward [7]. In order to keep FLASH a state-of-the-art FEL user facility, an upgrade project “FLASH2020+” is on-going [8–10], which includes an upgrade of the longitudinal diagnostics. Optimizing the performance of an FEL requires a precise knowledge of the longitudinal phase space distribution of the bunch. Transverse deflecting structures (TDSs) enable high resolution, direct measurement methods to determine the longitudinal properties of the bunch and allow to measure transverse-to-longitudinal correlations (centroid shift, mismatch, emittance, etc.) in the plane perpendicular to the streaking plane. The RF structures support an Eigenmode with a transverse electric field component, thereby deflecting electrons within the bunch transversely depending on the arrival time in respect to the RF wave. High amplitudes of the electric field and high RF frequency both improve the resolution. A collaboration between CERN, PSI and DESY has been established to develop and build an advanced modular X-band

TDS [11, 12]. The PolariX is an X-band (12 GHz) TDS with the new feature that the polarization of the transverse electric field can be varied by tuning the phase difference between two perpendicular in-coupling ports of the structure. This allows the measurement of the longitudinal distribution of emittance and mismatch in both transverse planes and even, to some extent, phase space tomography [13].

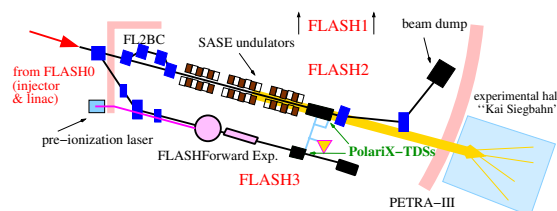


Figure 1: Schematic view of the FLASH2/3 beamlines with the 2+1 PolariXes and the shared X-band RF transmitter. Not to scale.

The prototype PolariX structure was installed in an optimized diagnostic section of the FLASHForward experiment in 2020 [14]. The prototype was pre-conditioned at CERN and some RF equipment could be pre-conditioned at a test assembly of klystron and modulator at DESY. In the winter shutdown 2020/2021 a system of two short (0.8 m long) PolariX-structures was installed in FLASH2 [15, 16]. Figure 1 gives a schematic overview of the layout of the FLASH2/3 beamlines and the installed PolariX system. In FLASH2 the RF structures were installed 2.0 m downstream of the end of the last SASE undulator and 2.40 m upstream, of the 3.5°-dipole separating the electron beam from FEL beam¹. Any single bunch in the standard 1 μ s timing pattern can be kicked onto a screen located 5.5 m downstream of the separator dipole. Immediately downstream of the PolariX section the beam of potentially several thousand bunches per second and a maximum beam power of 100 kW has to be prepared to be safely dumped. This set up is not optimal since there is not enough space for many quadrupoles *and* sufficient phase advance between them to achieve the wanted high temporal and energy- resolution with the streak from only one standard PolariX structure. However, with two PolariXes and a carefully designed beam optics this set up allows to measure the shape of the complete longitudinal bunch phase space distribution with temporal resolutions in the sub-10 fs range and supplies sufficient energy resolution

* vogtm@mail.desy.de

¹ Positions refer to *center* positions unless otherwise noted.

OPTIMIZATION AND FINE TUNING OF MACHINE PARAMETERS WITH MODEL-LESS ALGORITHM

F. Tripaldi, F. Galassi and G. Gaio, Elettra Sincrotrone Trieste, Trieste, Italy

Abstract

Despite the use in machine physics of high-performance software for calculating and predicting machine parameters, when these are applied to the real world, additional operating point search is often necessary to obtain the desired performance.

Furthermore, small configuration changes required by FEL users during running experiments, lead to search new optimal working points in a short time.

Use of tools based on model-less algorithms such as Nelder-Mead and 1D or 2D scans allow the automatic and online search for the best fine setup of machine and FEL parameters in short times.

The development of MIMOFB (Multi Input Multi Output Feedback) software used as optimizer with model-less algorithms has provided a versatile tool that can be applied in many situations.

The ability to concatenate optimizations with pre-programmed batch executions allows to develop complex optimization strategies and iterate them by refining algorithm's parameters.

At FERMI MIMOFB optimizers are currently used with good results for fine-tuning the electron beam magnetic optics and trajectory, by acting on the current of quadrupoles and correctors magnets for FEL signal optimization and terahertz parasitic signal maximization.

INTRODUCTION

A high-level software allowing to control the spatial and temporal overlap of the laser seed and electron beams in the undulator chain is currently in use at FERMI [1]. A good strategy to maintain the long-term stability of the FEL signal consists in minimizing the correlation between the FEL intensity itself and several machine parameters, acquired on the shot-to-shot basis [2, 3].

At the same time, stochastic optimization algorithms (SO) are strictly integrated into the trajectory feedback loops; they change at each shot the feedback set points, acquires sensors and actuators and couples them with the objective function [2, 3].

Until now, no optimization strategy had been implemented for the optimization of the electron transport and confinement magnetic optics.

The ultimate goal is to apply algorithms to optimize the FEL performance by tuning the electron-beam trajectory and the machine optics along the undulator chain. The optimization algorithms implemented in the tool developed at FERMI (called MIMOFB), were initially tested on a sim-

pler case, regarding the optimization of the THz signal generated by the exhausted electrons after the FEL line and transported to the TeraFERMI beamline [4]. After a brief introduction about the MIMOFB, we show the successful optimization of the TeraFERMI signal acting on the quadrupoles and steerers placed in the FERMI's main beam dump line. In the second part, we show how the MIMOFB can be used to improve the FEL intensity acting on the quadrupoles along the FEL undulator chain.

The optics matching procedure, which imposes the design values of the Twiss functions to the electron beam, is performed with dedicated tools that were developed during the FERMI commissioning and improved over time [5, 6].

However, although the emittance and Twiss parameter calculation tools are increasingly advanced and precise, their results depend significantly on the quality of the input data. These are represented in FERMI by electron beam sizes measured through the scan of quadrupole currents, from the analysis of CCD cameras images at various machine points. This kind of measurement is affected by many variables which are affected by systematic errors, non-standard procedures and settings that can compromise the reproducibility and the reliability of the measurement itself.

Similarly, small but significant last-minute changes to the machine configuration, for example due to changed required by the beamline running the experiment, require to optimize the new setup as quickly as possible.

MIMOFB AS OPTIMIZER

Starting from the aforementioned requirements and exploiting the experience gained on the Elettra synchrotron [7], we implemented the MIMOFB on FERMI, as optimizer based on mode-less algorithms (Nelder-Mead) [8]. In particular, we focused on the optimization of the electron beam optics in the spreader common line (SFEL1) and along the undulators (IUFEL1) to maximize the FEL intensity, and in the main beam dump (MBD) line to maximize the TeraFERMI signal.

Differently from the Elettra, MIMOFB optimization in FERMI has been configured adding some constraints. This is done by introducing another set of dedicated sensors with a very low weighting coefficients ($1e-6$) such as they do not impact significantly final objective function [7], but act as thresholds during optimization process.

This implementation was necessary for example because the control of the charge losses before the end of the elec-

VIRTUAL DIAGNOSTIC FOR LONGITUDINAL PHASE SPACE IMAGING FOR THE MAX IV SXL PROJECT

J. S. Lundquist*, S. Werin, F. Curbis, Department of Physics, Lund University, Lund, Sweden

Abstract

Accurate and high resolution detection of the Longitudinal Phase Space (LPS) of the electron beam is a great advantage for operating and setting up a FEL. In the case of the soft X-ray FEL being proposed at the MAX IV synchrotron facility in Lund, this information will mainly be supplied by a Transverse Deflecting Cavity (TDC) which is currently being installed and scheduled for commissioning in the autumn (2022). Performing the LPS measurement with the future TDC is limited in two regards: it is destructive and may be low in resolution as compared to the maximum compression possible in the MAX IV linac. In this project we propose using machine learning tools to implement a virtual diagnostic to retrieve the LPS information non-destructively using fast, non-invasive measurements and critical set-points in the linac as inputs for a neural network. In this paper we summarize the current progress of this project which thus far has focused on simulation studies of the TDC and the training of a virtual diagnostic using the TDC's simulated output.

INTRODUCTION

The Soft X-ray Laser (SXL) is a free electron laser currently being proposed as an expansion to the existing synchrotron light facility MAX IV in Lund, Sweden. The SXL is designed as an extension to the operating linac, currently used to drive two electron storage rings as well as a Short Pulse Facility (SPF). The SPF currently hosts only one end-station (FemtoMAX), but two more beamlines are currently planned as new branches at the end of the linac. One is the SXL, where the beam will pass through a 156 m long undulator hall before reaching two experimental end-stations; the other line is reserved for a Transverse Deflecting Cavity (TDC). This is a diagnostic beamline, meant to produce new information of the state of beam, useful for operating the SXL. Figure 1 shows a detailed layout of the MAX IV linac with these proposed beamlines present. The TDC line operates by allowing the beam to pass through a particular accelerating structure which kicks the beam transversely, in order to turn it, in this case horizontally. This allows for a longitudinal image of the beam as it impacts on a screen further down the beamline. One can also pass the beam through a dipole magnetic field before the screen to retrieve information of the energy distribution of the beam. With these two techniques used in tandem one can get a full image of the Longitudinal Phase Space (LPS) of the beam, crucial information for operating the SXL optimally [1].

As the TDC requires the beam to impact on a screen this measurement is destructive and can not be performed in par-

allel with studies at the SXL beamlines. A non-destructive tool for extracting the same diagnostic information is thus highly attractive. For this project, the possibility of using Machine Learning (ML) methods to develop a virtual diagnostic monitoring this information is being investigated. The virtual diagnostic in this case would interpret non-destructive signals from the entire linac and then produce predictions of the TDC image without interacting with the beam. If this can be achieved with high reliability and accuracy, the operations of the current linac and the future SXL could be significantly improved. Similar projects have shown promising results [2, 3].

In this paper, the early strides of this project are summarized. This includes two main results: predictions of the TDC output based on simulation data and predictions of the beam's transverse image in a dispersive section of the linac based on real data collected during study time on the accelerator. These are referred to as the *simulated* and *experimental* case respectively. The following two sections will go into more detail on the simulation and experiment performed to generate the data used in training the constructed virtual diagnostics, followed by a section covering the machine learning methods used in the virtual diagnostic itself.

DATA COLLECTION

A crucial early step is finding the input channels one could possibly use for training the ML structures. For this project, we require non-destructive, fast measurements which are also correlated to the result of the destructive measurement of the TDC, i.e., they should have a strong dependence or influence on the energy and temporal distribution of the final beam. Below in Table 1 a summary of the different input channels selected, both for the simulation and experimental case, can be seen. Here, L01 refers to a specific early accelerating structure separated from the remainder of the linac by a bunch compressor, L02-19 are then referring to the rest of the 18 accelerating structures which have synchronized setpoints for phase and voltage.

These setpoints were then used as input to different ML structures, either outputting images, or scalar values for the position of the beam centroid. The following two subsections summarize the methods for procuring the data through simulation and experiment.

Simulation

The accelerator simulation code elegant was used for the simulations of the TDC output. Scans were performed of the RF parameters summarized in Table 1, at first systematically to find the limits in each channel, then using 1000 random setpoints from the tested range to produce the final dataset.

* johan.lundquist@maxiv.lu.se

DEVELOPMENT OF THE RF SYSTEMS FOR THE PoFEL ACCELERATOR*

J. Szewiński[†], P. Bartoszek, K. Chmielewski, K. Kostrzewa, T. Kowalski, P. Krawczyk, R. Nietubyc, D. Rybka, Z. Wojciechowski, National Centre for Nuclear Research, Otwock-Świerk, Poland

Abstract

PoFEL stands for Polish Free Electron Laser, the first FEL research infrastructure in Poland. This facility is under development, and it will operate in three wavelength ranges: IR, THz and VUV, using different types of undulators. Machine will be driven by 200 MeV linear superconducting accelerator, which will operate in both, pulsed wave (PW) and continuous wave (CW) modes. This contribution will describe the concept, current status and the first results of the RF systems development.

INTRODUCTION

PoFEL will be a 4-th generation light source, based on the 200 MeV superconducting linear accelerator [1]. It will generate coherent light in 3 ranges: THz, IR and VUV.

To deliver proper beam conditions, a stable RF field is required in the accelerator cavities, and to achieve this, a high-power and low-level RF systems are required. PoFEL accelerator will be driven by a solid state amplifiers, in the single cavity regulation mode where one cavity will be driven by one amplifier. For such control mode, vector sum calculation is not needed, which simplifies the the RF control system in comparison to such Free Electron Lasers such as X-FEL or FLASH.

To simplify the LLRF system even more, a direct sampling technique is planned to be implemented in PoFEL [2]. This technique reduces the need for the separate devices such as downconverters and LO generation modules. The key part of the direct sampling LLRF system will be the clocking solution for the ADCs, but since the whole clock tree will be integrated into the ADC board, it can be optimized for this particular application.

HIGH POWER RF SYSTEM OVERVIEW

The aim of the RF system is to deliver power to accelerating modules which is needed to accelerate the electron beam. The accelerating modules of in PoFEL accelerator will be made of TESLA-type, 9-cell RF Structures. Each criomodule will have two such RF structures, but each structure will be driven and controlled individually. RF power from solid state amplifiers to the criomodules will be delivered using WR650 waveguides. Solid state amplifiers will be placed in the hall next to the accelerator tunnel. Because construction of PoFEL accelerator will utilize existing buildings, the design of the waveguides distribution system is not straight-forward and requires significant effort.

* Work supported by National Information Processing Institute, <https://opi.org.pl/>

[†] J.Szewinski@ncbj.gov.pl

Table 1: SSA Key Parameters

Parameter	Value
Lower frequency range (-3dB)	≤ 1270 MHz
Upper frequency range (-3dB)	≥ 1310 MHz
Output power in pulsed mode	≥ 7 kW
Maximal pulse duration	≥ 1 ms
Output power in continuous mode	≥ 5 kW
Maximal power of input signal	≥ 10 dBm
Amplifier gain	≥ 60 dB
Max. required power supply level	≤ 20 kW
Operational temperature range	$5^\circ\text{C} - 40^\circ\text{C}$

One of the features that helps in the waveguide design is single cavity regulation mode. Because of this, there is no need for splitting the RF power within the waveguide distribution system. Each waveguide will deliver RF power directly from the solid state RF amplifier to the RF structure. In such configuration, circulators and loads does not have to be placed close to the criomodules and can be placed next to the RF amplifiers out of radiation impact area, which also helps in the design.

Solid State Amplifier

The RF power in the PoFEL accelerator will be generated by solid state amplifiers (SSA). Because of PoFEL will operate in continuous mode a dedicated RF power source is needed. Dedicated RF amplifier for PoFEL will be designed and delivered by the Kubara Lamina S.A. company [3]. The requirements for the RF amplifier are following show in Table 1.

By the time of writing this paper, the prototype of the SSA amplifier was under development (Fig. 1).

LOW-LEVEL RF SYSTEM OVERVIEW

High speed and high bandwidth ADCs makes possible to sample directly the RF signal of the frequency 1.3 GHz. Well known and also evaluated [4,5] for this purpose is Texas Instruments ADS5474, which input bandwidth covers range up to 1.4 GHz. Possibility of direct RF sampling allows to significantly simplify the LLRF hardware.

The components of the PoFEL LLRF system are similar to the ones used at X-FEL [6] because of the same fundamental frequency 1.3 GHz, but the layout of the system is more like the one used at ESS [7], because ESS operates also in single cavity regulation mode.

LLRF system scheme in the Fig. 2 show the configuration used at ESS. Configuration used at ESS for controlling

RF CONDITIONING AND FIRST EXPERIENCES WITH THE PolariX TDS AT PSI

P. Craievich*, J. Alex, C. Beard, H.-H. Braun, M. D'Amico, R. Fortunati, R. Ganter,
Z. Geng, R. Kalt, T. Kleeb, T. G. Lucas, F. Marcellini, R. Menzel, M. Pedrozzi,
E. Prat, S. Reiche, W. Tron, R. Zennaro
Paul Scherrer Institut, Villigen-PSI, Switzerland

Abstract

In 2017, a collaboration between DESY, PSI and CERN was established with the aim of developing and building seven advanced X-Band Transverse Deflection Structures (TDS) with the novel feature of a variable polarization of the deflecting force. Seven deflectors were produced by PSI, of which, five were installed in three experiments at DESY while the remaining two were installed in the ATHOS soft X-ray beamline in SwissFEL. The ultimate goal of this project was to provide sub-fs resolution for soft X-ray pulse profiles. In early 2022, the X-band power source of the TDS for SwissFEL was completed and system commissioning began. This contribution summarizes the first deflection experiments performed.

INTRODUCTION

Several experiments at DESY (FLASH II, FLASHForward, SINBAD) and PSI (ATHOS at SwissFEL) were interested in the utilization of high gradient X-band Transverse Deflection Structure (TDS) systems for high resolution longitudinal diagnostics. In this context, a collaboration between DESY, PSI and CERN was established to develop and build an advanced modular X-Band TDS system which included the novel feature of providing variable polarization of the deflecting force. This structure was aptly named the Polarizable X-band (PolariX) TDS [1, 2]. In recent years, seven deflectors were built in total and installed at the various facilities. Currently, the two deflectors in FLASH II and the one FLASHForward are routinely used in operation while the two installed in SINBAD are ready for commissioning as soon as the RF system will be available. The remaining two were installed in the post-undulator diagnostic section in the ATHOS soft X-ray beamline at SwissFEL [3, 4], with the aim of providing sub-fs resolution for soft X-ray pulse profiles. In early 2022, the X-band power source for the TDS in ATHOS was completed and commissioning of the whole TDS system has begun. This contribution summarizes the progress of the project at PSI, including the results from the first month of RF conditioning and the first set of experiments performed with variable polarization.

THE PolariX TDS SYSTEM

The SwissFEL project at PSI consists of a 6 GeV accelerator facility feeding two undulator beamlines, Aramis [5]

* paolo.craievich@psi.ch

Table 1: RF parameters for two PolariX TDSs installed in ATHOS. The frequency corresponds to operational temperatures of 33.3° and 32.5° for the TDS1 and TDS2, respectively.

Cell parameter		Unit
Frequency	11995.2	MHz
Phase advance/cell	120	°
Iris radius	4	mm
Iris thickness	2.6	mm
Group velocity	-2.666	c/c
Quality factor	6490	
Shunt impedance	50	MΩ/m
1x TDS parameter		Unit
n. cells	120	
Filling time	129.5	ns
Total length	1160	mm
Power-to-voltage	6.1	MV/(MW) ^{1/2}
2x TDS + BOC		Unit
BOC Q ₀	157800	
BOC β	7.88	
RF pulse width	1.5 1.0	μs
Power-to-voltage	19.1 17.7	MV/(MW) ^{1/2}

and Athos [3, 4], operating in parallel at 100 Hz. The Athos line consists of a fast-kicker magnet placed at a beam energy of 3.2 GeV, a dog-leg transfer line, a small linac, and 16 APPLE X undulators [6]. It is designed to operate in advanced modes of operation slightly different from standard SASE operation and produce soft X-ray FEL radiation with pulse durations ranging from a few to several tens of femtoseconds [7]. Electron beam diagnostics based on a TDS system placed downstream of the undulators (post-undulator TDS) in conjunction with an electron beam energy spectrometer can indirectly measure the pulse length of these ultra-short photon pulses by analysing the induced energy spread on the electron bunch due to the FEL process.

Figure 1 shows a schematic layout of the ATHOS post-undulator diagnostic section. Beam slice emittance in both transverse planes are investigated by a multi-quadrupole scan technique combined with the TDS. By means of the TDS, the beam is vertically and horizontally streaked and a multi-quadrupole scan is performed in the horizontal and vertical direction, respectively, with the constraint of keeping the vertical/horizontal beam size constant over the whole scan. For this purpose, five quadrupoles were foreseen to be placed downstream of the TDS. Reconstruction of the longitudinal

SHORT PERIOD APPLE-X UNDULATOR MODELING FOR THE AQUA LINE OF THE FUTURE EuPRAXIA@SPARC_LAB FACILITY

A. Petralia^{1*}, M. Carpanese¹, M. Del Franco², A. Doria¹, F. Nguyen¹, L. Giannessi², A. Selce¹

¹ENEA Fusion and Technology for Nuclear Safety and Security Department,
R.C. Frascati, Frascati, Italy

²INFN Laboratori Nazionali di Frascati, Frascati, Italy

Abstract

The study for a short period Apple-X variable polarizing undulator is presented, with small gap of operation and high magnetic field. This will be the base module for the AQUA line of the EuPRAXIA@SPARC_LAB FEL facility, of next realization at the INFN Laboratory of Frascati. The undulator allows to achieve radiation between 3.5 and 6 nm with a 1 GeV electron beam energy, lower than other FELs operating in the world, so giving the possibility to have a Soft X-ray source with a full polarization control in a more cost effective way and with less required space than the state of the art devices. An overview of the magnetic design is given with the main parameters and performances in terms of the field properties, tuning capabilities and the effects on the electron beam motion.

INTRODUCTION

In the recent years some efforts have been done on research and experimentation on the possibility of using plasma accelerators to pilot Free Electron Lasers (FELs) [1]. The possibility to accelerate electron beams over short distances using plasma-based technology has the potential for a revolution in the field of particle accelerators. The much more compact nature of plasma-based accelerators would allow the construction of much smaller and therefore much less expensive machines capable of operating a FEL. Recently, some first experimental demonstrations have been obtained that encourage to continue on this path [2,3] (see also M. Galletti and M. Labat talks, these proceedings). In this direction the European project EuPRAXIA goes, aiming at the realization of the first user FEL machine driven by plasma accelerator [4]. In this context, a study and design work is in progress at the INFN National Laboratories of Frascati (INFN LNF), with the participation of the ENEA undulator experts, for a compact FEL piloted by an X-band RF accelerator but which also provides for the presence of a plasma acceleration stage, for a final maximum beam energy of 1 GeV. This machine, namely EuPRAXIA@SPARC_LAB [5], will be a user facility and two FEL lines are foreseen. The first one is a SASE FEL line, called AQUA, and will produce radiation at $\lambda = 4$ nm in the spectral region of the so called "water window" (see F.Nguyen poster, these proceedings). The second, called ARIA, will be a seeded FEL line operating in the wavelengths range 50-180 nm (see M. Opromolla poster, these proceedings). Regarding the AQUA line, the

value of the beam energy ($E = 1$ GeV) and the desired resonance require to have an undulator with short period λ_u and a magnetic peak field B that gives a value $K_{rms} \approx 1$ for the undulator deflection parameter, according to the FEL resonance formula

$$\lambda = \frac{\lambda_u}{2\gamma^2} (1 + K_{rms}^2) \quad (1)$$

being m_o and c respectively the rest mass of an electron and the speed of light and $\gamma = E/m_o c^2$ is the Lorentz factor. Furthermore the polarization control of the emitted radiation is desired, varying from Linear (LP) to Circular (CP) passing through all intermediate levels. For these reasons, the best choice is the use of an Apple-X type undulator. Starting from the initial scheme proposed in [6], in the last few years some Apple-X undulators have been made or are under construction [6–8]. Thanks to its geometry, the Apple-X allows to fit the required parameters for the EuPRAXIA@SPARC_LAB FEL operation. In addition, the characteristics of this type of undulator are such that the resonance wavelength and the tuning range are the same for all polarization setting.

UNDULATOR DESIGN

The undulator under development for AQUA has a much shorter period than other Apple-X built so far. The choice of the period is determined by the desired resonance wavelength with an energy beam equal to 1 GeV but also to have a good compromise between the tuning range and the value of the saturation length which has to be less than 30 meters (including beam optics), being this the maximum available space for the undulator line. For these reasons, the value $\lambda_u = 18$ mm is chosen for the undulator period. The value $K_{rms} = 0.8$ for the undulator parameter is hence required for the operation at 4 nm, according with Eq. (1).

The undulator structure is made of four Neodymium-Iron-Boron (NdFeB) permanent magnet blocks with octagonal shape with a magnetization at 45° and a remanent field $B_r = 1.35$ T, with a locking thoot to fix the block magnets to the holder. The magnets are disposed radially at equal distance around the electron beam axis. The resultant square hole in the centre of the structure allows the installation of a 5 mm external diameter vacuum pipe for the propagation of the electrons. Longitudinally we have four blocks per period arranged according to the Halbach configuration. The minimum achievable gap is settled as 1.5 mm, being this a good compromise between the maximum wanted magnetic field value (and hence the maximum K), and some constructive

* alberto.petralia@enea.it

DESIGN OF THE SUPERCONDUCTING UNDULATOR FOR EUPRAXIA@SPARC_LAB*

C. Boffo†, M. Turenne, Fermi National Accelerator Laboratory, Batavia, IL, USA

F.Nguyen, A. Petralia, ENEA-Frascati, Frascati, Italy

L. Giannessi, INFN-Laboratori Nazionali di Frascati, Frascati, Italy

Abstract

EuPRAXIA@SPARC_LAB is a new Free Electron Laser (FEL) facility that is currently under construction at the Laboratori Nazionali di Frascati of the INFN. Fermilab is contributing to the project with the design, manufacturing and qualification of a prototype conduction cooled superconducting undulator (SCU) that, if successful, could be integrated in the final machine.

The design of the SCU capitalizes on the extensive experience present at Fermilab on cryomodules. Specifically, the system is based on the warm strongback concept developed for the PIP-II project which enables a modular design with multiple undulator coils integrated in a single vacuum vessel. Here we focus on the overall design concept of the magnet system, its modularity, cost reduction potential and industrialization strategy.

INTRODUCTION

The INFN-LNF Laboratory is developing EuPRAXIA@SPARC_LAB [1], a 1 GeV compact light source facility directly driven by a plasma accelerator, which represents the first phase of the EuPRAXIA European project [2].

According to the present design, the machine will include two Free Electron Laser (FEL) beamlines, AQUA and ARIA. AQUA is a Self-Amplified Stimulated Emission (SASE) line with a 4 nm target wavelength. While the baseline for AQUA foresees the use of Apple-X permanent magnet undulators, superconducting undulators (SCU) could provide an advantage in terms of tunability and flexibility during machine operation. Fermilab is designing EuSCU16, a 16 mm period length SCU, aiming to demonstrate that this technology is mature for integration in a FEL user facility.

UNDULATOR SPECIFICATIONS

The main specifications for EuSCU16 required to meet the operating parameters of the AQUA beamline are summarized in Table 1. At present, SCUs installed in user facilities are stand-alone units cooled by means of cryocoolers, either utilizing a thermosiphon or a conduction cooling cryogenic scheme [3]. While this prototype includes only a single magnet array, its modular design allows for future expansions and installation of multiple units in a single

vacuum vessel as it is typically performed in cryomodules for both superconducting RF and accelerator magnets.

Table 1: EuSCU16 Specifications

Parameter	Value	Units
Period	16	mm
Beam stay clear	5	mm
FEL wavelength	4	nm
Peak field on axis at 5 mm beam stay clear	1.5	T
Cooling medium	Cryocoolers	-
Magnet length	1.2	m
Vacuum vessel length	< 1.5	m
Cooldown time	< 7	days
Operating temperature	≤ 4.2	K

In addition, the cryogenic scheme can be adapted to include liquid helium piping to support operation of multiple vacuum vessels in series connected to a cryogenic plant.

ELECTROMAGNETIC DESIGN

The geometry of the period and the choice of superconductor are the core SCU design elements with impact on performance. EuSCU16 uses a commercially available 0.5 mm by 0.7 mm (bare) NbTi rectangular enamel-insulated strand that is continuously wound without joints throughout each array. The rectangular shape was chosen to maximize the engineering current density within the winding packages.

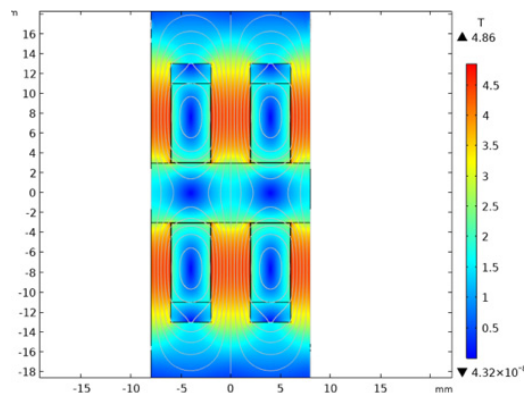


Figure 1: Electromagnetic design of the one period of EuSCU16. A peak field of 4.86 T is reached in the soft iron former at operating current of 500 A. Peak field on axis is 1.5 T.

* This work was produced by Fermi Research Alliance, LLC under Contract No. DE-AC02-07CH11359 with the U.S. Department of Energy.

† crboffo@fnal.gov

BEAM BASED ALIGNMENT OF A SEEDED FEL

E. Allaria[†], A. Brynes, B. Diviacco, L. Giannessi¹ and C. Spezzani

Elettra-Sincrotrone Trieste S.C.p.A. Trieste, Italy

¹also at INFN LFN, Frascati, Roma, Italy

Abstract

Optimal FEL gain in a seeded FEL requires the careful alignment of different components. As for SASE FELs, the gain is optimized when the electron bunch travels in a straight line along the axis of each undulator in the radiator section. We have recently developed an alignment strategy for the optimization of the FERMI FELs which combines the beam-based alignment of the magnetic elements (undulators and quadrupoles) with the collinear alignment of spontaneous emission from each undulator. The method is divided into 3 steps. In the first step, we measure the undulator spontaneous emission with a spectrometer to fine-tune each undulator gap and set the best electron beam trajectory for collinear emission of each module. In the second step, the alignment of the undulator axis on the electron trajectory previously defined is achieved by looking at the undulator focusing effect. Finally, the seed laser is superposed on the electrons and aligned to maximize the bunching along the defined direction. This procedure can lead to an improvement in the control over the electron beam trajectory and results in a more efficient FEL process characterized by more stable and larger energy per pulse and a cleaner optical mode. A description of the method with the obtained results are reported in this work.

INTRODUCTION

High gain single pass Free Electron Lasers such as FERMI [1] rely on the energy exchange between the electron beam and the FEL radiation occurring along a long radiator (~ 100 m) composed of several undulators. To optimally couple the electrons to the radiation several conditions need to be satisfied:

1. Electron trajectory should be straight;
2. Resonance condition to the FEL wavelength should be met in each undulator;
3. Undulator need to be aligned to the electron beam axis.

In case of seeded FEL such as FERMI it is also required that:

4. the seed laser is aligned to the same electron beam axis.

Due to the strong interplay between these conditions, it is required to establish a procedure that allows to individually adjust each of them. It has been observed that the emission mode of a seeded FEL is strongly affected by the pointing of the seed laser [2]. With the procedure recently implemented at FERMI the first 3 points are cured before the seed laser is aligned.

[†] enrico.allaria@elettra.eu

DEFINING THE BEAM TRAJECTORY

FEL pulses produced by both FEL lines at FERMI can be characterized using the PADReS setup [3,4] accounting various optical elements and diagnostic including a spectrometer and various FEL profiles relying on YAG screens and CCD (Figure 1).

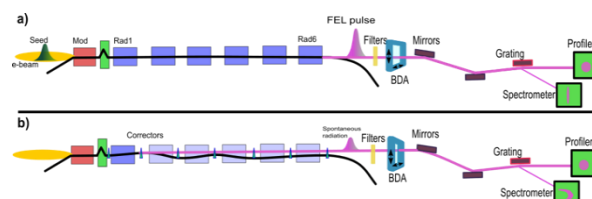


Figure 1: FEL-1 line and the used devices for the characterization of the FEL (top) and for the trajectory alignment procedure (bottom).

To define the straight trajectory on the long radiator, we use PADReS diagnostic on the spontaneous emission produced by the electron beam on a single undulator tuned at the desired wavelength while other undulators are open.

The PRESTO spectrometer collects the light dispersed in the horizontal plane by means of a diffraction grating onto a 2D detector, providing simultaneously the spectral distribution of the source (horizontal projection) and its intensity profile (vertical projection).

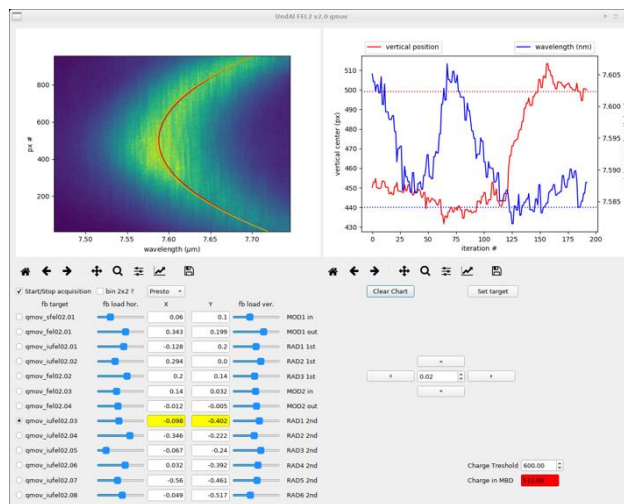


Figure 2: GUI used to monitor the evolution of the spontaneous emission mode while changing the trajectory in the resonant undulator.

DEVELOPMENT OF A PHOTOELECTRON SPECTROMETER FOR HARD X-RAY PHOTON DIAGNOSTICS AT THE EUROPEAN XFEL

J. Laksman*, F. Dietrich, J. Liu, Th. Maltezopoulos, M. Planas, W. Freund, R. Gautam, N. Kujala, S. Francoual¹, J. Grünert
European XFEL, Schenefeld, Germany

¹also Deutsches Elektronen-Synchrotron DESY, Hamburg, Germany

Abstract

We developed an angle-resolved photoelectron spectrometer, based on the electron time-of-flight concept, for hard X-ray photon diagnostics at the European Free-Electron Laser. The instrument shall provide users and operators with pulse-resolved, non-invasive spectral distribution diagnostics, which in the hard X-ray regime is a challenge due to the poor cross-section and high kinetic energy of photoelectrons for the available target gases. We report on the performance of this instrument as obtained using hard X-rays at the PETRA III synchrotron at DESY. We demonstrate a resolving power of 10 eV at incident photon energies up to 20 keV.

INTRODUCTION

The unique properties of X-ray Free-Electron Laser (XFEL) radiation offering high-intensity and coherent X-ray pulses at Ångström wavelengths have found applications where the ability to take snapshots of samples at unprecedented molecular length and time scales provides new scientific insights. However, the stochastic nature of Self-Amplification of Spontaneous Emission (SASE) has the consequence that every photon pulse displays individual characteristics in terms of spectral distribution and intensity. At the European XFEL (EuXFEL) facility in Schenefeld, Germany, the X-ray photon diagnostics group (XPD) utilizes a variety of dedicated techniques for providing beam parameters [1]. For soft X-rays, the angle-resolved Photo-Electron Spectrometer (PES) with 16 electron Time-Of-Flight (eTOF) flight-tubes as dispersive elements provides pulse resolved photon energy and polarization diagnostics [2]. Electron spectrometers based on the eTOF principle have flight-tubes with applied voltages that decelerate the electrons. Fast electronics register the time difference from ionization to detection which is related to the kinetic energy of the photoelectrons. The PES, in Fig.1, which uses gas targets is non-invasive and has found applications for soft X-ray photon diagnostics and experiments [3, 4]. Adapting the PES concept to the hard X-ray range is not straightforward due to the poor ionization cross-section and very high kinetic energies of photoelectrons in that regime. This contribution describes the development of the new PES dedicated to photon diagnostics at hard X-rays and presents results from measurements at the beamline P09 at PETRA III [5].

* joakim.laksman@xfel.eu

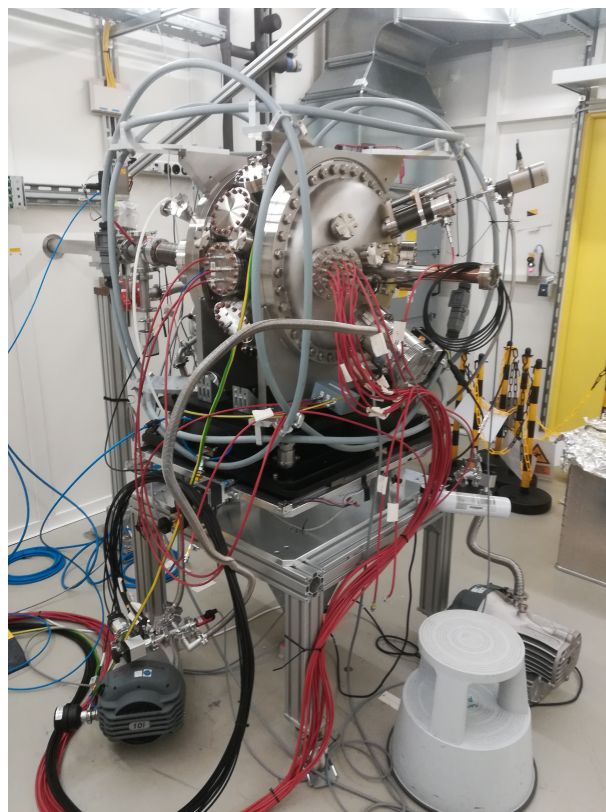


Figure 1: The hard X-ray PES installed at the P09 beamline at PETRA III. A target gas is injected into the center. Emitted photoelectrons are decelerated and focused through the electron optics of the flight-tubes before they reach the detector. Helmholtz coils encapsulate the device to cancel external magnetic fields, which otherwise influence the electron trajectories.

INSTRUMENT

A picture of the device installed at the P09 beamline is presented in Fig. 1. The spectrometer consists of 12 eTOF flight-tubes oriented perpendicular to the X-ray beam at angles of 0° , 30° , \dots , 330° . In order to maximize the flight-tubes performance as dispersive elements, while simultaneously focussing the photo-emitted electrons to the detector, we chose a design where the flight-tubes are divided in *retardation region* and *Einzel lens*, separated with a high transmission gold mesh to prevent field penetration between the two regions. An effusive gas jet is injected via a capillary in the interaction region where it interacts with the X-ray beam

CHARACTERISATION OF A DIAMOND CHANNEL CUT MONOCHROMATOR DESIGNED FOR HIGH REPETITION RATE OPERATION AT THE EuXFEL*

K. R. Tasca[†], L. Samoylova[‡], A. Madsen, I. Petrov, A. Rodriguez-Fernandez, R. Shayduk, M. Vannoni, A. Zozulya, European XFEL GmbH, 22986 Schenefeld, Germany
R. Barrett, T. N. Tran Thi, European Synchrotron Radiation Facility, 38000 Grenoble, France

Abstract

The European X-ray Free-Electron Laser (EuXFEL) is a unique FEL facility that provides X-ray pulses of high spectral brilliance and high photon flux at MHz repetition rate. However, the high peak power, produced in trains of up to 2700 fs pulses at a rate of 10 Hz, induces a periodic temperature increase of the hard X-ray monochromators, thereby reducing their transmitted intensity. To address this limitation, a diamond channel cut monochromator (DCCM) was proposed as an alternative to the currently used silicon monochromators. The heat load effect of typical EuXFEL pulses at 300 K and 100 K was simulated by finite element analysis (FEA) and indicates that the significant reduction of the transmitted intensity occurs after a higher number of pulses when compared to silicon. The DCCM first prototype was manufactured from an HPHT type IIa diamond single block and characterised by rocking curve imaging (RCI). The RCI results demonstrated the high crystalline quality of the DCCM with rocking curve widths of the same order as the width predicted by the dynamical theory and a uniformly reflected intensity over the surface. The performance as a monochromator was demonstrated by measuring the double bounce reflection. The resulting images after two successive reflections showed a diffracted beam of the same size and parallel to the incident beam and confirmed its applicability.

INTRODUCTION

The EuXFEL provides X-ray pulses of high spectral brilliance and high photon flux at MHz-repetition rate [1]. However, the high peak power of the EuXFEL beam imposes a high dynamical heat load on the optical elements, such as mirrors and monochromators. Currently, in the hard X-ray regime, cryo-cooled silicon (1 1 1) monochromators are used to reduce the spectral bandwidth of the beam generated by self-amplified spontaneous emission or as spectral purification elements in seeded operation mode [2–4]. Yet, the use of a silicon monochromator introduces some limitations on the instrument operation, since the transmission of the Si monochromator at MHz repetition rates is affected by the heat load, thus reducing the intensity of the transmitted pulses by a factor of two after around 150 pulses [5]. To address these challenges imposed by the MHz repetition rate photon beams to the hard X-ray monochromator, we pro-

posed a cryo-cooled diamond channel cut monochromator (DCCM) as an alternative to silicon. The monolithic design of the channel-cut ensures high mechanical stability and for hard X-rays, the diamond absorption cross section is one order lower than that of silicon, so the volumetric heat load effect is significantly reduced. In addition, diamond has a smaller thermal expansion coefficient and higher thermal conductivity compared to silicon, as well as high reflectivity and narrow Darwin widths [6–9].

The heat load from the EuXFEL high-energy pulses increases the temperature of the crystal and induces deformations in the crystal lattice with 10 Hz periodicity. This strongly affects the monochromator reflectivity properties and results in a decrease of the transmitted intensity through the monochromator with the accumulation of the absorbed energy in the first crystal [5]. Deformations of the lattice resulting from accumulated heat on the crystal affect the reflectivity curve. As a result of the lattice deformation with a change in d-spacing, the centre of the rocking curve is shifted, the width is broadened and the maximum intensity decreases. These variations of the diffraction profile result in a performance decrease of the monochromator, reducing the transmitted intensity and slightly increasing the bandwidth. The maximum acceptable shift of the peak position of the diffraction profile from the first crystal with respect to the second one is determined by the relative bandwidth that gives an estimation of the amount of heat that leads to the detuning of the monochromator and therefore the maximum acceptable temperature difference (ΔT) between the two crystals of the monochromator. Estimates of the acceptable ΔT between the two crystals of a diamond monochromator show that this temperature threshold is reached after a six to ten times higher number of pulses in comparison with a silicon monochromator in the same conditions, suggesting that diamond can be a suitable alternative to silicon [10, 11].

Due to the recent technological developments in the high pressure and high temperature (HPHT) crystal growth technique, diamond single crystals of type IIa with suitable size and high crystal quality suitable for X-ray optics applications are now available [8, 12, 13].

As mentioned above, an X-ray monochromator requires a high-quality perfect single-crystal. The most common techniques used to determine crystalline perfection are the measurement of X-ray diffraction profile and X-ray topography [9]. In this work, we present the X-ray characterisation results of the DCCM by the rocking curve imaging (RCI) method [14, 15], which combines rocking curve analysis and

* Work supported the R&D program of EuXFEL

[†] kelin.tasca@xfel.eu

[‡] liubov.samoylova@xfel.eu

MAGNETIC FIELD INVESTIGATION IN A COMPACT SUPERCONDUCTING UNDULATOR WITH HTS TAPE

D. Astapovych*, N. Glamann, A. W. Grau, B. Krasch, D. Saez de Jauregui, Karlsruhe Institute of Technology (KIT), Karlsruhe, Germany

Abstract

The superconducting undulator (SCU) based on the second-generation high-temperature superconducting (HTS) tapes is a promising application for building tabletop free-electron laser (FELs). The short period < 10 mm undulators with a narrow magnetic gap < 4 mm are especially relevant. The advantage of the HTS tape is that it shows both high critical current density and high critical magnetic field. Each tape has $50 \mu\text{m}$ thickness and 12 mm width and is further scribed by a laser to achieve a meander structure, hence, providing the desired magnetic field pattern.

Thus, a new approach to a superconducting undulator has been presented in the past and is further developed at KIT: each coil is wound with a single 15 m structured HTS tape. As a result, 30 layers of scribed sections lay above each other, and therefore, provide the required magnetic field. The results of the magnetic field measurements together with the results of the numerical investigation will be presented and discussed.

INTRODUCTION

An idea of the undulator using the meander-structured HTS tapes was proposed by Prestemon [1,2]. Figure 1 shows a photo of a second-generation HTS tape with a meander structure, which has been made in-house at KIT using the pulsed YAG laser system at the Institute of Technical Physics (ITeP). The main parameters of the laser-scribed tapes are presented in Table 1 and used later in the computations.



Figure 1: Segment of laser-scribed HTS tape.

Table 1: Main parameters of laser-scribed HTS tapes

Parameter	Value
HTS tape thickness (μm)	55
Period length (mm)	8.05
Period number	12.5
HTS tape groove section ($\mu\text{m mm}$)	25 4

A concept of a jointless undulator using the structured HTS tapes has been proposed by T. Holubek [3]. The design is the following: a 15 m single-piece of structured HTS tape

* daria.astapovych@kit.edu

is folded in half, resulting in the opposing current direction between two layers. Further, two non-magnetic stainless steel yokes are used to wind coils with such tapes, hence, 30 layers of scribed sections lay above each other and provide the needed magnetic field. Figure 2 shows the photo of the undulator prototype based on this winding concept.

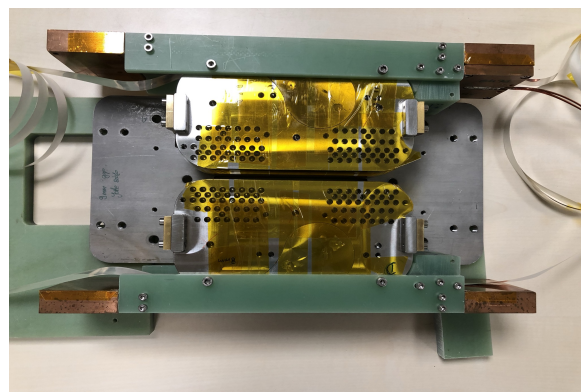


Figure 2: Undulator prototype: structured HTS tape wound around non-magnetic stainless steel core.

Setup for Magnetic Field Measurements

The magnetic field measurements station CASPER (ChAracterization Set-uP for Field Error Reduction), which was built and installed at our institute and is operated at KARA [4], is shown in Fig. 3. In principle, CASPER is a

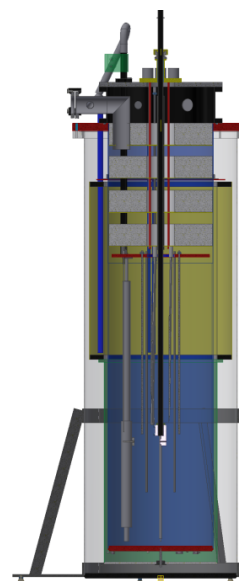


Figure 3: Magnetic field measurements station CASPER I.

DESIGN OF THE INNOVATIVE APPLE-X AX-55 FOR SABINA PROJECT, INFN - LABORATORI NAZIONALI DI FRASCATI

J. Počkar, M. Kokole, T. Milharčič, U. Primožič, Kyma Tehnologija d.o.o., Sežana, Slovenia
 M. Del Franco, G. Di Pirro, A. Selce, A. Ghigo, INFN Laboratori Nazionali di Frascati, Rome, Italy
 A. Peralta, ENEA, Rome, Italy
 R. Geometrante, Kyma S.p.A., Trieste, Italy
 L. Giannessi¹, Elettra Sincrotrone Trieste, Trieste, Italy
¹also at INFN Laboratori Nazionali di Frascati, Rome, Italy

Abstract

Kyma S.p.A. was awarded the design and production of the APPLE-X undulator for SABINA project at INFN - Laboratori Nazionali di Frascati. SABINA (Source of Advanced Beam Imaging for Novel Applications) is a project aimed at the enhancement of the SPARC_LAB research facility. The two user lines that are going to be implemented are; a power laser target area and a THz radiation line.

Here we present the magnetic design and a novel mechanical implementation of this APPLE-X undulator for the THz/MIR radiation line. Undulator is made from three 1.35 m long sections. Each section consists of an APPLE-X magnetic array with 55 mm undulator period, a minimum bore diameter of 14.85 mm and a mechanical frame. The undulator design is both compact and lightweight. This is achieved by novel mechanical design and implementation of the multiple dynamic corrections through the motion control system.

SABINA PROJECT

SABINA (Source of Advanced Beam Imaging for Novel Applications) is a project aimed at the enhancement of the SPARC_LAB research facility with the final goal to shape it into a facility opened for external users. A reduction of the number and extent of faults and consequential increase of the uptime is the first main objective of the project. The second objective is the improvement of the accelerator performances. Both objectives will be achieved through the consolidation of technological systems and updates of replacement of critical equipment [1].

THz/MIR Line

SABINA will implement a self-amplified spontaneous emission Free Electron Laser (SASE FEL) providing a wide spectral range of intense, short and variable polarization pulses for investigation in physics, chemistry, biology, cultural heritage, and material science.

This new THz/MIR radiation line will produce pulses covering a broad spectral region from 3 THz to 30 THz, obtained by tuning the electron beam produced at the SPARC photo-injector to an energy between 30 and 100 MeV. The high brightness electron beam will be transported up to an APPLE-X undulator where photon pulses in the picosecond range and energy of tens of μJ , with linear, circular and elliptical polarization will be produced.

UNDULATOR

In order to reach required photon wavelength, low beam energy and long undulator period are required. Since beam energy is restricted to the range 30-100 MeV as previously mentioned and because of physical constraints for which the total undulator length must be less than 4.5 meters, an undulator with a period length of 55 mm has been proposed [2].

The undulator is divided in three modules of ~ 1.3 meters each, separated by about 20 cm of drift space to allow the installation of holders for the vacuum pipe and beam position diagnostics. Magnetic correctors to handle the electron beam orbit will be placed externally, outside the undulator modules.

An additional constraint on the radiation properties required by the SABINA project is the generation of switchable left-right circular polarization. In order to accomplish this request an APPLE2-type undulator was initially proposed. Such device allows to produce vertically/horizontally linear polarized radiation and left/right-handed elliptical polarized radiation [3].

The magnetic configuration that was finally chosen is an APPLE-X that has also the property of focusing the beam on both the horizontal and vertical planes. This feature is not common to other variable polarization undulators based on permanent magnets such as the APPLE II [4].

Tender

The INFN National Laboratory of Frascati has put the supply of the APPLE-X undulator described above to tender on March 2021. Offerors with suitable technical credentials and experience in the field of Insertion Device (ID) fabrication have been asked to bid for the design, engineering, manufacturing, assembly, testing, and final delivery of three devices that were referred as AX-55. AX-55 will be the first APPLE-X device in the world designed and build by industry.

CONCEPTUAL DESIGN OF THE THz UNDULATOR FOR THE PoIFEL PROJECT

J. Wiechecki[†], National Synchrotron Radiation Centre SOLARIS, Kraków, Poland
P. Krawczyk, R. Nietubyć, National Centre for Nuclear Research, Otwock-Świerk, Poland
P. Romanowicz, D. Ziemiański, Cracow University of Technology, Kraków, Poland

Abstract

PoIFEL will be the first free-electron laser facility in Poland. It will be driven with RF continuous-wave superconducting linac including an SRF injector furnished with a lead film superconducting photocathode. PoIFEL will provide a wide wavelength range of electromagnetic radiation from 0.6 mm down to 60 nm. The linac will be split into three branches. Two of them will feed undulators chains dedicated for VUV, and IR radiation emission, respectively, and a single THz undulator will be settled in the third branch. The design of the THz undulator has been recently accomplished. It consists of a 1560 mm long permanent magnet structure ordered as a Halbach array of 8 periods. Large block dimensions, gap flux zeroing at full opening and 0.5 THz – 5 THz wavelengths range imposed on the undulator significantly influenced the final shape of the device, including block holders, girders and frame robustness unto magnetic forces, and hindered manufacturing and assembling processes. The following publication presents the challenges and solutions that were accompanying the conceptual phase.

PoIFEL FACILITY

PoIFEL Superconducting Free electron laser is an ongoing project led by NCBJ with 9 contortions members onboard. Superconducting Electron Gun based on the sub-micrometre Pb film deposited onto a head of Nb dismountable plug, impinging by 257 nm light laser beam used to liberate electrons to the linear accelerator. The linear accelerator will consist of 5 Rossendorf-RI-type cryomodels (CM), two energy branches up to 187 MeV (High Energy) and a second up to 72 MeV (Low Energy). This configuration will guide the electron beam through succeeding three CMs, boosts their energy and supply the VUV undulators chain (HE) and IR undulator chain or pass it by, on the way towards the THz undulator (LE, respectively).

DESIGN CHALLENGES

The boundary conditions given for both the THz branch and the THz undulator are very demanding. They must be considered simultaneously with all two other types of undulators embedded into the PoIFEL project. The device consists of 100 x 100 x 40 mm size NdFeB magnet blocks, ordered in 8 periods 1560 mm long Halbach array. The electron beam high is 1400 mm above the floor level.

[†] jaroslaw.wiechecki@uj.edu.pl

The required gap range is 100 – 600 mm. These typical parameters must be compiled with imposed tolerances (see Table 1).

Table 1: Selected Tolerances Required for the Undulator

Parameter	Value
Undulator period length variation $\Delta\lambda$ (RMS)	<160 μm
Magnet block centre straightness (RMS) in the horizontal plane	<400 μm
The relative angle between the corresponding block surface in the upper and lower girder	< $1 \cdot 10^{-2}$ rad
Maximum change of the gap width Δg along the undulator	<30 μm
The maximum deflection of the undulator beam	<15 μm
Absolute accuracy of undulator beam vertical positioning	<2 μm
First integral IB1 of the transverse magnetic field along the undulator	< $3 \cdot 10^{-6}$ T·m
Second integral IB2 of the transverse magnetic field along the undulator	< $3 \cdot 10^{-6}$ T·m ²
Beam parallelism tolerance: relative beam twist angle along the magnetic z-axis (roll)	< $1 \cdot 10^{-2}$ rad
Beam parallelism tolerance: relative beam twist angle along the undulation x-axis (pitch)	$\pm 30 \cdot 10^{-6}$ rad
Beam parallelism tolerance: relative beam twist angle along the vertical y-axis (yaw)	$\pm 0,5 \cdot 10^{-3}$ rad
Tolerance of the undulator magnetic axis vertical positioning concerning the electron beam Δy	< 150 μm
Tolerance of the undulator magnetic axis horizontal positioning concerning the electron beam Δx	< 1000 μm

These requirements force the following considerations:

- Wide range of gap requires more space (from 100 mm to 600 mm)
- Three different types of undulators require a unified design
- Wide range of adjustment pulleys for magnet blocks (up to 1.5 mm)

CONTROLLING BEAM TRAJECTORY AND BEAM TRANSPORT IN A TAPERED HELICAL UNDULATOR

A. Fisher*, J. Jin, P. Musumeci

Department of Physics and Astronomy, University of California Los Angeles, CA, USA

Abstract

A helical undulator provides a stronger FEL coupling than common planar geometries as the beam transverse velocity never vanishes. However, a significant challenge lies in tuning and measuring the fields with limited access to the beam axis along the undulator. Confirming the good field region off axis is difficult given the limited space available for 3D hall probe scans, and is important for low energy beams used to create THz radiation which have large amplitude oscillations. We present our tuning procedures developed for the meter-long THESEUS undulators, consisting of two orthogonal permanent magnet Halbach arrays shifted by a quarter period relative to one another. The Hall probe and pulsed wire measurements are guided by the general field expansion of helical undulators to correctly tune fields on and near the axis.

INTRODUCTION

The helical geometry of the THESEUS undulators allows for stronger FEL coupling at the cost of increased engineering complexity and limited tuning access to the beam axis in the undulator [1]. Accurate tuning of the tapered undulator fields is necessary to provide straight trajectories with the correct slippage. In addition to Hall probe measurements, pulsed-wire measurements can provide an independent measurement of the electron beam transverse velocity and trajectory in tight arrangements. We also investigate using 3D pulse-wire measurements to ensure the electrons sample accurate fields far off-axis in the THz waveguide FEL [2].

In this paper, we present the tuning procedures developed for the THESEUS undulators at UCLA and organize as follows. First we derive the form of the undulator field expansion and fit the free parameters to a numerical simulation for the magnetic fields. Next we describe our Hall probe tuning procedure, including corrections to probe angle and transverse offset. Finally we present a pulsed-wire measurement setup developed at UCLA and discuss corrections, fiducialization, and our 3D pulse-wire measurements.

UNDULATOR FIELD EXPANSION

The tuning procedure for the THESEUS undulators utilizes a theoretical expansion for fields off-axis. For static fields with no current sources, $\nabla \times \vec{B} = 0$ implies the existence of a scalar magnetic potential $\vec{B} = -\nabla\phi$ that satisfies Laplace's equation.

$$\nabla \cdot \vec{B} = \nabla^2\phi = 0 \quad (1)$$

* afisher000@g.ucla.edu

Considering first a planar undulator with period $\lambda_u = \frac{2\pi}{k_u}$ and peak field $B_y = B_0$ at the origin, we assume a separation of variables solution with constant ϕ_0 , such that $\phi = \phi_0 X(x)Y(y) \cos(k_u z)$.

Dividing Eq. (1) by ϕ constrains

$$\frac{1}{X} \frac{\partial^2 X}{\partial x^2} + \frac{1}{Y} \frac{\partial^2 Y}{\partial y^2} - k_u^2 = 0. \quad (2)$$

To hold for all space, $X(x)$ and $Y(y)$ must be trigonometric or hyperbolic trigonometric functions. Physically, we expect B_y to be an even function with positive concavity and so identify $Y(y) = \sinh(\alpha k_u y)$ where α is a real parameter. Therefore, $X(x) = \cos(\beta k_u x)$ with $\beta^2 = \alpha^2 - 1$ and $\phi_0 = -\frac{B_0}{\alpha k_u}$ such that

$$\phi = \frac{-B_0}{\alpha k_u} \cos(\beta k_u x) \sinh(\alpha k_u y) \cos(k_u z). \quad (3)$$

The potential for an undulator with flat faces (infinite in x) is given by $\alpha = 1, \beta = 0$ whereas an undulator with equal focusing due to parabolic-pole shaped faces is given by $\alpha = 1/\sqrt{2}, \beta = i/\sqrt{2}$.

The THESEUS undulators are a helical geometry composed of two permanent magnet Halbach arrays shifted by a quarter period relative to each other. The full potential is given by

$$\phi = \frac{B_0}{\alpha k_u} \sinh(\alpha k_u x) \cos(\beta k_u y) \sin(k_u z) - \frac{B_0}{\alpha k_u} \cos(\beta k_u x) \sinh(\alpha k_u y) \cos(k_u z) \quad (4)$$

The undulators were designed with the magnetic code RADIA [3]. By fitting α in Eq. (4) to the design fields (for $\sqrt{x^2 + y^2} < 1$ mm), we find $\alpha = 1.53$ and $\beta = \sqrt{\alpha^2 - 1} = 1.16$. We emphasize that the THESEUS undulator differs from common textbook definitions as the strength of the peak magnetic fields forms a saddlefunction in the transverse dimension[4, 5].

HALL PROBE

The enclosed geometry of a helical undulator increases the difficulty of Hall probe tuning. Our design uses a flat metal piece that slides along a notched, hollowed out rod. The rod fits snugly in the tensioned vacuum pipe and is held fixed relative to the undulator with set screws at both ends. A 3-axis hall probe is glued to the flat piece and pulled along the undulator with a 1-m translation stage.

Errors in the probe roll angle and transverse offset can be inferred from measurements as seen in Fig. 1. A roll angle

DEVELOPMENT OF DIAMOND-BASED PASS-THROUGH DIAGNOSTICS FOR NEXT-GENERATION XFELs

R. Padilla†, E. Gonzalez, S. Kachiguine, F. Martinez-Mckinney, S. Mazza, M. Nizam, N. Norvell, E. Potter, E. Ryan, B. Schumm, M. Tarka, M. Wilder, Santa Cruz Institute for Particle Physics and the University of California at Santa Cruz, Santa Cruz, CA, USA

B. Jacobson, J. MacArthur, I. Silva Torrecilla, D. Zhu, SLAC National Accelerator Laboratory, Menlo Park, CA, USA

J. Bohon, D. Kim, J. Smedley, Los Alamos National Laboratory, Los Alamos, NM, USA

C. Grace, T. Prakashc, Lawrence Berkeley National Laboratory, Berkeley, CA, USA

C. T. Harris, Sandia National Laboratory, Albuquerque, NM, USA

D. Stuart, University of California, Santa Barbara, CA, USA

E. Prebys, University of California, Davis, CA, USA

Abstract

FELs deliver intense pulses on the femtosecond scale, with peak intensities and positions that fluctuate strongly on a pulse-to-pulse basis. The fast drift velocity and high radiation tolerance properties of chemical vapor deposition (CVD) diamonds make these crystals a good candidate material for developing a high frame rate pass-through diagnostic for the next generation of X-ray Free Electron Lasers (XFELs). We report on two diamond based diagnostic systems being developed by a collaboration of a UC campuses and National Laboratories supported by the University of California and the SLAC National Laboratory.

For the first of these diagnostic systems, we have developed a new approach to the readout of diamond diagnostic sensors designed to facilitate operation as a pass-through detection system for high frame rate XFEL diagnostics. Making use of the X-ray Pump Probe (XPP) beam at the Linac Coherent Light Source (LCLS), the performance of this new diamond sensor system has been characterized. Limits in the magnitude and speed of signal charge collection are explored as a function of the generated electron-hole plasma density.

A leading proposal for improving the efficiency of producing longitudinally coherent FEL pulses is the cavity-based X-ray free electron laser (CBFEL). In this configuration, the FEL pulses are recirculated within an X-ray cavity in such a way that the fresh electron bunches interact with the FEL pulses stored in the cavity over multiple passes. This creates a need for diagnostics that can measure the intensity and centroid of the X-ray beam on every pass around the recirculatory path. For the second of these diagnostic systems, we have created a four-channel, position-sensitive pass-through diagnostic system that can measure the intensity and centroid of the circulating beam with a repetition rate up to 50 MHz. The diagnostic makes use of a planar diamond sensor thinned to 43 μm to allow for minimal absorption and wave-front distortion of the circulating beam. A single-pulse resolution of 3 μm was achieved for nJ scale pulses.

† remopadi@ucsc.edu

INTRODUCTION

Advanced X-ray Free Electron Lasers (XFELs) will provide high-intensity, high repetition rate (up to 10 GHz) pulses of coherent X-rays. However, the unstable nature of XFELs causes fluctuations in the intensity as well as in its centroid position of each pulse. Developing a pass-through diagnostic capable of measuring the intensity and centroid location pulse-by-pulse over a large dynamic range can be beneficial as a diagnostic for accelerator operations and experiments making use of XFEL beams.

Monocrystalline diamond presents specific characteristics that can be taken advantage of in sensor applications. Diamond shows a fast saturated drift velocity of approximately 200 $\mu\text{m}/\text{ns}$ [1] and an exceptional thermal conductivity of about 2200 W/m·K. As an example of diamond performance: for a 30 μm diamond sensor the expected charge collection time with saturated drift velocity is about 150 ps. Additionally, diamond has a large band gap of 5.5 eV leading to an electron/hole pair creation energy of 13.3 eV [2], which limits the amount of signal charge generated inside the diamond. These characteristics differentiates diamond from other semiconductor materials and makes it a good candidate for a high-intensity, multi-GHz X-ray beam pass-through diagnostic.

In this proceeding we report on two studies making use of pass-through diamond sensors. In the first, making use of a specially designed fast readout scheme, we investigated the intrinsic charge collection efficiency and speed of diamond sensors. In the second, we characterized the performance of a position and intensity monitor designed to operate at repetition rates up to 50 MHz. These diagnostics made use of 4x4 mm² electronic-grade diamonds from the Element 6 corporation, thinned to 37 μm and 43 μm , respectively, and with the surface electrode divided into four equal quadrants for the position monitor. The studies were done on April 5-6, 2021, and April 16, 2022, in the X-ray Pump Probe (XPP) beamline of the Linac Coherent Light Source (LCLS) at the SLAC National Accelerator Laboratory (SLAC). During both runs, we made use of a monochromatic X-ray beam of 11.9 keV with single pulse intensities varying from 0.2 μJ to 80 μJ . In the first case,

INVESTIGATION OF HIGH ABSORBED DOSES IN THE INTERSECTIONS OF THE EUROPEAN XFEL UNDULATOR SYSTEMS

O. Falowska–Pietrzak[†], A. Hedqvist, F. Hellberg, Stockholm University, Stockholm, Sweden
 G. Lopez Basurco, Autonomous University of Madrid, Madrid, Spain
 F. Wolff-Fabris, European XFEL GmbH, Schenefeld, Germany

Abstract

This work presents measurements of the absorbed doses in the vicinity of phase shifter (PS) installed in intersections of the Undulator Systems at the European X-Ray Free Electron Laser (XFEL). In addition, Geant4 Monte Carlo simulations were performed to further investigate the radiation field present in these intersections. Measurements in the downstream undulator cell in SASE3 showed similar doses for the films placed at the PS entrance and near PS motors. Both measurements and simulations indicate that the radiation field near PS motors is not caused by the high-energy electron interactions with the beam pipe close to the PS. The measurements of the absorbed doses at the PS entrance in the upstream undulator cells are also presented.

INTRODUCTION

The European XFEL GmbH is a free-electron laser facility located in Schenefeld, Germany. It operates three undulator systems called SASE1, SASE2 and SASE3 since 2017, and the radiation damage to the undulators is the matter of concern [1]. In each of these systems, electron bunches of GeV energies that propagate along the undulators in the vacuum beam pipe generate high brilliance X-ray pulses. Each system consists of numerous undulator segments (5 m long) separated by intersections (1.1 m long). The intersection together with the undulator segment is called the undulator cell. There are 35 undulator cells in SASE1 and SASE2, while SASE3 consists of 21 cells. Each intersection contains vacuum systems and correction and diagnostic equipment such as beam position monitor (BPM), beam loss monitor (BLM) and quadrupole magnet (QM). Downstream of the QM a PS is located. It has a movable gap and is composed by permanent magnets from the same type as employed in the undulator segments. It matches the phase of electrons and photons produced through the Self-Amplification Spontaneous Emission (SASE) process [2].

At the entrance of each undulator segment, Radfet dosimeters continuously measure the absorbed doses and are online readable [3]. The radiation field close to the beam pipe can arise from several factors, such as spontaneous undulator radiation and electron interaction with gas molecules. In addition, electrons may hit the beam pipe which results in emission of stray radiation. However, no dosimetry system is installed in the intersections. Recently, it was noticed that the movement of gaps in some PS in SASE3 could not be performed due to PS motor or encoder damage. It might be caused by the radiation present

between undulator segments.

In this work, we present the results of gafchromic film measurements at the PS entrance and near PS motors. The measurements are presented together with the Monte Carlo simulations of electron beam losses to better understand the radiation field in the intersections.

METHODS

Gafchromic films

The absorbed doses in the intersections were measured with gafchromic film dosimeters. Film dosimetry is mostly used for medical radiation purposes, but they are also useful for measurements in the high-energy radiation fields. They can be cut in various shapes without changing their properties. Therefore, they can be placed in areas that are difficult to access with other detectors. In addition, film dosimeters give information on 2D dose distributions.

The films undergo polymerization during exposure to ionizing radiation. The subsequent colour change is proportional to the absorbed dose, which can be evaluated through Red (R), Green (G) and Blue (B) values of scanned films through multichannel analysis [4].

In this work, the GAFCHROMIC™ EBT3 films were placed at the PS entrance, perpendicularly to the beam pipe (referred later as PS films) in different SASE1 and SASE3 undulator cells. Films were removed from SASE1 and SASE3 after approximately five and two months, respectively. In addition, in SASE3 the absorbed doses were measured next to the PS motors, located approximately 10 cm above the PS and 40 cm above the beam pipe. The PS and position of the PS motor are shown in Fig. 1.

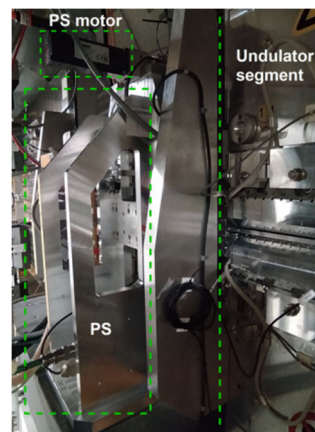


Figure 1: PS and PS motor seen from the downstream side of the undulator system.

[†] olga.falowskapietrzak@fysik.su.se

MILLIMETER-WAVE UNDULATORS FOR COMPACT X-RAY FREE-ELECTRON LASERS*

L. Zhang^{†1}, J. Easton, C. Donaldson¹, C. Whyte, A. Cross¹, University of Strathclyde, Glasgow, UK
Jim Clarke¹, ASTeC, STFC Daresbury Laboratory, Sci-Tech Daresbury, Daresbury, UK
¹also at Cockcroft Institute, Daresbury, UK

Abstract

Electromagnetic wave undulators have the advantage of a shorter period compared with the permanent magnet undulators when operating at high frequency, therefore producing FEL radiation at the same wavelength with less electron energy. This paper presents the design of a Ka-band microwave undulator. The ongoing research is to prototype a millimeter-wave undulator operating at ~100 GHz, which will have an undulator period of about 1/10 of the state-of-the-art permanent magnet undulators. The millimeter-wave undulator will allow the generation of soft X-ray radiation at much lower beam energy, such as hundreds of MeV, enabling a reduction in the cost of a compact XFEL facility.

INTRODUCTION

Free-electron lasers (FELs) [1, 2] are capable to produce high-power ultrashort-wavelength, and spatially coherent radiation. The coherent radiation at X-ray wavelength opens various applications and allows the exploration of new studies in biophysical and materials science, surface studies, chemical technology, medical applications, solid-state physics, and others. The FEL radiation is produced in an undulator which is traditionally made of periodic permanent magnets. The radiation wavelength produced by such a permanent magnet undulator (PMU) is

$$\lambda = \frac{\lambda_u}{2\gamma^2} \left(1 + \frac{K^2}{2} + \gamma^2 \theta^2\right) \quad (1)$$

where λ_u is the undulator period determined by the period of the magnet, γ is the relativistic factor governed by the electron beam energy. θ is the observation angle, which is normally set as 0. K is the undulator strength parameter. It is defined by the peak transverse magnetic field strength of the undulator and the undulator period, as

$$K = 0.0931 B_u [\text{T}] \lambda_u [\text{mm}] \quad (2)$$

Table 1 lists the parameters of PMUs used in Swiss XFEL and Europe XFEL [3, 4]. They show the scale of the periods of the state-of-the-art PMUs. The production of FEL radiation at X-ray wavelength requires high electron beam energy with a few GeV.

Table 1: Examples of the PMU parameters

	Swiss XFEL (Aramis)	Europe XFEL
Structure	Planar hybrid	Planar hybrid
Material	NdFeB	NdFeB
K	1.2	3.0
Period	15 mm	26 mm
Peak field	0.85 T	1.24 T
Gap type	Variable	Variable
Gap	4.7 mm	6.0 mm

The periodic transverse magnetic field in the undulator can also be created from the electromagnetic (EM) waves. The EM undulators [5-7] have the advantage of a shorter period compared with the permanent magnet undulators when operating at high frequency, therefore producing FEL radiation at the same wavelength with less electron energy. Early research on the microwave undulator was hampered by the limited power of the drive source. In 2014, SLAC demonstrated the FEL radiation with an X-band microwave undulator driven by a 50 MW klystron in the experiment [8-10]. It achieved an equivalent B_u of 0.65 T and a period of 13.9 mm. The experiment also demonstrated tuneable radiation at 400-600 nm using an electron bunch with an energy of 50 MeV to 70 MeV and seeded coherent harmonic generation (SCHG) at 160-240 nm using a 120 MeV electron bunch.

Microwave undulators operating at higher frequency allow shorter periods, therefore, achieving shorter FEL radiation wavelength at the same energy of the electron bunch energy. In this paper, the properties of a Ka-band microwave undulator operating at 36 GHz are presented.

MICROWAVE UNDULATOR

The main body of the undulator cavity was composed of a corrugated waveguide that supports the low-loss HE_{11} modes, as shown in Fig. 1. The field pattern satisfies the requirements of an undulator, including the low loss to increase the equivalent magnetic field strength at the same driving power, a maximum field strength at the waveguide center in which the beam propagates to maximize the interaction between the EM wave and the electron bunch, a TE-like mode to maximize the transverse magnetic field and avoid the axial electric field modulating the electron beam, and an overmoded structure to reduce the effect of the forward wave components in the cavity structure.

* Work supported by Science and Technology Facilities Council (STFC) U.K., Cockcroft Phase 4 grant ST/V001612/1.

[†] liang.zhang@strath.ac.uk

STUDY OF AN ERL-BASED X-RAY FEL*

F. Lin[†], V.S. Morozov, Oak Ridge National Laboratory, Oak Ridge, TN, USA
 J. Guo, Y. Zhang, Thomas Jefferson National Accelerator Facility, Newport News, VA, USA

Abstract

We propose to develop an energy-recovery-linac (ERL)-based X-ray free-electron laser (FEL). Taking advantage of the demonstrated high-efficiency energy recovery of the beam power in the ERL, the proposed concept offers the following benefits: i) recirculating the electron beam through high-gradient SRF cavities shortens the linac, ii) energy recovery in the SRF linac saves the klystron power and reduces the beam dump power, iii) the high average beam power produces a high average photon brightness. In addition, such a concept has the capability of optimized high-brightness CW X-ray FEL performance at different energies with simultaneous multipole sources. In this paper, we will present the preliminary results on the study of optics design and beam dynamics.

INTRODUCTION

A Free-Electron Laser (FEL) that has been invented and experimentally demonstrated in the 1970s [1, 2] holds a great potential to serve as a high-power and coherent source. FEL performance extends beyond the limitations of fully coherent laser light sources by covering a broad range of wavelength from infrared down to X-ray with a stable and well-characterized temporal structure in the femtosecond time domain. Particularly, XFEL allows scientists to probe the structure of various molecules in detail, and simultaneously explore the dynamics of atomic and molecular processes on their own time scales. XFEL allows for the exploration of new areas in physics, chemistry, biology, medicine and materials.

Techniques have been developed and improved to amplify the spontaneous radiation to provide intense quasi-coherent radiation [3 - 6]. The FEL process strongly depends on the local electron beam properties: current, energy, emittance and energy spread. Therefore, all existing XFELs [7 - 15] are driven by linear accelerators to ensure preservation of the electron beam quality from the source for achieving a high peak brightness. Normal conducting RF cavities, with very high accelerating gradients of up to 60 MV/m, are used to keep the linac length as short as possible. This limits the bunch repetition rate up to about 100Hz in a pulsed beam operation mode, resulting in average photon brightness of as much as 10 orders of magnitude lower than the peak one. Therefore, several XFEL facilities [9, 13] have started considering a CW beam operation mode that is made possible by the high-gradient SRF technology. There were two ERL-based concepts [16, 17]

explored to produce FELs in the UV and/or soft X-ray regions.

CONCEPT

We propose an ERL-based compact XFEL facility, schematically illustrated in Fig. 1. Note that the energy gain of 2 GeV from the SRF is chosen for this study only, considering relatively realistic SRF gradient, magnet fields, and geometric footprint of such a facility. Optimization of these parameters can be carried out in each individual case. We leverage the ongoing world-wide efforts on the further improvement of injector and XFEL techniques and focus on the feasibility study of the accelerator system.

Electron beams are generated from the source and accelerated to 250 MeV before the first bunch compression (BC). Then the beams are accelerated in the ERL by SRF cavities with the desired energy gain of 2 GeV. Since space charge effects are significantly suppressed at the GeV electron beam energy, one can utilize the first arc to compress the beam for the second time if needed. The electron beams are either directed into different undulators that can be designed and optimized for particular XFEL radiations parameters or bypass the undulator sections. Electron beams that have been used to produce XFEL can be energy recovered in the ERL after the second arc and dumped downstream. The bypassed electron beams will double energy up to ~ 4 GeV after the ERL and propagate through the third arc. Same as in the first ~ 2 GeV energy loop, the ~ 4 GeV electron beams will either be directed into different undulator sections or bypass the undulators. Again, the electron beams that have produced XFEL will be energy recovered and dumped, and the bypassed electron beams will be further accelerated to ~ 6 GeV for XFEL production and energy-recovered in the ERL before the final dump.

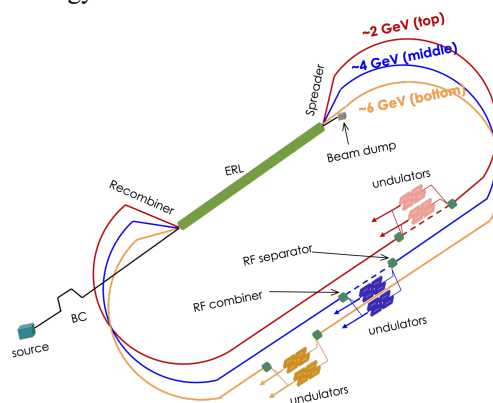


Figure 1: Schematic drawing of the proposed ERL-based XFEL facility.

* Work supported by UT-Battelle, LLC, under contract DE-AC05-00OR22725, and by Jefferson Science Associates, LLC, under contract DE-AC05-06OR23177

[†] Email: linf@ornl.gov

COHERENT 3D MICROSTRUCTURE OF LASER-WAKEFIELD-ACCELERATED ELECTRON BUNCHES*

M. LaBerge¹, A. Hannasch, B. Bowers, R. Zgadzaj, M. C. Downer
University of Texas – Austin, Austin, USA

O. Zarini, A. Debus, J. Couperus Cabadağ, P. Ufer, S. Schöbel, Y.Y. Chang, A. Koehler,
R. Pausch, U. Schramm, A. Irman

Helmholtz-Zentrum Dresden-Rossendorf, Dresden, Germany

A. H. Lumpkin, Fermi National Accelerator Laboratory, Batavia, USA

¹also at Helmholtz-Zentrum Dresden-Rossendorf

Abstract

We present experimental results across three different laser wakefield accelerator (LWFA) injection regimes demonstrating extreme visible microbunching (up to 10%). In each regime we examine the near field (NF) coherent optical transition radiation (COTR) at eight different wavelengths from a foil directly after the end of the accelerator. Depending on the LWFA operating regime, we observe different levels of bunch substructure. How this structure evolves across optical wavelengths is also LWFA-regime dependent. Utilizing multi-wavelength images of the foil, we observe features in the 3D beam that are unresolvable using other techniques. Moreover, with the aid of physically reasonable assumptions about the bunch profile, we present a candidate reconstruction of a 3D electron bunch.

INTRODUCTION

The micron-scale size of electron bunches from laser wakefield accelerators [1] make them ideal short, coherent radiation sources. They are inherently coherent in the terahertz and infrared [2], and with seeding, or through self-amplification, they can be microbunched into the ultraviolet spectrum [3, 4]. However, even without seeding LWFA electron beams have inherent visible microbunching due to LWFA processes [5, 6]. These pre-bunched portions of the beam can be used to jump start the self-amplification process in a free electron laser (FEL) [7]. LWFA electron bunches have also been proposed for use in electron-position colliders [8]. A low transverse beam emittance is of interest for the FEL, staged accelerator, and collider applications. However, measuring the transverse bunch size at the beam waist is particularly difficult in LWFAs. NF incoherent optical transition radiation (IOTR) has traditionally been used in conventional accelerators to monitor small transverse beam sizes [9]. Recently, NF COTR has been used to measure the transverse size of microbunches as well as put a sub-micron upper limit on their normalized emittance [6, 10]. It has been shown that the beam emittance from a LWFA is dependent on the injection regime [11]. We observe that the structure of the visibly microbunched portion of the beam also varies with injection regime. Using models from particle in cell

(PIC) simulations or electron spectrum data in tandem with multi-spectral NF COTR imaging, we glean 3D information about LWFA electron bunches, culminating in a candidate 3D reconstruction of the microbunched portion of the beam.

COTR CALCULATIONS

The transverse radiated field produced by a single highly relativistic particle transiting a foil and imaged by a single ideal lens can be described as

$$\frac{d^2 \mathbf{E}_\perp(\mathbf{r}_\perp)}{d\omega d\mathbf{r}_\perp} \propto \int_0^{\theta_m} d\theta \frac{\theta^2}{\gamma^{-2} + \theta^2} J_1(\theta k|\mathbf{r}_\perp|) \hat{\mathbf{r}}_\perp, \quad (1)$$

where \mathbf{E}_\perp is the transverse field, \mathbf{r}_\perp is the transverse radial coordinate, ω is the angular frequency of the radiation, θ_m is the angular acceptance of the lens, γ is the Lorentz factor, J_1 is the first Bessel function of the first kind, and k is $2\pi/\lambda$ with λ being the imaged wavelength [12]. The magnitude squared this equation is known as the OTR point spread function (PSF) [9]. For NF incoherent OTR, the radiated energy (W_{IOTR}) from a normalized charge density $\rho(\mathbf{r}_\perp, z)$ can be written as

$$\frac{d^2 W_{IOTR}}{d\omega d\mathbf{r}_\perp} \propto N_e \int d\mathbf{r}' \left| \frac{d^2 \mathbf{E}_\perp(\mathbf{r}_\perp - \mathbf{r}')}{d\omega d\mathbf{r}_\perp} \right|^2 \int dz \rho(\mathbf{r}', z), \quad (2)$$

which is simply a convolution of the PSF and the longitudinally integrated charge density. N_e is the total electron count in the bunch. On the other hand, radiated energy from coherent OTR (W_{COTR}) can be expressed as

$$\frac{d^2 W_{COTR}}{d\omega d\mathbf{r}_\perp} \propto N_e^2 \left| \int dz \int d\mathbf{r}' \frac{d^2 \mathbf{E}(\mathbf{r}_\perp - \mathbf{r}')}{d\omega d\mathbf{r}_\perp} e^{ikz} \rho(\mathbf{r}', z) \right|^2 \quad (3)$$

The subtle differences in these formulas lead to several significant consequences. First, IOTR scales as N_e where COTR scales as N_e^2 . If a portion of the beam is radiating coherently, it is likely that the COTR will dominate the IOTR. However, the portion of the bunch that is coherent depends on the longitudinal Fourier transform of the beam density distribution. If the beam is neither shorter than nor microbunched at the desired wavelength, there will be no COTR. Finally, for COTR, the transverse field is convolved with the charge distribution before taking the magnitude squared. This allows fields from transversely separated electrons to interfere.

* U. Texas authors acknowledge support from DOE Grant No. DE-SC0011617, and M. C. D. from the Alexander von Humboldt Foundation.

AC/DC: THE FERMI FEL SPLIT AND DELAY OPTICAL DEVICE FOR ULTRAFAST X-RAYS SCIENCE

A. Simoncig[†], M. Manfredda, G. Gaio, L. Raimondi, C. Fava,
S. Gerusina, R. Gobessi, A. Abrami, F. Capotondi, D. De Angelis,
R. H. Menk^{1,2}, M. Pancaldi, E. Pedersoli and M. Zangrando³, Elettra Sincrotrone Trieste S.C.p.A.,
Area Science Park, Basovizza, Italy

N. Mahne, Istituto Officina dei Materiali, CNR, Area Science Park, Basovizza, Italy

¹also at Istituto Nazionale di Fisica Nucleare section of Trieste, Trieste, Italy

² also at Department of Medical Imaging, University of Saskatchewan, Saskatoon, Canada

³ also at Istituto Officina dei Materiali, CNR, Area Science Park, Basovizza, Italy

Abstract

Free-electron lasers (FELs) are the most advanced class of light sources, thanks to their unique capability to lase high-brightness and ultrashort pulses marked by wavelengths spanning the Extreme-Ultraviolet (EUV), the Soft (SXR) and Hard (HXR) X-Ray spectral domains, alongside with temporal duration lying in the femtosecond (fs) timescale. Particularly, the FERMI FEL, located at the Elettra Sincrotrone Trieste campus (Italy), and based on the external laser seeding scheme, has recently set new standards in terms of EUV/SXR pulses emission. FERMI is a single-pass FEL able to lase nearly transform-limited and fully coherent pulses between 100 nm and 4 nm (in first harmonic), alongside the full control of the radiation polarization state, too. Thanks to these almost unique features, FERMI has recently allowed to extend, in a time-resolved approach, both established spectroscopies, daily implemented at synchrotron light sources, and novel non-linear optical methods, combining FELs and laser pulses. Nonetheless, the next step to push the ultrafast X-Ray science standards is widely recognized to the capability to perform experiments engaging exclusively EUV, SXR and HXR pulses. Indeed, exciting (and probing) matter at its (or nearby) electronic resonances, is largely speculated to be the key for disclosing the microscopic mechanisms hiding behind some of the most exotic phases of physical, chemical, and biological systems. Such a goal calls the design of optical devices capable to both split and delay (in time) FEL pulses, without impacting on their unique coherence properties, and required to be fully user-friendly in terms of preserving the perfect overlap of the resulting focal spots, even in the tightest focusing conditions achievable on the sample (few microns).

INTRODUCTION

At FERMI, such a goal is addressed by an optical device installed along the Photon Analysis Delivery and Reduction System (PADReS) and known as AC/DC, which stands for the Auto Correlator/Delay Creator [1-3]. AC/DC is designed to split the incoming FEL photons beam by inserting a grazing incidence flat mirror to create two exact half-spots. These resulting two pulse replicas are free to

travel along separate optical paths, being the first one marked by a fixed-length, while the second optical path is characterized by a mobile-length, which can be tuned by moving the relative longitudinal positions of two grazing incidence mirrors mounted onto two specular mechanical rails. In this way, it is possible to introduce a controlled temporal delay between these two EUV/SXR pulses and address the challenge to perform time-resolved experiments within a FEL-FEL configuration. Moreover, AC/DC is designed to exploit multi-colour time-resolved experiments characterized by non-degenerate (in wavelength) pump and the probe pulses to perform multidimensional spectroscopy studies, too. Indeed, thanks to its double cascade scheme, FERMI can deliver two (or more) FEL pulses marked by different wavelengths [4-6]. AC/DC can both a) isolate these FEL pulses, by means of the insertion of free-standing solid-state filters, separately intercepting the beams travelling along the mobile or the fixed-length optical branches, and b) delaying (in time) one respect to the other.

OPTICAL DESIGN

AC/DC can be easily described as composed of four different units (see Fig. 1), which are a) the first grazing incidence mirror (M1), in charge to split the incoming FEL photons beam in two exact half-spots, b) the two, fixed- and mobile-length optical branches (see blue and red lines in Fig. 1), c) the grazing incidence mirror (M4) recombining the two half-spots in the far-field, and d) the (laser) pointing feedback system (see black line in Fig.1), implemented to preserve the spots overlap at the focal plane of the experimental end-station. M1 is mounted onto a vertical actuator to intercept the incoming FEL photons beam along the optical transport trajectory and to split its quasi TEM₀₀ gaussian transverse intensity distribution into two exact half-spots. Several Ce:YAG screens, positioned downstream of M1, are used for checking in real-time the proper splitting. The radiation reflected by M1 is steered into the fixed-length optical branch (see blue line in Fig. 1). The grazing incidence angle for this first set of mirrors (M1 and M4) is 2 degrees. M4 is also mounted onto a vertical actuator, which allows its complete extraction during ordinary FEL operations. The pulses propagated after M1 (not reflected) intercept the second set of mirrors (M5 and

[†] alberto.simoncig@elettra.eu

PROBING TRANSIENT STRUCTURES OF NANOPARTICLES BY SINGLE-PARTICLE X-RAY DIFFRACTION

A. Niozu*, Hiroshima University, Higashi-Hiroshima, Japan
 Y. Kumagai, Tokyo University of Agriculture and Technology, Tokyo, Japan
 T. N. Hiraki, K. Asa, Y. Sato, N. Yokono, K. Nagaya, Kyoto University, Kyoto, Japan
 K. Matsuda, Kumamoto University, Kumamoto, Japan
 H. Fukuzawa, K. Motomura, Y. Ito, D. You, T. Ono, Y. Li,
 S. Saito, Y. Luo, K. Ueda, Tohoku University, Sendai, Japan
 M. Bucher, L. Young, Argonne National Laboratory, Argonne, USA
 E. Kukk, University of Turku, Turku, Finland
 C. Cirelli, C. Bostedt, PSI, Villigen PSI, Switzerland
 C. Miron, Universite Paris-Saclay, Paris, France
 L. Neagu, National Institute for Lasers, Plasma and Radiation Physics, Bucharest, Romania
 C. Callegari, M. Di Fraia, Elettra - Sincrotrone Trieste S.C.p.A., Trieste, Italy
 G. Rossi, D. E. Galli, T. Pincelli, Università degli Studi di Milano, Milano, Italy
 A. Colombo, Department of Physics, ETH Zürich, Zürich, Switzerland
 J. Rist, I. Vela-Pérez, Johann Wolfgang Goethe-Universität, Frankfurt, Germany
 M. Yabashi, RIKEN SPring-8 Center, Hyogo, Japan
 S. Owada, T. Kameshima, Y. Joti, T. Katayama, T. Togashi, K. Tono, JASRI, Hyogo, Japan

Abstract

We report on our recent experimental results of single-shot and single-particle X-ray diffraction of rare-gas nanoparticles at SACLA. The single-shot diffraction data provided insights into the crystallization kinetics of Xe nanoparticles, where the nanoparticles initially crystallize in the metastable stacking-disordered phase and then transform into the stable face-centered cubic phase. In addition, we investigated the ultrafast structural dynamics of nanoplasma induced by an intense near-infrared laser pulse. We found a relation between the timescale of structural disordering and the speed of ejected ions from nanoplasma. We demonstrate the effectiveness of single-particle diffraction for investigating non-equilibrium structural dynamics at the nanoscale.

INTRODUCTION

The availability of ultrashort and intense X-ray pulses from free-electron lasers (FELs) [1, 2] has opened novel opportunities for probing transient states of matter with unprecedented temporal resolutions. Particularly, single-particle X-ray diffraction is a promising technique for investigating structural dynamics of nanoparticles. Rare-gas nanoparticles have been employed as a model system in several FEL experiments due to their size tunability and simple interatomic interaction.

In this contribution, we report on applications of single-particle X-ray diffraction of rare-gas nanoparticles for the investigations of crystallization dynamics [3, 4] and ultrafast dynamics of laser-induced nanoplasma [5]. The experiments were carried out at SACLA BL3 [6, 7]. Please refer to the

references [3–5] for the detailed results and discussions and the reference [8] for the experimental setup.

CRYSTALLIZATION KINETICS OF XENON NANOPARTICLES

Crystallization is one of the most ubiquitous physical phenomena in nature; nevertheless, the atomic-scale structural dynamics upon crystallization is still a subject of controversy. The classical theory of nucleation assumes that crystallization starts from a small spherical nucleus having the structure of the stable phase in bulk. On the other hand, more than a hundred years ago, Ostwald proposed his step rule [9], stating that phase transition can proceed via intermediate metastable phases. Recent computational studies have provided novel insights into the microscopic structural pathway of crystallization [10]. In contrast, owing to several technical challenges to observe the atomic-scale dynamics, experimental observations have been so far mostly restricted to slow dynamics, such as crystallization of colloidal systems [11].

We investigated the structure of single Xe nanoparticles crystallized in a supercooled Xe gas jet. Our experiment realized an ideal condition for crystallization, i.e. in the absence of interaction with the surroundings and impurities. The single-particle structures of Xe nanoparticles were probed by FEL pulses ($h\nu = 11$ keV) several hundreds of microseconds after the growth. The diffraction signals were recorded on a shot-by-shot basis with the multiport CCD sensor detector [12].

The accumulated virtual powder X-ray diffraction pattern of the Xe nanoparticles showed peaks corresponding to the face-centered cubic (fcc) structure (the bulk stable phase of Xe) but also peaks from a structure composed of randomly

* niozu@hiroshima-u.ac.jp

NOVEL LATTICE INSTABILITY IN ULTRAFAST PHOTOEXCITED SNSE *

Y. Huang, S. Teitelbaum, G. De la Peña, D. A. Reis, M. Trigo,
 SIMES, SLAC National Accelerator Laboratory, Menlo Park, California, USA
 S. Yang, J. L. Niedziela, D. Bansal, O. Delaire,
 Department of Mechanical Engineering and Materials Science,
 Duke University, Durham, North Carolina, USA
 T. Sato, M. Chollet, D. Zhu,
 LCLS, SLAC National Accelerator Laboratory, Menlo Park, California, USA

Abstract

We use ultrafast X-ray scattering to study SnSe, a resonantly bonded material, with an emphasis on its non-equilibrium states. The work presented advances the methodology of ultrafast X-ray scattering enabled by the free-electron lasers (FELs), and shows how these novel methodologies help us understand how electrons and phonons interact in their natural length scale and time scale, and how new non-equilibrium states of matter, possibly related to new functionalities, are created.

INTRODUCTION

We use ultrafast X-ray scattering to study SnSe, a resonantly bonded material. Resonantly bonded materials have various functional properties directly associated with the structures, including ferroelectricity, high thermoelectric figure of merit, and large change of optical constants upon crystallization and amorphization (or phase change materials). They host a number of structural phases that are sensitive to external parameters (e.g., temperature, pressure, and chemical doping) and are expected to exhibit tunability by the light field. The large polarizability in resonantly bonded materials means pronounced coupling between phonons and electronic states, which yields large responses of the X-ray probe. We show that using a combination of ultrafast optical and X-ray lasers, we can understand materials on the natural time and length scales of their chemical bonding, which is not achievable with purely optical probes. The knowledge of the microscopic interactions in the non-equilibrium states will ultimately help us explore possible new functionalities in the non-equilibrium phases.

In particular, we use time-resolved X-ray diffraction to obtain amplitude as well as the phase of atomic motion, which allows us to reconstruct the lattice structure of SnSe. The structural distortions and the related new phase are unexpected, and cannot be correctly concluded from a purely optical (e.g., Raman scattering) measurement. We also use time-resolved X-ray diffuse scattering to access the excited-state dispersion of SnSe, which elucidates how photoexcitation alters the strength of specific bonds leading to this the novel lattice instability observed in diffraction.

* huangyj@stanford.edu

PROBING PHOTOINDUCED LATTICE INSTABILITY IN SNSE

Using time-resolved X-ray diffraction, we demonstrate that SnSe, one of the IV-VI resonantly bonded compounds, hosts a novel photoinduced lattice instability associated with an orthorhombic distortion of the rock-salt structure. This lattice instability is distinct from the one associated with the high-temperature phase, providing a counterexample of the conventional wisdom that laser pump pulse serves as a heat dump. See Fig. 1.

The new lattice instability is accompanied by a drastic softening of the lowest frequency A_g phonon. This mode was previously identified as the soft mode in the thermally driven phase transition to a Cmcm structure. Time-resolved X-ray diffraction directly reveals the phase of motion of the lowest frequency A_g phonon ($A_g^{(1)}$), which is opposite to a motion towards Cmcm. The identification of the distorted structure is made possible by summing up the contributions of several phonon modes. The amplitude, as well as the phase of the motion of each mode, are calculated by fitting the time-resolved X-ray scattering intensity. The findings highlight the importance of diffraction technique, which reveals the phase and amplitude of motion instead of just frequencies compared to conventional optical ultrafast spectroscopies.

We show that the driving mechanism for this new lattice instability is related to the removal of valence electrons from the lone pair orbital. Lone pair electrons tend to locally distort a symmetric structure, in the case of SnSe, the octahedral environment shown in Fig. 1. The Se $4p$ - and Sn $5s$ -derived bands that largely constitute that lone pair, are about 0.7 eV below the top of valence bands, which can be reached with the pump photons of 1.55 eV but not the thermal excitations. Density functional theory (DFT) calculations from our collaborators at Duke University confirm the origin of photoinduced Immm lattice instability.

Our findings have implications in other rocksalt distorted IV-VI semiconductors, several of which have topological states protected by lattice symmetry in the cubic or tetragonal phases. More generally, our work suggests that pump wavelength could provide additional control of structural distortions through orbitally-selective above-gap excitation. This could be exploited to direct a particular structural distortion to desirable outcomes with particular functionality beyond those accessible in thermal equilibrium.

FLASH2020+ PUMP-PROBE LASER UPGRADE: CONCEPT AND CURRENT STATUS

S. Ališauskas[†], A.-L. Viotti¹, M. Seidel, A. Tajalli, B. Manschwetus, H. Cankaya, and I. Hartl
Deutsches Elektronen-Synchrotron DESY, Hamburg, Germany
¹also at Department of Physics, Lund University, Lund, Sweden

Abstract

Time-resolved experiments are increasingly relevant in modern FEL user facilities. With the FLASH2020+ upgrade project, the pump-probe capabilities of FLASH will be extended. Besides offering high power fixed wavelengths (1030 nm fundamental and its harmonics), tunable wavelengths are under development: sub-150 fs 2-5 μm mid-infrared pulses for the condensed matter community and sub-40 fs long 200-500 nm UV-Visible pulses for the general chemistry, atomic molecular and optical physics (AMO) communities. Here, we present our pump-probe laser concept.

CONCEPT OF PUMP-PROBE LASER

By 2025, two new pump-probe laser systems will be operational in both the FLASH1 and FLASH2 FEL beamlines, allowing users to perform femtosecond pump-probe experiments [1]. Pump-probe lasers will be placed for both FEL beamlines in laser hutches in the FLASH experimental halls to provide temperature and humidity-stabilized environments, which are essential for laser stability. Both the FLASH1 and FLASH2 pump-probe lasers are of similar construction, see Fig. 1. The primary requirement for user experiments is that the pump-probe laser must be synchronized with the FEL radiation, and should therefore operate in bursts at 10 Hz (with an intra-burst repetition rate up to 1 MHz and a burst duration $>600 \mu\text{s}$) with a precisely controllable time delay. Utilizing Yb amplifiers based on fiber, thin disk, Innoslab, or cryogenic technology can accomplish this [2-5]. The Yb:YAG Innoslab technology is our preference because it has proven to be the most cost-effective solution and has already been implemented in a few FEL facilities, including European XFEL and LCLS II [6,7]. Due to the gain bandwidth limitations, a high-power Yb:YAG laser generates relatively long pulses (~ 1 ps FWHM). Frequently, lasers of this type are used to drive a broadband optical parametric amplifier (OPA) to generate the short pulses required for FEL pump-probe experiments [6,7]. Unfortunately, OPCPA has quite a low efficiency, and the final laser system power drops by one order of magnitude.

In our upgrade scheme, we plan to use external pulse post-compression: the pulse will be spectrally broadened by self-phase modulation in multi-pass cells (MPCs). MPCs offer large compression ratios (up to 40 times for one cell) and efficiency levels higher than 90%, while being still very compact and supporting excellent pulse-to-pulse stability [8]. We have been successfully testing the

[†] skirmantas.alisauskas@desy.de

nonlinear compression technique in the recent years [9-12]. We will install gas-filled MPCs in the FLASH1 as well as FLASH2 laser hutches. By tuning the gas pressure, we can control the bandwidth of the output pulses (see Fig. 2 for more details), and subsequently, adjust the laser pulse durations to the experimental needs. A vacuum beamline system will then transport the uncompressed, spectrally broadened pulses with a Fourier limit of as small as 35 fs from the laser hutch to several modular optical delivery stations (MODs) within reach of the instruments, where pulse compressor, frequency conversion, and user controls will be installed. Afterward, the beam is coupled to the instrument and focused onto the interaction point. A single colour laser transport beamline with a modest spectral bandwidth becomes rather simple and will allow us to use high-quality AR and HR optics resulting in very high transmission (close to 99%).

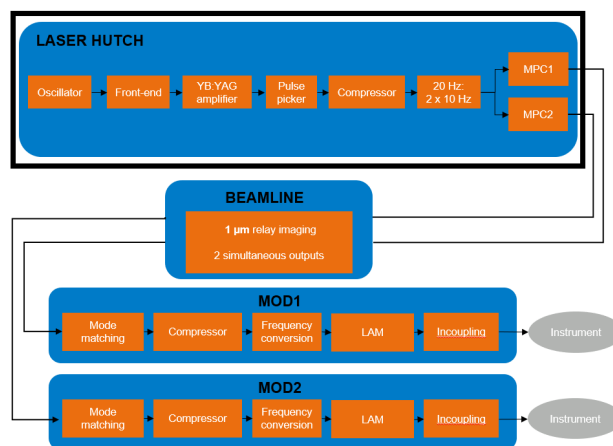


Figure 1: An illustration of the pump-probe laser and its delivery to the experiment.

FLASH's pump-probe laser's will run at 20 Hz and split the output into two 10 Hz pulse trains, one synchronized with the FEL and another shifted by 50 ns. This splitting will be achieved with a fast rotating waveplate and a polarizer. Simultaneously, these two outputs will be sent to MPCs for spectral broadening and afterward send to two MODs: one MOD where users will run the experiment and another MOD where we will prepare for the next user experiment. We are targeting to deliver 1030 nm few millijoule level pulses at the MODs. Currently, the Yb:YAG amplifier intraburst repetition rate is limited to 100 kHz, and in the future, we are considering increasing the intraburst rate to 1 MHz by keeping the same pulse energy. The pulse picker will adjust the burst length after the amplifier. The